PROPERTIES OF CONCRETE WITH GROUND GRANULATED BLAST FURNACE SLAG

EFFECT OF THE ADDITION ON THE FROST SCALING RESISTANCE AND CLHORIDE MIGRATION

Vera Mónica Ferreira Correia

Dissertação para obtenção do Grau de Mestre em

Engenharia Civil

Orientador: Professor Doutor João Paulo Janeiro Gomes Ferreira

Orientador: Professor Doutor Luping Tang (Chalmers University of Technology)

Júri:

Presidente: Professor Doutor Augusto Martins Gomes

Orientador: Professor Doutor João Paulo Janeiro Gomes Ferreira

Vogal: Professora Doutora Ana Paula Patrício Teixeira Ferreira Pinto França de Santana

Outubro 2015

RESUMO

Escória de Alto Forno (GGBS), um resíduo da produção de aço em alto forno, pode ser usado para substituir parcialmente o cimento Portland (CEM I) no betão. A adição de escória de alto forno na produção do betão melhora certas características do betão, quando comparado com betão produzido apenas com cimento Portland como ligante. No entanto, preocupações relacionadas com o comportamento do betão com escória de alto forno em ambientes de gelo/degelo têm sido levantadas. O objectivo da presente investigação foi averiguar as propriedades de betão com adição de escória de alto forno, em especial no que se toca à resistencia ao gelo/degelo na presença de sais descongelantes, e à resistencia à penetração de cloretos, e se é possível produzir betão resistente ao gelo/degelo com percentagens de escória de alto forno superiores às permitidas na norma sueca SS 13 70 03 (2008) para a classe de exposição XF4 (25% da massa de CEM I).

A presente dissertação consistiu maioritariamente numa investigação laboratorial. Betões com diferentes percentagens de substituição de cimento por escória de alto forno (0%, 25%, 50% e 100% da massa de cimento), com factores de eficiência diferentes (k=0.6 e k=1.0), e diferentes teores de ar (4.5% e 6.0%) foram produzidos e testados, num total de 8 composições diferentes. A influência de outros parâmetros (cura a temperatura elevada, uso de superplastificantes, hidratação prolongada) foi também averiguada.

Os resultados revelam também que a resistência ao gelo/degelo diminui com o aumento da percentagem de adição. No entanto, a presente investigação mostrou que é possível produzir betão com adição de escória de alto forno com percentagens de substituição até 50% que apresente resistência ao gelo/degelo considerada aceitável, através do ajuste de certas propriedades da mistura (como por exemplo, aumentando o teor em ar). Isto é, é possível produzir betão resistente ao gelo/degelo com percentagens de escória superiores às permitidas na norma SS 13 70 03 (2008). Os resultados obtidos mostram também uma melhoria significativa da resistência à penetração de cloretos com o aumento da adição de escória de alto forno.

Palavras-chave: betão, adições, Escória de Alto Forno (GGBS), durabilidade, resistência ao gelo/degelo na presença de sais, migração de cloretos

ABSTRACT

Ground Granulated Blast-Furnace Slag (GGBS), which is a by-product of the manufacturing of iron in the blast furnace, can partially replace cement in concrete. The use of GGBS in concrete has proved to improve certain properties, when compared to Portland cement concretes. However, some concerns regarding its performance in freezing environments have been raised. The aims of the research project conducted were to investigate the properties of the concrete with GGBS, with special focus on its frost scaling resistance and resistance against chloride ingress, and to assess if it is possible to produce salt-frost resistant concrete with amounts of GGBS higher than the permitted in the Swedish Standard SS 13 70 03 (2008) for exposure class XF4.

The research was carried out mainly as a laboratory study. Concretes with different amounts of GGBS (0%, 25%, 50% and 100% of the cement weight), different efficiency factors (k=0.6 and k=1.0), and different air content (4.5% and 6.0%), on a total of 8 mixes, have been tested. The effects of other parameters (curing at higher temperature, use of superplasticizer, prolonged hydration) have also been investigated.

The results showed that the frost resistance of concrete generally decreases with the increase of the amount of GGBS. However, this research showed that it is possible to produce frost resistant concrete with up to 50% of GGBS by changing some properties of the mix (such as increasing the air content), i.e., it is possible to produce sat-frost resistant concrete with amounts of replacement higher than the limit defined in SS 13 70 03 (2008). The results also showed a significant improvement of the resistance against chloride ingress for concrete with high additions of GGBS.

Key words: concrete, additions, Ground Granulated Blast Furnace Slag (GGBS), durability, salt frost resistance, chloride migration

ACKNOWLEDGEMENTS

First, I would like to express my sincere gratitude to Professor Luping Tang (Chalmers University of Technology) and Anders Lindvall (Thomas Concrete Group AB) for introducing me to this field and giving me the opportunity of working in such a challenging project, and for their support, guidance and sharing of knowledge throughout the entire research.

I am, too, grateful to Professor João Gomes Ferreira for his advice, patience and availability to discuss some topics of great relevance to this thesis, and for his precious insight and suggestions which enriched this thesis.

I would like to acknowledge Thomas Concrete Group AB, for providing their installations and all the materials and equipment necessary during the experimental campaign.

I would also like to thank Pernilla Kamperin (TCG) and Andreas Karlsson (TCG), and Marek Machowski (Chalmers University of Technology) and all the staff from both laboratories for their advice and help during the experimental campaign.

Last but not least, I would like to express my deepest gratitude to my family, especially my father, for their unconditional love, support and encouragement.

I would also like to thank my friends for all the complicity, understanding, encouragement and company throughout the entire duration of this project. A special thanks to Tiago Barroqueiro for his patience and invaluable help with the preparations for the presentation of this project.

TABLE OF CONTENTS

LIST OF FIGURES

LIST OF TABLES

NOTATION

(w/b)	water/binder ratio
(w/c)	water/cement ratio
$(w/c)_{eq}$	equivalent water/cement ratio
A	area of the test surface
A_c	area of the cross-section of the specimen
D_{nssm}	chloride migration coefficient from non-steady-state migration (NT BUILD 492)
F	maximum load applied in the compressive strength test
f_c	compressive resistance
k (k-factor)	cementing efficiency factor
L	thickness of the specimen
m_n	mass of material loss per area
Mn	accumulated mass of scaled material after n cycles
mn	scaled material after n cycles (SS 13 72 44)
p	total pore volume
S	Degree of saturation
S_{cr}	Critical degree of saturation
T	Temperature (°C);
t	time
U	absolute value of the applied voltage (V) (NT BUILD 492)
w_e	evaporable water content
x_d	average value of the penetration depths (NT BUILD 492)

Acronyms

AEA	Air Entraining Agent
AVA	Air Void Analyser
GGBS	Ground Granulated Blast Furnace Slag

1. Introduction

1.1. Background

Since its development, by Joseph Aspdin, in 1824, Portland cement represents the great majority of the binders all over the world. However, in the last 100 years some other materials have been used to partially replace cement – the so-called supplementary cementitious materials, or additions. These materials are almost always inorganic, with particle sizes similar or smaller to that of Portland cement [Domone and Illston (2010)].

The rising interest in using alternative binders is mainly due to their ability to enhance some properties of concrete, often in the fresh concrete, but mostly in the hardened concrete. For a long time, Portland cement was regarded as *the* binder by excellence. When other cementitious materials were introduced, they were considered merely as replacements of cement, with their properties and effects on concrete being always confronted with that of Portland cement-only concrete. Currently, however, it is widely accepted that concrete with additions performs better in certain environments than Portland cement concrete, being the type and dosage of supplementary cementitious material studied to optimize concrete properties, depending on the mechanical and durability requirements. High performance concrete often features a combination of Portland cement and one or more of these materials additions [Neville (2003)].

Other reason for using alternative binders is the rising concern about the environmental impact of the construction industry, and particularly that of the production of cement. The carbon dioxide emissions by the cement industry comprise not only the burning of the fuels to produce energy to extract the raw material and the high temperatures needed for the decomposition of the calcium carbonate, but also the grinding of the clinker and the transport of the cement. In 2006 alone, the cement industry was responsible for 5.5% of the CO_2 emissions to the atmosphere. Since those emissions are unavoidable when producing cement, one way to reduce the negative environmental impact of the concrete manufacture is to replace a certain amount of cement with other materials whose production is more sustainable. Moreover, being most of these alternative cementitious materials a by-product of other industrial processes, the use of this products will reduce the need for extraction of raw materials to produce cement (which are finite resources), while also reducing the industrial waste, further contributing for a lower negative impact of the construction industry in the global environment [Domone and Illston (2010)].

The main reason for the introduction of these alternative binders was, however, economical. The extraction of raw materials is a costly process. Being these supplementary cementitious materials mostly by-products of other industrial processes, their production requires little processing, which reduces the cost of production. For that reason, these additions are usually cheaper than Portland cement [Domone and Illston (2010)].

In Europe, the use of additions in concrete is guided by the European Standard EN 206-1, Concrete: *Specification, Performance, Production and Conformity*. EN 206-1 defines two types of additions: Type I (nearly inert additions) and Type II (pozzolanic or latent hydraulic additions). Type I additions do not present pozzolanic behaviour. They improve the properties of concrete acting as "filler", which results on a more cohesive and compact concrete paste and, therefore, on an increased compressive strength and lower permeability. One example of a Type I addition is limestone [Neville (2003)].

Type II additions contain active silica (SiO_2) in a glassy or amorphous state, which provides the pozzolanic behaviour. These additions do not usually possess hydraulic properties on their own. Instead, when broken to a finely divided powder, and used together with Portland cement, the active silica will react with the calcium hydroxide released during the hydration of Portland cement to form cementitious compounds (calcium silicates). The main Type II additions are Fly Ash, Ground Granulated Blast Furnace Slag, Silica Fume and Natural Pozzolans [Neville (2003)]:

- **Fly Ash** is the most common artificial pozzolan. Fly ash is a finely divided powder which is a residue of the combustion of pulverized coal used to fire power plants. Fly ash is mainly composed by silica (SiO_2), aluminium oxide (Al_2O_3), iron oxide (Fe_2O_3) and calcium oxide (CaO). Due to the incomplete combustion and the organic additives used in the collecting process, fly ash also contains some unburned carbon. Two classes of fly ash are usually considered: **Class C Fly Ash**, and **Class F Fly Ash**. Class C fly ash originates from subbituminous and some lignite coals, whilst Class F fly ash originates primarily from burning anthracite and bituminous coals. The chemical composition of both fly ash qualities is very similar, though the CaO content of Class C fly ash is higher (usually 10% to 30%) than Class F fly ash (typically 0.7% to 7.5%). Hydration of Class F fly ash requires an activator, unlike Class C fly ash, which presents slightly hydraulic properties [ACI Committee 232 (1996)].

- **Ground Granulated Blast Furnace Slag (GGBS)**, also known as slag, is a granular material formed when molten iron blast furnace slag (a by-product of the manufacture of iron and steel) is quenched by immersion in water, and then ground to a fineness similar to that of Portland Cement. The chemical composition of GGBS is very similar to that of Portland cement, though GGBS is composed mainly (90% to 95%) by glassy calcium silicates and calcium aluminosilicates, and presents a lower content of lime (CaO) than Portland cement. GGBS is, to a certain extent, cementitious on itself, even though continued hydration requires an activator [Ramachandran (1995)].

- **Condensed silica fume**, also known as silica fume or microsilica, is a by-product of the reduction of high-purity quartz with coal in an electric arc furnace during the manufacture of metallic silicon or ferrosilicon alloys. Silica fume consists of at least 85% silicon dioxide, in an amorphous (non-crystalline) form. Silica fume particles are extremely small when compared to other cementitious materials, with an average diameter of 0.1μm, i.e., $1/100^{th}$ of a Portland

cement particle. Because of its extreme fineness and high silica content, silica fume is a very effective latent hydraulic material [Ramachandran (1995)].

- **Natural Pozzolans** are natural materials displaying latent hydraulic properties. The most common natural pozzolans are volcanic ashes, calcined clay, calcined diatomaceous earth, opaline shale and high-reactivity metakaolin [Neville (2003)].

Traditionally, only one supplementary cementitious addition was used in each concrete mix, being introduced either as a separate material added in the mixer, or blended and ground with the Portland cement. Currently, due to improved access to these materials, concrete producers can combine two or more of these materials. Mixes using three cementitious materials, the so-called ternary mixes, are becoming more common, typically for economic reasons, but also for optimizing engineering properties [ACI Committee 233 (2000)].

The present investigation focused on the behaviour of concrete with addition of GGBS. GGBS, or slag, can be present in concrete as a separate material added in the mixer, or blended in the Portland cement: either as Portland-slag cement, CEM II-S (with up to 35% of GGBS of the total binder content) or as Blast furnace cement, CEM III (also called Blast Furnace Slag cement, containing 35% to 95% of GGBS of the total binder content) [EN 206-1].

GGBS is often used in concrete to improve certain properties, both in fresh and hardened concrete. GGBS is frequently used in the production of low heat cement. Ternary systems composed by Portland cement, slag and silica fume have also been used in the production of high-strength concrete. However, the main application of GGBS as a supplementary cementitious material is in concrete structures placed in marine environments, due to its proven influence in reducing chloride ingress in concrete. An improved performance of concrete mixes produced with GGBS in the protection against sulphate attack and alkali-silica reaction has also been widely reported [ACI Committee 233 (2000)].

However, some concerns have been raised regarding the durability of concrete with addition of GGBS in freezing environments. The freeze/thaw durability of concrete, especially when de-icing agents are used, is of the utmost importance in countries with cold climates, and has been widely studied both in Northern Europe and North America. The use of de-icing salts may result in a type of frost attack in concrete called surface scaling. In this type of frost attack in concrete, small chips of the cement paste are removed from the concrete surface, exposing the aggregate. The continuation of this mechanism can lead to severe consequences for the structures: the thickness of the protective layer above the reinforcement is reduced, which may lead to initiation of corrosion and consequent loss of load capacity [Neville (2003)].

Several investigations report reduced salt-frost resistance of concrete with additions of GGBS, when compared to that of Portland cement concrete, especially when large additions of GGBS are used. However, this conclusion is not consensual – even though laboratory tests usually result in a poorer

performance, many researchers have found that, in field exposure, the resistance of concrete with additions of slag is comparable to that of Portland cement concrete [ACI Committee 233 (2000)].

The present investigation aims at providing more information about the behaviour of slag concrete in freezing conditions when de-icing agents are used.

1.2. Aims of the investigation

The present research project aims at investigating the properties of concrete containing additions of GGBS, especially in what concerns its compressive strength, resistance against chloride penetration, and salt-frost resistance. The investigation was carried out mainly as a laboratory study. The experimental study was carried out at Thomas Concrete Group AB in Göteborg, Sweden, in partnership with Chalmers University of Technology.

The use of GGBS in concrete in Sweden is regulated by the Swedish Standard SS 13 70 03 (2008), which is the Swedish adaptation of EN 206-1. In this standard, the addition of GGBS is limited to 50 weight -% of CEM I for exposure classes XF1-3 (frost attack without de-icing agents), and 25 weight-% of CEM I in exposure class XF4 (frost attack in the presence of salts). The present research project aims at investigating whether it is possible to produce GGBS concrete with adequate resistance against frost attack in the presence of de-icing agents using higher amounts of GGBS than the 25% per weight of CEM I permitted by SS 13 70 03 (2008).

To that end, air-entrained concrete mixes with an equivalent water/cement ratio of 0.45 and with different percentages of replacement of Portland cement by GGBS were produced and tested. The influence of the air entrainment and curing temperature on the properties of the hardened GGBS concrete has also been investigated.

In the present investigation the GGBS was added separately in the mixer, since CEM II or CEM III are not currently available in Sweden. In Europe, the requirements for the GGBS to be used in concrete are regulated by the European Standard EN 15167: *Ground Granulated Blast Furnace Slag for use in concrete, mortar and grout*. In Sweden, the Swedish adaptation of this standard, SS-EN 15167-1, is used. The GGBS used in the present research project complies with the requirements defined in SS-EN 15167-1 (2006).

1.3. Methodology and organization of the project

The experimental research that resulted on the present thesis was preceded by a literature review that included not only the chemical and physical properties of Ground Granulated Blast Furnace Slag

and the influence of the addition in the properties of concrete, but also the mechanisms of frost attack in concrete and the factors that influence its resistance. An extensive review of previous investigations on the frost resistance of concrete with slag additions was also carried out. The experimental plan was then prepared: the concrete mixes were designed, the parameters to be investigated were defined and the tests to be performed were decided. The concrete mixes were then prepared, the specimens were casted and the properties of fresh and hardened concrete were tested. The results of the tests were collected, analysed and compared with the results provided in the literature. To conclude, the main research findings and the perspectives for future research were formulated.

The present thesis is organized in six chapters:

Chapter 1 gives an outline of the thesis, including the background, aims and methodology of the research project.

Chapter 2 describes the properties of GGBS used as a supplementary cementitious material in concrete, and its effects on the properties of fresh and hardened concrete.

Chapter 3 gives a brief description of the most well-known freeze/thaw mechanisms and factors that influence the frost resistance of concrete, and presents a literature review of previous work on the effect of the addition of GGBS regarding the frost resistance of concrete.

Chapter 4 presents the experimental study, including the mix proportions of the concrete qualities produced, the tests performed, and modifications made to the standardized test methods to study a particular property.

Chapter 5 reports the results of the experimental study. These results are carefully analysed and discussed considering the results presented in the literature.

Chapter 6 outlines the main conclusions of this research project, as well as some suggestions for future investigations.

2. Concrete with addition of GGBS

Ground Granulated Blast Furnace Slag (GGBS) has been used as a cementitious material in concrete since the beginning of the 20th century. GGBS can partially replace cement in concrete, either as a separated cementitious material added in the mixer, or blended in the cement. This chapter describes the properties of the GGBS used in concrete, and explains the mechanisms behind its influence on the fresh and hardened properties of concrete.

2.1. Production and properties of GGBS

Blast-Furnace Slag is a by-product of the production of iron. When the iron ore is melted in the blast furnace, some impurities ascend to the surface, which are called iron blast-furnace slag. The molten slag that ascends to the surface at a temperature of about 1500ºC is rapidly cooled as soon as it leaves the blast furnace, becoming a vitrified material. The rate of cooling determines the mineralogy of slag, and consequently, its reactivity: rapid cooling results in a high percentage of reactive glassy materials and small amounts of crystalline matter. Slow cooling results in an undesirable amorphous material, with no hydraulic properties [Hewlett (2004), Neville (2003)]. The most common process of cooling is quenching with water, also known as granulation. Pelletizing, a cooling process that requires less water than quenching, may also be used. The result are fine-aggregate-size particles called granulated blast furnace slag, which are composed of at least two thirds by mass of glass, and possess hydraulic properties when suitably activated. This compound is then dewatered, dried and ground to the desired fineness (usually similar or finer than that of Portland Cement), becoming the Ground Granulated Blast-Furnace Slag (GGBS) [ACI Committee 233 (2000), SS-EN 15167-1 (2006)].

Chemically, GGBS is the supplementary cementitious material which composition is more similar to Portland cement, though with a higher content of silica (SiO_2), alumina (Al_2O_3) and magnesia (MgO), and a lower content of lime (CaO), when compared to Portland cement [Ramachandran (1995), Chen (2006)].

Ground Granulated Blast Furnace Slag is both a pozzolanic and a cementitious material, due to its glassy nature and chemical composition. Even though it is not a fully hydraulic material, the presence of CaO in its chemical composition makes it self-cementing to some extent, when suitably activated by the presence of an activator, which can be alkalis, sulfates, gypsum or lime [Hewlett (2004)]. When used in combination with Portland cement, the calcium and sodium hydroxides produced during the hydration of the cement will take part in the pozzolanic reaction, working as activators, by initiating the hydration of the glass present in the slag, and forming cementing compounds [Ramachandran (1995)].

The Swedish Standard *SS-EN 15167-1 (2006): Ground Granulated Blast Furnace Slag for use in concrete, mortar and grout*, specifies the requirements for chemical and physical properties, as well as quality control procedures for GGBS to be used as a Type II addition in the production of concrete conforming with the European Standard *EN 206-1: Concrete: Specification, performance, production and conformity.*

According to SS-EN 15167-1 (2006), the GGBS to be used in concrete shall consist of at least 2/3 by mass of calcium oxide (CaO), magnesium oxide (MgO) and silicon dioxide (SiO_2). The remainder shall consist of aluminium oxide (Al_2O_3) and a small amount of other compounds. The ratio (CaO+MgO)/(SiO_2) by mass must exceed 1.0. This ratio ensures high alkalinity, without which the slag would be hydraulically inert [SS-EN 15167-1 (2006), Neville (2003)].

According to SS-EN 15167-1 (2006), the chemical properties of the GGBS suitable to be used in concrete shall conform to the requirements presented in Table 2.1, and be tested according to the reference tests described. EN 196-2 is the European Standard that describes the methods for chemical analysis for cement. Appendix A is part of the SS-EN 15167-1 (2006).

Table 2.1 - Requirements of GGBS, according to SS-EN 15167-1 (2006), given as characteristic values

Property	Test reference	Requirements
magnesium oxide	EN 196-2	≤ 18%
sulfide	EN 196-2	≤ 2,0%
sulfate	EN 196-2	≤ 2,5%
loss on ignition (correct for oxidation of sulfide)	EN 196-2	≤ 3,0%
chloride	EN 196-2	≤ 0,10%
moisture content	Annex A	≤ 1,0%

The standard also states a minimum specific surface (determined according to Blaine's air permeability method) of 275 m2/kg [SS-EN 15167-1 (2006)]. The surface area is a parameter that measures the fineness of a powder, whose value increases with an increase in the fineness, i.e., with a decrease in the size of the particles that compose the powder. The specific surface of the slag influences its hydraulic activity (and, consequently, the rate of strength development), increasing with a higher specific surface. For that reason, other authors recommend a higher value of the specific surface for slags to exhibit satisfactory cementitious and pozzolanic properties: Ramachandran (1995) recommends a Blaine surface area between 400 and 600 m2/kg.

Since the surface area is directly related with the particle size distribution, Ramachandran (1995) recommends the grinding of slag to particle sizes between 10 µm and 45 µm, with a large amount of particles bellow 10 µm. The particles up to 10 µm contribute to the strength development up to 28 days of age, whereas the particles between 10-40 µm contribute to the long-term strength

development. However, the European Standard SS-EN 15167-1 (2006) does not limit the size of the particles of GGBS. Instead, this parameter is controlled indirectly, by defining a minimum allowable specific surface. Unlike the European Standard, the North-American Standard ASTM Specification C989-93 limits the particles coarser than 45 µm to 20% of the total [Neville (2003)].

The specific gravity for GGBS is usually between 2.85 and 2.95, being therefore lower than the specific gravity of Portland Cement (which is around 3.15). The specific surface of the blended cement will therefore be affected correspondingly [Neville (2003)].

The GGBS to be used in the production of concrete shall be tested in combination with CEM I. The requirements for the test cement are specified in SS-EN 15167-1 (2006). When tested with Portland cement, a mortar sample using a combination by mass of 50% GGBS and 50% CEM I shall be used, and compared with a reference sample of 100% CEM I.

The initial setting time of the mortar with 50% of GGBS addition is determined according to the European Standard EN 196-3, and shall not be more than twice of the reference Portland cement sample, according to the standard SS-EN 15167-1 (2006).

The activity index shall also be determined. The activity index is an indication of the reactivity of an addition, being therefore a very important parameter of the GGBS: very low reactive slags may take too long to reach the desirable compressive strength, especially when high percentages of replacement are used. According to SS-EN 15167-1 (2006), the activity index it is the ratio (in percentage) of the compressive strength between a mortar sample with 50% of GGBS replacement, an a sample of Portland cement mortar, both prepared with an water/(cementitious material) ratio of 0.5, and tested according to the European Standard EN 196-1. Since the hydration of slag is slower than the hydration of Portland cement, the strength development of concrete (or mortar) with a percentage of replacement of GGBS will be slower than the strength development of OPC concrete (or mortar), i.e., the activity index will be lower than 1. SS-EN 15167-1 (2006), defines minimum values of activity index of 45% at 7 days and 70% at 28 days.

The activity index depends on the cement with which the addition is mixed, and not only on the addition itself [SS-EN 15167-1 (2006)].

The chemical and physical requirements for GGBS to be used in concrete prescribed in SS-EN 15167-1 (2006) do not include strength or durability requirements per se. Instead, the standard presents the properties that the GGBS must possess so that, when concrete with addition of slag is produced fulfilling all the requirements of the relevant standards and/or regulations, the mechanical properties and durability requirements of concrete are fulfilled.

2.2. Use of GGBS in concrete

Ground Granulated Blast Furnace Slag complying with SS-EN 15167-1 (2006) can be used as a cementinious material in concrete supplied either as a separate material added in the concrete mixer, or interground with the Portland cement. The Swedish Standard SS-EN 197-1: Cement: compositions, specifications and conformity criteria for common cements (which is the Swedish adaptation of the European Standard EN 197-1) recognizes two cement types with GGBS interground with the Portland cement: Type II cement, or Portland-slag cement, which consists mainly of Portland cement, with up to 35% of GGBS by mass of cementitious material; and Type III cement, also known as Portland Blastfurnace cement, which consists predominantly of GGBS.

These cement types are subdivided in classes, according to the mass of GGBS as percentage of mass of cementitious material (Table 2.2).

Table 2.2 - Classification of the main cements containing GGBS, according to the Swedish Standard SS-EN 197-1

Type	Designation	Mass as percentage of mass of cementitous material	
		Portland cement clinker	GGBS
I	Portland	95 - 100	-
II/A	Portland-slag cement	80 - 94	6 - 20
II/B		65 - 79	21 - 35
III/A	Portland Blastfurnace cement	35 - 64	36 - 65
III/B		20 - 34	66 - 80
III/C		5 - 19	81 - 95

The GGBS can also be added directly in the mixer. Supplying the addition separately presents some advantages: it is possible to grind the GGBS to its own optimum fineness (therefore increasing its reactivity), and to apply the efficiency factor depending on the activity of the slag used. Also, the proportions of the addition can be adjusted to suit any particular project requirements. However, when the addition is fed directly into the mixer, an additional silo is needed to store it [ACI Committee 233 (2000)].

When using the GGBS as a separate cementitious material together with CEM I in concrete, the k-value concept is introduced. This k-factor, or efficiency factor, is a measure of the relative contribution of the addition to the strength of concrete, compared to an equivalent mass of Portland cement.

The efficiency factor concept is based on the fact that, since the hydration of the GGBS is slower than the hydration of Portland cement (as it will be explained further in this chapter), if CEM I is replaced by

slag on a one-to-one basis, the strength at early ages will be lower. Since the compressive strength of concrete is highly dependent on the water/cement ratio, it follows that one way to achieve higher strength at early ages when using GGBS is to decrease the water/(cementitious material) content, i.e., the mass of GGBS used will be higher than the mass of Portland cement that it is replacing [Domone and Illston (2010)].

This means that x kg/m3 of GGBS is equivalent to kx kg/m3 of Portland cement, with k ≤1.0 to achieve the same compressive strength as Portland cement concrete at a given age (usually 28 days), and the total equivalent cement content is C+kS, being C the mass of cement and S the amount of slag. Therefore, instead of using the water/cement ratio or water/binder ratio, the equivalent water/cement ratio ((w/c)eq) is used, which is defined in the following equation (1) [SS 13 70 03 (2008)]:

$$(w/c)_{eq} = \frac{w}{C + k\,S} \quad (1)$$

where:

- *w* is the water content (by mass)
- *C* is the content of Portland cement (by mass)
- *k* is the efficiency factor
- *S* is the content of GGBS (by mass)

A k-factor of 1 would mean that the slag would replace the Portland cement concrete on a one-to-one basis without strength loss. Since the strength development of the GGBS concrete is slower than that of the Portland cement concrete, it results that the k-factor should be lower than 1 [Domone and Illston (2010)].

The Swedish Standard SS 13 70 03 (2008), which is the application of EN 206-1 in Sweden, presents the requirements for concrete and all of its constituents to be used in the country. Therefore, concrete with additions of GGBS must address the global requirements for strength and durability of concrete, and also the requirements for the use of this addition.

The Swedish Standard SS 13 70 03 (2008) defines a maximum k-factor of 0.6 when GGBS complying with SS-EN 15167-1 is used with CEM I. However, the standard allows the use of a k-factor of 0.8 if the following conditions are fulfilled by the GGBS and cement used:

1. The activity index at 28 days determined according to the method described in SS-EN 15167-1 is at least 80%, with a permitted deviation for single values of 5%-units under the required value (with sampling, testing and evaluation of conformity carried out under a third party independent surveillance);

2. The maximum amount of GGBS to be used together with CEM I shall be slag/cement ≤ 1,0, by mass, i.e., the amount of slag shall not exceed 50% of the total binder content, by mass.

The maximum amount of GGBS used together with CEM I depends on the exposure classes, and is defined in Table 5.3.2a of SS 13 70 03 (2008). The requirements related with the exposure classes will be explained in this chapter.

2.3. Properties of concrete with additions of GGBS

Currently, the main reason behind the use of supplementary cementitious materials in general, and GGBS in particular, is not the environmental concern or economical reason, but the effect of this addition in improving some desirable properties of concrete. In the following sub-chapters, the influence of the replacement of Portland cement by GGBS in the properties of fresh and hardened concrete will be discussed.

2.3.1. Influence on fresh concrete

2.3.1.1. Workability and water demand

The addition of GGBS usually results on a slight increase in the workability of concrete, when compared with Portland cement concrete [Neville (2003)]. Bortz (2010) attributes this fact to the better dispersion of the cementitious particles and the limited amount of water that the slag absorbs during mixing. Fulton (1974) suggested that the improvement of workability of concrete with GGBS is due to the increased cohesiveness of the paste. Concrete produced with GGBS is more cohesive, but also more “mobile”. Therefore, the effect on the workability and placeability of concrete may not be noticeable in terms of slump; instead, for the same slump, slag concrete presents an increased workability, and is easier to compact [Neville (2003)].

The addition of GGBS may also result in a decrease in the water demand, for the same slump, depending on the dosage of addition [Neville (2003)]. Tests performed by Osborne (1989), cited in the ACI Committee report 233 (2000), showed that, as the percentage of GGBS increased, the ratio of water-cementitious materials had to be decreased, in order to maintain the same slump as the reference CEM I concrete. Wimpenny et al. (1989), also cited in the ACI Committee report 233 (2000) concluded that, for concretes with the same water/(cementitious material) ratio, the slump increased with the increasing addition of GGBS. Contrarily, Sivasundaram and Malhotra (1992) reported that, for replacement rates above 50%, the water demand may increase for the same workability.

2.3.1.2. Time of setting

The addition of GGBS usually prolongs the setting time of concrete, due to its slower pozzolanic reaction, since the hydration of the GGBS must await the hydration of Portland cement. When Portland cement hydrates, it releases hydroxyl ions that will break down the glass present in the slag, initiating its hydration. The degree of set retardation depends on factors such as the initial

temperature, the water/(cementitious material) ratio, the amount and type of Portland cement and the reactivity and dosage of the GGBS. Retardation of the setting time is in most cases an advantage in hot climates. However, the prolonged setting time in cold climates can significantly delay the finishing of the structure, increasing the risk of plastic shrinkage cracking, being therefore undesirable. However, in these situations, this effect may be offset by adding accelerating admixtures [ACI Committee 233 (2000)].

2.3.1.3. Bleeding and segregation

The bleeding of concrete (the emergence of mix water to the surface of concrete during and after placement) is mainly affected by the ratio of the surface area of solids to the unit of volume of water, i.e., it depends on the fineness of the cementitious material. Therefore, when GGBS ground to a coarser or similar fineness of the Portland cement is used to partially replace Portland cement, the rate and amount of bleeding may increase [ACI Committee 233 (2000)]. However, this fact appears not to affect segregation. Inversely, if the GGBS particles are ground to smaller sizes than the Portland cement, bleeding will usually be delayed and reduced [Neville (2003)].

2.3.1.4. Heat of hydration

The heat of hydration is the heat liberated in the exothermic reaction between a cementitious material and water. This reaction causes a temperature rise in concrete, which is usually dissipated to the surrounding environment, and the temperature changes within the structure are not significant. However, in structures that present large volumes of concrete (such as dams), the heat is not released as easily. These temperature rises will cause expansion when the concrete is hardening. If this rise in temperature is significantly high, and concrete suffers an uneven cooling, the stresses due to thermal contraction (and possibly structural constraints) may cause cracks in the concrete [Neville (2003)].

GGBS presents a lower heat of hydration than Portland cement. This property of GGBS makes the slag concrete suitable to be used as low heat cement in structures where a large volume of concrete needs to be placed, to control the temperature rise in the early ages [ACI Committee 233 (2000)].

2.3.1.5. Rate of strength development

The rate of strength gain is usually lower for concrete with GGBS than for Portland cement concrete. This fact is due to the slower pozzolanic reaction of the GGBS. When the water is added to mix, some hydration of the GGBS occurs immediately. This reaction creates a protective layer in the surface of the slag particles that inhibits the penetration of water, preventing further hydration of the slag. The GGBS must thus await the hydration of the Portland cement, which will release hydroxyl ions (NaOH, KOH, $Ca(OH)_2$) that work as activators which will break down the inhibitive coating and enable the hydration of the remaining slag particles [Ramachandran (1995)].

The slower hydration of GGBS concrete leads to a lower rate of strength development, taking about 3 days for the contribution of the cementitious properties of the GGBS to become noticeable. The lower rate of hydration of GGBS results, therefore, in a lower strength at early ages of slag concrete, when compared to Portland cement concrete [Ramachandran (1995)]. Given the slower hydration of GGBS, when compared to CEM I, it results that the rate of strength development of a concrete mix usually decreases as the amount of slag increases, and, consequently, the early-age strength will be lower for mixes with higher slag contents.

However, the effect of the addition of slag in the strength development of a concrete mix depends not only on the percentage of replacement, but also on the reactivity of the GGBS. The reactivity of the slag is typically lower than that of the CEM I, i.e., the activity index of the slag is usually lower than 1. However, concretes made with highly reactive GGBS (activity index equal or higher than 1.0) may present a similar or higher strength than Portland cement concrete even at early ages [ACI Committee 233 (2000)].

Since the hydration of GGBS concrete is usually slower than that of Portland cement concrete, the strength development of concrete with GGBS is more affected by the curing conditions than the Portland cement concrete. The lower rate of hydration leads to a loss of moisture that would otherwise be available for the hydration reactions. Therefore, concrete with GGBS requires prolonged (moisture) curing to avoid decrease in strength development [ACI Committee 233 (2000)].

2.3.2. Influence on hardened concrete

2.3.2.1. Compressive strength

The influence of the addition of GGBS in the compressive strength of concrete depends on various factors, which define the extent to which the amount of GGBS affects this property of the concrete.

As explained before, the lower rate of hydration of concrete with addition of GGBS and consequent reduced formation of hydrate at early ages leads to a lower compressive strength at early ages, when compared to Portland cement concrete. However, if proper curing is ensured, concrete with addition of GGBS continues to develop strength over longer periods of time than Portland cement concrete. This fact is due to the continuing release of alkalis by the GGBS, allied to the continuing formation of calcium hydroxide by the Portland cement, which results in a continuing slag reaction much further than the 28 days. This usually leads to a higher ultimate compressive strength of concrete with GGBS [Neville (2003)].

On the other hand, even though the chemical composition of CEM I and GGBS is similar, and, therefore, the products of hydration of the two cementitious materials are also quite similar, the fact that GGBS contains more silica and less lime results on a higher amount of C-S-H and lower amount of lime in the hydrated paste of concrete incorporating GGBS. This results in a smaller average pore size, since the pores are partially filled with C-S-H, which results in a more refined and dense

microstructure of the cement paste, contributing, therefore, for a higher compressive strength [Neville (2003)].

The ultimate compressive strength achieved by concrete with addition of GGBS depends on the amount of slag in the mix, and is usually higher for higher percentages of replacement [ACI Committee 233 (2000)]. However, for very high percentages of replacement, the strength development may be very slow, and may result in lower strength at all ages, compared to the reference concrete. An investigation carried out by Gruyaert (2011) showed that the hydration degree of slag in concrete with 50% of GGBS of the total cementitious material is about 70% at 2 years, whereas for higher percentages of replacement that value strongly decreases (to approximately 39% for 85% of GGBS replacement). The author found that, for concrete with very high GGBS content, only cement and part of the slag can hydrate, presenting a high amount of unhydrated slag particles in the paste even at later ages. This fact is understandable, since the hydration of the slag depends on the progressive formation of hydroxyl ions from the hydration of the cement. Therefore, when the hydration of cement is complete, the hydration of slag is interrupted, and, if the amount of GGBS is too high, some unhydrated particles will remain in the paste. Thus, several authors suggest a maximum amount of replacement of GGBS of 50% of the total of cementitious material to obtain the highest medium-term compressive strength (at 28 to 90 days) [ACI Committee 233 (2000)].

Tensile, flexural, torsional and bond strength are affected by the addition of GGBS in the same manner as compressive strength [Neville (2003), Hogan and Meusel (1981)].

2.3.2.2. Permeability of concrete

The permeability of the paste is probably the most relevant factor that determines the durability of concrete. In fact, the main deteriorating mechanisms acting on concrete (chemical attack, chloride and carbon initiated corrosion, expansion due to alkali-silica reaction, freeze/thaw attack) depend on the penetration and transport of liquids or gas into the concrete. Hence, producing concrete with lower permeability is of the utmost importance for its good performance during its service life, especially when exposed to aggressive environments.

The lower permeability of concrete incorporating GGBS, compared to mixes containing Portland cement only, is well documented. This is a result of the chemical nature of the hydrated paste and its microstructure. The permeability of concrete depends not only on its porosity, but also on the size, distribution and continuity of the pores. The flow of water (or gas) is easier through the large capillary pores than through the much smaller gel pores. When Portland cement and GGBS start to hydrate, and hydration products occupy less space than the original constituents of the paste, capillary pores are formed. The continuing hydration of the cementitious materials will produce C-S-H gel that will fill part of the capillary pores. Thus, the permeability of the paste changes continuously, and decreases with progressing hydration [Gruyaert (2011)].

As explained in the previous section, the hydration of GGBS concrete results in a higher amount of C-S-H gel being produced than the hydration of Portland cement concrete. Thus, in slag concrete, more of the pore space is filled with C-S-H than in Portland cement concrete, which results in a denser and more refined pore structure and, consequently, a lower permeability of concrete is obtained [Neville (2003)]. Besides, GGBS is usually ground to a higher fineness than Portland cement, which results in improving particle packing and, consequently, reduced permeability. Therefore, the decrease of the permeability of concrete is proportional to the increase of GGBS addition, provided that enough time has elapsed for sufficient slag hydration [ACI Committee 233 (2000)].

2.3.2.3. Sulphate Attack

The ingress of sulphates in concrete structures can cause damage, such as: cracking, spalling, increased permeability and loss of strength. Sulphates in the solid state do not attack concrete. However, when dissolved in water, they react with the compounds of the hydrated cement paste, causing severe deterioration of concrete. The most common sulphates that attack concrete are the ones present in soil or groundwater, such as sulphates of sodium, potassium, calcium or magnesium [Neville (2003)].

The deterioration of concrete due to sulphate attack is due to both chemical and physical processes. When the sulphate ions react with the compounds of the hydrated cement, different products are formed that cause damage of concrete. The most important is ettringite, which is, in presence of water, an expansive compound. The volume expansion due to the formation of ettringite causes internal tensions that may cause cracking of concrete. The cracking of concrete will, in turn, increase its permeability to other harmful agents, which will result in further damage [Gruyaert (2011)].

Concrete with addition of GGBS is reported to improve resistance against sulphate attack, when compared to Portland cement concrete, particularly when larger amounts of replacement are used. In fact, several authors report that concretes containing at least 50% of GGBS by mass of the total binder content exhibit the same sulphate resistance as concrete produced with sulphate-resistant (Type V) cement (Portland cement containing a low amount of calcium aluminate, C_3A) [ACI Committee 233 (2000), Neville (2003)].

The higher resistance of concrete with GGBS to sulphate attack is related with the lower permeability of the hydrated paste and the different chemical composition of the binder. Sulphate attack is greatly dependent on the permeability of concrete to the penetration of the damaging sulphates, and thus, the improved microstructure of the cement enhances the resistance of concrete to sulphate attack. On the other hand, the use of GGBS lowers the concentration of calcium hydroxide (CH) and calcium aluminate (C_3A) in the pore solution, which are the main compounds that react with the sulphates to produce ettringite [ACI Committee 233 (2000), Jain et al. (2007)]. However, a minimum amount of GGBS is required to provide high sulphate resistance of concrete. Neville (2003) recommends amounts higher that 50% by mass of the total binder (ideally, 60 to 70%).

2.3.2.4. Expansion due to Alkali-Silica Reaction (ASR)

Alkali-Silica reaction (ASR) is a chemical reaction between the active silica minerals of the aggregate and the alkali hydroxides in the cement paste. This reaction leads to the formation of a hygroscopic gel, which absorbs water and swells, increasing the volume of the paste. The volume expansion may cause tensile stresses in concrete and consequent formation of internal micro cracks and surface cracks. Even though the alkali-silica reaction affects mainly the serviceability conditions of a structure, rather than its mechanical properties, the cracking of concrete facilitates the ingress of deteriorating agents, which may contribute to further damage [Neville (2003)].

Concrete with GGBS is known to reduce the risk of expansion of concrete due to alkali-silica reaction. This positive effect is attributed to several factors. One of the most influencing factors is the reduced penetrability provided by the dense GGBS concrete, which offers higher resistance to the ingress and diffusion of alkali-ions. Furthermore, the presence of slag contributes to a decrease in the concentration of calcium hydroxide in the paste, which is necessary to support the alkali-silica reaction, since the $Ca(OH)_2$ released during the hydration of Portland cement is used to activate the slag. Moreover, the addition of GGBS reduces the amount of alkali available for the reactions with the aggregate. GGBS contains only a small amount of water soluble alkalis, so the replacement of Portland cement by GGBS will result in a lower concentration of alkalis in the cement paste. On the other hand, the low Calcium/Silica ratio in the hydration products of concrete with additions of GGBS increases the alkali binding capacity. This means that a great proportion of the available alkalis (present both in the pore solution and provided by the hydration of Portland cement) will bound by the hydration products of slag cement, reducing its availability to participate in ASR [Gruyaert (2011), ACI Committee 233 (2000)].

The positive effect of GGBS in reducing or preventing the alkali-silica reaction in concrete is verified both for low and high percentages of cement replacement of GGBS, even though it is more effective for higher amounts of GGBS [Gruyaert (2001)]. In fact, it is usually assumed that there is a minimum amount of GGBS replacement above which the alkali-silica reactions are supressed. Hogan and Meusel (1981) report that replacing 40% to 65% of cement by GGBS is effective in mitigating the expansion due to alkali-silica reactions. The North-American Standard ASTM C989 considers that concrete with replacement of at least 40% of GGBS is resistant to alkali-silica reaction, with no further tests required, unless GGBS is combined with high-alkali Portland cement. However, even when used with high-alkali cement, replacements of a minimum of 40% seem to be effective in reducing the potential of ASR [ACI Committee 233 (2000)].

Although, research carried out by Gruyaert (2001) found that replacement of cement by 50% to 70% was effective in mitigating ASR, whereas the performance of concrete with 85% replacement by GGBS was poorer than that of the previous mixes (even though it showed better results than the reference Portland cement concrete). In fact, it is widely accepted that the increase of cement replacement by GGBS improves the resistance of concrete to alkali-silica reaction, but the amount of replacement in the literature rarely exceeds 70%. The author thus suggests that not only a minimum,

but also a maximum allowable amount of GGBS replacement shall be prescribed to consider the concrete ASR resistant. Neville (2003) recommends 50 to 65% of GGBS replacement for effective ASR resistance.

2.3.2.5. Carbonaton

Carbonation of concrete is a process by which the carbon dioxide (CO_2) present in the surrounding environment penetrates the concrete and reacts with the hydrated compounds of the cement paste (such as calcium hydroxide) to form calcium carbonate (CaCO). Carbonation does not cause damage in concrete *per se*, but the ingress of CO_2 can induce corrosion of the reinforcement, by lowering the alkalinity of the pore solution (the so-called carbon-initiated corrosion) [Gruyaert (2011)].

Steel imbedded in the hydrated products of cement forms a passivity layer of oxide which adheres to the steel, protecting it from the reactions with water and oxygen. This passivation of the reinforcement is maintained when the water in contact with the passivation layer presents a pH between 12.6 and 13.5. When the pH drops below 9, the passivity layer that protects the steel reinforcement is destructed, opening a path for aggressive agents to reach the reinforcement and, in the presence of oxygen and water, the corrosion process is initiated. Corrosion of the reinforcement results in the reduction of the cross-sectional area of the steel bars, and consequent loss of structural capacity [Neville (2003)].

The effect of cement replacement by GGBS in the carbonation of concrete is two-fold. On the one hand, the silica in the GGBS reacts with the calcium hydroxide that results from the hydration of Portland cement. This means that the hydrated paste of concrete with GGBS presents a lower content of calcium hydroxide, thus a smaller amount of CO_2 is required to bind all the $Ca(OH)_2$ to form calcium carbonate, which results in a faster rate of carbonation (and increased depth of carbonation at early ages). However, the low permeability of GGBS concrete prevents the continuing diffusion of carbon dioxide, preventing the continuing increase in the depth of carbonation [Neville (2003)]. This theory is supported by an investigation carried out by Bouikni, et al (2009), which found that the reduced permeability of GGBS concrete confines the high rate of carbonation to the initial 10 mm, further penetration being slowed down, which led the authors to conclude that GGBS concrete provides proper protection against carbonation, and consequent corrosion of steel.

On the other hand, carbonation of Portland cement concrete results in a more refined pore structure with part of the products from the carbonation reaction filling part of the pores, which results on a denser paste and reduced permeability of the carbonated Portland cement paste. However, this is not the case for GGBS concrete. The carbonation of GGBS concrete results in the coarsening of the pore structure, i.e, reduction of the number of air pores, but increase in their average size. An increase in the amount of large capillary pores will in turn facilitate the further penetration of CO_2. For this reason, GGBS usually presents a lower resistance to carbonation, when compared to Portland cement concrete, especially for higher percentages of replacement [Gruyaert (2011)].

Research carried out by Gruyaert (2011) in concrete containing different amounts of GGBS replacement (50%, 70% and 85% of the cement content) clearly showed a decrease in the carbonation resistance of concrete with the increase of slag content. The author also developed a method to estimate the carbonation depth of concrete after a service life of 50 years from the results of accelerated carbonation tests. The results revealed that, even though concrete with 50% of GGBS replacement presents a high carbonation coefficient, steel corrosion can be prevented for normal environments (containing up to 0.3% CO_2). However, for higher percentages of replacement, the risk of steel corrosion is not excluded, even though, according to the author, it may be largely reduced if proper prolonged moisture curing is provided.

Therefore, an adequate mix proportioning, with a low w/c ratio and low percentage of GGBS, and an adequate (preferably prolonged) wet-curing are of the utmost importance to reduce the carbonation attack of slag concrete [Neville (2003)].

2.3.2.6. Chloride penetration

As for carbonation, the main adverse consequence of the ingress of chlorides in concrete is the corrosion of the steel reinforcement: the so-called chloride-initiated corrosion. The ingress of chloride ions in concrete destroys the passivity layer that protects the steel reinforcement from corrosion and, once the chloride ions reach the surface of steel, they act as an anode, being the passivation surface the cathode. As a result, in the presence of water and oxygen, corrosion occurs [Neville (2003)].

The corrosion of the steel is, primarily, an expansive reaction, with the products of the corrosion reactions occupying a larger volume than the original steel. This volume expansion leads to the development of stresses in the concrete paste, which may lead to cracks, spalling or delamination of concrete. The damage caused by the volume expansion in the concrete paste will, in turn, enable the ingress of additional chlorides in the concrete, accelerating the corrosion rate. The continuation of the corrosion will then damage the steel, leading to a reduction of the cross-section area of reinforcement bars, which results in loss of load-bearing capacity of the structure [Neville (2003)].

The improved resistance of GGBS concrete against chloride ingress has been widely reported [Ellis et al. (1991)]. In fact, the use of additions of GGBS in concrete has gained momentum due to its improved durability in structures placed in marine environment [Ramachandran (1995)].

The positive effect of the addition of GGBS is mainly due to its lower penetrability. The chloride ions that attack concrete are usually found dissolved in water. When the water is in contact with concrete, it may penetrate the concrete by capillary suction, and the chloride ions are transported in the interior of concrete by diffusion and/or sorption. The denser and more refined microstructure of the GGBS concrete reduces the capillary suction and slows the diffusion rate down, therefore reducing the transport of the chloride ions inside the concrete, and lowering the concentration of available chloride ions in the paste. On the other hand, the lower concentration of hydroxyl ions in the pore solution of the GGBS concrete reduces its capacity to exchange anions, which also contributes for the reduction

of the diffusion rate of the Cl^- ions. The transport of oxygen and the availability of moisture necessary for the corrosion reaction to occur is also influenced in the same manner by finer pore structure, which further contributes for the higher resistance to concrete damage due to steel corrosion [Gruyaert (2011)]

Chlorides are present in concrete in different forms: they can be chemically bound, being incorporated in the hydration products of the cement; they can be physically bound, being absorbed on the surface of the gel pore. Only the chlorides that are not bound during the hydration reactions, the so-called free chlorides intervene in the chloride induced corrosion of concrete [Neville (2003)]. GGBS has been shown to improve the chemical and physical binding of chloride ions, with further contributes for the reduction of the available free chlorides in the paste. The chemical binding is enhanced by the reaction of the C_3A formed in the hydration of slag with the chloride ions, which forms Friedel's salt. This compound is, in turn, able to physically bind chlorides. The physical binding of the Cl^- ions is improved by the larger amount of C-S-H gel present in the hydrated paste of the slag concrete, which provides a higher surface area for the absorption of chlorides, thus blocking the diffusion path [Gruyaert (2011)].

The resistance of GGBS concrete against chloride ingress has been investigated and reported by several authors. Ellis et al. (1991) studied the permeability of concrete with 50% of GGBS of the total binder content, by testing the specimens according to the Rapid Determination of the Chloride Permeability of Concrete test (AASTHO T-277) at the age of 56 days. The results for 50% GGBS concrete rated between "Negligible" and "Very Low" in the Chloride Ion Penetrability Rating established in the standard, for relatively high-quality, low water/(cementitious material) ratio. The tests also revealed that concrete with GGBS shows low permeability even for relatively high water/(cementitious material) ratios. These results coincide with the results achieved by Ozyildirim (1994), who found that additions of slag are more effective in reducing the permeability of concrete than lowering the water/cement ratio of Portland cement concrete. The author concluded that the permeability and chloride penetration for GGBS concrete are lower than for Portland cement concrete at all ages, even though an improvement of the chloride resistance at later ages was registered for both concrete qualities. The performance of GGBS concrete against chloride ingress improves with an increase of GGBS content. Gruyaert (2011) found that the mean chloride migration and diffusion coefficients generally decreased with an increase in the replacement levels of GGBS. The author also found that the continuing hydration of GGBS concrete results on a significant decrease in the migration coefficient at later ages, which does not occur in Portland cement concrete. Daube and Bakker, cited by Neville (2003), reported that concrete with at least 60% by mass of cementitious material and water/cement ratio of 0.5 shows a chloride diffusion coefficient ten times smaller than Portland cement concrete.

2.3.2.7. Frost resistance

The performance of concrete with addition of GGBS in freezing environments has been object of extensive debate. In literature, it is generally assumed that concrete with GGBS addition has inferior

resistance to frost attack than Portland cement concrete, especially when de-icing agents are used. However, even though laboratory tests usually result in a poorer performance, many researchers have found that, in field exposure, the resistance of concrete with additions of slag is comparable to that of Portland cement concrete [ACI Committee 233 (2000)].

The lower frost resistance of concrete with GGBS is usually assumed to be related with the coarsening of the pore structure of the carbonated GGBS concrete. An increase in the amount of large capillary pores results on an increase of the freezable water in the concrete paste, and, consequently, increased frost damage. Nevertheless, several authors report that, with proper mix proportioning and curing, it is possible to produce slag concrete with acceptable salt-frost resistance. ACI Committee 233 (2000) states that concrete mixes with a maximum of 50% by mass of cementitious materials, low water/(cementitious material) ratio, and proper air entrainment usually show acceptable salt-frost resistance. Neville (2003), however, refers that for GGBS concrete to achieve the same deicer scaling resistance as Portland cement concrete, prolonged wet curing before exposure is crucial.

The mechanisms of frost attack and the factors that influence the performance of GGBS concrete under freezing conditions will be discussed later with detail.

2.3.2.8. Appearance

The addition of GGBS in concrete will result in a near-white colour of the concrete, much lighter than the grey Portland cement concrete. However, in the second to forth days after casting, a greenish colouration appears, due to a reaction of the sulphide sulphur in the GGBS with some compounds of the cement. This colouration disappears after some time, as oxidation takes place [ACI Committee 233 (2000)].

2.3.3. Requirements of concrete with GGBS

The production of concrete in Europe must comply with the requirements in the European Standard EN 206-1: *Concrete: Specification performance, production and conformity*. EN 206-1 establishes the basic requirements for all the constituents of concrete, as well as requirements regarding the composition of concrete, its mechanical properties and durability (depending on the exposure classes). The Swedish Standard SS 13 70 03 (2008) is the application of EN 206-1 in Sweden, i.e., it deals with the materials and test methods that are not included in EN 206-1, but which are used in Sweden. Concrete produced with Ground Granulated Blast Furnace Slag complying with SS-EN 15167-1 (2006) must always comply with the requirements of SS 13 70 03 (2008).

The requirements regarding durability of concrete depend on the environment in which the concrete will be placed, being stricter the harsher the environment. The Swedish Standard SS 13 70 03 (2008) defines several exposure classes, as follows:

1. No risk of corrosion or attack

   X0: For concrete without reinforcement or embedded metal: all exposures except where there is freeze/thaw, abrasion or chemical attack;
   For concrete with reinforcement or embedded metal: Very dry.

2. Corrosion induced by carbonation: where concrete containing reinforcement or other embedded metal is exposed to air and moisture, the exposure shall be classified as follows:

   XC1: Dry or permanently wet
   XC2: Wet, rarely dry
   XC3: Moderate humidity
   XC4: Cyclic wet and dry

3. Corrosion induced by chlorides other than from sea water: Where concrete containing reinforcement or other embedded metal is subject to contact with water containing chlorides, including de-icing salts, from sources other than from sea water, the exposure shall be classified as follows:

   XD1: Moderate humidity
   XD2: Wet, rarely dry
   XD3: Cyclic wet and dry

4. Corrosion induced by chlorides from sea water: Where concrete containing reinforcement or other embedded metal is subject to contact with chlorides from sea water or air carrying salt originating from sea water, the exposure shall be classified as follows:

   XS1: Exposed to air borne salt but not in direct contact with sea water
   XS2: Permanently submerged
   XS3: Tidal, splash and spray zones

5. Freeze/thaw attack with or without de-icing agents: Where concrete is exposed to significant attack by freeze/thaw cycles whilst wet, the exposure shall be classified as follows:

   XF1: Moderate water saturation, without de-icing agent
   XF2: Moderate water saturation, with de-icing agent
   XF3: High water saturation, without de-icing agent
   XF4: High water saturation, with de-icing agent or sea water

6. Chemical attack: Where concrete is exposed to chemical attack from natural soils and ground water as given in table 2 of EN 206-1 (2000), the exposure shall be classified as given below:

   XA1: Slightly aggressive chemical environment
   XA2: Moderately aggressive chemical environment
   XA3: Highly aggressive chemical environment

For each exposure class, the durability requirements are expressed in terms of maximum water/cement ratio, minimum cement content, and minimum cement strength class. In the Swedish standard SS 13 70 03 (2008), the limiting values and requirements of concrete with regard to durability in different exposure classes based on a service life of 50 years are displayed in Table 2.3.

Table 2.3 – Limiting values and requirements on the composition of concrete with regard to durability in different exposure classes [SS 13 70 03 (2008)].

Requirements		Exposure classes																
		No risk of corrosion	Carbonation-induced corrosion				Chloride-induced corrosion					Freeze/thaw attack				Aggressive chemical environments		
							Sea water			Chloride other than from sea water								
		X0	XC 1 [5]	XC 2	XC 3	XC 4	XS 1	XS 2	XS 3	XD 1	XD 2	XD 3	XF 1	XF 2	XF 3	XF 4	XA 1	XA 2	XA 3
Maximum vct_{ekv}		–	0,90	0,60	0,55	0,55	0,45	0,45	0,40	0,45	0,45	0,40	0,60	0,45	0,55	0,45	0,50	0,45	0,40
Minimum binder content [7] C_{ekv} kg/m^3		–	–	200	200	200	200	200	200	200	200	200	200	200	200	200	200	200	200
Cement conforming to EN 197-1 with established suitability in the respective exposure class		I II/A-S II/B-S II/A-D II/A-V II/B-V II/A-LL II/A-M II/B-M[8] III/A III/B	I II/A-S II/B-S II/A-D II/A-V II/B-V II/A-LL II/A-M II/B-M[8] III/A	I II/A-S II/B-S II/A-D II/A-V II/B-V II/A-LL II/A-M II/B-M[8] III/A	I II/A-S II/B-S II/A-D II/A-V II/B-V II/A-LL II/A-M II/B-M[8]	I II/A-S II/B-S II/A-D II/A-V II/B-V II/A-LL II/A-M II/B-M[8]	I II/A-S II/B-S II/A-D II/A-V II/B-V II/A-LL II/A-M II/B-M[8]	I II/A-S II/B-S II/A-D II/A-V II/B-V II/A-LL II/A-M II/B-M[8]	I II/A-S II/A-D II/A-V II/A-LL II/A-M	I II/A-S II/B-S II/A-D II/A-V II/B-V II/A-LL II/A-M II/B-M[8]	I II/A-S II/B-S II/A-D II/A-V II/B-V II/A-LL II/A-M II/B-M[8]	I II/A-S II/A-D II/A-V II/A-LL II/A-M	I II/A-S II/B-S II/A-D II/A-V II/B-V II/A-LL II/A-M II/B-M[8]	I II/A-S II/B-S[9] II/A-V II/B-V[9] II/A-LL II/A-M[10] II/B-M[8,9,10]	I II/A-S II/A-V II/A-LL II/A-M[10] II/B-M[8,10]	[3]	I II/A-S II/B-S II/A-D II/A-V II/B-V II/A-LL II/A-M II/B-M[8] III/A III/B	[2]
Strength class		≥ 32,5	≥ 32,5	≥ 32,5	≥ 42,5	≥ 42,5	≥ 42,5	≥ 42,5	≥ 42,5	≥ 42,5	≥ 42,5	≥ 42,5	≥ 42,5	≥ 42,5	≥ 42,5	≥ 42,5	≥ 42,5	≥ 42,5	≥ 42,5
Maximum amount of addition per amount CEM I [4), 6)]	Silica fume	0,11	0,11	0,11	0,11	0,11	0,11	0,11	0,11	0,11	0,11	0,11	0,11	0,11	0,06	0,06	0,11	0,11	[2]
	Fly ash	0,50	0,50	0,50	0,50	0,50	0,50	0,50	0,25	0,50	0,50	0,25	0,50	0,50	0,50[9]	0,25	0,50	0,50[1]	
	Slag	2,30	1,50	1,50	0,50	0,50	0,50	0,50	0,25	0,50	0,50	0,25	0,50	0,50	0,50[9]	0,25	2,30	0,50[1]	
	Total	2,30	1,50	1,50	0,50	0,50	0,50	0,50	0,25	0,50	0,50	0,25	0,50	0,50	0,50[9]	0,25	2,30	0,50	
Freeze/thaw resistant aggregate		–	–	–	–	–	–	–	–	–	–	–	yes	yes	yes	yes	–	–	–
Testing of the freeze/thaw resistance of the concrete		–	–	–	–	–	–	–	–	–	–	–	–	–	–	yes	–	–	–
Minimum air content or testing of the freeze/thaw resistance of the concrete		–	–	–	–	–	–	–	–	–	–	–	–	yes	yes	–	–	–	–

As it can be observed in the Table 2.3, additions up 2.3 times the amount per weight of Portland cement are allowed for mild exposure classes. However, for XD3 and XF4 exposure classes, the use of GGBS combined with CEM I is limited to 25% of the amount of CEM I by weight. Besides the maximum amount of addition, the rules of the *k*-value concept must also be taken into account when using slag together with Portland cement, as well as any other type II addition. Moreover, when additions are used together with CEM II and CEM III, the total amount of the respective type II addition per amount of Portland cement clinker, including the amount incorporated as a main constituent of the cement, shall not exceed 1.05 the value given in Table 2.3 for the addition in question, and for the respective exposure class [SS 13 70 03 (2008)].

For all environments susceptible to freeze/thaw attack, frost resistant aggregate is required by the standard. For exposure class XF1, concrete with an equivalent water/cement ratio equal or lower than 0.6 is considered frost resistance, even without air entrainment. For XF2 and XF3 exposure classes, a minimum air content in the fresh concrete is required, for concrete to be considered frost resistance without further testing. The minimum air content required depends on the maximum dimension of the aggregate, and ranges between 4% for D_{max} of 32mm to and 5% for D_{max} of 8mm. However, for these exposure classes, a lower air content may be used in concrete, by demonstrating that the concrete mix presents adequate frost resistant through testing according to the Swedish Standard SS 13 72 44, using method A for concrete in exposure class XF2, and method B for concrete in exposure class XF3. Contrarily, for exposure class XF4, minimum air content is not required. Instead, the freeze/thaw resistance of concrete to be placed in XF4 conditions must be verified through testing according by to the method A described in the SS 13 72 44, and the results shall be at least acceptable [SS 13 70 03 (2008)].

3. Frost resistance of concrete

Frost attack is, together with corrosion of the reinforcement, the most severe damaging mechanism acting on concrete. There are two types of frost damage that can occur in concrete: internal cracking and surface scaling.

Internal cracking of concrete in cold climates results from a combination of a high degree of saturation and freezing temperatures. The freezing of the water inside concrete will exert pressure in the cement paste, leading to the development of micro and macro-cracks throughout the entire volume of concrete. Contrarily to surface scaling, the cracking may start in the interior and not be perceptive on the outside. The internal cracking of concrete results in volume expansion and loss of mechanical properties of concrete (such as elasticity modulus or compressive strength). It also results in higher permeability, which enables the penetration of other damaging agents, thus accelerating the deterioration of the material [Utgennant (2004), Rønning (2001)].

Surface scaling, or salt-frost scaling, is characterized by a loss of material on the concrete surface. Surface scaling of concrete occurs when saturated concrete is exposed to a freezing environment in the presence of salts. The process starts at the surface, with small chips of mortar flaking off, and gradually advances to the interior, leaving the coarse aggregate exposed. Surface scaling is, initially, an aesthetically problem, with the removal of material leaving an unappealing rough concrete surface. However, even though surface scaling does not affect the mechanical properties of concrete, the reduction of cement paste at the concrete surface leads to a reduction of the concrete cover that protects the reinforcement, which may accelerate the corrosion of the reinforcing steel [Bortz (2010), Utgennant (2004)].

The salt-frost scaling of concrete is dominant in environments with saline sea water or where de-icing salts are used, and is mainly observed on road structures, bridge decks and paving blocks. Internal cracking is less common, though it may be observed on parts of structures in direct contact with water and subjected to capillary suction, such as the lower parts of supporting walls and dam structures above the water surface [Rønning (2001)].

The production of concrete with good frost resistance is of the utmost importance in cold climates. Therefore, the mechanisms causing deterioration and the parameters that influence the performance of concrete in freezing environments must be well studied and understood.

3.1. Frost Mechanisms

Knowledge of the mechanisms influencing the frost resistance of concrete is crucial in order to know how to produce frost resistant concrete, and how to develop reliable test methods that enable an adequate prediction of the service life of a structure in freezing environments.

3.1.1. Mechanisms of plain frost damage

3.1.1.1. Freezing without moisture transport

The basic mechanism of frost damage is referred to as “closed container mechanism” or “freezing without moisture transport”. It is based on the fact that the volume of ice is 9% higher than that of liquid water. Thus, given a material whose permeability is zero (closed container), the 9% increase of volume when water freezes will exert pressure. If the material is more than 91,7% filled with water, the built-up stresses caused by the volumetric expansion may cause damage to the material [Çopuroğlu (2006)].

However, concrete is a porous material, i.e., its permeability is not zero. This means that the water flow is possible. Therefore, when ice starts to form in the large capillary pores, the increase in volume of the ice already formed will force the unfrozen water out of the pore. If there is enough space in the cement paste to accommodate the water expelled, damage will not occur. Thus, for a given concrete quality, there is a maximum amount of moisture content which, if exceeded, causes damage, i.e., a critical degree of saturation [Lindmark (1998)].

3.1.1.2. Critical degree of saturation

The degree of saturation, S, is defined as the ratio between the total evaporable water content, w_e (m^3/m^3), and the total pore volume, p (m^3/m^3), as shown in equation (2) [Fagerlund (1982)]:

$$S = \frac{w_e}{p} \tag{2}$$

The critical degree of saturation is, therefore, the maximum amount of freezable water that can be present in concrete which, when subjected to freezing and thawing cycles, does not cause damage. The critical degree of saturation can be estimated using a method developed by Fagerlund (1977).

Fagerlund (1977) conducted a series of experiments in concrete specimens with w/c ratios ranging from 0.4 to 0.5 without entrained air. The specimens were pre-conditioned to different levels of saturation and the modulus of elasticity (E-modulus) was measured. The specimens were then subjected to freeze/thaw cycles in moisture sealed conditions, and the E-modulus was measured after the freezing cycles. Figure 3.1 shows no decrease in E-modulus as long as the saturation of the specimen stood lower than 0.845, which means that damage did not occur. However, when the saturation exceeded 0.845, the E-modulus of the specimens decreased significantly, which indicates

extensive damage. Therefore, the critical degree of saturation, S_{cr}, is around 84,5% [Schulson (1998)]. This means that if concrete is not more than 84% saturated with water, damage will not occur, as there is enough space to accommodate the volume increase.

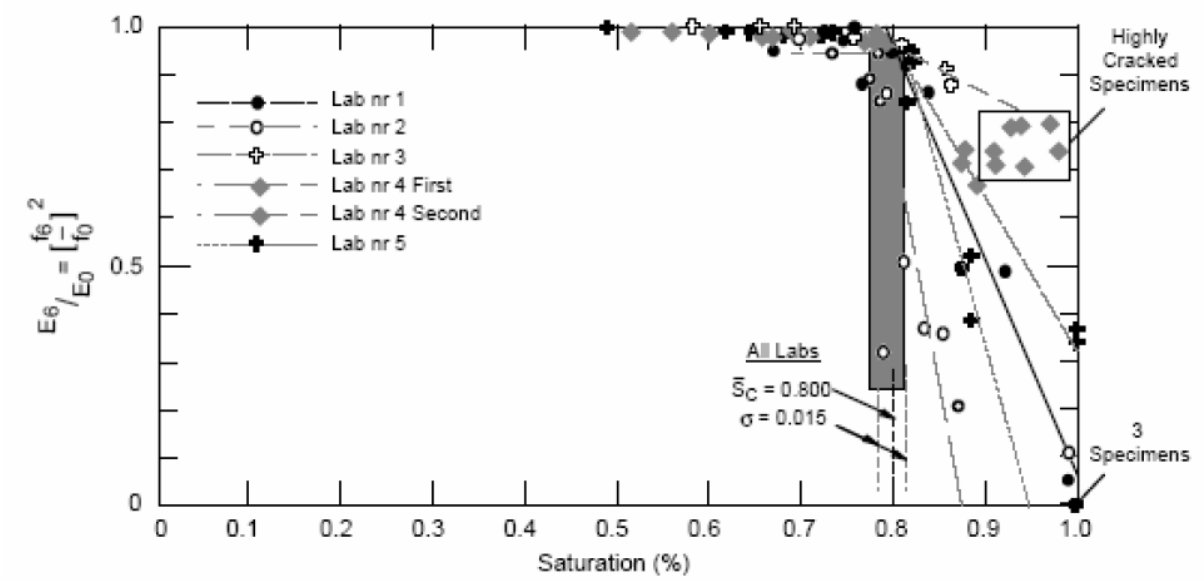

Figure 3.1 - Relation between the Dynamic Elasticity Modulus (normalized) and the degree of saturation of concrete under freezing and thawing, measured in five different laboratories [Schulson (1998)]

When the critical degree of saturation of the material is determined, the main question to be answered is how long it takes for concrete to reach such degree of saturation, i.e., how long may the concrete be in continuous contact with water until freezing causes damage. This time frame is a determining factor for the service life of the concrete, and depends, mainly, on the permeability of concrete and the pore size distribution. The lower the permeability of concrete and the better the distribution of the air pores in the paste, the longer it takes for the critical degree of saturation to be reached. It also depends on the climate conditions to which the concrete is exposed. Concretes placed in dry environments may never reach they critical saturation, whereas concrete on moist environments will rapidly reach it [Utgennant (2004)].

3.1.1.3. Hydraulic pressure

In 1949, Powers presented a new theory for the frost damage of concrete. Powers had found that, even though concrete often presents enough volume of air pores to accommodate the water forced out of the capillary pores where freezing takes place, i.e., the degree of saturation is not reached, deterioration due to freezing would still occur. Therefore, Powers proposed that the main cause for frost damage was not the pressure due to volumetric expansion when water turns to ice, but instead the hydraulic pressure that develops as the water is squeezed out of the pore where ice started to form [Powers (1949), Lindmark (1998)].

The temperature at which freezing starts depends on the size of the pore, and the concentration and type of dissolved chemicals. Freezing usually starts in the large capillary pores. When the temperature is sufficiently low, the first ice crystals start to form. The increase of volume when water freezes in a critically saturated pore forces the liquid water to be spelled out of the water-filled pore into the unfrozen pore system of the paste. The transport of water from the capillary pore to the air pore through a thin tube-shaped pore causes pressure in the cement paste (Figure 3.2). If the pressure is higher than the tensile strength of the cement paste, damage will occur [Çopuroğlu (2006), Utgennant (2004)].

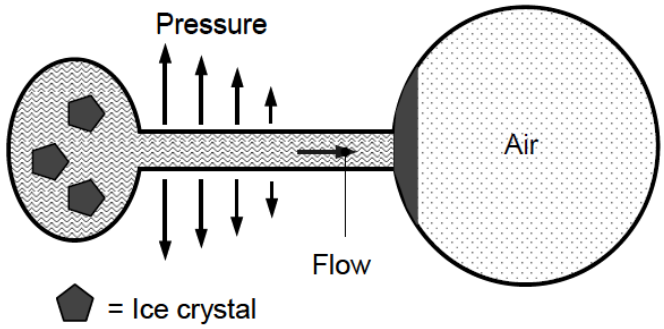

Figure 3.2 – Illustration of the hydraulic pressure mechanism [Utgennant (2004)].

The hydraulic pressure is lower in a paste with high permeability, and increases with an increase in the water flow rate, with an increase of the cooling rate and with an increase in the distance between the water filled pores and the air pores. The shorter the path that the water has to travel between the pores, the lower the stresses that are imposed in the paste, and the higher the frost resistance of concrete. Hence, the hydraulic pressure mechanism introduces a new parameter that influences the frost resistance of concrete: the spacing factor.

3.1.1.4. Spacing factor

The spacing factor can be defined as the mean distance between the water filled pores where ice crystals form and the air pores in concrete. When the spacing factor is large, the water expelled from the capillary pores will have a longer distance to travel to reach the air pores, and the pressure built up in the tube-shaped pore that connects them may be high enough to cause disruption. Inversely, if the capillary pore and air pore are close enough, the water expelled can reach the air pore without increased stresses, therefore preventing damage. This means that for each pore system, temperature (below 0ºC) and time at this temperature, there is a critical spacing factor, i.e., a maximum distance between the pores that, if exceeded, will lead to stresses that may cause damage in concrete [Utgennant (2004)].

The critical spacing factor depends on the temperature, the rate of cooling and the flow rate of water. Several authors have attempted to calculate the critical spacing factor. However, the values reached do not always match. Powers, cited by Neville (2003), calculated that an average spacing factor of

0.25mm is required for concrete to be frost resistant. Ivey and Thomas (1970) studied the relationship between the “durability factor” determined by the test method described in ASTM 666 and the Powers spacing factor in concrete mixes freezing in pure water. They noticed a change from good to bad frost resistance when the spacing factor was between 0.22mm and 0.25mm. Fagerlund (1988) tested specimens on a salt sealed environment with 3% NaCl (sodium chloride) solution, and concluded that when a spacing factor of 0.16mm is exceeded, the specimens start to show poor salt-scaling resistance.

It seems that the critical spacing factor is lower for freezing environments in the presence of salts than for freezing in pure water. Nevertheless, no exact values for the critical spacing factor for each of the cases have been reached. This means that the Power’s spacing factor cannot be used as a general criterion to ensure frost resistant concrete. There is, however, a critical spacing factor for each quality concrete that, when exceeded, causes damage [Fagerlund (1985)]. Nowadays the critical spacing factor usually recommended to ensure frost resistant concrete is to be about 0.20mm [Fagerlund (1985), Neville (2003)].

The concept of spacing factor also helps to explain the positive influence of air entrainment in the durability of concrete in cold climates, as will be explain in the next section.

3.1.1.5. Microscopic ice lenses growth

According to Power’s hydraulic pressure theory, the internal pressures that cause disruption increase with an increase in the rate of ice formation, which in turn increases with an increase in the cooling rate. Therefore, when the cooling rate is zero, i.e., when the temperature is held constant, the internal pressure is zero and the expansion stops. When cooling is resumed, dilation starts again, i.e., frost attack caused by hydraulic pressure depends on the cooling rate [Utgennant (2004)].

However, Powers and Helmuth (1953) observed that non air-entrained pastes of concrete specimens expanded during cooling, and kept expanded even during periods where the temperature was held constant (below 0ºC), whereas air-entrained specimens would contract. The expansion of the paste at steady temperature contradicted the hydraulic pressure theory, and a new mechanism was proposed by the authors. The Microscopic Ice Lenses Growth theory was the proposed by Powers and Helmuth in 1953, and was later developed by Setzer in 2002. According to this theory, the cement paste is in a thermodynamic equilibrium until ice starts to form. When the temperature drops and the first ice crystals form in the large pores (and the entrained air voids, if they contain water), the equilibrium is broken, since, at a given temperature and pressure, the chemical potential of the ice is lower than that of the liquid water. In order to re-establish equilibrium, the water will move from the saturated small capillaries and gel pores towards the ice bodies where ice started to form (Figure 3.3). This movement of water will continue until equilibrium is reached again [Lindmark (1998), Setzer (2002)].

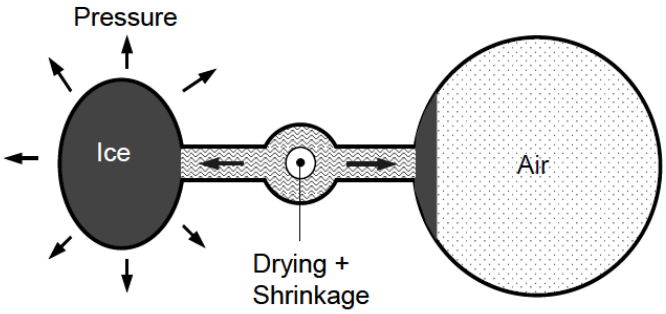

Figure 3.3– Illustration of the microscopic ice lenses growth [Utgennant (2004)].

In a moisture-isolated specimen, the water drawn from the small pores will cause shrinkage of the paste. However, if there is available water from outside sources, it will be sucked into the pores, and water uptake will continue until the air void system is saturated and/or equilibrium is reached. In that case, if the temperature continues to decrease, the volumetric expansion of the freezing of water will exert pressure in the pore walls. If these stresses are stronger than the tensile strength of the concrete paste, damage will occur [Lindmark (1999), Setzer (2002)].

For concrete with low w/c ratio, this mechanism may lead to shrinkage of the paste, at least in the first freeze-thaw cycles, while water uptake is not sufficient to saturate the paste. However, for concrete qualities with high water/cement ratio and high permeability, volume expansion is to be expected, even in the first freeze/thaw cycles [Bager (2010)].

3.1.1.6. Osmotic pressure

The micro ice lenses growth theory assumes that the water in the gel pores is pure water, without any dissolved chemicals. In 1975, Powers introduced the osmotic pressure concept, which took into consideration the effect of the dissolved chemicals in the energy state of the water [Utgennant (2004)].

Before freezing starts, the concentration of dissolved substances in the pore water is the same in the whole structure of the material. When the water starts to freeze in the first capillary pore, the concentration of the remaining unfrozen solution becomes higher. This will create an osmotic effect, causing unfrozen water in solutions with lower concentrations to move towards solutions with higher concentration (Figure 3.4). When the concentration of the dissolved substances is lowered by the water transported, the freezing temperature of the solution will increase, and ice starts to form again. The redistribution of water, the growth of the ice lenses and increase of the pressure in the pore walls will continue until equilibrium is re-established [Utgennant (2004), Çopuroğlu (2006)].

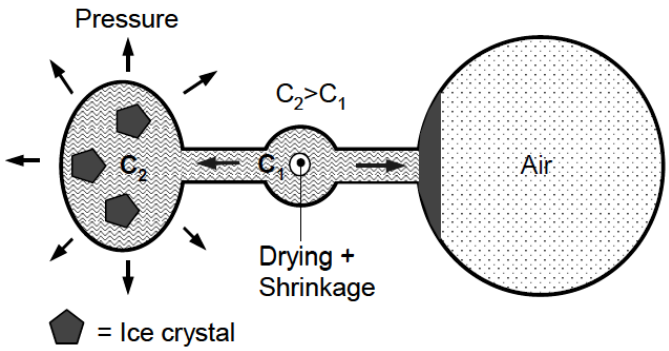

Figure 3.4 – Illustration of the osmotic pressure [Utgennant (2004)].

The redistribution of water due to osmotic phenomena is often regarded as the main cause for salt-frost scaling. The salt increases the solute concentration in the surface pores. Thus, the concrete will absorb more water in order to re-establish chemical equilibrium. This leads to a higher degree of saturation, which in turn leads to increased pressure in the pore walls and, therefore, higher risk of frost damage [Neville (2003)].

This theory must be regarded not as a separate theory, but as a complement of the micro ice lenses growth mechanism. In reality, it is believed that the frost deterioration of concrete is a combined effect of the two mechanisms. Theoretically, the hydraulic pressure should be dominant for concrete with high amounts of freezable water (high w/c ratios), whereas the micro ice bodies growth should be the prevailing mechanism for concrete with low w/c ratio (large portion of unfreezable water) [Utgennant (2004), Fagerlund (1995)].

3.1.1.7. Conclusion

Even though different theories have been developed trying to explain the frost damage in concrete, there is not a single one that explains all the phenomena of frost attack. Instead, it is believed that all mechanisms act in most of the concrete qualities at a given point, and damage occurs in consequence of the combined effect of the various degradation mechanisms described.

However, for each situation, there may be a mechanism that is more relevant, depending on the w/c ratio, the pore size distribution in the concrete paste, the freezing temperature to which the material is subjected, and the time at that temperature.

3.1.2. Mechanisms of salt frost scaling

Even though the effects of internal cracking and surface scaling are different, and internal cracking occurs even in environments with no presence of salt, whereas the surface scaling occurs mainly in structures in contact with salt, the mechanisms behind both types of frost damage are usually assumed to be the same. Both surface scaling and internal cracking damage occurs at freezing temperatures when the degree of saturation exceeds a critical value. However, the strong damaging influence of the presence of de-icing salts is not yet completely understood.

Several researchers have proposed different mechanisms to explain the negative effect of the presence of salts in the frost resistance of concrete. Some examples of proposed theories are presented.

3.1.2.1. Powers, 1965

One of the first hypotheses to explain the salt-frost scaling of concrete was proposed by Powers (1965). The author proposed that the harmful effect of de-icing salts was due to a combined effect of osmotic and hydraulic pressures. The presence of salts would attract more moisture into the pores, and consequently, the hydraulic pressure generated when freezing started would be higher. Powers (1965) also refers that de-icing salts spread faster in the capillary pores than in the gel pores, and thus the salt concentration gradients generated between the gel pores and capillary pores would promote this mechanism.

This theory has been found dubious. Lindmark (1998) gives the following explanation: after freezing has started in a salt solution, the chemical potential of the remaining salt solution will be equal to that of the ice. Thus, at a given temperature, the combined ice and salt solution mixture would have no more intense ability to attract water than would a pure ice body at the same temperature. Investigation carried out by Lindmark (1998) found that the presence of salts in the pores reduces the pressure difference needed for equilibrium between ice and pore water. Hence, the presence of salts in the pores should reduce the hydraulic pressure. Moreover, Lindmark (1998) also demonstrated that it is the outer salt concentration, and not of the inner salt concentration, that is determinant in the salt frost scaling of concrete.

3.1.2.2. Rösli and Harnik, 1980 – Thermal Shock Effect

Rösli and Harnik (1980) proposed that the severe tensions in a concrete surface may be caused by thermal shock when an ice cover is removed by salting. The use of de-icing salts will lower the melting point below the ambient temperature. Since melting is an endothermic reaction, the heat required to melt the ice is drawn from the concrete surface layer. The internal tensile stresses that arise from the temperature gradient between the top layer and the underlining concrete may cause superficial cracking.

This mechanism is also found dubious. First, the mechanism does not explain why salt scaling occurs when the salt solution is already present on the surface when freezing begins (as is the case in most laboratory testing and also in marine environments). On the other hand, while in laboratory conditions, it is possible to obtain temperature shocks which may produce tensions of up to 4 MPa (with an ice layer of 2 mm of thickness and strong salt solutions), field tests show that that the temperature shocks are never large enough to cause destructive stresses [Lindmark (1998)].

3.1.2.3. Valenza and Scherer, 2004 – Glue Spall mechanism

According to Valenza and Scherer (2004), the glue spall mechanism seems to give the only plausible explanation for the salt-frost scaling of concrete. According to this theory, after freezing, the de-icing salts are entrapped on the frozen layer, creating week brine pockets, and leading to cracking of the ice layer. The crack development penetrates the underlying concrete, and, when the crack reaches a critical depth, it runs parallel to the surface. When cracks in the paste connect, a thin piece of cement paste scaled from the surface.

The glue spall theory can explain the greater deterioration of pessimum salt concentration under frost. However, it does not explain the positive effect of air entrainment. In fact, according to the glue-spall theory, an increase in the air content should result in more scaling, which contradicts the experimental results. The authors gave as a possible explanation the reduced bleeding provided by the use of air entraining agents, thus resulting on a stronger surface layer [Çopuroğlu (2006)].

3.1.2.4. Conclusion

Even though several authors have attempted to explain the salt-frost scaling of concrete, none of the proposed hypotheses has been recognised as fully satisfactory. In fact, the production of concrete to be exposed to a freezing environment with presence of salts is still based on experience. It has been observed that the parameters that influence the internal frost damage of concrete (water/cement ratio, air entrainment), influence salt scaling in the same manner. Hence, the common practices when producing salt frost resistance concrete are basically the same as for plain frost attack.

3.2. Test Methods

The several mechanisms that occur simultaneously during frost action and all the different parameters that influence the resistance of concrete against salt frost attack result in a great difficulty in predicting the durability of concrete. Consequently, the usual practice is to apply design guidelines that are based on “local” practice. However, this “experience based” concept poses as a restriction to the use of new materials. There is, therefore, the need for an accurate method of evaluation of the durability of concrete under salt-frost scaling during its service life. To that purpose, different test methods have been developed [Rønning (2001)].

The aim of the test methods is to simulate the harmful actions to which concrete will be exposed in the field conditions during its service life, and decide between acceptable and not acceptable performance. It is, however, somewhat difficult to accurately simulate the field conditions in laboratory. The main difficulty is to reproduce a deterioration process that may take years in a much shorter period of time. Moreover, it is also hard to replicate the true climatic conditions to which concrete will be exposed in the field.

There has been extensive debate on the accuracy of the existent test methods, and its correlation with the field performance of the concrete tested. The most important feature of a test method is that it classifies the material as acceptable or unacceptable exactly as the field conditions would, i.e., it must not give false-positives, eliminating potentially durable concrete, but it must absolutely not allow the use of inferior concrete qualities [Lindmark (1998)].

Some authors alert that the laboratory conditions prescribed in the standards may be too mild, therefore allowing the use of concrete of poor quality. Lindmark (1998) refers that test methods like the Swedish Standard SS 13 72 44 apply the minimum temperature for a short period of time. In reality, the concrete structures are frequently under sub-freezing temperatures for a longer period of time, which, as explained in the previous section, results in increased damage.

On the other hand, some authors argue that the most common test procedures may be too restrictive. Çopuroğlu (2006) refers that, in the most common test procedures, the specimens are always in contact with the solution, becoming wetter and wetter after each cycle. In reality, concrete would probably not reach such a high degree of saturation.

In fact, several authors have studied the correlation between laboratory and field performance of concrete, and have reported several cases in which concrete placed in field conditions outperformed concrete tested in laboratory. Marchand et al. (2005) compared laboratory test moulds and cores from a sidewalk of the same concrete quality, and reported that field cores performed better than laboratory specimens. One of the reasons pointed out is the small surface of the test mould, which can be easily finished prematurely or overworked, when compared to an actual field placing. Similar results were obtained by Boyd and Hooton (2007), who prepared two sets of laboratory specimens, one to be cured in laboratory and tested after 28 days, and another cured in actual field conditions for 127 days.

The authors report that the specimens cured in the field outperformed the specimens cured in laboratory.

Another limitation usually pointed out to the standard test methods is that they were produced to evaluate Portland cement concrete. Its applicability for concrete produced with supplementary cementitious materials has not yet been verified.

Some of the most common test methods used to evaluate the frost resistance of concrete are briefly described below.

3.2.1. Swedish Standard SS 13 72 44 (Borås method), Procedure IA (Edition 3)

The Swedish Standard SS 13 72 44 (2005) is used to determine the resistance to scaling of a horizontal concrete surface exposed to freezing and thawing cycles with or without the presence of de-icing chemicals.

Concrete cubes 150x150x150mm are cured in water 20±2°C until the 7th day of age, after which they are placed in a climate chamber at 20±2°C and 65±5% R.H.. At 21±2 days of age, a 50mm slab is sawn of the cube. The specimen is then returned to the climate chamber for 7 days, during which a rubber sheet is glued in all surfaces of the specimen except the test surface.

At 28 days of age, the specimen is re-saturated by pouring tap water onto the freezing surface. After 72±2 hours, the tap water is removed and the freezing medium (pure water or saline solution) is applied at a depth of 3mm. The specimen is thermally insulated with 20mm of polystyrene, and covered with a tight plastic foil to prevent evaporation. The test set-up is shown in Figure 3.5. The specimen is then placed in the freezer and the test begins.

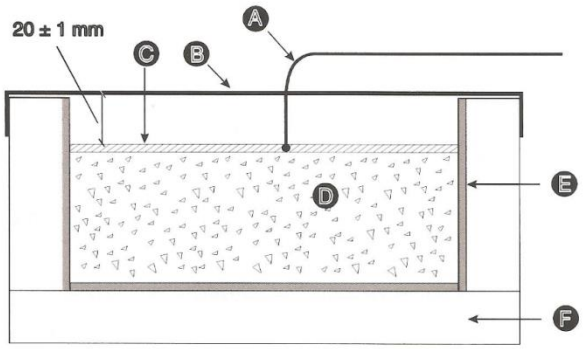

Figure 3.5 - Freeze-thaw test set-up. A: Thermo element; B: Protection against evaporation; C: Freezing medium; D: Test specimen; E: Rubber cloth; F: Thermal insulation. [SS 13 72 44 (2005)]

In the freezer, the specimens are subjected to repeated freezing and thawing. The temperature in the freezing medium cycles from -20ºc to 20ºC over a period of 24 hours, with the temperature exceeding 0ºC for at least 7 hours, but not more than 9 hours in each cycle.

After 7, 14, 28, 42, 56, 70, 84, 98 and 112 cycles, the scaled-off material is collected and weighted. The results are expressed as accumulated mass of scaled material per area of freeze surface.

Concrete is considered acceptable if the mean value of the scaled material after 56 cycles is lower than 1.0kg/m^2.

3.2.2. ASTM C 672: Scaling Resistance of Concrete Surfaces Exposed to De-icing Chemicals

ASTM C 672 (2003), used in the U.S.A., is very similar to SS 13 72 44, with some modifications. Specimens must have test surface area of at least 0.045 m^2 (72 in.^{2}), and a depth of at least 75 mm (3 in.). After casting, moulding and finishing the surface, a 20 mm (0.75 in.) high dike is placed along the perimeter of the top surface of the specimen, as seen in Figure 3.6. The specimens are then covered with a polyethylene sheet. Moulds are removed after 24 hours, and the specimens are then placed in a moisture room with temperature 23±2ºC (73.5±3.5ºF) and RH≥95%. After 14 days, the specimens are stored in air, in a room with relative humidity of 45-55% and temperature 23±2ºC (73.5±3.5 ºF) for another 14 days.

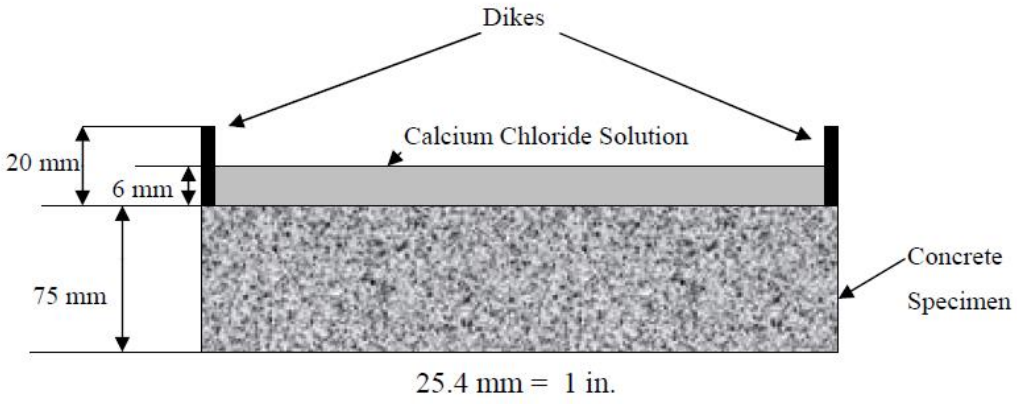

Figure 3.6 - ASTM C672 salt-scaling test specimen setup [Bortz, (2010)]

After curing, a 6-mm (0.25 in.) layer of calcium chloride solution is applied to the freeze surface, and the freeze/thaw test begins. The solution must contain 4 grams (0.14 oz.) of anhydrous calcium chloride per 100 ml (3.38 fl. oz.) of solution.

The specimens are then subjected to 24-hour freeze/thaw cycles, being in a freezing environment (-18±3ºC) for 16 to 18 hours. The specimens are then removed and placed in laboratory air at 23±2ºC (73.5±3.5ºF) for the remaining 6 to 8 hours, during which solution is added to maintain the depth of the solution.

After every 5 cycles, the solution flushed off, and a visual inspection of the freezes surface of the specimen is performed. The test continues for at least 50 cycles. The specimens are then rated according to Figure 3.7 and the following rating scale:

- 0 - No scaling
- 1 - Very slight scaling (max. 3.2 mm depth, no coarse aggregate visible)
- 2 - Slight to moderate scaling
- 3 - Moderate scaling (some coarse aggregate visible)

- 4 - Moderate to severe scaling
- 5 - Severe scaling (coarse aggregate visible over entire surface)

:

Figure 3.7 - ASTM C672 salt-scaling test rating [Bortz, (2010)]

3.2.3. CDF: Capillary Suction of De-icing Chemicals and Freeze-Thaw Tests

Like the Swedish Standard SS 13 72 44, the CDF test, developed in Germany, is used to determine the mass of scaling per freeze surface area. The specimens are casted in 150x150x150mm cubes. The specimens are removed from the moulds 24 hours after casting, and cured in tap water at 20±2ºC for 6 days. On the 7th day of age, the specimens are moved to the climate chamber at 20ºC and 65% RH up to the age of 28 days, when pre-saturation starts. The evaporation in the climate chamber must be 45±15g/m^{2}hr for free water.

Between 7 and 2 days before pre-saturation, the lateral faces of the specimens are sealed. The specimens are then placed on top of racks 10 mm above the base of the test container. The freezing medium (a sodium-chloride solution, 3% by weight) is the added to the container, to a level of 15mm (Figure 3.8). The test containers are placed at 20±2ºC during 7 days to allow capillary suction.

After 7 days of pre-saturation, the specimens undergo a ultrasonic bath to remove any loose material, after which they are placed in the freezes, and the freeze/thaw cycles are applied.

Each freeze/thaw cycle lasts 12 hours. Starting in 20ºC, the temperature is lowered to -20ºC in 4 hours. The temperature of -20ºC is kept during 3 hours, after which it starts to increase at a rate of 10ºC/hour, until it reaches +20ºC. The temperature is kept constant at +20ºC during one hour.

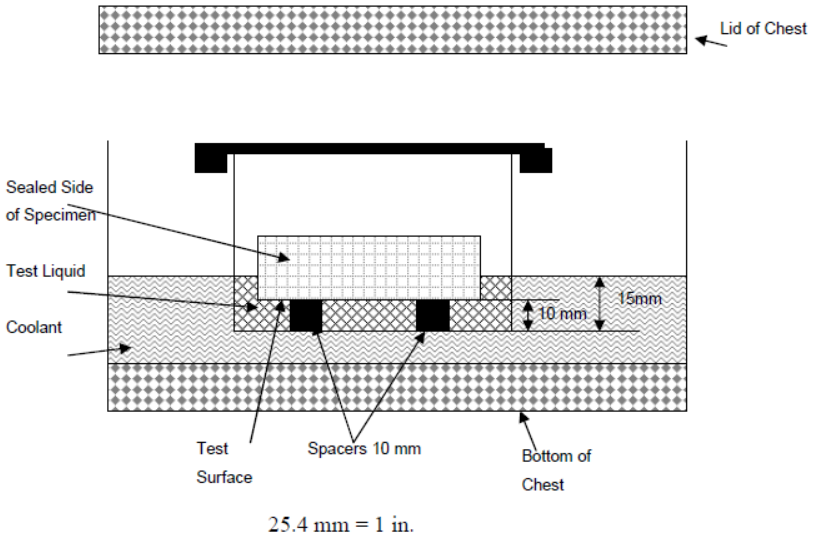

Figure 3.8 - CDF test set-up [Bortz (2010)]

After 14 and 28 cycles, when the temperature is +15ºC, an ultrasonic bath is used to remove the loose particles from the surface of the specimen. The scaled material is then dried and weighted. Concrete is considered acceptable if the scaled material after 28 cycles does not exceed 1500g/m^2.

3.2.4. Comparison between test methods

The different test methods described differ mainly in specimen dimensions, curing and pre-treatment procedures, and number and temperature cycles. Even though the representativeness of the results from all the standard test methods presented is considered acceptable, some remarks may be made.

The ASTM C672 test, unlike the CFD or the SS 13 72 44 relies on visual rating of the specimen, and is, therefore, somewhat dependent on the subjectivity of the operator. For that reason, some authors have proposed an additional step of measuring of the mass of scaled material [Valenza and Schrerer (2007)]. As a guideline, the amount of scaled material is usually compared with the limits presented by standards such as SS 13 72 44, i.e., the mass of scaled material shall be less than 1000g/m^2 after 50 cycles [Pigeon (1995)].

The use of the CDF test presents the advantage of being able to separate the different phenomena that influence the salt-frost scaling of concrete. The test allows the separation between initial scaling and later, continuous scaling, as well as the effects of the chemical and physical phenomena [Setzer (2007)].

Unlike the CDF and ASTM C 672 tests, in the SS 13 72 44 test, the specimens are thermally insulated on all sides except the freezing surface. This results in a uniaxial temperature attack, and a freeze surface progressing vertically from the surface to the interior of the specimen, which is more representative of the field conditions [Pigeon (1995)].

As referred previously, one of the main drawbacks of these test methods is that they were developed for Portland cement concrete, and its representativeness when testing concrete produced with supplementary cementitious additions has not yet been verified. For all test methods, the specimens are subjected to the freeze/thaw cycles around the 28th day of age, or some days later, which may underestimate the performance of concrete produced with cements with slower hydration rates. Further investigation is needed to assess the correlation between the results of the test methods to the field performance of concrete containing additions, as well as to determine if changes in curing and/or pre-conditioning methods should be introduced to the standards to estimate more accurately the performance of concrete produced with supplementary cementitious materials.

3.3. Factors that influence the frost resistance of concrete

Even with all the investigation carried out over the years on the frost mechanisms acting in concrete, it is still difficult to design concrete with good resistance against frost attack. The main reasons for this are: the complicated structure and chemical composition of concrete, the difficulty in predicting the real exposure conditions, the combined effects of different degradation mechanisms, and the ageing of concrete [Lindmark (1998)]. The effect of most relevant factors that influence the frost resistance of concrete are discussed in this section.

3.3.1. Water/cement ratio

The primary influence of the water-to-cement (w/c) ratio on the freeze/thaw durability of concrete is its effect on the capillary pore volume, i.e., its permeability and ability to absorb freezable water. In fact, according to the hydraulic pressure theory, the pressure increases with an increase in the amount of freezable water in concrete, i.e., the degree of saturation. Therefore, the critical degree of saturation will be reached faster for more permeable concretes. Hence, in order to ensure good frost resistance, the volume of capillary pores should be minimized, i.e., concretes with low water/cement ratio should be used. [Bager (2010), Neville (2003)].

The influence of the water/cement ratio in the resistance of concrete to frost attack usually translates on the limitation of the water/cement ratio of concrete to be used in structures placed in freezing environments. The Swedish standard SS 13 70 03 (2008) allows w/c ratios up to 0.6 for exposure class XF1, but limits the w/c ratio to 0.45 for XF4 exposure class. The American Standard ACI 201.2R limits the w/c ratio for concrete exposed to freeze/thaw cycles to 0.50, and sets the limit of 0.45 for extreme environments where de-icing agents are used (such as bridge decks and kerbs) [Neville (2003)].

The positive effect of a low w/c ratio on the resistance of concrete against freezing and thawing has been investigated and verified by many authors. It has even been hypothesised that there is a maximum w/c ratio below which concrete is always frost resistant, even without the use of air entraining agents [Tang]. Many authors tested specimens with a salt scaling resistance test similar to that described in the Swedish Standard SS 13 72 44, and obtained very good salt frost resistance with concrete qualities with w/c ratio lower than 0.35. However, presently, there is no way to predict if possible microstructure changes occurring during field applications will affect the frost resistance of high quality concretes. Therefore, air entrainment must always be used when producing concrete to be subjected to freeze/thaw cycles [Lindmark (1998)].

A low water/cement ratio also contributes for a better performance of concrete against frost action by increasing the mechanical strength of the concrete. Low w/c ratios in concrete result in higher tensile strength of the paste, and the higher the tensile strength of the material, the higher the expansion stresses due to the freezing of water in the capillary pores the concrete can withstand [Bager (2010)].

3.3.2. Air entrainment

Air entrainment is a common practice and is always recommended when producing concrete to be placed in freezing environments. The positive effect of air entrainment in the frost resistance of concrete is explained by the various frost damage mechanisms described: spacing factor, micro ice lenses growth and osmotic pressure.

Entrained air bubbles protect against frost damage by providing sites for water to migrate and for ice crystals to grow without development of stresses, thus preventing pressure built up in the pore walls [Ramachandran (1995)].

According to the hydraulic pressure theory, the positive effect of air entrainment is due to the fact that well-distributed air pores in the cement paste will reduce the distance that the water expelled out of the large pores where freezing takes place will have to travel. This means that the air entrainment in concrete is closely related with the spacing factor. In fact, the aim of air entrainment is to provide concrete with enough sites for water to freeze without stress increase, and sites that must be uniformly dispersed through the paste so that the average distance between two pores does not exceed the critical spacing factor [Utgennant (2004)].

According to the micro ice lenses growth and osmotic pressure mechanisms, the entrained air bubbles will receive a small amount of water that is expelled from the capillary pores by hydraulic pressure when freezing is initiated. This water will then freeze and compete with the large pores for the unfrozen water in the finer pore system. Thus, the unfrozen water can either move towards the ice filled pore, or the ice in the air bubble. Due to the low chemical potential of the ice in the entrained air bubble, the thermodynamic impulse is for water to move towards the air bubble. Therefore, the water intake of the large pores will be lower, and, consequently, the disruptive stresses due to expansion will not increase [Utgennant (2004), Domone and Illston (2010)].

3.3.2.1. Influence of the pore structure in the freeze/thaw resistance of concrete

The key parameters that characterize the air void system of concrete are its total air content, its spacing factor and its specific surface [Çopuroğlu (2006)].

The air content of concrete is the ratio between the volume of air voids in the paste and the total volume of concrete [Ramachandran (1995)]. Even though air entrainment is widely accepted as a way to prevent frost damage, there is not a minimum amount of air above which resistance of concrete against frost attack is guaranteed. On the other hand, there is also no indication of an air content below which the concrete will always fail [Fagerlund (1988)].

This may be due to the fact that increased air content does not necessarily correlate with a good distribution of air pores through the cement paste, i.e., an adequate spacing factor [Bortz (2010)]. The total air content includes both entrained air (which are equidistant air bubbles with a typical diameter of about 0.05mm) and entrapped air (larger irregular cavities, sometimes larger than 1 mm). These large

entrapped bubbles will accommodate a larger amount of water, therefore contributing for an increase in volume of freezable water in the paste. Thus, in order for air entrained concrete to present an adequate frost resistance, the size of entrained air bubbles should not exceed 0.10mm [Pigeon and Pleau (1995)]. On the other hand, for the same air content, the spacing factor will be smaller for a higher amount of air voids. Therefore, to ensure good frost resistance of the concrete, the air void structure should be composed of a system with a large amount of small air voids, equidistant and relatively close to each other (Figure 3.9) [Ramachandran (1995)].

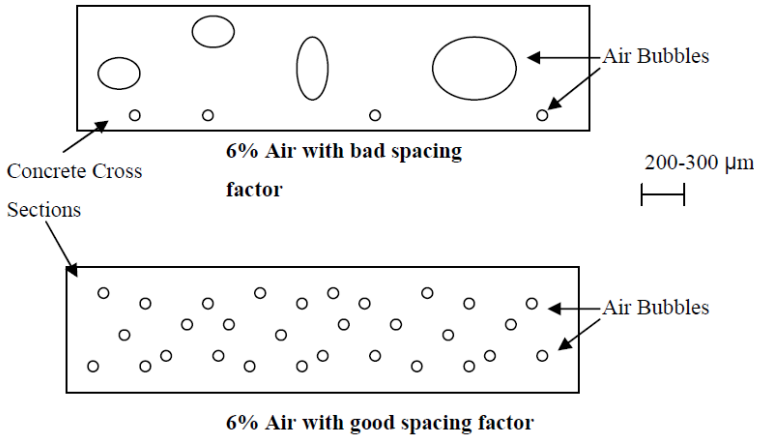

Figure 3.9 – Schematic representation of concrete with 6% if air content, with good and bad spacing factor [Bortz (2010)]

The specific surface is another indication of the adequacy of the air void system. The specific surface is defined as the surface area of the air bubbles divided by their total volume. This means that a higher specific surface is a result of a higher amount of small sized air pores. However, the specific surface does not reveal the number of air voids of a specific size. Instead, there are a number of different air pore size distributions that result in the same specific surface. The specific surface is, however, a good indicator of the pore size distribution for concrete with similar air content. Nevertheless, it is usually assumed that the minimum specific surface for air-entrained concrete of satisfactory freeze/thaw resistance shall vary between 16 and 24 mm^{-1}. Specific surfaces lower than 12 mm^{-1} indicate a poor air void structure, with a high amount of entrapped air bubbles [Ramachandran (1995), Neville (2003)].

The amount of entrained air that effectively protects concrete from frost attack depends also on the freezing medium. In fact, the minimum air content necessary to protect concrete against frost attack in pure water seems to be lower than when freezing occurs in the presence of a salt solution. Lindmark (1998) refers that the usual air content required for concrete to be resistant to plain frost attack is between 2 and 3%, whereas for salt scaling resistance a minimum of 4.5% of air is usually required. This fact may be explained by the lower spacing factor required for resistance against salt frost scaling (between 0.16 and 0.2mm) than for pure frost attack (around 0.25mm) [Fagerlund (1988)].

The recommended air content of concrete under frost attack depends on the maximum aggregate size and usually lies between 4% and 8% by volume of concrete [Domone and Illston (2010), Ramachandran (1995)]. The Swedish Standard SS 13 70 03 (2008), which is the application of EN

206-1 in Sweden, sets the minimum air content for XF2 and XF3 exposure classes to 4% for a maximum aggregate size of 32 mm, 4.5% for 16mm and 5.0% for 8mm of maximum aggregate size.

The air void structure of concrete is, therefore, one of the most important factors that influence its resistance against salt frost scaling. For an adequate air content and pore system to be achieved, air entraining agents are used [Çopuroğlu (2006)].

3.3.2.2. Use of air entraining agents (AEA)

Air entraining agents (AEA) are admixtures which, when added to the mix water, entrain a controlled quantity of air in the form of small closely-spaced bubbles in the concrete paste. The entrained air bubbles are incorporated into the concrete and become part of the matrix that binds the aggregate together. The entrained air bubbles must be stable enough so that the air pore system is unaffected by placing, compaction, setting and hardening of concrete [Domone and Illston (2010), Ramachandran (1995)].

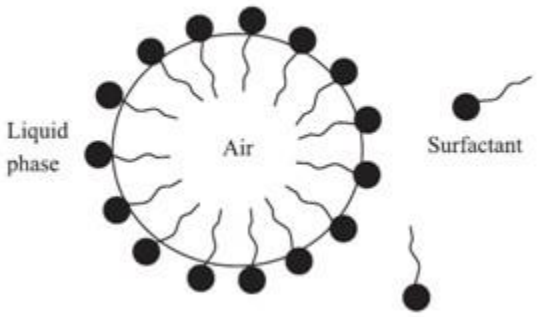

Figure 3.10 – Illustration of an air bubble produced by an air entraining agent [Due and Folliard (2004)].

Chemically, the air entraining agents are powerful surface-active agents, or surfactants, which act at the air-water interface in the cement paste. The AEA molecules are constituted by a hydrocarbon tail (non-polar) that orients towards the air within the bubble, and a hydrophilic head (polar group) that becomes oriented towards the aqueous phase (Figure 3.10). The hydrophilic heads are negatively charged. The electrostatic repulsion between the hydrophilic heads of the molecules results in stable bubbles, which prevents coalescence to form larger bubbles, thus creating a stable air void system in the cement paste [Hewlett (2004), Due and Folliard (2004)].

The average size of the entrained air bubbles ranges between 0.01 and 0.1mm [Bortz (2010)], with and average spacing of about 0.25mm [Neville (2003)].

The air entraining agents are usually supplied and used as dilute solutions that are added directly into the concrete mix. For each concrete quality, and for each air entraining admixture, there is a recommended dosage to obtain the desired air content in concrete. The usual dosages of AEA lie between 0.3 and 1.0ml/kg, which corresponds to 0.01% of the mass of cement [Ramachandran (1995)]. However, it is very hard to achieve the desired amount of entrained air and air void

distribution. Air entrainment of concrete is a complex process, which depends on many factors, such as the mixing process (including mixer type and mixing time), the mix proportions, the properties of the Portland cement, the use of additions and its properties, the amount and quality of the mixing water, the temperature of the mix, the dosage and properties of air entraining agent used and other admixtures (such as superplasticizers) and the slump [Due and Folliard (2004)].

Generally, higher amounts of air entraining agent will result in higher air content in concrete. However, for each AEA, there is a maximum dosage beyond which there is no increase in the air content of concrete [Neville (2003)].

3.3.2.3. Further effects of air entrainment

The main purpose of using air entraining admixtures in concrete is to improve its frost resistance. However, incorporating air in concrete also influences other properties [Neville (2003)].

Since the compressive strength of concrete is directly correlated with its density ratio, the increase in the volume of air voids will result in lower compressive strength of concrete, unless this effect is offset by changes in the mix proportions (for instance, by lowering the w/c ratio). The average drop in compressive strength is about 5.5% to 6% for each 1% of air content [Domone and Illston (2010), Neville (2003)].

Another effect of the use of air entraining admixtures is an improvement in the workability of concrete, for the same water/cement ratio. The reason for the higher workability of air entrained concrete mixes is that the small air bubbles introduced by the AEA act as fine aggregate of high elasticity and low surface friction. Neville (2003) refers an increase in slump between 15 to 50mm with an air entrainment of 5%. Therefore, the increased workability due to the AEA can compensate for the loss of compressive strength, by allowing a reduction in the w/c ratio, for the same workability [Hewlett (2004), Neville (2003)].

The air entrainment of concrete also causes a reduction in the bleeding and segregation of concrete. The introduction of air bubbles results in a more cohesive and homogeneous concrete paste, preventing the emergence of mix water on the surface of concrete and the settlement of the solid particles on the bottom. This fact may partially explain the positive effect of air-entrained concrete in the resistance against salt-frost scaling. The rise of mix water to the surface of concrete results in a lower strength of the top layer. By reducing this phenomena, higher tensile strength on the top layer is achieved, and, consequently, the surface layer will be more resistant to frost attack [Neville (2003), Ramachandran (1995)].

3.3.3. Influence of the superplasticizers in the pore structure

Superplasticizers are water-soluble polymers used as admixtures to improve the workability of the concrete for the same water/cement ratio, or to decrease the water demand for the same workability.

Superplasticizers, much like the AEA, present a hydrophilic group, which allows its dissolution in water, and a hydrophobic group. The repulsion forces created by these two groups result in a dispersion of the cement particles in suspension, and, thus, in an improved workability of concrete [Ramachandran (1995)].

Superplasticizers are often used to produce high-quality concrete, by reducing the need of water for the same workability, i.e., reducing the w/c ratio, which results on a higher compressive strength and lower permeability [Ramachandran (1995)]. However, some concerns have been raised regarding the use of superplasticizers together with AEA.

Some superplasticizers are known to entrain some air (1 to 2%) in concrete. However, the increase in air content due to the incorporation of superplasticizers is mainly due to a phenomenon named bubbling of concrete, in which large air bubbles are entrapped in the concrete during mixing, even when adequate vibration is provided. Therefore, obtaining an adequate air void system, with adequate bubble sizes and spacing factor is made more difficult by the use of superplasticizers [Domone and Illston (2010), Ramachandran (1995)].

On the other hand, the added cohesion provided by the air entraining agents and the dispersing action caused by the superplasticizers are mutually competitive, which may result in the disruption of the stable air void system created by the AEA and in the coalescence of the air bubbles [Hewlett (2004), Ramachandran (1995)].

The use of superplasticizers together with air entraining agents was studied by Fagerlund (1995). The author carried out tests in concrete with 4 different air contents, and two types of air-entraining agents used alone, and one air-entraining agent used together with a superplasticizer. The results showed that the use of superplasticizers decreased the frost resistance of concrete, when compared to the case where only air-entraining agents were used.

Nevertheless, some studies show that effect of the use of superplasticizers on the pore structure of concrete is rather small. Schulson (1998) refers studies by Pigeon and Langlois (1991) that showed through test methods described in ASTM C 666 that the critical air spacing factor of two superplasticized Portland cement concretes with w/c ratio of 0.5 with was not significantly affected by superplasticizers. Thorpe et al. (1996), also cited by Schulson (1998), concluded from similar tests on 60 different mixes that mixes containing superplasticizers presented an adequate air pore system regarding freeze/thaw durability. Experiments conducted by Dhir et al. (1996) even showed better frost resistance for Porland cement concrete with superplasticizer admixtures than for concrete without superplasticizer. However, none of the concrete qualities tested were air-entrained. The superplasticized concrete mixes presented an air content on average 0.7% higher than the plain concrete. Since the frost durability of concrete is influenced by differences in air content between 0.5 to 1%, the positive effect of the superplasticizer was probably due to the increase in air content.

The use of superplasticizers introduces a new variable in the production of air entrained concrete, thus possibly having consequences in its performance in freezing conditions. Nevertheless, obtaining a

stable air void system of concrete containing superplasticizer is possible. Hewlett (2004) recommends the use of the air entraining agent to provide the adequate amount of stable air first, and only then adding the superplasticizer. Moreover, the compatibility of the AEA and the superplasticizer to be used together must always be verified [Neville (2003)].

3.3.4. Finishing

The scaling of concrete due to the frost attack where de-icing agents are used occurs mainly in the concrete surface. Therefore, the surface finishing operations affect the salt-frost scaling resistance of concrete.

The effect of finishing in the salt-frost resistance was observed by Johnston (1994), cited by Çopuroğlu (2006), and Afrani and Rogers (1994), cited by Bortz (2010), who tested the top and bottom surfaces of the same specimen, and found that the bottom moulded surfaces showed little to no salt-frost scaling, whereas the finished top surface resulted in severe scaling. The poorer performance of the top surface is probably due to the bleeding of concrete. The emergence of mix water to the surface of concrete results in a different air void system, and higher w/c ratio, which results in lower strength and higher permeability of the top layer and, hence, the top layer will be more susceptible to salt-frost attack [Çopuroğlu (2006), Bortz (2010)].

As formerly referred, the positive effect of the air entraining agents in the salt-frost resistance of concrete is often attributed to the reduced bleeding provided by the air entrainment: the air bubbles keep the solid particles in suspension, thus reducing sedimentation and emergence of mix water to the surface of concrete [Neville (2003)].

Bortz (2010) also refers that the salt-frost scaling will be higher when concrete is finished prematurely, i.e., before bleeding is complete. The finished surface stops the emergence of water, trapping it under the hardened surface layer. The trapped water near the surface results in an increase of the water/cement ratio and higher porosity of that layer, and, therefore, lower resistance against frost attack.

Prolonged vibration of concrete may also contribute for the emergence of mix water and finer cement particles to the surface, therefore resulting in changes in the microstructure of the paste in the concrete surface, becoming more porous and weak. Overworking the concrete surface may also result in an increased spacing factor, and must therefore be avoided [Çopuroğlu (2006)].

3.3.5. Curing

Curing conditions have been shown to have a significant effect on salt scaling resistance of concrete.

Extended wet curing may improve the durability of concrete under frost action by increasing the degree of hydration of the cementitious materials and, therefore, increasing the tensile strength of the surface [Bortz (2010)].

The effect of the curing conditions is even more important for concrete with additions (such as GGBS), than for Portland cement concrete with the same workability and water/cement ratio. Since the rate of hydration of slag is lower than the Portland cement, prolonged wet curing is needed to provide water for the ongoing hydration of slag. However, when GGBS concrete is designed to have a similar strength development than Portland cement concrete, the influence of prolonged curing would be rather small [Çopuroğlu (2006)].

The curing temperature also affects the frost resistance of concrete. Curing temperatures higher than 65ºC have shown to have a detrimental effect on the salt-scaling resistance of concrete. This effect is attributed to the increased porosity and lower strength at later ages presented by concrete qualities cured at high temperatures [Pigeon and Pleau (1995)].

Besides curing with water, some curing compounds may also be used. Some curing compounds have shown to reduce the amount of scaling of certain specimens, when compared to similar water-cured concretes. Curing compounds seal the surface layer during curing, thus reducing evaporation. This increases the degree of hydration of cement at the surface, hence increasing its strength [Bortz (2010), Çopuroğlu (2006)].

3.3.6. Temperature

According to Power's hydraulic pressure theory, the internal pressure in critically saturated concrete increases with an increase in the ice formation rate, which in turn increases with the increasing cooling rate, i.e., with a decrease in temperature. According to the micro ice lenses growth, a decrease in temperature rises the chemical potential of water, therefore breaking the thermodynamic equilibrium. In order to re-establish equilibrium, the water is drawn from saturated small capillaries and gel pores to the micro ice bodies where ice started to form [Lindmark (1999)].

The previous explanations indicate that the damage is more extensive the lower the temperature reached during the freeze/thaw cycles. This has been verified by different authors. Valenza and Scherer (2007), showed that no salt-scaling damage occurs when the minimum temperature is held above -10ºC. Tests conducted by Studer (1993) also showed that scaling is more severe the lower the temperature reached. However, the author found that the relation between the frost damage and minimum temperature reached is non-linear, with the mass of scaled material reducing between 38 to 52% for an increase in temperature from -18ºC to -16ºC, whilst a 2 degree increase from -13ºC to -11ºC resulted only in a 4 to 22% reduction in the amount of scaled material.

Lindmark (1998) reported that freezing temperatures of -7ºC cause only slight scaling, and that the scaling increases for lower temperatures reached. The author concluded that a lower minimum temperature will result in higher scaling, at least for temperatures ranging from 0ºC to -20ºC.

The duration at minimum temperature has also shown to affect the amount of scaling. Valenza and Scherer (2007) reported that the amount of damage for temperatures below -10ºC increases with a longer duration at minimum temperature. Jacobsen (1995), cited by Lindmark (1998), also showed that scaling increased for longer time at minimum temperature. This fact is explained by the

continuous formation of ice at low temperatures. According to the osmotic pressure theory, when ice starts to form, the concentration of the remaining unfrozen solution becomes higher, which drives the water towards the pores where the ice starts to form. This movement of water will lower again the concentration of the solution and, if the temperature does not increase, the more ice is formed. This phenomenon will continue until equilibrium is reached [Utgennant (2004), Çopuroğlu (2006)]. If the temperature increases, the formation of ice stops. If the temperature remains lower than the freezing temperature of the solution, formation of ice continues, and the probability of damage in concrete increases. This explains the higher amount of damage observed for concrete that remains for long periods of time at freezing temperatures.

3.3.7. Pessimum concentration

Several authors have reported that, not only the presence of salts results in a much lower frost resistance of concrete, by inducing the so-called salt-frost scaling of the concrete surfaces, but there is also a pessimum concentration of salt solution that causes the maximum amount of damage. A salt solution with a concentration of about 3%-by-weight has been found to be the pessimum concentration for concrete [Bortz (2010)].

Tests performed by Lindmark (1998) for concrete with a w/c ratio of 0.4 and moderate air content showed that the most severe damage was registered when the concentration of the outer salt solution was about 3%. Similar results were also reported by Verbeck and Klieger [Lindmark (1999)]. Fagerlund (1995) also showed that concrete specimens tested with a 2.5% salt solution always resulted in a higher volume expansion than other concentrations. Moreover, Fagerlund (1995) performed tests on the degree of saturation of several concrete mixes in isothermal conditions and different salt concentrations, and concluded that a solution of 2.5% to 5% sodium chloride resulted in the highest degree of saturation of concrete.

The reasons why such a pessimum concentration occurs are not clear. Fagerlund (1995) hypothesised that the amount of freezable water may decrease with an increase of the salt concentration, thus reducing the hydraulic pressure for high concentrations. On the other hand, when some of the capillary water freezes, the capillary pore will contain an ice body, but also water with increased salt concentration, when compared to the water in the pores where freezing has not started. This will cause an osmotic effect inside the concrete that may offset the normal pressure between ice and unfrozen water.

The pessimum concentration does not depend on the type of salt used (Valenza and Scherer 2005). It is also independent on the inner salt concentration of concrete, the rate of freezing and the lowest freezing temperature reached [Fagerlund (1995)].

3.3.8. Ageing of the concrete

The ageing of concrete, and the age at which a concrete mix is exposed to the first freeze/thaw cycle seem to be two of the most relevant parameters influencing the frost resistance of concrete. It is crucial that substantial hydration takes place before exposing concrete to freezing temperatures. At early ages, concrete presents a higher permeability, therefore absorbing higher amounts of water in wet conditions, which increases the degree of saturation of the paste. On the other hand, unhydrated cementitious particles do not contribute to the strength of the paste, which results in concrete being more susceptible to damaging stresses at early ages [Neville (2003)].

Utgennant (2004) conducted a comprehensive investigation on the effects of the ageing of concrete in its salt-frost scaling resistance, by studying the effects of the different ageing phenomena (hydration, drying and carbonation), both in Portland cement and slag concrete.

The effect of hydration was investigated on wet-cured, never dried specimens, stored in water until the start of the salt freeze/thaw test. Thus, the test evaluated not only the effect of hydration, but also the possible effect of water curing, and the increase of the degree of saturation with time.

The drying of concrete was studied by comparing the wet-cured, never-dried specimens with specimens dried for 7 days and re-saturated for three days before the beginning of the scaling test.

For all concrete qualities, the effect of hydration and drying on the salt-scaling resistance was only significant at early ages (up to 30 days). The tests showed that the scaling resistance of concrete is improved by short drying before exposure, at least at early ages. From 31 days onwards, the effect of drying and hydration on the salt-frost resistance of uncarbonated specimens is negligible.

However, the most important ageing effect that influences the salt-scaling resistance was found to be carbonation. Carbonation influences the scaling of concrete at all ages, though its effect is dominant at later ages (over 30 days).

Utgennant (2004) found that, for all the investigated concrete qualities, carbonation leads to a decrease in total porosity. However, the effect was different for Portland cement concrete and for slag concrete. For Portland cement concrete, carbonation results in a densification of the pore system, leading to a significant reduction in the amount of freezable water in the paste. For concrete with small amounts of slag, carbonation leads to a decrease in both coarse and fine pores, and thus reduction of the freezable water content. However, for concrete qualities with high amounts of GGBS, carbonation results in a substantial coarsening of the pore structure, thus leading to an increase of the amount of freezable water. These changes in the pore structure of carbonated concrete with different binders explains the improved salt scaling resistance of carbonated Portand cement concrete, and the reduced scaling resistance displayed by concrete with high amounts of GGBS, also investigated by the author.

Similar results for Portland cement concrete were obtained by Petersson (1996) on a field investigation carried out on marine environment. Concrete qualities with different w/c ratios were

subjected to salt-frost scaling test according to SS 13 72 44 at 31 days of age. Specimens from the same mixes were placed on aggressive marine environment (above sea level) and, after 3 years of exposure, the specimens were taken to the laboratory and the exposed surfaces were tested according to the same method. The author reports that, for almost all concrete qualities, the aged specimens showed lower scaling than the specimens tested at the age of testing prescribed in the standard. Moreover, some of the field-exposed specimens were tested after removing the top layer, and the improvement in the salt scaling resistance during the field exposure was lost. This result is probably due to the fact that the denser carbonated layer was removed from the concrete surface [Lindmark (1998)].

The results obtained by Utgennant (2004) for GGBS concrete verify the previous investigations carried out by Fagerlund (1995). Fagerlund (1995) tested uncarbonated concrete qualities containing different types of binders against freeze/thaw damage. Then, the specimens were exposed to two types of natural ageing, and were frost tested again. For uncarbonated specimens, slag cement has a comparable (or even better) frost resistance than Portland cement concrete. However, the aged slag specimens showed extensive damage due to salt-frost scaling, whereas the performance of Portland cement concrete was improved or unchanged after ageing.

Stark and Ludwig (1997) give a chemical explanation for the lower frost resistance of carbonated GGBS concrete. The authors found that the carbonated cement paste of OPC contains only calcium carbonate in the form of calcite, whereas carbonated cement paste of concrete with high contents of slag presents considerable amounts of aragonite and vaterite, in addition to calcite. According to the authors, aragonite and vaterite dissolve in the presence of sodium chloride, resulting in “badly crystalline calcite” which is easily removed under freeze/thaw cycles. However, the authors do not explain whether the dissolution of these products would cause damage to concrete in the absence of freezing. Therefore, the physical explanation is usually more widely accepted [Lindmark (1998)].

3.3.9. Conclusion

There are several different mechanisms and factors that influence the frost attack on concrete placed in cold saline environments. Most of the times, some of these mechanisms act simultaneously, which makes it hard to predict the durability of concrete solely based on material properties and exposure conditions. For that reason, current practice is to use concrete types that have proved durable by local experience. However, this restrains the application of new materials, for lack of experience and field results [Rønning (2001)]. Standards such as EN 206 give guidelines to produce salt frost resisting concrete, such as minimum cement content, minimum strength class for cement, w/c ratio and air content. However, the permitted amounts of supplementary cementitious materials are relatively low. Further investigation needs to be carried out.

3.4. Frost resistance of concrete with GGBS

The performance of concrete with addition of GGBS when subjected to salt-frost scaling has been object of broad discussion. Several authors have expressed concern about the scaling resistance of concrete containing slag, especially when the dosage of slag exceeds 50% of the total cementitious material. However, while some authors believe that this concern is mostly related with the results of tests carried out in laboratory environment, which are in poor correlation with field observations, other authors report that the test methods do evaluate adequately the frost resistance of concrete with additions of GGBS [Schlorholtz and Hooton (2008)].

Several authors have investigated the effect of slag replacement in the frost resistance of concrete, both in laboratory and in the field. Some relevant investigations are presented in this section.

3.4.1. Laboratory studies

3.4.1.1. Virtanen, 1982

Virtanen (1982) performed a comprehensive study on the effect of the use of supplementary cementitious materials in the frost resistance of concrete, by studying the different parameters that usually influence the frost attack in concrete (both internal damage and surface scaling). Virtanen studied the effect of GGBS, Fly Ash and Condensed Silica Fume using five different test methods:

- Protective Pore Ratio (according to Finish standard SFS-4475);
- Freezing Expansion;
- Frost-salt test at the age of 7 and 35 days;
- Critical degree of saturation (according to the method developed by Fagerlund);
- Optical analysis of the pore structure of the hardened concrete.

The GGBS was added separately in the mixer, and represented 50% of the cement weight. Both air entrained and non-air-entrained concretes were tested. The targeted air-content for the air-entrained mixes was 4%. The concrete mixes were studied to have similar consistency and 28-day compressive strength.

The five different test methods gave somewhat different results. Therefore, the concretes were ranked according to the results obtained by different test results. The ranking order provided by the author is presented in Table 3.1:

Table 3.1 – Results of the frost resistance of concrete qualities, ordered from the most resistant to the least resistant [Virtanen (1982)]

Mix	Type of Concrete	Air content
C-4	Cement	7,0%
S-2	Silica Fume	4,6%
F-4	Fly Ash	6,2%
B-3	**GGBS**	**4,1%**
F-3	Fly Ash	5,2%
C-3	Cement	5,0%
F-2	Fly Ash	4,2%
C-2	Cement	3,7%
B-2	**GGBS**	**2,0%**
S-1	Silica Fume	non-air-entrained
F-1	Fly Ash	non-air-entrained
C-1	Cement	non-air-entrained
B-1	**GGBS**	**non-air-entrained**

The results presented on Table 3.1 demonstrate the great influence of air content on the freeze-thaw resistance of concrete, both for Portland cement concrete and for concrete with additions. According to the ranking, GGBS concrete with an air content of 4.1% shows better frost resistance than Portland cement and fly ash concretes with similar or higher air content. Thus, the author concluded that GGBS addition may result in a slight improvement in the freeze-thaw resistance of concrete, when compared to Portland cement concrete qualities with the same compressive strength and air content.

Only one of the tests performed measured the frost-scaling of concrete in the presence of de-icing agents. The salt-scaling resistance test used by Virtanen follows the Finish method SFS-5449. Three test cubes with dimensions 100 x 100 x 100 mm^3 were tested per mix. The cubes were taken out of the moulds after 24 hours, and a 7 day curing under water began. The specimens to be tested at 7 days of age were subjected to the freeze-thaw test, and the cubes to be tested at 35 days of age were exposed to relative humidity of 70% until the freeze/thaw test started.

The test consists of a freezing bath on a saturated solution of sodium chloride at -15ºC during 8 hours, and a thawing bath of pure water at 20ºC during 16 hours. The deterioration was measured by measuring the change in volume after 25 cycles. The Finish requirement states that concrete is considered resistant to salt frost scaling if the volume change does not exceed 5% after 25 cycles.

The results for the salt-scaling resistance of Portland cement concrete and GGBS concrete are presented on Table 3.2.. Table 3.2 also displays the air content in the freshly mixed concrete and the air content in the hardened state, measured by optical analysis:

Table 3.2 – Results for the salt frost scaling damage in concrete qualities with Portland cement (C) and for concrete qualities with 50% GGBS of the weight of CEM I (B), for different air contents [Virtanen (1982)]

Mix	Frost-salt test Volume change, %		Air content (fresh concrete)	Air content (hardened concrete)
	7 d	35 d		
C-1	34,7	4,3	1,5 (NAE*)	0,76
C-2	6,9	0,3	3,7	3,68
C-3	4,2	0,5	5,0	6,37
C-4	2,9	0,5	7,0	7,93
B-1	29,5	5,8	1,0 (NAE*)	0,53
B-2	6,3	2,9	2,0	1,57
B-3	3,0	1,7	4,1	5,06

(*) NAE (not air entrained)

The results show that Portland cement concrete presents, generally, a better salt-frost resistance than GGBS concrete. The results also show the strong influence of air entrainment in the salt-frost scaling resistance of concrete, with non-air-entrained concretes displaying a much higher volume change than the air-entrained qualities.

The volume change for specimens tested at 7 days of age is extremely high on both concrete qualities, especially for non-air-entrained mixes. These results are explained by the low maturity concrete at 7 days: at early ages, the hydration of the cementitious materials is still ongoing, which means that concrete presents high capillary porosity. Therefore, the moisture uptake is very high, which results on the critical degree of hydration to be reached in a short time. On the other hand, the tensile strength of the paste before hydration is complete is low, and thus, lower pressure needs to develop to cause damage in concrete.

For specimens tested at 35 days of age, only non-air-entrained concrete with GGBS failed. Even though the volume change for slag concrete is systematically higher than for Portland cement concrete, which indicates worse performance of slag concrete, the present investigation showed that it is possible to produce salt-frost resistant concrete with replacement up to 50% of GGBS of the cement weight, as long as proper air entrainment is provided.

Nevertheless, this investigation did not consider the effect of the ageing of concrete (particularly carbonation), which may adversely influence the performance of GGBS concrete.

3.4.1.2. LaBarca et al., 2007

LaBarca et al. (2007) studied the deicer scaling resistance of concrete with different replacements of GGBS according to the modified North-American standard ASTM C 672. The salt-scaling resistance testing considered one brand of Grade 120 slag at 0%, 30%, and 50% percentages of replacement of the total cementitious material, two brands of CEM I, two types of coarse aggregate, and six different

curing regimes, on a total of 12 mixes. The concrete mixes presented a water/(cementitious material) ratio of 0.45%, and the targeted air content was 6±0.5%.

The salt-scaling test began after a curing period of 28 days. The freezing medium was a 4% NaCl (sodium chloride) solution. Every fifth cycle, the specimens were rinsed and the scaled material was collected, dried and then weighted. The test was carried out until 60 freeze/thaw cycles were completed. The results for the cumulative scaling loss after 60 freeze/thaw cycles averaged for slag cement replacement, for different curing conditions is presented in Figure 3.11:

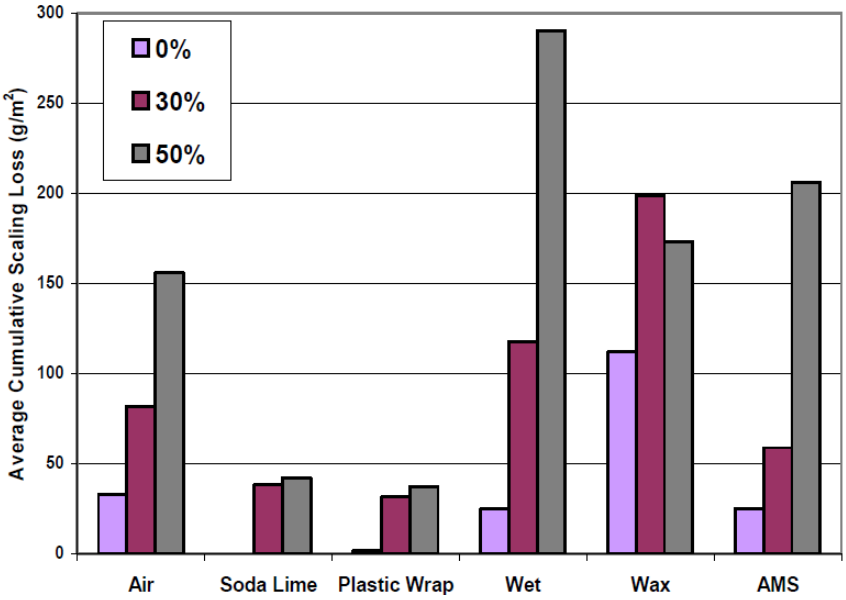

Figure 3.11 - Cumulative scaling loss after 60 freeze-thaw cycles averaged over slag cement replacement, for different curing conditions [LaBarca et al. (2007)]

The ASTM C672 standard does not require any collection and weighting of the scaled material. Instead, a visual evaluation of the specimen, following the rating system indicated in the standard is performed. There is not, therefore, a quantitative limit for the scaled material measured below which a concrete mix is considered acceptable, according to the ASTM C672 method. However, in this investigation, the limits defined by other standards were used as a guideline. The Swedish Standard limits the scaling mass loss at 1 kg/m^2 after 56 cycles, whilst the Canadian standard limits the scaling mass loss at 500g/m^2 at the 56th cycle.

Figure 3.11 shows that for all the replacement levels, no average accumulated scaled material surpassed 1 kg/m^2 or 500 g/m^2 after 60 cycles. However, the raw data show that one mix (wet cured, with 50% GGBS and igneous coarse aggregate) reached 583 g/m^2 after 60 cycles.

The results clearly show that an increase in GGBS replacement results in a decrease in salt-frost scaling resistance of concrete, regardless of the type of curing performed. However, the scaling resistance was acceptable at all GGBS replacement levels. The authors also found a pronounced effect of the curing method on the deicer scaling resistance of concrete, being the wet curing the most harmful for all of the mixes. Wet curing provides concrete with higher volume of freezable water, thus

resulting in a higher degree of saturation, and, consequently, on a lower resistance against frost attack. In the present investigation, it can also be observed that air-cured concrete generally displayed higher scaling resistance than concrete cured with commercial compounds.

The authors also investigated the depth of carbonation of the specimens, cured according to the same curing procedures followed for the salt-scaling test up to 28 days of age. After the 28th day, the carbonation specimens remained in laboratory conditions until the age of testing. Figure 3.12 shows the average carbonation depth of concrete for different percentages of slag replacement, and for different curing methods, at 28 and 80 days of age.

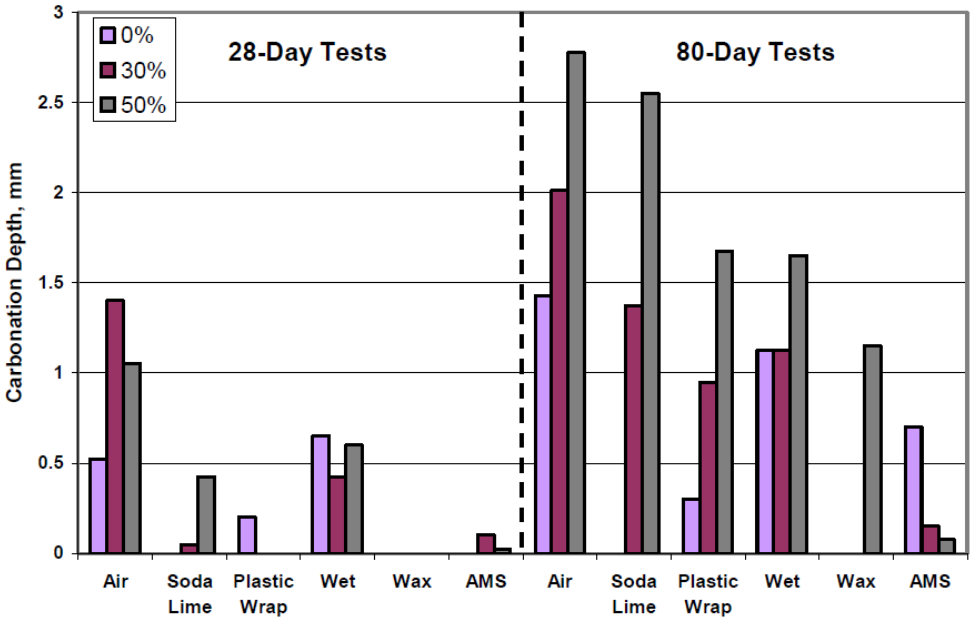

Figure 3.12 – Carbonation depth averaged over slag cement replacement level, for different curing conditions [LaBarca et al. (2007)]

Carbonation depth was higher for 80 days than for 28 days of age (Figure 3.12), which is expected, since carbonation of concrete depends on the time that concrete has been exposed to CO_2. Therefore, it is also expected that carbonation continues after 80 days.

The results also show that the carbonation depth generally increases as the level of slag cement replacement increases (Figure 3.12). In fact, at 80 days of age, the carbonation depth in 30% slag cement concrete was on average 1.5 times that of the reference Portland cement concrete, and the carbonation depth of 50% slag cement concrete was about twice that of concrete with 30% slag.

The poorer resistance of concrete with GGBS additions against salt scaling is usually attributed to the changes in the microstructure of the carbonated slag cement paste. This would mean that a curing medium that reduces carbon dioxide exposure (and thus reduces carbonation) would result in the most resistant slag concrete. However, the present results contradict this theory. In fact, concrete with 50% slag replacement shows higher carbonation for air-cured concrete, yet it presented the forth lower scaling loss. Furthermore, soda lime curing results in high carbonation, but low scaling of GGBS concrete. On the other hand, even though wet curing resulted in lower carbonation depth, it

represented the highest scaling loss for GGBS concrete. These results indicate that the degree of saturation and amount of freezable water may be more influential on the salt-scaling resistance of GGBS than the carbonation depth.

This investigation showed that, even though deicer scaling resistance decreased as the level of slag cement replacement increased, it is possible to produce salt-scaling resistance concrete with GGBS replacement levels up to 50% of the total cementitious material, by changing some parameters of the mix or curing conditions.

3.4.1.3. Utgennant, 2004

Utgennant (2004) studied the effect of ageing, and particularly carbonation, in concrete qualities with different amounts of GGBS replacement, and compared the results with Portland cement concrete. The concrete mixes produced and tested were as follows:

- **OPC-35 air** – Air-entrained Portland cement concrete with w/c of 0.35
- **OPC-45 air** - Air-entrained Portland cement concrete with w/c of 0.45
- **OPC-55 air** – Air-entrained Portland cement concrete with w/c of 0.55
- **20%slag-45** – Not air-entrained concrete with 20% GGBS of the total cementitious material, with a (w/c)eq of 0.45.
- **35%slag-45** – Not air-entrained concrete with 35% GGBS of the total cementitious material, with a (w/c)eq of 0.45.
- **65%slag-45** - Not air-entrained concrete with 65% GGBS of the total cementitious material, with a (w/c)eq of 0.45.

Mixes with 5% silica fume were also produced and tested, though the results for this mixes will not be further discussed.

When producing the concrete qualities to be tested, the aim was to produce frost-resistance qualities with similar air pore structures, i.e., similar spacing factor and specific surface. The spacing factor was aimed at 0.2mm. This led to different target values of the air content for each mix. Several trial mixes were produced until the proper mix proportioning was achieved. For qualities with GGBS, it was found that air entrainment was not necessary to obtain the desired air void structure.

The effect of carbonation in the salt-frost resistance of concrete was studied by placing the specimens seven days in a climate chamber at 65% RH/+20°C and with increased carbon dioxide content of ~1 vol-%, followed by a three-day-long re-saturation period before start of the freeze/thaw testing. The curing and pre-conditioning regime used in the investigation for the evaluation of the effect of carbonation in the frost resistance of concrete is schematically presented in Figure 3.13. The reference non-carbonated specimens followed the same cure and pre-conditioning, though were placed at climate chambers without carbon dioxide. The effect of drying was investigated by comparing the non-

carbonated specimens (dried during 7 days in the climate chamber 65% RH/+20°C) with never dried specimens.

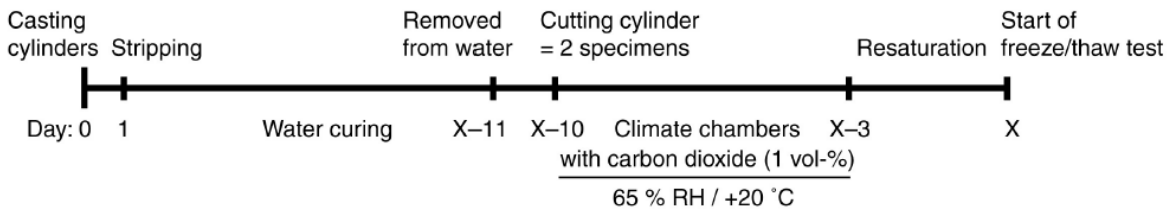

Figure 3.13 – Curing and pre-conditioning regime of the specimens to be subjected to freeze/thaw testing [Utgennant (2004)].

The effect of the increasing age in the salt-frost resistance of concrete was evaluated by starting the freeze/thaw testing of the specimens at different ages. In the illustration presented above, *X* is the age in days after casting when the freeze/thaw test of concrete starts.

- For Portland cement concrete qualities (OPC), testing started at seven different ages (*X*): 17, 24, 31, 38, 66, 122 and 276 days after casting.
- For GGBS concrete qualities the freeze/thaw testing was started at four different ages (*X*): 17, 31, 73, 122 days after casting.

Large concrete cylindrical specimens (with 100mm of diameter and 105mm of height) were casted. Each cylinder was cut in half, resulting in two cylindrical specimens with a thickness of around 50mm. One day before cutting, the specimens were insulated. After preconditioning and re-saturation, the specimens were placed with the test surface downwards in a cylindrical glass cup with a diameter of 135mm. The cup was filled with a 12mm deep layer of 3% NaCl solution. A plastic ring on the bottom of the cup maintained a 10mm space between the test surface and the bottom of the cup. The temperature was measured in the salt solution under the test surface. The glass cup was thermally insulated on all sides except the bottom of the cup.

The method used is similar to the earlier version of SS 13 72 44, called SS 13 72 36. However, the temperature curve used is the same as is used in SS 13 72 44.

Results at the age of 31 days

Figure 3.14 a) shows the results for freeze-thaw tests that started at 31 days of age, for specimens conditioned in climate chambers with and without carbon dioxide. As it can be seen, carbonated Portland cement concrete specimens show much lower scaling than specimens conditioned in an environment without carbon dioxide. For both carbonated and uncarbonated Portland cement concrete qualities, the resistance against salt-frost scaling is reduced for an increase in w/b ratio. However, the effect of the water/binder ratio is marked for uncarbonated specimens, whereas for carbonated concrete, the increase in the mass of scaled material due to the increase of w/b ratio is only noticeable for concrete qualities with w/b ratio of 0.55, being negligible for lower w/b ratios (0.45 and 0.35).

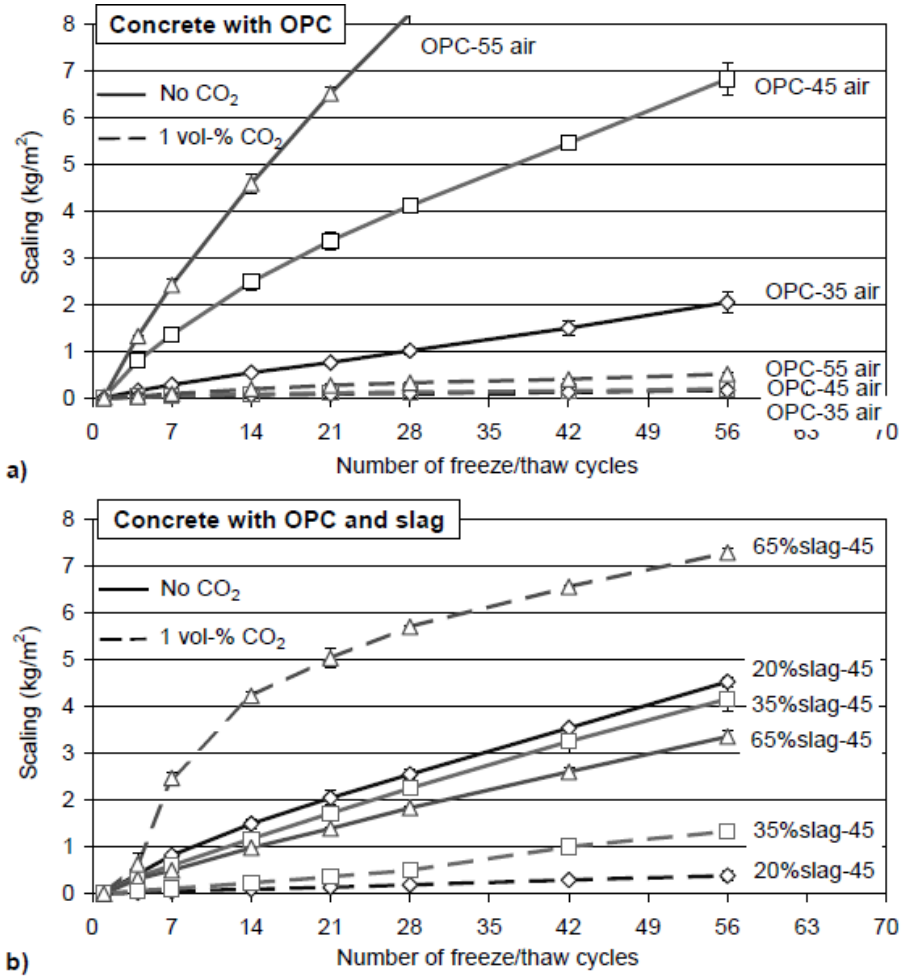

Figure 3.14 - Scaling as a function of the number of freeze/thaw cycles for concrete with different binder types/combinations, conditioned in climate chambers with and without carbon dioxide. The age at the start of the freeze/thaw test was 31 days. a) OPC, b) OPC + slag [Utgennant (2004)]

As for concrete with additions of GGBS, Figure 3.14 b) shows that the scaling resistance of uncarbonated concrete increases with increasing slag content, with concrete with 65% of GGBS content presenting the lowest amount of scaling. Carbonation, however, affects the salt frost scaling of the specimens with different slag contents in a different manner: for concrete with small additions of slag (up to 35% of replacement), carbonation leads to a significant reduction of the accumulated scaled material. Contrarily, it seems that for concrete qualities with high GGBS content the effect is the opposite: according to the results, carbonation results on significant deterioration due to salt-frost scaling, at least for concrete qualities with 65% of GGBS as part of the binder.

From the appearance of the scaling curve for the carbonated concrete with 65% GGBS, it seems clear that severe scaling takes place during the first 14 freeze/thaw cycles, after which the rate of scaling slows down and becomes about the same as for non-carbonated concrete. This fact points to the existence of a layer, probably the carbonated layer, which is scaled off during the initial part of the freeze/thaw test. When the carbonated layer is scaled off, the rate of scaling becomes the same as for uncarbonated concrete.

Similar results have been reported by Stark and Ludwig (1997), who showed that the initial large scaling of carbonated concrete containing high amounts of slag as part of the binder correlates very well with the thickness of the carbonated layer. The authors reached that conclusion by comparing the depth of the scaling with the depth of carbonation for different concrete qualities containing more than 60% slag, and with and without entrained air.

Influence of drying and carbonation on the scaling results - testing at different ages

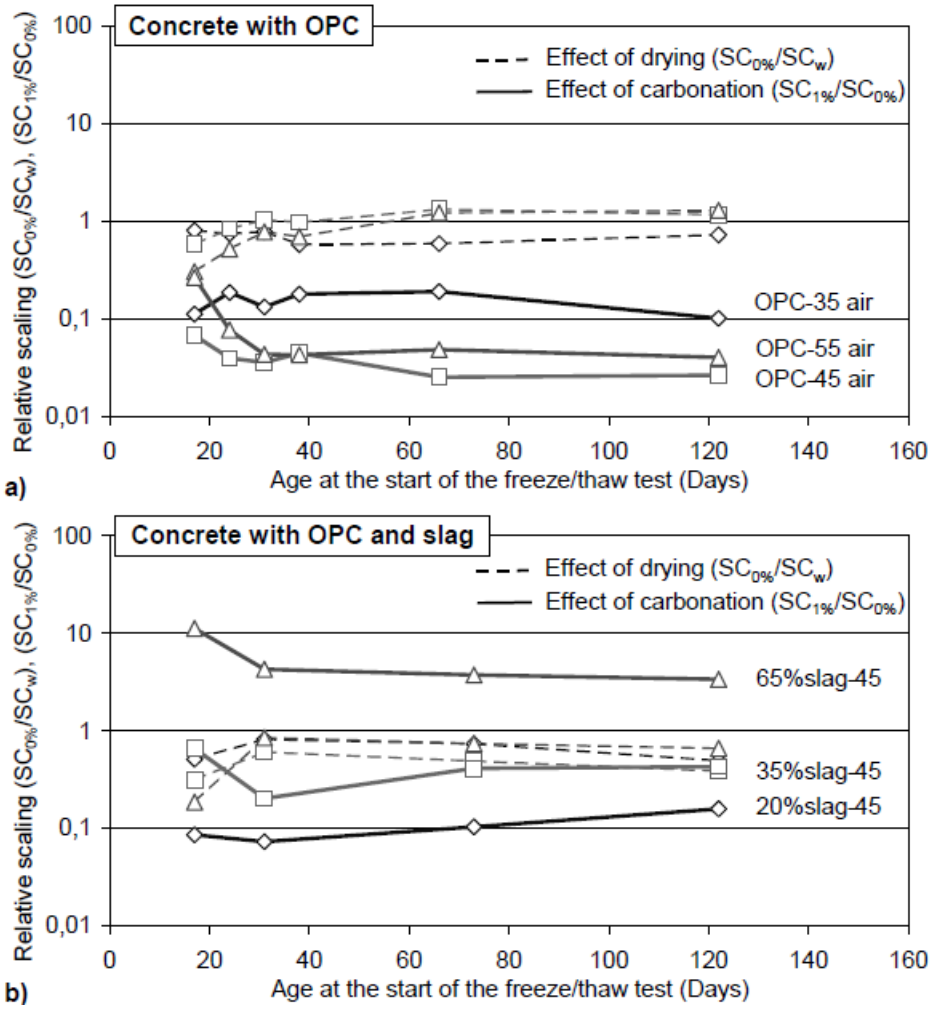

Figure 3.15 - Relative scaling after 14 freeze/thaw cycles as a function of age at start of the freeze-/thaw test. Effect of carbonation = scaling (carbonated) / scaling (uncarbonated): (SC1%/SC0%). Effect of drying = scaling (uncarbonated) / scaling (water cured):(SC0%/SCw). a) OPC, b) OPC + slag [Utgennant (2004)].

The results presented in Figure 3.15 a) show that the effect of carbonation in Portland cement concrete qualities is markedly positive for all w/b ratios, and at all ages, though being less pronounced at early ages, at least for w/b ratios of 0.45 and 0.55. At an age of 31 days or more, however, the scaling of these concrete qualities is significantly reduced due to carbonation, when compared to the uncarbonated mixes. The relative effect of carbonation for concrete qualities with low w/b ratio (0.35),

though positive, is less pronounced. This fact is attributed to the high scaling resistance of the uncarbonated material, which results on a higher value of the SC1%/SC0% ratio.

As for concrete with GGBS as part of the binder, a significant difference of the influence of carbonation is shown, depending on the slag content. For concrete with 20% slag as part of the binder, the effect of carbonation is considerably positive at all ages, as it can be seen in Figure 3.15 b). For concrete with 35% GGBS, only a small positive effect of carbonation is noticed at early ages. At 31 days of age or more, on the other hand, the effect of carbonation is significantly positive, with this concrete quality presenting less than half the scaling of the comparable uncarbonated concrete.

Conversely, for concrete with 65% slag as part of the binder, the effect of carbonation is negative at all test ages. This negative effect of carbonation is most noticeable at early ages. At an age of 31 days or more, the negative effect of carbonation is not so obvious, but the scaling for carbonated concrete is still over three times the scaling for the uncarbonated material. For concrete specimens older than 31 days of age at the start of testing, the relative effect of carbonation is almost the same regardless of the age at the start of testing.

The results presented in Figure 3.15 a) and b) also show that the effect of drying is usually positive, though rather small, when compared to the effect of carbonation.

Conclusion

Utgennant (2004) found a strong correlation between carbonation and salt frost resistance of concrete with additions of GGBS. For concrete with slag as part of the binder, the results have shown that carbonation improves the scaling resistance for concrete with low to medium amounts of slag as part of the binder (up to 35% of the binder content), even though the positive effect of carbonation is not as high as for concrete with OPC alone as the binder. However, this positive effect is considerably reduced with increasing slag content, changing from positive for concrete with low slag contents to negative for concrete with high slag contents (with 65% of binder weight). The main reason for this observation was attributed to the formation of a carbonated layer, where the properties of the material are altered in a way that leads to a considerable reduction of the scaling resistance (for instance, a coarser pore structure, which increases the capillary suction and, consequently, the amount of freezable water in this layer).

Utgennant (2004) conducted further studies to evaluate the effect of carbonation in the parameters that influence the salt-frost resistance of concrete (capillary suction, freezable water content, critical degree of saturation), both for Portland cement concrete and for GGBS concrete. The results showed that, during long-time water absorption, carbonation of concrete with high amounts of slag leads to an increase in degree of saturation, in opposition to Portland cement concrete. The author also found that carbonation results in a reduced total porosity for all concrete qualities tested. However, for Portland cement concrete, carbonation results in a denser pore structure, with a larger part of the porosity belonging to the fine porosity, whereas for slag concrete, carbonation leads to a coarsening of the pore structure, i.e., fine porosity is reduced, but coarse porosity is increased. The increase in coarse

porosity of carbonated GGBS concrete was also found to be strongly related with the increase of freezable water content reported for these concrete qualities.

Utgennant (2004) showed the strong influence of ageing of concrete in the salt-frost scaling of concrete. The influence of ageing increases the difficulty in predicting the field behaviour of a concrete mix, especially considering that in the majority of the standard test methods that evaluate the salt-frost scaling of concrete the first freeze-thaw cycle occurs between 28 and 31 days of age.

3.4.2. Field Studies

3.4.2.1. Utgennant, 2004

Utgennant (2004) complemented his laboratory study with a field investigation carried out at 3 field exposure sites during five winter seasons. Two of these exposure sites were situated in saline environments: one being a marine environment (Träslövsläge harbour) and one a highway environment (where de-icing agents are frequently used). The third exposure site was located in a salt-free environment (premises of SP, the Swedish National Testing and Research Institute).

Concrete qualities with five different water/binder (w/b) ratios (0.30, 0.35, 0.40, 0.50 and 0.75), and with and without entrained air were produced for different binder combinations:

- Portland cement concrete (reference);
- Concrete with 30% of GGBS (of the total weight of cementitious materials) added in the mixer;
- Concrete produced with Dutch slag cement CEM III/B, with approximately 70% of slag.

One mix with 5% silica fume was also produced and tested, though the results for this mix will not be further discussed.

The cubic specimens to be placed at the field exposure sites were, after water curing for 7 days, stored in climate chambers with 50% R.H. and temperature of +20ºC, during a period between one and a half and three months. Between eight and twelve days before the specimens were placed in the field, the cubes were cut, resulting in two specimens with the shape of a half 150mm cube with one cut surface and the rest mould surfaces. After cutting, the specimens were returned to the climate chamber until they were placed at the test sites. Two specimens of each quality were placed at each test site.

The damage of the specimens was evaluated by measuring the volume of the specimens. A decrease in volume means loss of material due to scaling of the specimens. An increase in volume means internal damage of concrete. The volume of the specimens was calculated from the results obtained for the measurements of the weight of the specimens in water and surface-dry in air. In order to assess the internal damage of concrete, ultrasonic pulse transmission time was also measured on a regular basis.

The first measurement was carried out before placing the specimens at the test sites. The specimens placed at the highway site were then measured once a year, and the specimens located at the other two sites were measured after two, four and five years. The specimens sited at highway environment were also measured after seven years, though only the results up to 5 years will be presented, for direct comparison of the results for the tree sites.

Highway environment

Figure 3.16 shows the results for the highway environment after five winter seasons. As it can be observed, all non-air-entrained concrete qualities with w/b ratio of 0.75 displayed a significant volume reduction, with both concrete qualities containing slag presenting the most damage, and Portland cement concrete presenting somewhat better resistance (Figure 3.16 a)). For lower w/b ratios, the damage is lower for all concrete qualities. However, CEM III/B concrete still shows poor resistance even for w/b ratios as low as 0.50 or 0.40, whereas for all other concrete qualities, no significant damage is registered for w/b ratios bellow 0.50.

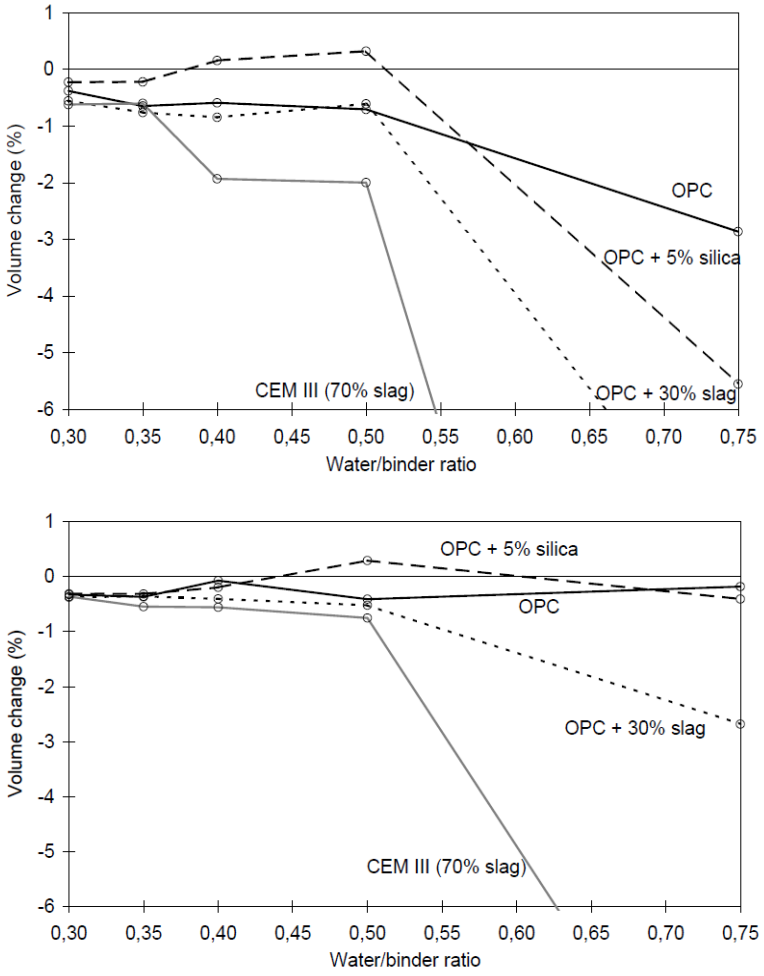

Figure 3.16 -Volume change after five winter seasons at the highway exposure site. Concrete with different binder combinations and water/binder-ratios: a) Not air entrained; b) 4,5 % air.

As for air-entrained concrete qualities, Figure 3.16 b) shows volume reduction for all specimens with w/b ratio of 0.75 placed at highway environment. However, the volume reduction for Portland cement

concrete is relatively low, at least when compared to the volume reduction of the specimens with slag as part of the binder, which show increasing damage with increasing slag content.

All air entrained concrete qualities with w/b ratios up to 0.5 show limited volume reduction after five years exposure, except CEM III/B concrete, which shows significant decrease in volume (Figure 3.16b)). For these qualities, air entrainment does not seem to have a noticeable positive effect on the salt frost resistance, at least in the aggressive highway environment.

Marine environment

Figure 3.17 presents the results for the frost resistance of specimens placed in marine environment during 5 winter seasons.

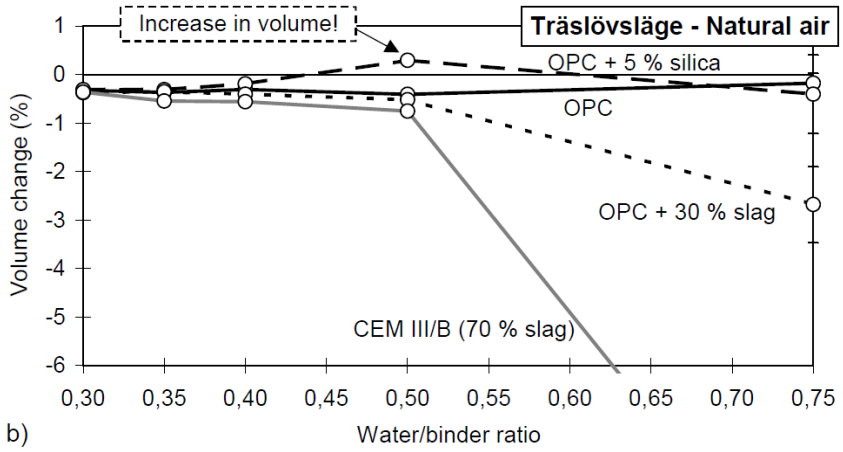

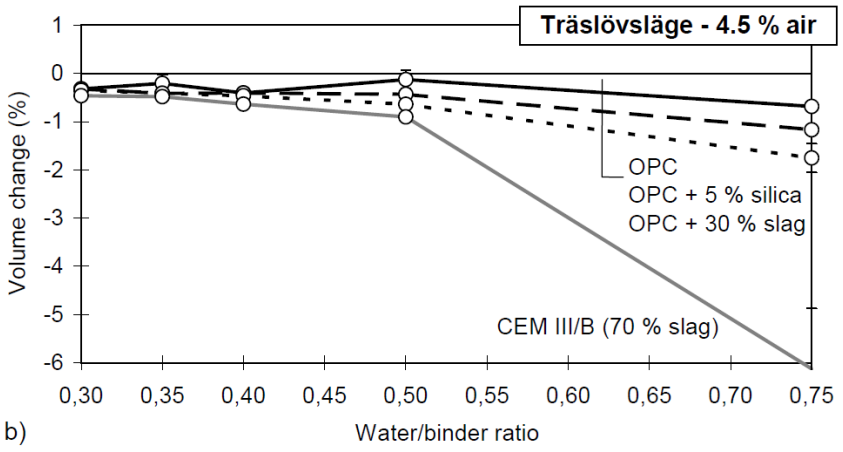

Figure 3.17 - Volume change after five winter seasons at the marine exposure site. Concrete with different binder combinations and water/binder-ratios: a) Not air entrained; b) 4.5% air.

As it can be seen in Figure 3.17 a), for non-air entrained concrete qualities, only concrete qualities with high w/b ratios and containing slag show signs of damage, with the damage increasing with an increase in the slag content. As for air-entrained concrete, only CEM II/B concrete with w/b ratio of

0.75 showed significant damage (Figure 3.17 b)). For all other concrete qualities with w/b ratio of 0.75, the volume reduction detected was not significant, and no damage was detected for any on the concrete qualities with w/b ratio lower than 0.50.

The results also revealed that concrete in marine environments, exposed only to salts that naturally exist in sea water, is much less severely damaged than concrete in highway environments, where the temperature is usually lower and where de-icing agents are used. Similar observations were also reported by Peterson (1995).

Environment without salt exposure

Figure 3.18 displays the results for the volume change of the concrete qualities placed in an environment without salt exposure during 5 winter seasons.

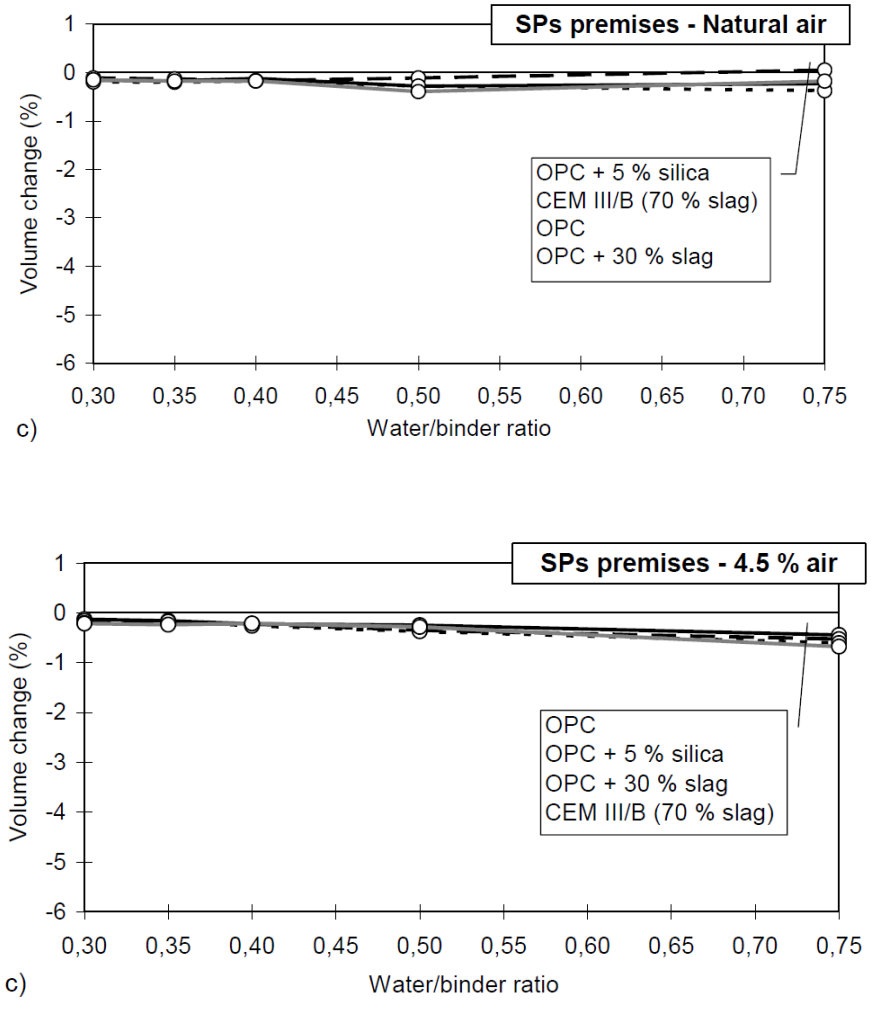

Figure 3.18 - Volume change after five winter seasons at the salt-free exposure site. Concrete with different binder combinations and water/binder-ratios: a) Not air entrained; b) 4.5% air.

For all concrete qualities placed on an environment without salt exposure, both with or without entrained air, no noticeable damage was detected after five winter seasons, even for w/b ratios as high as 0.75 (Figure 3.18).

The results from the field investigation carried out by Utgennant (2004) show that, in general, air entrainment improves the salt-frost resistance of concrete, even for high water/binder ratios. However, this does not seem to be valid for concrete qualities with high slag content. The investigation showed that air entrained concrete qualities with CEM III/B as a binder presented damage of the same order as - and sometimes even greater - than non-entrained concrete of the same quality, as is the case for the specimens placed in highway environment (Figure 3.16 a) and b)). For concrete qualities with 70% of slag content, entrained air does not seem to improve the scaling resistance.

On the other hand, the investigation showed the use of slag as part of the binder leads to a poorer resistance of concrete against salt scaling, particularly when high amounts of GGBS are used. In fact, concrete with CEM III/B as a binder showed considerable scaling, even with w/b-ratio as low as 0.40 and with entrained air (at least for harsh environments as highways). On the other hand, even though some damage was registered for 30% GGBS concrete with a w/b ratio of 0.50, for air-entrained qualities with a w/b ratio of 0.40 or below, no signs of either external or internal damage were detected.

The investigation then reveals that it is possible to produce slag concrete resistant against salt frost scaling, even for environments as severe as highways, at least for concrete with slag replacements up to 30%, as long as proper air entrainment is provided, along with low w/b ratios.

3.4.2.2. Schlorholtz and Hooton, 2008

Schlorholtz and Hooton (2008) studied the field performance of existing concrete pavements and bridge decks made with slag cement that have been exposed to freeze-thaw cycles in the presence of deicing chemicals during their service life.

Field sites containing ternary mixtures (Portland cement with the addition of slag and another supplementary cementitious material, usually fly ash or silica fume) were investigated. The field study was limited to sites in freezing environments were de-icing agents are used during winter, mainly bridge decks and road pavements. The sites were also selected to provide a wide a range of slag content in concrete. The slag content in the samples extracted and tested varied between 20% replacement (typically in bridge decks containing ternary mixtures with silica fume) and 50% (pavement concrete). In addition, an attempt was made to obtain cores from concrete with a wide range of ages.

Table 3.3 shows the sites investigated, the date of construction of the structures, the slag content and the visual observation of the surface scaling carried out in situ. Table 3.3 shows that bridge decks are usually more susceptive to salt-scaling damage than highway pavements. However, it can be observed there are concrete mixes with up to 50% of GGBS of the total binder content that do not show scaling, even in environments where deicer salts are used (highway pavements).

Table 3.3 – Location, type of site, the date of construction, slag content in the concrete mix and visual observation of the slag scaling in situ for all the sites investigated.

Site	Location - Type of Site	Date Constructed	% Slag (others)	Scaling
1a	IA, Highway 520 EB, Hamilton County milepost 156.45 - Pavement	12/10/1999	35% (15% Class C Fly Ash)	None observed
1b	IA, Highway 520 EB, Hamilton County milepost 157.20 - Pavement	14/10/1999	35% (15% Class C Fly Ash)	Inconclusive due to surface problems
1c	IA, Highway 520 EB, Hamilton County milepost 157.85 - Pavement	15/10/1999	35% (15% Class C Fly Ash)	None observed
2a	IA, I-35 NB, Hamilton County milepost 143.45 - Pavement	30/06 to 03/07/2003	35% (15% Class C Fly Ash)	None observed
2b	IA, I-35 NB, Hamilton County milepost 143.55 - Pavement	30/06 to 03/07/2003	35% (15% Class C Fly Ash)	None observed
3	IA, Euclid Bridge EB, Polk County - Bridge Deck	10/11 and 13/11/2003	35% (15% Class C Fly Ash)	Gutter and deck
4	IA, Euclid Bridge WB, Polk County - Bridge Deck	17/06 and 19/06/2003	35% (15% Class C Fly Ash)	Gutter only
5	CT, Bridge deck #1863	2005 (April ?)	20% (5% silica fume)	Gutter and deck
6	DE, SR 896 SB, New Castle County - Pavement	10/1990 to 8/1991	25% (10-15% fly ash)	Inconclusive (scale or abrasion?)
7	DE, SR 1 SB, Kent County - Pavement	10/1992 to 6/1993	50%	None observed
8	KS, Lamar Roundabout, Overland Park - Pavement	2002	35%	Cover panels
9	KS, Nall Avenue, Leawood - Pavement	2005	25%	None observed
10	MI, M 45 EB, Kent County - Bridge Deck	10/2001	30%	None observed
11	MI, M45 WB, Kent County - Bridge Deck	05/2002	30%	None observed
12	NY, SR 378 EB, Albany County - Bridge Deck	03/08/2004	20% (6% silica fume)	Inconclusive (scale or abrasion?)
13	NY, Taconic State Parkway, Columbia County - Bridge Deck	17/10/2002	20% (6% silica fume)	Gutter and deck

Core samples with 6 in. (152mm) of diameter and 3 in. (76mm) thick were extracted from 12 field sites: 6 pavement sites and 6 bridge decks. Two or three test specimens from each site were subjected to the scaling tests following the procedures described in the North-American Standard ASTM C 672/C 672 M-03. A petrographic examination of the specimens was also performed.

The test specimens used for the scaling tests consisted of the top sections of the concrete cores that were extracted from the sites. In order to pour the salt solution on the top surface of the cores, the sides of the cores were sealed with a bituminous membrane with a berm about 1.8 in. (45mm) above the exposed concrete surface. Silicone sealant was applied around the edges at the top and at the

bottom of the specimens. The surface of each specimen was then covered with approximately 0.25 in. (6mm) of a 4% calcium chloride solution, according to ASTM C 672/C 672 M-03.

The specimens were exposed to 50 cycles of freezing (for approximately 16 hours) and thawing (approximately 8 hours) per day. At every five cycles the solution was changed, the surface of each test specimen was visually evaluated, and the surface mass loss was measured. This process was continued for 50 freeze thaw cycles. The results of the scaling tests are presented in Table 3.4.

Table 3.4 – Salt-scaling results for the cores extracted from the sites

Site	Location	Visual Rating (at start of test)	Visual Rating (at end of test)	Mass loss lb/yd^2 / (kg/m^2)
1a	IA, Highway 520 EB milepost 156.45	0	0	0.35 / (0.159)
1b	IA, Highway 520 EB milepost 157.20	1	1	0.39 / (0.177)
1c	IA, Highway 520 EB milepost 157.85	0	0	0.29 / (0.132)
2a	IA, I-35 NB, milepost 143.45	0	0	0.17 / (0.077)
2b	IA, I-35 NB, milepost 143.55	0	0	0.18 / (0.082)
6	DE, SR 896 SB, New Castle County	0	0	0
7	DE, SR 1 SB, Kent County	0	0	0.24 / (0.109)
10	MI, M 45 EB, Kent County	0	0	0.66 / (0.299)
11	MI, M 45 WB, Kent County	0	0	0.53 / (0.240)
13	NY, Taconic State Parkway	1	2+	1.95 / (0.885)

According to the Ontario Provincial Standard OPSS LS-412 (a modification of the North-American Standard ASTM C 672), the allowable scaling loss after 50 cycles is 1.5 lb/yd^2 (0.680 kg/m^2). The results in Table 3.4 show that only cores extracted from Site 13 (20% slag and 6% silica fume) exhibited scaling mass loss higher than this value. However, the authors refer that problems in the extraction of the core for this site have probably contributed to some of the mass loss, especially around the edges of the specimen.

The results also show that bridge deck cores presented more mass of scaled material than pavement cores, which is in accordance with the assessment carried out in situ. Bridge decks are more vulnerable to freeze/thaw cycles than road pavements, as they remain wet for longer periods [Neville (2003)].

After the testing had been completed, a section of the test specimen (or the entire test specimen) from each site was subjected to petrographic examination. Petrographic examinations of the core specimens from the different sites indicated that four out of the seven sites that exhibited scaling showed evidence of retempering, i.e., addition of water on site to restore workability (which indicates that these concretes may in fact present a higher water/binder ratio than the initially assumed). In fact, two of the sites whose specimens revealed higher scaling tended to have significantly higher water-cementitious material ratios than was expected from the nominal mix design information that was

provided. Hence, the authors concluded that, for this study, the construction-related issues had a higher influence in the scaling resistance of concrete than the amount of slag.

Furthermore, spacing factors of 0.008 in. (0.2mm) or less, when combined with an adequate volume of entrained–air voids, are usually considered to indicate that concrete will exhibit good resistance to freeze-thaw deterioration. The only spacing factors obtained above 0.008 in. were observed in cores from Site 7, with 50% of GGBS replacement (tested on three separate cores, resulting in values of 0.012 in., 0.010 in., and 0.007 in.). The high spacing factors at this site appeared to be related to a very coarse air-void system, which agrees with the literature, which points to a coarsening of the pore structure of the carbonated slag concrete [Utgennant (2004)]. Nevertheless, specimens from Site 7 revealed acceptable salt-frost resistance.

The present investigation showed that scaling is occasionally observed on field concrete pavements and bridge decks that contain slag cement. However, the field scaling that was observed was slight and appeared to have little impact on the long-term durability of the structure. From the results of this investigation, it seems that it is possible to use slag replacements up to 50% without significant salt-scaling damage, even for harsh environments such as highway pavements.

4. Experimental study

4.1. Introduction

The aim of the laboratory study carried out during this project was to evaluate the effect of the replacement of Portland cement by GGBS on the properties of fresh and hardened concrete, with emphasis on its salt-frost resistance, and to assess whether it is possible to produce concrete with GGBS that presents acceptable resistance against frost attack in the presence of salts with higher amounts of slag than the limit of 25% by CEM I weight described in SS 13 70 03 (2008). Air entrained concrete mixes with different amounts of replacement were produced and tested (0%, 25%, 50% and 100% of GGBS by weight of CEM I).

The present chapter describes the materials used, the proportions of the different concrete mixes, the specimens casted, and the tests performed (main purpose, standard followed, material used, number of samples and expression of the results).

The tests performed on the freshly mixed concrete were the following:

- Slump test, according to SS-EN 12350-2 (2009);
- Air content, according to SS-EN 12350-7 (2009);
- Air void analysis.

The tests performed on the hardened concrete included:

- Compressive strength, according to SS-EN 12390-3 (2009);
- Rapid chloride migration, according to NT Build 492 (1999);
- Salt-frost scaling, according to SS 13 72 44 (2005).

4.2. Materials

As a main binder, a moderate heat, low-alkali, sulphate-resistant Portland cement was used: *Cementa Degerhamn Anläggningscement* (CEM I 42.5 N MH/SR/LA), produced by Cementa AB. The cement is CE-marked, and complies with SS-EN 197-1. Its compact density is 3200±20 kg/m^3 and Blain specific surface is 310±30 m^2/kg.

The coarse aggregates used were Swedish natural and crushed stone, *Tagene* (4-8 mm and 8-16 mm). The fine aggregates used were *Sjösand* (0-4 mm) and *Hol* (0-8 mm).

The Ground Granulated Blast Furnace Slag used was *Slagg Bremen*, imported by Thomas Cement from Holcim Deutschland A.G. The GGBS complies with all the specifications required by SS-EN 15167-1 (see Table 4.1), and was added separately in the mixer. The main properties of the GGBS used, according to its technical sheet (tested according to SS-EN 15167-1, with mortar

samples of 50% of CEM I 42.5 or 52.5, and 50% of GGBS, compared with samples with 100% of Portland Cement) are presented below:

Table 4.1- Properties of the GGBS used (*Slagg Bremen*) and requirements in SS-EN 15167-1 [Thomas Concrete Group (2012)]

Property	Characteristic values	Requirements in SS-EN 15167-1
Specific surface	420±20 m^2/kg	≥ 275 m^2/kg
Activity index (7/28 days)	≥ 55/75 %	≥ 45/70 %
Setting Time	≤ 1,3	≤ 2,0

Thomas Concrete Group AB tested the activity index of the GGBS used in this experimental work (*Slagg Bremen*) with different cements, including the *Cementa Anläggningscem*ent (CEM I 42.5 MH/SR/LA) used in the project. The results obtained (mean values) are presented in Figure 4.1.

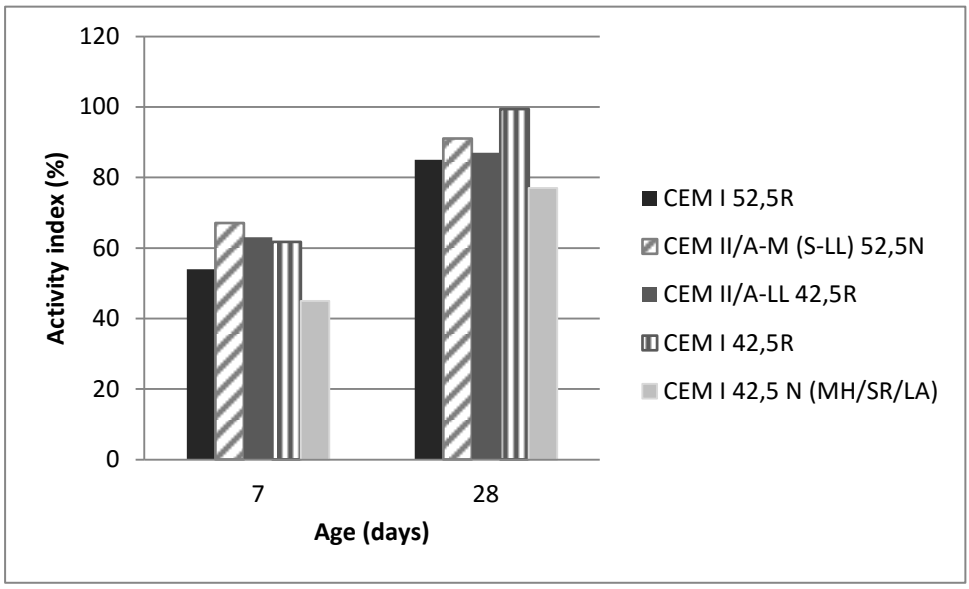

Figure 4.1 - Activity index of the GGBS in combination with different types of cement, tested at 7 and 28 days of age. Test according to EN 196-1.

As shown in Figure 4.1, the combination of the GGBS with the CEM I 42.5 N (MH/SR/LA) results on an activity index of 45% at 7 days and 77% at 28 days of age, which complies with the requirements of SS-EN 15167-1 (2006) (Table 4.1). The activity index obtained in combination with CEM I 42.5 N (MH/SR/LA) at 7 days of age at was, however, lower than the 55% described in the catalogue. Nevertheless, for all cement types tested by Thomas Concrete Group, the GGBS used complied with the requirements presented in SS-EN 15167-1 (2006).

4.3. Concrete mixes

Concrete qualities with four different GGBS contents were produced. The Swedish Standard SS 13 70 03 (2008) expresses the GGBS content in a concrete mix as percentage of mass of CEM I. The four different GGBS contents studied were:

- 0% GGBS, reference (Mix 1);
- 25% GGBS (which is the maximum amount of GGBS allowed for XF4 exposure class according to SS 13 70 03 (2008), see Table 2.3) (Mix 2);
- 50% GGBS (Mix 3);
- 100% GGBS (Mix 4).

The concrete mixes were prepared so that its compressive strength would fall on the C32/40 class of strength defined in SS 13 70 03 (2008) (with a minimum characteristic cube strength of 40 MPa).

The equivalent water/cement ratio used was 0.45 for all of the mixes, which is the maximum allowed in SS 13 70 03 (2008) for exposure class XF4 (Table 2.3).

The efficiency factor considered in the present investigation was 0.6, which is the highest *k*-factor allowed for GGBS added in the mixer together with CEM I, according to SS 13 70 03 (2008). Therefore, according to equation (1), the equivalent water-cement ratio, $(w/c)_{eq}$ is given by:

$$(w/c)_{eq} = \frac{w}{c + 0.6\,S} \qquad (1)$$

An additional concrete mix (Mix 6) with 50% GGBS was defined using a *k*-factor of 1, i.e., in this mix, the mass of slag replaces the exact same mass of Portland cement.

All concrete qualities were air entrained. The air content was targeted at 4.5±0.5%. The targeted air content for each mix was achieved using a synthetic tenside air entraining agent by Sika, *SikaAer*-S (1:10). *SikaAer-S* is produced by Sika Sverige AB in Sweden. The properties of *Sika-S* are shown in Table 4.2 below.

In order to evaluate the effect of an increased air content on the different properties of the hardened concrete, particularly the salt-scaling resistance of concrete with GGBS, an additional mix with 50% of slag replacement and targeted air content of 6.0±0.5% was produced (Mix 5).

The proportion of each concrete mix was chosen so that its consistency would correspond to an S3 class of slump (between 100 and 150mm). The desired slump was achieved with help of a superplasticizer. A third generation Polycarboxylate Ether (PCE) based superplasticizer produced by Sika Sverige AB, *Sikament* 56/50, was used.

Table 4.2 - Properties of SikaAer-S

Property	Characteristic values
Density	1.01 kg/dm³
pH value	≈ 7
Chloride content	<0.10% by weight of the solvent
Alkaline Content, eq. Na_2O	<0.5% by weight of the solvent
Solids	≈ 4.5%
Viscosity	Light liquid
Colour and shape	Transparent liquid

In order to achieve the targeted $(w/c)_{eq}$ and air contents, there were cases in which it was not possible to maintain consistency within the class S3 limits mentioned above. Since the equivalent water/cement ratio and the air content are the factors which influence the most the frost resistance of concrete, these parameters were kept constant, and only the amount of superplasticizer was adjusted. Nevertheless, even after some trial mixes were casted to assess the amount of superplasticizer needed to achieve the targeted slump, some mixes still fell outside the targeted slump limits.

Two additional mixes were produced without superplasticizer: one with 0% GGBS (Mix 7), and another with 50% GGBS (Mix 8), both with a targeted air content of 4.5±0.5%. The aims of producing these mixes were: to investigate if there is a significant influence of the use of superplasticizer together with AEA in the air void systems of the mixes; to evaluate if using superplasticizer together with AEA influences the salt frost scaling of concrete; and to investigate if it was possible to entrain the desired amount of air in the concrete by using only the air entraining agent, without exceeding the dosage recommended by the producer of the AEA.

Summarizing, a total of eight different mixes were produced:

- **Mix 1** - 0% GGBS, 4,5±0.5% Air (reference concrete);
- **Mix 2** - 25% GGBS, 4.5±0.5% Air, efficiency factor *k*=0.6;
- **Mix 3** - 50% GGBS, 4.5±0.5% Air, efficiency factor *k*=0.6;
- **Mix 4 -** 100% GGBS, 4.5±0.5% Air, efficiency factor *k*=0.6;
- **Mix 5** - 50% GGBS, 6.0±0.5% Air, efficiency factor *k*=0.6;
- **Mix 6 -** 50% GGBS, 4.5±0.5% Air, efficiency factor *k*=1;
- **Mix 7 -** 0% GGBS, 4.5±0.5% Air, no superplasticizer;
- **Mix 8 -** 50% GGBS, 4.5±0.5% Air, efficiency factor *k*=0.6, no superplasticizer;

The proportions of all the components of the final mixes are presented in the Table 4.3 below:

Table 4.3 – Final mix design

	Mix							
	1	2	3	4	5	6	7	8
Amount of GGBS (as % of CEM I)	0	25	50	100	50	50	0	50
***k*-factor**	-	0.6	0.6	0.6	0.6	1.0	-	0.6
Targeted air content [+/-0,5%] (%)	4.5	4.5	4.5	4.5	6.0	4.5	4.5	4.5
$(w/c)_{eff}$ ratio	0.45	0.52	0.59	0.72	0.59	0.68	0.45	0.59
(w/b) ratio	0.45	0.41	0.39	0.36	0.39	0.45	0.45	0.39
$(w/c)_{eq}$ ratio	0.45	0.45	0.45	0.45	0.45	0.45	0.45	0.45
Cement [kg/m^3]	390	330	330	280	330	250	390	330
GGBS [kg/m^3]	0	82.5	165	280	165	125	0	165
(GGBS/total binder) ratio	0.00	0.20	0.33	0.50	0.33	0.33	0.00	0.33
Equivalent cement content	390	379.5	429	448	429	375	390	429
Aggregate								
Sjösand (0-4mm) [kg/m3]	449.8	446.4	410.7	388.6	410.7	455.0	449.5	411.5
Hol (0-8mm) [kg/m3]	274.7	272.7	250.8	237.3	250.8	277.9	274.5	251.3
Tagene (4-8mm) [kg/m3]	121.6	120.7	111.1	105.0	111.1	123.0	121.5	111.2
Tagene (8-16mm) [kg/m3]	885.7	879.0	809.2	765.1	809.2	896.0	885.1	810.2
Water [kg/m3]	175.5	170.8	193.1	201.6	193.1	168.8	175.5	193.1
AEA [kg/m3]	0.975	0.990	1.155	1.120	2.475	1.000	2.730	2.970
AEA [% of cement by weight]	0.25	0.30	0.35	0.40	0.75	0.40	0.70	0.90
AEA [% of binder by weight]	0.25	0.24	0.23	0.20	0.50	0.27	0.70	0.60
Superplasticizer [kg/m3]	1.365	1.320	2.145	1.400	1.155	1.125	0	0
Superplasticizer [% of cement by weight]	0.35	0.40	0.65	0.50	0.35	0.45	0	0
Superplasticizer [% of binder by weight]	0.35	0.32	0.43	0.25	0.23	0.30	0	0

4.4. Mixing and casting

For each concrete quality, two mixes of about 30 liters were produced using a Zyklos rotating pan mixer. The surface of the mixer was moist, and all dry materials (aggregates and binders) were added, followed by the water. After mixing these components for 30 seconds, the air entraining agent and the superplasticizer were added, and the concrete was mixed for another 120 seconds.

Directly after mixing, the following tests on the freshly mixed concrete were performed:

- Slump test, according to SS-EN 12350-2 (2009);
- Air content, according to SS-EN 12350-7 (2009);
- Air void analysis in the fresh state.

The test procedures followed are described in the next sections.

After mixing, concrete was cast in cylindrical and cubical moulds that comply with specifications in SS-EN 12390-1 (2001) for testing hardened concrete. About 1 cylinder and 5/6 cubes were cast from

each concrete mix, on a total of 2 cylinders and 11 cubes per concrete quality (2 mixes per concrete quality). During casting, the moulds were filled in two stages, being compacted during 15 seconds between the fillings. A vibrating table (frequency 50-60Hz, amplitude ±0.5mm) was used for compaction. After 24 hours, the specimens were removed from the moulds and curing began. The number of specimens per test, the age at which they were tested and the geometry of the specimen are described in Table 4.4.

Table 4.4 – Specimens casted, geometry of the moulds and age of testing of the hardened concrete

Test in the hardened concrete	Age (days)	Number of specimens	Geometry (mm)
Compressive Strength (EN 12390-2)	7	2	Cube, 150 (e)
	28	3	
	56	2	
Rapid Chloride Migration (NT Build 492)	28	1	Cylinder, 100 x 200 (Ø x h)
	56	1	
Scaling under freeze/thaw (SS 13 72 44)	31	4	150x150x50 slabs cut from cube, 150 (e)

4.5. Curing

4.5.1. Standard curing

After 24 hours in the moulds, the specimens were unmoulded and the curing began. The curing procedure followed by each specimen depends on the test in the hardened concrete that the specimen would be subjected to, and are described below.

- Specimens to be tested for compressive strength (according to SS-EN 12390-3)

The curing procedure followed the standard *SS-EN 12390-2 (2009): Testing hardened concrete. Making and curing specimens for strength tests*. After demoulding, the concrete specimens were placed in water at 20ºC until the time of testing (7, 28 or 56 days of age).

- Specimens to be tested for Rapid Chloride Migration (standard NT Build 492)

For the Rapid Chloride Migration test, the specimens were also cured according to SS-EN 12390-2 (2009) (water curing at 20ºC) until the start of the pre-conditioning. The pre-conditioning starts 24 hours before the test, which means that specimens tested at 28 days were water cured (at 20ºC) up to the 27th day of age, and specimens tested at the age of 56 days followed the same curing procedure up until the 55th day.

- Specimens to be tested against scaling at freezing (according to SS 13 72 44)

The curing of the specimens followed the procedure in *SS 13 72 45 (1995): Concrete Testing. Hardened Concrete. Concrete cubes for frost testing.* After 24 hours, the specimens were placed

in water at 20ºC for 6 days. In the 7th day, the specimens were placed in the climate chamber at (20±2)ºC, with (65±5)% of relative humidity, where they were stored during the next 14 days. At the 21 days of age, a 50 mm slab was sawn off the cube, and the pre-treatment started. The pre-treatment procedure followed the method described in SS 13 72 44: Concrete testing. Hardened concrete. Frost resistance., and will be described later in this chapter.

4.5.2. Curing at increased temperature

Some specimens were cured in water at increased temperature (55ºC), in order to evaluate the effect of curing at higher temperature in the strength development of slag concrete. The rate of hydration, and, therefore, the strength development increases with an increase in temperature. Given that the hydration of slag is slower than that of Portland Cement, the main purpose of increased curing temperature was to evaluate the effect of the curing temperature on the hardened properties of concrete with the higher amounts of slag replacement. Specimens of Mix 4 (100% GGBS) and Mix 6 (50% GGBS, *k*=1) were chosen to be cured at higher temperature, and tested against compressive strength, Rapid Chloride Migration and salt-frost scaling.

The differences between the standard curing procedure and the procedure followed for the specimens cured at higher temperature, and the number of specimens cured at higher temperature, for each test method, are described below:

- Compressive strength

  One cube from Mix 4 (100% GGBS) was cured at higher temperature, and then tested at 28 days of age. After demoulding, the specimen was cured in water at 20ºC for 6 days; at the 7th day of age, the specimen was moved to water curing at 55ºC, until the age of testing (28th day).

- Rapid Chloride Migration

  Two cylindrical specimens from Mix 4 (100% GGBS) were cured at higher temperature: one to be tested at 28 days, and another to be tested at 56 days of age, respectively. The specimens were stripped out of the moulds 24h after casting, and placed in the water tank at 20ºC until the 7th day of age. Then, the specimens were placed in water at 55ºC, and curing at higher temperature continued until the pre-conditioning started: 27th day for the specimen to be tested at 28 days of age, and 55th day for specimen to be tested at 56 days of age.

- Scaling at freezing

  Three specimens from Mix 4 (100% GGBS) and three specimens from Mix 6 (50% GGBS, k=1) were cured at increased temperature: after the specimens were taken out of the moulds, they were water-cured at 20ºC for 6 days. On the 7th day, they were moved to the water at increased temperature (55ºC). On the 14th day, the specimens were placed in the climate chamber at (20±2)ºC, with (65±5)% RH, where they sat for 7 days. At the 21st day, a 50 mm slab was sawn off each cube, and the pre-treatment started.

The mixes subjected to curing at increased temperature and the tests performed are summarized in the Table 4.5 below:

Table 4.5 - Mixes cured at 55ºC and tests performed

				Curing 55ºC		
Mix	**%GGBS**	***k* factor**	**Air content (%)**	**Compressive Strength**	**RCM**	**Scaling at Freezing**
1	0	-	4,5			
2	25	0,6	4,5			
3	50	0,6	4,5			
4	100	0,6	4,5	X	X	X
5	50	0,6	4,5			
6	50	1	6			X
7	0	-	4,5			
8	50	0,6	4,5			

4.6. Tests in the fresh concrete

The consistency (slump), the total air content and the air pore structure were the parameters evaluated in the fresh concrete.

4.6.1. Slump test

The consistency of a freshly mixed concrete paste can be defined as the ease with which it flows, i.e., its relative mobility. The consistency of concrete influences mainly its workability, i.e., the effort required to manipulate (place, compact and finish) a freshly mixed concrete quality with minimum segregation. It may, also, influence other properties of concrete, such as the air entrainment. According to Neville (2003) and Ramachandran (1995), a very flowable concrete may allow the entrained air pores to “escape” the paste (which might lead to a poorer frost resistance of the mix). On the other hand, it may be difficult to entrain air on a very stiff concrete.

The consistency of the fresh concrete was determined following the procedure in *SS-EN 12350-2: Testing fresh concrete. Slump-test*. The slump test consists of filling a standard steel cone with three layers of freshly mixed concrete, each layer with the thickness that corresponds to 1/3 of the height of the steel cone. After placing one layer inside de cone, the layer is compacted with 25 strokes from a steel rod, and the next layer is added. When the cone is filled, the excess concrete is removed by sliding the steel rod across the top with a sawing motion. The steel cone is then vertically and carefully lifted up. The slump is defined as the downward movement of the concrete, being the result of the test the difference between the height of the cone and the height of the concrete at the highest point, as shown in Figure 4.2. The sample used for testing was collected from all over the mixer, in order to represent the concrete as accurately as possible. Only true slumps were considered and measured.

Figure 4.2 – Slump test

The proportions of the concrete qualities were studied so that its slump would fall on an S3 class (100-150 mm). The slump classes defined by SS-EN 206-1 (2005) are shown in Table 4.6.

Table 4.6 - Slump classes according to SS-EN 206-1 (2005).

Slump Class	Slump (mm)
1	10 to 40
2	50 to 90
3	100 to 150
4	150 to 210
5	≥ 220

4.6.2. Air content in the fresh state

The total air content of the fresh concrete was measured following the procedure for the Pressure Gauge method described in *SS-EN 12350-7 (2005): Testing fresh concrete. Air content. Pressure methods.* This method is based on the Boyle-Mariotte's law, which states that, at constant temperature, the volume is inversely proportional to the applied pressure. This method consists, therefore, of measuring the decrease in the volume of a sample of concrete when subjected to a known pressure.

An adequate vessel, with a volume larger than 5l (shown in Figure 4.3) was filled with a sample of concrete in two layers, being compacted in the vibrating table after each filling. The excess concrete was removed so that the container was full and the surface was even. The cover was then placed and clamped, in order to tightly seal the vessel. After sealing the container, water was added through one petcock, forcing the entrapped air to escape through the second petcock. Water continued to be added to the petcock until the water expelled by the second petcock was free of air. Then, both

petcocks were closed, and the vessel was pressurized using the pump to pump air into the vessel, and using the bleeder valve to stabilize the air back to the initial pressure. After pressurizing the vessel, the valve was released, and remained opened until the gauge needle stabilized. Since the pressure increased above the atmospheric pressure, the volume of air in the concrete was reduced, which resulted on a decrease of the level of the water above the concrete. Since we were using a calibrated equipment, the total air content of the sample was read directly from the gauge (in percentage by volume of concrete).

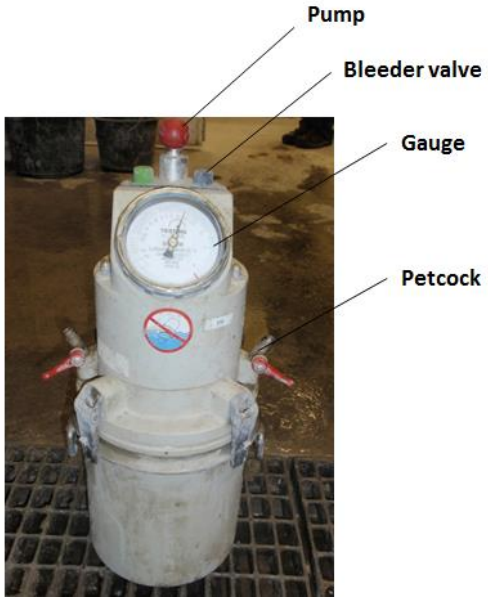

Figure 4.3 – Vessel used for measuring the total air content of concrete in the fresh state, according to SS-EN 12350-7 (2005).

This method measures the total air content, i.e. both entrained air and entrapped air, but does not give any information about the air pore size distribution or the spacing factor. In order to obtain more information about the air void system, an air void analysis in the fresh concrete was performed.

4.6.3. Air void analysis in the fresh concrete

The Air Void Analyser (AVA) is used to characterize the air void structure of the freshly mixed concrete. The characterization of the air pore system is achieved by measuring the spacing factor (the maximum distance between a point in the paste and the edge of the nearest air void) and the specific surface (the ratio of surface area of the air voids to their volume, which gives an indication of the size of the air voids) [German Instruments (2009)].

The Air Void Analyser is not a standardized test method. There are, instead, standard test methods that measure the air void parameters of hardened concrete. One example is the North American standard ASTM C 457-90 – *Test Method for Microscopical Determination of Parameters of the Air-Void System in Hardened concrete*, which requires a sample cored from the hardened concrete on-site. The air void parameters are then measured either manually, using the linear transverse

technique with the help of a microscope, or using an automated image analysis system. However, the information provided by this method can only be obtained after the concrete has already been placed, being therefore impossible to perform adjustments during the mixing process if the parameters are not satisfactory [German Instruments (2009), Neville (2003)]. On the contrary, the AVA is able to provide information regarding the air void parameters of a concrete mix within half an hour of its casting.

According to the manufacturer, the results obtained with the Air Void Analyser have been correlated with the results obtained by ASTM C 457, being the results generally within ± 10 % of those obtained by the latter [German Instruments (2009)].

Since the equipment for the AVA was available in the laboratory, unlike the equipment necessary to measure the air pore parameters in the hardened concrete, the AVA was the method chosen to determine the air void parameters of concrete.

4.6.3.1. Test procedure

The concrete sample to be analysed was taken from the vessel were the air content was measured, after vibration (and before the air content test was performed). The sample was obtained by vibrating a wire cage (Figure 4.4) into the fresh concrete. The wire cage excludes particles larger than 6mm, which means that the sample will be a mortar fraction of the original concrete. A syringe placed inside the cage will be filled with 20cm^3 of mortar, which will be the sample of the test [German Instruments (2009)].

Figure 4.4 – Wire cage surrounding the syringe used to collect the sample for the AVA test [German Instruments (2009)].

Figure 4.5 – AVA test set-up. Riser column with inverted pan on (on the right) and computer and printer that process the information (on the left).

The sample collected was then injected into the riser column (Figure 4.5). The riser column contains the “blue AVA release liquid” at the bottom, and water on the top. The blue AVA release liquid has the adequate viscosity and hydrophilic character to prevent the air bubbles of the mortar sample from

coalescence or disintegrate into smaller bubbles, thus maintaining the original size [German Instruments (2009)].

After injected in the riser column, the mortar and liquid are gently stirred by a magnetic stirrer during 30 seconds, forcing the air bubbles to be released from the mortar sample to the liquid. The air bubbles will rise through the column of water above the AVA release liquid. The rate of rising through the liquid depends on the bubble size, with larger bubbles rising faster than smaller bubbles, according to Stoke's Law. This leads to bubbles of different sizes reaching the top of the column at different times [German Instruments (2009)].

The air bubbles are then collected on an inverted and submerged pan (Figure 4.5) that is attached to a very sensitive scale. As the air bubbles accumulate on top of the pan, the apparent mass of the pan decreases, since water is replaced by air. A computer attached to the scale records the change in apparent mass of the pan over time (Figure 4.5) [German Instruments (2009)].

Since larger air bubbles rise faster, in the early stages of the measurement the size distribution of the air bubbles varies from a few mm to a few µm, and will continue to decrease with time. The measurement will continue during 25 minutes, or until no mass change is registered in the inverted pan for 2 consecutive minutes [German Instruments (2009)].

4.6.3.2. Test results

The AVA software processes the information gathered using an algorithm that calculates the size distribution of the collected air bubbles based on the change in apparent mass of the pan. The spacing factor and the specific surface are then calculated from the results obtained for the air pore size distribution. The algorithm ensures the parameters are the same as obtained from ASTM C 457 linear traverse measurements. The software then produces a graph of the bubble size distribution and a histogram of the different bubble sizes [German Instruments (2009)].

4.7. Tests in the hardened concrete

The tests performed in the hardened concrete were: compressive strength, Rapid Chloride Migration and salt scaling under freeze/thaw. The principles, standards and methodology followed for each test method are described in the following chapters.

4.7.1. Compressive strength

The aim of the compressive strength test is to estimate the resistance of different concrete mixes when subjected to uniform compression, by compressing the specimens until failure and recording the ultimate compressive strength. The compressive strength test followed the methodology described in *SS-EN 12390-3 (2009): Testing hardened concrete. Compressive strength of test specimens*. The

test specimens used were cubes with 150mm of length, as described in *SS-EN 12390-1 (2001): Testing hardened concrete. Shape, dimensions and other requirements for specimens and moulds*. As explained in Chapter 4.5, the curing of the specimens followed the procedure defined in *SS-EN 12390-2 (2009): Testing hardened concrete. Making and curing specimens for strength tests*. One additional cube of Mix 4 (100% GGBS replacement) was subjected to curing at increased temperature, as explained in section 4.5.

The compressive strength of each mix was measured at 3 different ages: 7 days, 28 days and 56 days of age. The standard SS-EN 12390-3 (2009) states that, in order for the result to be representative, at least three specimens of each mix (and at each age) should be tested. Due to lack of space in the water tank (for curing), 3 specimens from each concrete quality were tested at 28 days of age, but only 2 specimens were tested at 7 and 56 days of age. The number of cubes tested at each age is shown in Table 4.7.

Table 4.7 - Number of cubes tested for strength at each age of all mixes

Mix	Curing	%GGBS	*k* factor	Air content (%)	Age of testing		
					7 days	28 days	56 days
1	20ºC	0	-	4.5	2	3	2
2	20ºC	25	0.6	4.5	2	3	3
3	20ºC	50	0.6	4.5	2	3	2
4	20ºC	100	0.6	4.5	1	2	1
	55ºC	100	0.6	4.5	0	1	0
5	20ºC	50	0.6	4.5	2	3	2
6	20ºC	50	1	6.0	1	3	2
7	20ºC	0	-	4.5	2	3	2
8	20ºC	50	0.6	4.5	3	3	2

The compressive strength test followed the procedure described in SS-EN 12390-3 (2009). At the age of testing, the specimen was taken out of the water tank and was cleaned with a cloth in order to remove the excess moisture in the surface. Then, the mass of the cube was measured on a scale with precision up to 0.1g. The specimen was then placed on the bottom plate of the cube-testing machine (Figure 4.6). The load was applied in two opposite faces that were casted against the mould, to ensure they were even, smooth and parallel, thus avoiding concentration of local stresses. The cubes were subjected to a load of 13.5kN/s until failure. Only cracking patterns considered satisfactory by SS-EN 12390-3 (2009) were registered.

Figure 4.6 – Compressive strength test set-up.

The compressive resistance of each cube is given by equation (3):

$$f_c = \frac{F}{A_c} \tag{3}$$

- f_c is the compressive resistance (in MPa)
- F is the maximum load (in N)
- A_c is the area of the cross-section of the specimen (in mm^2).

The results obtained for the compressive strength of each mix are presented and discussed in Chapter 5.

The mass of the specimens, measured before the compressive strength test, was used to calculate density of concrete. Knowing the density of the test specimens might be useful to assess the viability of an anomalous result (for instance, the presence of holes inside of the specimen due to deficient vibration may lead to a lower ultimate compressive strength, and a lower density).

4.7.2. Rapid Chloride Migration

The resistance against chloride ingress was evaluated according to the method described in NT Build 492 (1999), which determines the chloride migration coefficient of hardened concrete specimens from non-steady-state migration experiments. This method consists of applying an external electrical potential axially across the concrete specimen, forcing the chloride ions to migrate into the specimen. After a certain period of time, the specimens are split and the penetration depth is

measured by spraying a silver nitrate solution on the split sections. The non-steady state coefficient is then calculated based on the penetration depth.

The non-steady state migration coefficient measured by this method does not correlate directly with chloride diffusion coefficients obtained with other test methods. The Rapid Chloride Migration test is, however, an accurate method to compare the resistance against chloride ingress of different concrete qualities. The test procedure, as well as the materials used and pre-conditioning of the specimens are detailed below.

4.7.2.1. Preparation of the specimens

Cylinders with a base diameter of 100mm and a height of 200mm were casted and cured according to the procedures explained in sections 4.4 and 4.5. For each concrete quality, specimens were tested at 28 days and 56 days of age. Specimens from Mix 4 cured at 55ºC were also tested at both ages.

The pre-conditioning starts one day before the start of the test. The cylinders are removed from de water tank and sawn perpendicularly to the its axis into 3 slices with 50±2mm of thickness. The slices are sawn from the inner part of the cylinder, using a water cooled diamond saw. NT Build 492 recommends that 3 specimens from each concrete quality should be tested. Since it was not possible to store 6 cylinders for each concrete mix in the laboratory, 3 specimens sawn from the same cylinder were tested for each mix and at each age (28 and 56 days).

After sawing, the specimens are washed and the excess water was removed with a cloth. When the specimens were surface-dried, they were placed in a vacuum container and pre-conditioning began.

4.7.2.2. Pre-conditioning

After placing the specimens in the vacuum container, the absolute pressure of the container was reduced to 10-50 mbar (1-5kPa) and kept constant for three hours. After three hours, with the vacuum pump still running, the container was filled with a saturated Ca(OH)2 (calcium hydroxide) solution. The vacuum continues during another hour, after which it is turned off, and air is allowed inside the container (Figure 4.7). The pre-conditioning continues for 18±2 hours.

The aim of this pre-conditioning procedure is to completely saturate the concrete specimen with liquid, in order to obtain a uniform decay of the applied voltage throughout the thickness of the sample (linear electrical field distribution), which results on the chlorides being accelerated by the electrical field evenly in the entire volume of the sample. The air is first removed from the sample with the vacuum pump, and the sample is later saturated with limewater (saturated $Ca(OH)_2$ solution).

Figure 4.7 – Vaccum container holding the test specimens covered in the $Ca(OH)_2$ solution, after being disconnected from the vaccum pump.

4.7.2.3. Test procedure

After the pre-conditioning, the specimens were removed from the solution and cleaned with a cloth. A rubber sleeve was then fitted around the specimen, and tightly secured with two clamps to prevent leakage (Figure 4.8 and Figure 4.9).

Figure 4.8 – Specimens for the Rapid Chloride Migration test fitted inside the rubber sleeve.

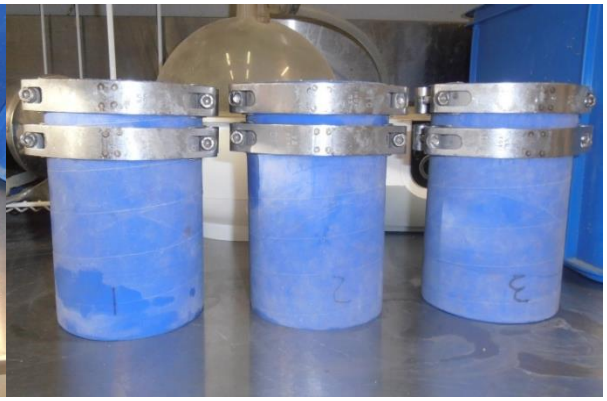

Figure 4.9 – Specimens for the Rapid Chloride Migration test secured with clamps to prevent leakage.

The specimens were then placed in the catholyte reservoir, which consists of a plastic box filled with a catholyte solution, and the cathode - a stainless steel plate about 0.5mm thick. The stainless steel plate (cathode) must be placed in a 45º angle to the longitudinal walls of the reservoir, as shown in Figure 4.10. The specimens were then placed on top of the cathode, with the bottom surface of the specimens in contact with the catholyte solution. The catholyte solution consists of a solution of 10% NaCl (sodium chloride) by mass in tap water.

The rubber sleeve was filled with 300 mL of the anolyte solution, which is a 0.3N NaOH (sodium hydroxide) solution in de-ionised water. The anode, which consists of a stainless steel mesh or plate

with holes, with a thickness about 0.5 mm thick and a diameter similar to that of the cylindrical specimens, was then placed inside the rubber sleeve, immersed in the anolyte solution, and in contact with the top surface of the specimen. Figure 4.10 and Figure 4.11 show, respectively, the schematic and the real arrangement of the migration test set-up. As it can be seen in Figure 4.11, a thermometer was used to control the temperature of the solution and specimens, which should be kept between 20 to 25ºC during the test.

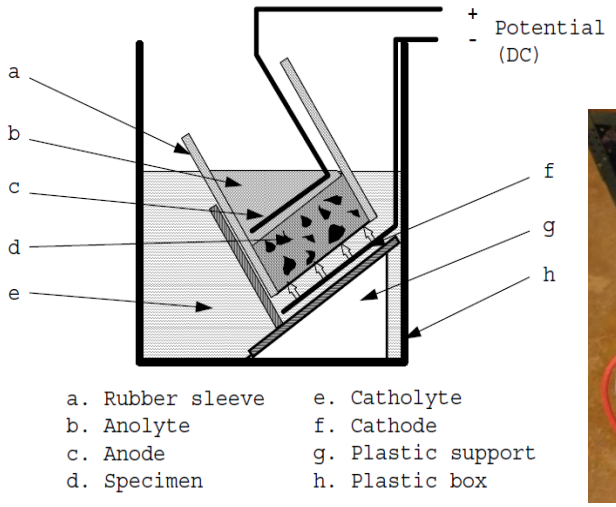

Figure 4.10 – Schematic representation of the test set-up [NT Build 492 (1999)].

Figure 4.11 – Rapid Chloride Migration test set-up.

The test beggins when the cathode is connected to the negative pole and the anode is connected to the positive pole of the power supply, and the power is turned on. The voltage was pre-set at 30V, and the initial current was recorded for each specimen. The initial temperature of each anolyte solution was also registered. The test duration was chosen as 24 hours, in accordance with the standard. Before finishing the test, the final current and temperatures were recorded.

After striping the specimens out of the rubber sleeves, they were washed with tap water, and cleaned with a cloth. The specimens were then split axially into two pieces, which were then sprayed with a 0.1M AgNO3 (silver nitrate) solution. When the white silver chloride precipitation was visible (Figure 4.12)), the penetration depths were measured with the help of a ruler, from center to both edges at intervals of 10 mm, as represented in Figure 4.13, with an accuracy of 0.1mm.

Figure 4.12 – Test specimens for the Rapid Chloride Migration test after being sprayed with silver nitrate solution.

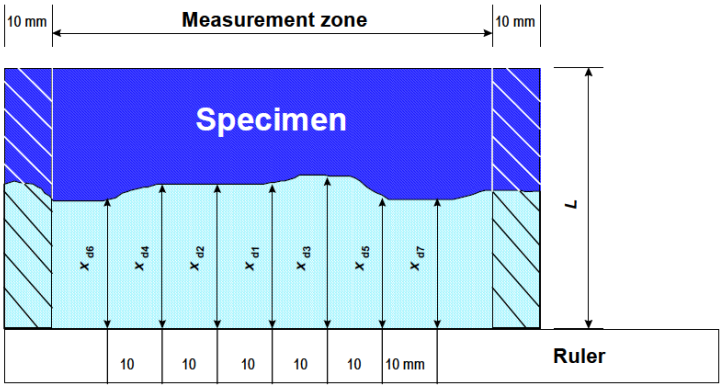

Figure 4.13 – Illustration of measurement of chloride penetration depths [NT Build 492 (1999)].

4.7.2.4. Test results

The non-steady state migration coefficient was calculated according to the following equation (4):

$$D_{nssm} = \frac{0.0239(273+T)L}{(U-2)t}\left(x_d - 0.0238\sqrt{\frac{(273+T)L\,x_d}{U-2}}\right) \quad (4)$$

In which:

D_{nssm} is non-steady-state migration coefficient (x10-12 m²/s);

U is absolute value of the applied voltage (V);

T is average value of the initial and final temperatures in the anolyte solution (°C);

L is thickness of the specimen (mm);

x_d is average value of the penetration depths (mm);

t is test duration (hours)

The results obtained for the non-steady state migration coefficient are presented and discussed in Chapter 5.

4.7.3. Salt-frost scaling

The salt-frost scaling resistance of the concrete qualities was tested according to the Swedish Standard SS 13 72 44 (2008). Some modifications to the test procedure were performed in certain cases to provide relevant information about the factors that influence the salt-frost scaling resistance of concrete. These modifications will be carefully explained.

The Swedish Standard SS 13 72 44 (2008) describes four procedures for the freeze/thaw testing of concrete: Procedures I and II, which are intended for pre-testing of concrete (i.e. before the concrete is used in a construction), and Procedures III and IV, which are intended for concrete products or drilled out cores from structures (Table 4.8). Procedures II and IV are used when the frost resistance of the cast surface is of particular interest, whereas for procedures I and III, the surface to be tested is the interior surface (i.e., a cut surface) of the specimen (Figure 4.14). For each of the procedures, pre-treatment of the specimens may follow method A, which evaluates the salt-frost scaling resistance of concrete, in which the specimen is exposed to a 3% NaCl solution during freezing, or method B, which evaluates the freeze/thaw resistance of concrete without the presence of de-icing agents, where the freezing medium is pure water. The present investigation followed procedure IA.

Table 4.8 - Procedures for freeze/thaw testing described in SS 13 72 44 (2008)

Procedure	Application	Freeze surface
I	Pre-testing	Interior
II	Pre-testing	Cast
III	Drilled	Interior
IV	Drilled	Cast

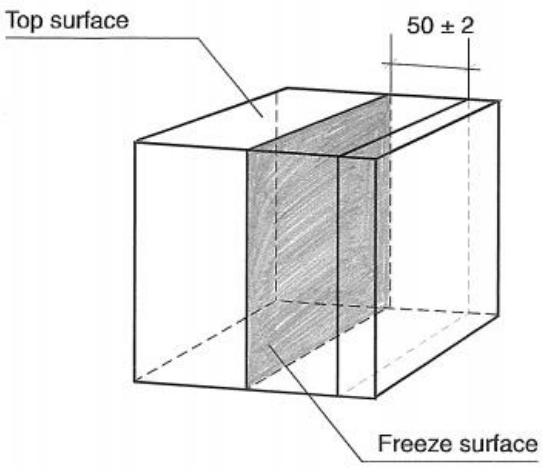

Figure 4.14 – Test specimen according to procedure I. Dimensions in mm [SS 13 72 44 (2005)]

Concrete cubes, 150x150x150mm^3 were casted and cured according to SS 13 72 45, as explained in section 4.5. At the age of 21±2 days, a 50 mm thick slab was cut out of each cube so that the freeze surface would come in the centre of the cube (Figure 4.14), SS 13 72 44 recommends at least 4 specimens from each mix to be tested. This was the case for all mixes, except in the ones cured at 55ºC, in which only 3 specimens of each concrete quality were tested.

After cutting, the slab specimens were rinsed with tap water and the excess water was removed with a moisture sponge. The specimens were subsequently returned to the climate chamber for pre-treatment.

4.7.3.1. Pre-treatment of the specimens

Right after sawing, the specimens were returned to the climate chamber at (20 ± 2)ºC and (65±5)% RH, where they were stored for 7 days, in accordance to the pre-treatment procedure described in SS 13 72 44 (Figure 4.15). During that time, a rubber cloth was glued to all the surfaces of the specimen except the test surface. The interface between the specimen and the rubber sheet in the test surface was sealed with silicone applied in a strip in the corner between the rubber sheet and the test surface, to prevent leakage (Figure 4.16).

Figure 4.15 – Slab specimens pre-conditioned in the climate chamber.

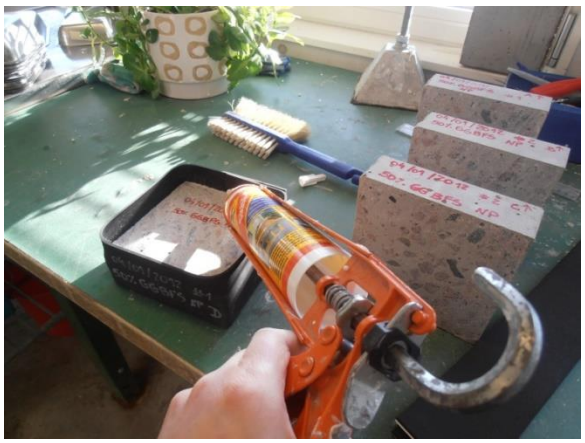

Figure 4.16 – Application of the rubber cloth and silicone sealant on the test specimens.

After 7 days in the climate chamber, pure water was poured onto the freezing surface to a height of 3mm. This pre-conditioning procedure was carried out for 72±2 hours (until the 31st day of age of the concrete, when the freezing test started).

On the day the test started, the water in the test surface was replaced by a 3% NaCl solution. The specimens were insulated in all surfaces except the test surface, to ensure a one-dimensional heat flow. In order to prevent the freezing medium (sodium chloride solution) from evaporating, the test surface was covered by a tight plastic foil. The set-up of the specimen is schematically shown in Figure 4.17.

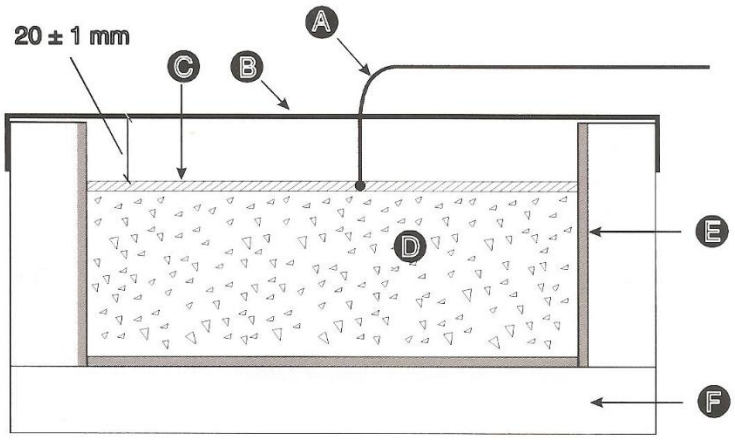

Figure 4.17 – Freeze-thaw test set-up. A: Thermo element; B: Protection against evaporation; C: Freezing medium; D: Test specimen; E: Rubber cloth; F: Thermal insulation. [SS 13 72 44 (2005)]

After the specimens were prepared, they were placed in the freezer and the freeze-thaw test began (Figure 4.18).

Figure 4.18 - Salt-frost scaling test specimens placed in the freezer.

4.7.3.2. Specimens subjected to prolonged pre-treatment

GGBS concrete presents a slower rate of hydration than Portland cement concrete, which may lead to a lower degree of hydration at the age of 28 days. A lower degree of hydration usually results on a more porous concrete, with lower compressive and tensile strengths. Given that the freeze/thaw test starts at 31 days of age, the salt-frost resistance of concrete with GGBS may be adversely affected by its lower hydration degree, when compared with Portland cement concrete. In order to evaluate the effect of a prolonged hydration of the concrete specimens with GGBS before being exposed to the freeze/thaw cycles, 3 specimens from each of the mixes with 50% of GGBS replacement and different air content (Mix 3 and Mix 5) were subjected to prolonged pre-treatment. From each cube of these mixes, two slabs were cut and tested (instead of one). One slab was pre-conditioned according to the standard procedure described in the previous section. The other slab was kept in the climate chamber for 14 more days (after the rubber sheets were glued), and only afterwards the water was poured onto the test surface. For these specimens, the test started at the 45th day of age, instead of the 31st day.

4.7.3.3. Test procedure

The specimens were exposed to 24-hour long freeze/thaw cycles, with the temperature varying between about +20°C and –18°C. The temperature in the salt solution shall fall within the shaded area in Figure 4.19 for a 24 hour cycle. The time of T>0°C shall be between 7 to 9 hours.

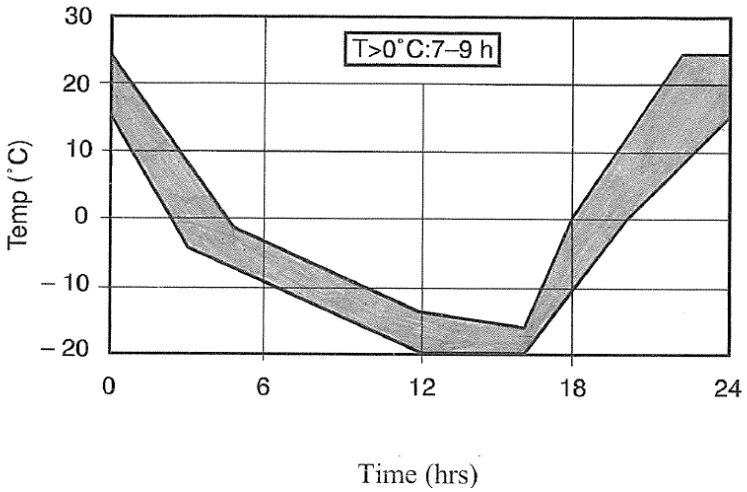

Figure 4.19 – Time-temperature cycle in the freezing medium [SS 13 72 44 (2005)].

The standard requires the collection of the scaled-off material after 7, 14, 28, 42, 56, 70, 84, 98 and 112 cycles. It was decided to collect and weight the scaled material every 7 cycles, up until the 112th cycle, so as to follow the results more precisely.

The material scaled from the test surface was collected in a steel vessel (Figure 4.20), by brushing the surface of the specimen with a brush and rinsing with pure water. After collection of the material, the new freezing medium was applied at a depth of 3mm, after which the specimen was returned to the freezing chamber. After the scaled material was dried, the total dry weight was determined with an accuracy of 0.1g (Figure 4.21).

Figure 4.20 – Scaled-off material collected on a steel vessel.

Figure 4.21 – Determination of the mass of scaled material.

4.7.3.4. Test results

The results of the frost resistance test according to SS 13 72 44 are expressed as accumulated mass of scaled material per area of freeze surface, as function of number of freeze/thaw cycles. At every 7th cycle, the scaled material is collected and weighted, and the mass loss per area, m_n (kg/m^2), is determined and registered, according to equation (5),

$$m_n = \frac{M_n}{A} \quad (5)$$

where:

- *Mn* is the accumulated mass of scaled material after *n* cycles (kg);
- *A* is the area of the test surface (m^2).

The frost resistance of a concrete quality is evaluated according to the following criteria (

Table **4.9**):

Table 4.9 - Acceptance criteria for the frost scaling resistance of concrete according to SS 13 72 44 (2005).

Frost resistance	Requirements
Very good	The mean value of the scaled material after 56 cycles (m_{56}) is less than 0.10 kg/m^2.
Good	The mean value of the scaled material after 56 cycles (m_{56}) is less than 0.20 kg/m^2 **and** m_{56}/m_{28} is less than 2; or The mean value of the scaled material after 112 cycles (m_{112}) is less than 0.50 kg/m^2.
Acceptable	The mean value of the scaled material after 56 cycles (m_{56}) is less than 1.00 kg/m^2 **and** m_{56}/m_{28} is less than 2 Or The mean value of the scaled material after 112 cycles (m_{112}) is less than 1.00 kg/m^2.
Unacceptable	The requirements for acceptable frost resistance are not met.

5. Results and Discussion

5.1. Properties of the fresh concrete

5.1.1. Slump Test

Table 5.1 summarizes the test results for slump (according to SS-EN 12350-2) performed in the fresh concrete.

Table 5.1 - Results for the slump measured according to SS-EN 12350-2(2009) for each concrete batch.

Mixes		Slump (mm)
Mix 1 (0% GGBS, air=4,5%)	**#1**	130 (S3)
	#2	130 (S3)
Mix 2 (25% GGBS, air=4,5%, k=0,6)	**#1**	110 (S3)
	#2	120 (S3)
Mix 3 (50% GGBS, air=4,5%, k=0,6)	**#1**	210 (S4)
	#2	220 (S5)
Mix 4 (100% GGBS, air=4,5%, k=0,6)	**#1**	220 (S5)
	#2	210 (S4)
Mix 5 (50% GGBS, air=6%, k=0,6)	**#1**	170 (S4)
	#2	170 (S4)
Mix 6 (50% GGBS, air=4,5%, k=1,0)	**#1**	130 (S3)
	#2	140 (S3)
Mix 7 (0% GGBS, NSP, air=4,5%)	**#1**	80 (S2)
	#2	90 (S2)
Mix 8 (50% GGBS, NSP, air=4,5%, k=0,6)	**#1**	130 (S3)
	#2	120 (S3)

As explained in Chapter 4, the mix proportions for each concrete quality were designed so that the consistency of each mix would fall on the S3 class of slump (which corresponds to a downward movement of between 100 and 150mm). In order to achieve the targeted slump without loss of mechanical strength, a superplasticizer was used in mixes 1 to 6. Mixes 7 and 8 were produced without adding superplasticizer. However, and even after some trial mixes were cast to adjust the mix proportions to the desired properties, this was not the case for some concrete qualities. In fact, only mixes 1, 2, 6 and 8 presented a slump within the limits (100 to 150mm) for both batches.

The increased slump presented by both batches of Mix 3 (210 and 220mm, which correspond to slump classes S4 and S5, respectively) is probably due to the increase in dosage of superplasticizer (by total binder weight). As shown on Table 4.3, the percentage of superplasticizer per weight of binder increases from 0.32% for Mix 2 (with 25% of GGBS replacement) to 0.43% for Mix 3 (with 50% of slag

replacement). For Mix 4 (with 100% GGBS replacement), the mix proportions were readjusted, in consequence of the results obtained for Mix 3. Therefore, the dosage of superplasticizer was reduced to 0.25% of the total binder content. Regardless of this fact, slump values as high as 210mm (S4) and 220mm (S5) were also obtained for the batches produced for Mix 4.

The dosage of superplasticizer used for Mix 5 was lower than the dosage used for Mix 3 (both with 50% of GGBS replacement), for two reasons. On the one hand, the targeted air content for Mix 5 is 6.0%, whereas for Mix 3 is 4.5%. Therefore, more air entraining agent was used in Mix 5. As explained in Chapter 3, the use of air entraining agents usually improves the flowability and workability of concrete, which, therefore, results in a higher slump. In order to offset the effect of the increase of AEA in the consistency of Mix 5, the dosage of superplasticizer was reduced. On the other hand, as it was the case for Mix 4, Mix 5 was casted after Mix 3. The results of the slump test for Mix 3 showed that the dosage of superplasticizer needed to be further reduced, in order to achieve the desired consistency. Consequently, a new adjustment to the mix proportions was performed, and a dosage of 0.23% of the total binder content was used. Nevertheless, both batches casted for Mix 5 presented a slump of 170mm (class S4), still higher than targeted 100 - 150mm interval of class S3.

The analysis of the mix proportions and the results obtained for the slump test indicates that an increase in the dosage of GGBS in concrete results in a reduced consistency of concrete. In fact, for Mix 2 (with 25% of GGBS) the dosage of superplasticizer was reduced, when compared to Portland cement concrete (Mix 1), and the same slump class was obtained, even with a decrease in the water/binder ratio for Mix 2, when compared with Mix 1 (Table 4.3). For Mix 4, with 100% of slag replacement, the dosage of superplasticizer was reduced about 33%, when compared to Portland cement concrete, and slumps up to 220mm were obtained (even with a water/binder ratio as low as 0.36). On the other hand, for Mix 6 (with 50% of GGBS replacement, and *k*-factor of 1), where the GGBS replaces the slag on a one-to-one basis, the dosage of superplasticizer was also lower than that of Portland cement concrete (Mix 1), and slumps within the S3 class were achieved. The addition of GGBS has been reported to improve the workability of concrete, as referred in Chapter 2.3.1.1, as a consequence of the better dispersion of the cement particles and the limited amount of water that the slag particles absorb during mixing [Neville (2003)].

An improvement in the workability/placeability of concrete with addition of GGBS means that it is possible to produce a concrete quality with the desired consistency using a lower water/cement ratio, when compared to Portland cement concrete with similar properties. This improvement in workability due to the addition of slag may, thus, contribute to offset the effect of the addition in the compressive strength at early ages, by allowing a reduction in the water/binder ratio of concrete.

Both batches casted for Mix 5 presented a slump of 170mm, which corresponds to the S4 class of slump. Even though this value was not within the targeted interval, it is still within acceptable limits. However, one of the batches for Mixes 3 and 4 and reached the S5 slump class (with 220mm of slump), being the other batch still within the limits of S4 class, though reaching a slump as high as 210mm. As explained in Chapter 4, the consistency of a concrete mix may affect the effectiveness of

the air entrainment. Even though the entrained air can be more easily incorporated in a more flowable concrete [Ramachandran (1995)], it is also more likely to escape from a very fluid concrete. Ramachandran (1995) refers that, for concrete slumps higher than 178mm, a decrease in consistency results in easier loss of air during handling and placing. This means that, for Mixes 3 and 4, there is a risk that the actual air content in the hardened concrete is lower than the measured in the fresh concrete, which may in turn influence the salt-frost resistance of the specimens of these mixes.

Mixes 7 (Portland cement concrete) and 8 (with 50% GGBS replacement) were produced without addition of superplasticizer. In order to achieve the desired consistency, the dosage of air entraining agent was increased for both of these mixes. In fact, the percentage of AEA by total binder weight increased from 0.25% for Mix 1 to 0.7% for the comparable Mix 7, and from 0.23% for Mix 3 to 0.7% for Mix 8. The usage of AEA is known to enhance the workability and increase the slump of concrete, for the same water/cement ratio [Ramachandran (1995), Hewlett (2004)]. For Portland cement concrete (Mix 7), however, it was not possible to obtain a slump higher than 90mm (S2 class). As for Mix 8, on the other hand, a combined effect of an increased dosage of AEA and a 50% of the weight of cement replaced by slag resulted in a concrete with a consistency within the targeted limits (class S3 of slump).

5.1.2. Air content

It is somewhat difficult to achieve the desired air content in concrete, especially when air entraining agents are used together with superplasticizers. In order to assess the compatibility of the AEA and superplasticizer chosen to produce the concrete mixes, and also to adjust the amount of AEA necessary to achieve the desired air content for each mix, trial mixes were casted. No incompatibility was found between the superplasticizer and the AEA. However, and even after the adjustments made to the initial mix proportions, some concrete batches fell out of the targeted limits for the air content (4.5±0.5% for all mixes except Mix 5, whose targeted air content was 6±0.5%).

Two methods were used to measure the air content of the concrete mixes. The first was the pressure gauge method described in the SS-EN 12350-7 (2009). However, this method is only able to measure the total air content of the sample, which consists of both entrained air and entrapped air. As explained in section 3.2.2, the positive effect of air entrainment on the salt-frost resistance of concrete is not strictly related with its total air content, but also with the properties of the air pore structure, such as pore size, and average distance between the air pores. Therefore, in order to obtain more information about the air void system of the concrete mixes casted, an additional air void analysis in the fresh concrete was performed.

Table 5.2 compares the results obtained for each batch, measured according to both the pressure gauge method described in SS-EN 12350-7 (2009) and the Air Void Analyser (AVA). For one of the batches of Mixes 7 and 8, an error occurred during the measurements with the air void analyser (AVA), which resulted in incorrect values for the air pore parameters (such as negative spacing factors). Those results were, therefore, dismissed.

Table 5.2 - Comparison between the air content results obtained by the test method described in SS-EN 12350-7 and the Air Void Analyser (AVA)

Mixes		Air Content (EN 12350-7)	Air content (Air Void Analyser)
Mix 1	**#1**	4,80%	4,70%
(0% GGBS, air=4,5%)	**#2**	4,60%	8,40%
Mix 2	**#1**	5,30%	4,10%
(25% GGBS, air=4,5%, k=0,6)	**#2**	5,00%	9,00%
Mix 3	**#1**	4,90%	6,20%
(50% GGBS, air=4,5%, k=0,6)	**#2**	4,10%	5,50%
Mix 4	**#1**	4,50%	4,90%
(100% GGBS, air=4,5%, k=0,6)	**#2**	4,20%	8,80%
Mix 5	**#1**	5,50%	9,20%
(50% GGBS, air=6%, k=0,6)	**#2**	5,60%	9,40%
Mix 6	**#1**	4,50%	6,00%
(50% GGBS, air=4,5%, k=1,0)	**#2**	4,50%	7,10%
Mix 7	**#1**	5,80%	
(0% GGBS, NSP, air=4,5%)	**#2**	5,10%	12,10%
Mix 8	**#1**	4,00%	2,20%
(50% GGBS, NSP, air=4,5%, k=0,6)	**#2**	5,30%	

As shown in Table 5.2, according to SS-EN 12350-7 (2009), the air content obtained was within the targeted limits for all concrete batches, except for both batches casted for Mix 7, and one batch for Mixes 2 and 8. In all of these cases, the percentage of air obtained was higher than the targeted values.

By analysing the mix proportions of each concrete quality (Table 4.3), it can be observed that the amount of air entraining agent per weight of cementitious material varies only slightly for Mixes 1 to 4, being the dosage reduced as the amount of GGBS replacement increases. This tendency is not, however, followed in Mix 6. Mix 6, with 50% GGBS replacement and *k*-factor of 1, i.e., with a higher ratio of slag to Portland cement, when compared Mix 3, required a higher dosage of air entraining agent to achieve the same air content (0.27% for Mix 6, and 0.23% for Mix 3). The effect of the replacement of cement by GGBS on the ability to entrain air in concrete is, therefore, not clear. As for Mix 5, which targeted air content was 1.5% higher than the other mixes (6%), the dosage of AEA per binder weight (0.5%) was more than double the dosage used for the comparable Mix 3 (0.23%) (with 50% slag replacement, and 4.5% targeted air content). As expected, the amount of air entrained is not proportional to the dosage of AEA. In fact, as there is a minimum required dosage of AEA that ensures its effectiveness, there is also a maximum amount of admixture above which there is no more increase in entrained air [Due and Folliard (2004)].

As for both mixes produced without superplasticizer (Mix 7, Portland cement only concrete and Mix 8, with 50% GGBS replacement), and as explained in the previous section, the dosage of AEA used was

higher in order to improve the workability of concrete. Also, the use of superplasticizers may increase air entrainment [Due and Folliard (2004), Domone and Illston (2010)]. Therefore, in order to reach the desired air content for mixes produced without superplasticizer, the dosage of AEA should be increased. The percentage of AEA by total binder weight increased from 0.25% for Mix 1 to 0.7% for the comparable Mix 7, and from 0.23% for Mix 3 to 0.7% for Mix 8. The higher dosage of AEA used is probably the cause for the increased air content obtained for both batches of Mix 7, and one batch of Mix 8.

The results obtained reveal the difficulty in achieving an accurate air content when designing and producing concrete. Both batches for each mix were produced with the exact same dosage of each component. Regardless, for Mixes 3 and 7, the difference between the air content obtained for the two batches casted is 0.8% and 0.7%, respectively. As for Mix 8 the difference is even greater: the air content varies from 4.0% for batch number 1 to 5.3% for batch number 2. Morevover, the result obtained for batch number 1 of Mix 8 was lower than the results obtained for both batches for the comparable Mix 3, even if the amount of AEA was almost 3 times higher (Table 4.3).

Table 5.2 shows an excessive discrepancy between the results obtained by the two methods, being the air content obtained by the AVA higher in almost all cases, except for batches batch number 1 from Mixes 1, 2, and 8. On the other hand, significant differences between the air content measured with the AVA for two batches of the same mix are observed for all mixes, except Mix 5. These differences are particularly pronounced in Mixes 1, 2 and 7, where the results obtained for batch number 2 are almost double than the results obtained for batch number one.

Furthermore, according to the AVA, Mix 7 displays an air content of 12.10%, which is excessively high for concrete, and more than twice the air content obtained for both batches according to SS-EN 12350-7 (5.10 and 5.80%). The recommendations for the air content of concrete in freeing environments is usually given as a minimum percentage of air of the total concrete volume, and varies between 4% and 8%, depending on the maximum aggregate size [Neville (2003), Domone and Illston (2010)]. Excessively high air contents (above 8% or 9%) may have severe adverse consequences on other mechanical and durability aspects of the hardened concrete, such as compressive strength and permeability, and are not, therefore, recommended. Mix 8, on the other hand, presents only 2.20% of air content (slightly higher than half the air content obtained with the pressure gauge method described in SS-EN 12350-7), which is lower than recommended for concrete in freezing environments.

The reasons for these differences are unclear. Small sampling size for the AVA might be one of the reasons. Unlike the test method described in SS-EN 12350-7, which uses samples of at least 5 litres, and is used for concrete made with aggregate of maximum size up to 63 mm [SS-EN 12350-7 (2009)], the AVA uses samples of only 20cm^3, and excludes aggregates larger than 6mm [German Instruments (2009)]. The sample used in the AVA is not, therefore, a sample of “concrete”, but of a “mortar fraction” of that concrete, with aggregate size up to 6mm. This means that the AVA removes all of the coarse aggregate, and also some fine aggregate whose particle sizes are higher than 6mm.

Other reasons include the great sensitivity of the AVA to the precision of the operator during the collection of the sample, and to external vibrations during the test. For these reasons, and even though the results obtained with the AVA were not dismissed, it was decided to take the results measured according to SS-EN 12350-7 (2009) as the relevant ones. Nevertheless, the discrepancy in the measurements was kept in mind, in case there was any unexplained result in the tests performed in the hardened concrete.

Table 5.3 presents the results for all the air void system parameters measured with the air void analyser (AVA).

Table 5.3 – Air pore structure parameters obtained by the AVA

Mixes		Air content (Air Void Analyser)	Specific Surface (mm^{-1})	Spacing factor (mm)
Mix 1 (0% GGBS, air=4,5%)	**#1**	4,70%	15,9	0,30
	#2	8,40%	24,1	0,12
Mix 2 (25% GGBS, air=4,5%, k=0,6)	**#1**	4,10%	17,9	0,28
	#2	9,00%	27,3	0,10
Mix 3 (50% GGBS, air=4,5%, k=0,6)	**#1**	6,20%	19,4	0,21
	#2	5,50%	20,2	0,22
Mix 4 (100% GGBS, air=4,5%, k=0,6)	**#1**	4,90%	15,1	0,31
	#2	8,80%	28,3	0,10
Mix 5 (50% GGBS, air=6%, k=0,6)	**#1**	9,20%	22,7	0,12
	#2	9,40%	22,7	0,12
Mix 6 (50% GGBS, air=4,5%, k=1,0)	**#1**	6,00%	23,7	0,18
	#2	7,10%	22,7	0,14
Mix 7 (0% GGBS, NSP, air=4,5%)	**#2**	12,10%	25,9	0,08
Mix 8 (50% GGBS, NSP, air=4,5%, k=0,6)	**#1**	2,20%	26,4	0,26

The results presented in Table 5.3 display a marked correlation between the air content and the spacing factor in concrete: the spacing factor generally decreases with an increase in air content. This correlation was expected, even though it is not always linear. For the same average pore size, the greater the air content, the larger the number of air pores and, therefore, the closer they will be to each other. The fact that the spacing factor decreases with an increase in the air content is one of the reasons for the good performance against salt-frost scaling of entrained air.

However, this is not true for all the cases. Batches number 1 of Mixes 1, 2 and 4 present an air content between 4.1% and 4.9%, and a spacing factor between 0.28 and 0.31 mm. On the other hand, even though batch number 1 of Mix 8 presents a lower air content (2.2%), the spacing factor is also lower (0.26mm) than the previous batches. This means that the air voids in the concrete of Mix 8

are more evenly distributed throughout the paste than in the previous cases, i.e., there is probably a larger amount of air pores in the paste. Since the air content is lower, it is likely that the air pores present a much smaller size.

According to the specifications of the AVA, the spacing factor should be smaller than 0.20mm in order for concrete to be considered frost resistant [German Instruments; Petersen, (2009)], which is in agreement with the recommendations of Fagerlund (1985) and Neville (2003). This value is exceeded in one of the batches for Mixes 1, 2, 4 and 8, and both batches for Mix 3.

Even though the spacing factor exceeds 0.20mm in both batches of Mix 3, spacing factors of 0.21mm or 0.22mm may still prove frost resistant. In fact, even though a maximum spacing factor of 0.20mm is nowadays usually recommended, Powers, cited by Neville (2003), calculated that an average spacing factor of 0.25mm is enough for adequate protection against frost damage. On the other hand, for the other Mixes, all spacing factors are higher than 0.25mm, which may adversely affect the frost resistance of these mixes.

As for the mixes presenting a spacing factor larger than 0.20mm for one of the batches, and a lower spacing factor for the other, this difference may explain any variation in the amount of scaling presented by different specimens casted for the same mix (since 2 cubes from each batch were tested). For that reason, for Mix 4, all the specimens tested against frost attack were casted from batch number 2, which presents a lower spacing factor (0.10mm). The results of the frost resistance of Mix 4 are not, therefore, affected by the difference in the spacing factor measured in the two batches.

The air void analysis also measures the specific surface of the air pores. The specific surface is the ratio between the surface area of the air pores and their total volume, i.e., it is a measure of the size of the air pores. A high specific surface is usually a result of a fine air pore system. However, the specific surface does not indicate the number of pores of each size that exist in concrete, i.e., the same value of specific surface may represent a variety of different pore size distributions. Nevertheless, for different concrete qualities with the same air content, the specific surface is a good indication of the air pore size distribution, being a higher specific surface the result of a greater amount of small sized air pores.

According to the specifications of the AVA, the specific surface must be greater 25mm^{-1} in order for concrete to be considered frost resistant [German Instruments, Petersen (2009)]. Ramachandran (1995) and Neville (2003), on the other hand, refer that concrete can present a satisfactory freeze/thaw resistance even with specific surfaces as low as 16mm^{-1}. The authors refer that the specific surface of air-entrained concrete with adequate frost resistance should range between 16 and 24 mm^{-1}, sometimes reaching 48 mm^{-1}. On the contrary, specific surfaces lower than 12 mm^{-1} usually indicate a poor air void structure, with a high amount of entrapped air bubbles (i.e., air bubbles larger than 1mm) [Ramachandran (1995), Neville (2003)].

Specific surfaces higher than 25mm^{-1} were obtained only for one of the batches of Mixes 2, 4, 7 and 8. On the other hand, one of the batches of Mixes 1 and 4 present a specific surface lower than 16mm^{-1}.

The results display a clear correlation between the specific surface and the spacing factor, with the specific surface increasing with a decrease in the spacing factor. This tendency was expected. Considering a sample of two different concrete mixes with the same volume of air, the smaller the size of the pores (higher specific surface), the larger the number of pores must exist in the sample to achieve the same volume. The larger the number of air pores that exist in a sample of concrete, the lower the average distance between them, i.e., the lower the spacing factor.

This is not the case, however for Mix 8. Mix 8 presents a large spacing factor (0.26mm), to which corresponds an also large specific surface (26.4mm^{-1}). According to the results, Mix 8 presents a specific surface higher than 25mm^{-1}, which is considered satisfactory in what concerns the frost resistance of concrete. Contrarily, the spacing factor obtained was much larger than the recommended for frost resistant concrete (0.20mm). These results are probably explained by the very low air content obtained for Mix 8 (2.20%). As previously mentioned, the specific surface is the surface area of the air pores divided by their volume. This means that, if the surface area of the pores is small, and the volume of air is also low, a high specific surface will be obtained. Since the total volume of air is low, it means that the number of air pores will also be reduced, which results on an increase in the distance between pores, i.e., a high spacing factor.

These results show that the adequacy of the air pore system of a concrete quality to be placed in freezing environments cannot be evaluated by analysing only one of the parameters of the air pore structure. Instead, the total air content, the spacing factor and the specific surface must be known.

Nevertheless, the results for the air void structure parameters obtained by the AVA show that there is usually a correlation between the total air content, the spacing factor and the specific surface, with the spacing factor generally decreasing and the specific surface usually increasing with an increase in the air content. Even if the results for the total air content obtained with the AVA are somewhat questionable (not only because of the differences between the measurements with the AVA and the test method described in SS-EN 12350-7 (2009), but also because of the differences between the results for two batches of the same mix), the correlation between the air pore parameters obtained shows how introducing air in concrete (and the amount of air introduced) may affect the air pore structure and, consequently, the performance of concrete under freeze/thaw cycles.

According to the results shown in Table 5.3, almost all concrete qualities with air content higher than 6% present values for specific surface and spacing factor considered satisfactory for freeze/thaw resistance. For air contents between 4.1% and 4.9%, on the other hand, it appears not to be possible to ensure a suitable air pore structure for adequate protection against salt-frost scaling. These results demonstrate the positive effect of an increase in the air content of concrete to be placed in freezing environments.

Two mixes (Mix 7 and Mix 8) were cast without superplasticizer in order to evaluate the effect of the use of superplasticizer in the air void structure of the concrete. According to the results obtained with the AVA, at least for Mix 8, when contrasted to the comparable superplasticized Mix 3, it seems that not using superplasticizers results on a much more refined pore structure. In fact, even for a low air content (2.20%), Mix 8 reveals a specific surface higher than the minimum recommended for satisfactory frost resistance (25mm^{-1}). The spacing factor, however, was higher than the maximum recommended, which seems to be related with the low air content of the mix, rather than quality of the entrained air. Nevertheless, the spacing factor was still lower for Mix 8 than for other superplasticized mixes with higher air contents, such as batches number 1 of Mixes 1, 2 and 4.

As for Mix 7, the extremely high air content obtained resulted on an expected high specific surface and very low spacing factor (Table 5.3). Comparing the results obtained for the air void parameters of Mixes 1 and 7, no apparent negative effect of the use of superplasticizer is noticeable. The differences obtained for the spacing factor and specific surface for Mix 7 and the comparable Mix 1 are probably due to the differences in the actual air content, instead of the use of superplasticizer.

These results reveal, once again, the difficulty in achieving an adequate air pore structure in concrete, even when the air entraining agent is the only admixture added during the production of concrete.

5.2. Properties of the hardened concrete

5.2.1. Compressive strength

The results for the compressive strength of the concrete mixes tested at different ages are presented and discussed in this section. The results presented in this section correspond to the average values obtained for all the specimens of each of the concrete mixes tested. The raw data from the tests performed is presented in Appendix C.

5.2.1.1. Influence of the amount of Portland cement replacement by GGBS

Figure 5.1 displays the results for the average compressive strength at 7, 28 and 56 days of age, for concrete with varying amounts of GGBS replacement, for the same targeted air content (4.5±0.5%) and efficiency factor (*k*=0.6), and cured according to the standard procedures.

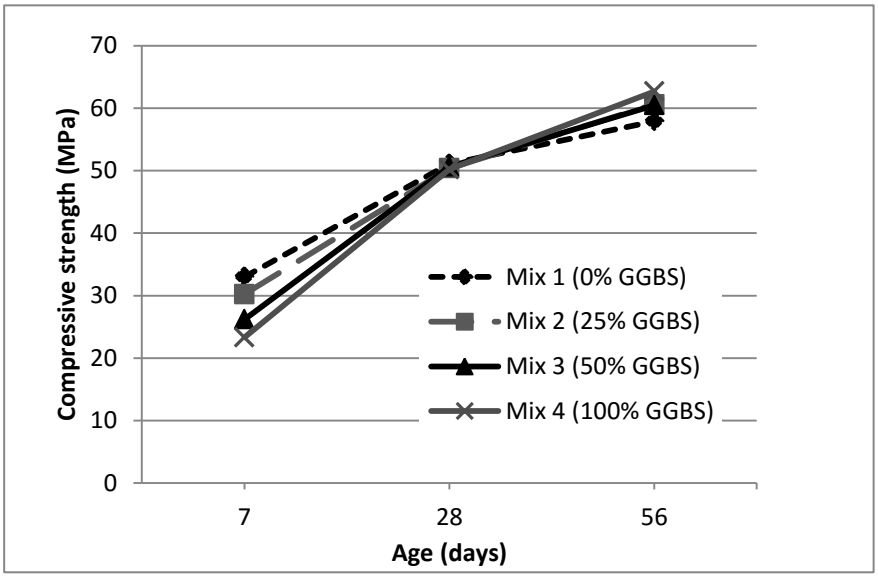

Figure 5.1 - Compressive strength development for concretes with different additions of GGBS, k=0.6, targeted air content of 4.5%±0.5%, cured at 20ºC. Test performed at 7, 28 and 56 days of age. Tested according to SS-EN 12390-3 (2009).

As shown in Figure 5.1, the compressive strength at 7 days of age is higher for Portland cement-only concrete, and decreases with an increase in the addition of GGBS. At 28 days of age, the compressive strength is very similar for all concrete mixes. At the age of 56 days, the reference Portland cement concrete presents the lowest compressive strength, and the compressive strength for concrete mixes with GGBS gradually increases with the increase in slag content.

The rate of hydration of GGBS is usually lower than that of Portland cement, which results on a lower rate of strength gain for concrete with additions of slag. Consequently, GGBS concrete will present a lower compressive strength, at least at early ages. As seen in Figure 5.1, the compressive strength of

GGBS concrete at the age of 7 days is lower at all percentages of replacement than for Portland cement concrete.

The results also show that the compressive strength at this age increases with a decrease in slag content. Again, given that the reactivity of the slag is lower than that of the Portland cement concrete, the compressive strength at early ages will be lower for concretes in which the contribution of slag for the compressive strength is higher, i.e., concrete mixes where slag replaces a higher amount of cement. These results are in accordance with the ACI Committee Report (2000), which refers that early strength of concrete with GGBS is inversely proportional to the amount of slag in the mix. Similar results were obtained by Gruyaert (2011), who tested the compressive strength of concrete mixes with 0% to 85% of slag replacement, cured at 20ºC and with a relative humidity of 95%. The author found that the compressive strength up to 7 days after mixing decreased with an increase in slag content.

The rate of strength development depends not only on the amount of replacement, but also on the activity index of the GGBS combined with the Portland cement used. For the combination of Slagg Bremmen with *Anläggningscement* (CEM I 42.5 N MH/SR/LA), the activity index at 7 days is around 45% (Figure 4.1). The activity index is calculated for a mix where 50% of slag replaces Portland cement in a one-to-one basis. This would mean that the compressive strength of Mix 4 (where the GGBS replaces 50% of the total binder content) would be about 45% of the compressive strength of Mix 1. However, the 7-day compressive strength of Mix 4 (23.3 MPa) is approximately 70% of the compressive strength obtained for Mix 1 (33.0 MPa). This fact has to do with the use of a *k*-factor lower than 1.0 in the mix proportioning.

As explained previously, the efficiency factor represents the relative contribution of the amount of addition in the compressive strength, compared to an equivalent weight of Portland cement [Domone and Illston (2010)]. The efficiency factor is used in mixes containing additions in order to achieve the same compressive strength at 28 days that a comparable Portland cement concrete would achieve, by considering that only a percentage of the addition used contributes to the strength development. In the present case, the *k*-factor is 0.6, which means that only 60% of the total slag content contributes to the strength development. Thus, the *S* amount of slag is replaced by 0.6*S* in equation (1), i.e., only 60% of the total slag content is considered in the calculation of the equivalent water/cement ratio, which results on an actual water/binder ratio lower for mixes with GGBS additions than for the comparable Portland cement concrete. The efficiency factor is, therefore, used to offset the slower hydration of the supplementary cementitious materials, which results on a higher compressive strength than it would be obtained if slag would replace Portland cement on a one-to-one basis.

Figure 5.1 also shows that, even though the rate of strength development is different for all the mixes, the average compressive strength obtained for all concrete qualities at 28 days is very similar. There may be two reasons that explain these results: first, the equivalent cement content was higher for Mixes 3 and 4, which may have contributed to offset the effect of the high slag replacement levels in the strength development of these mixes. On the other hand, even though the equivalent

water/cement ratio was the same for all the mixes, the actual water/binder ratio was lower for mixes with higher slag contents. As already explained, the efficiency factor concept is used in order to obtain the same compressive strength at 28 days for concrete with additions as the comparable Portland-cement concrete by offsetting the slower hydration of the additions with a decrease in the w/b content. The results obtained show the adequacy of the use of the efficiency factor in the production of concrete with additions to obtain similar compressive strength at 28 days of age.

The efficiency factor recommended in SS 13 70 03 (2008) for GGBS added in the mixer together with CEM I is 0.6, regardless of the type and amount of slag and cement used. However, the *k*-factor also depends on the reactivity of the slag, which in turn depends on its chemical composition, glass content, and fineness [Neville (2003)]. Moreover, the reactivity of each slag depends on the cement with which it is mixed (as seen in Figure 4.1), i.e., there is one *k*-factor for each type of slag mixed with each type of cement. The activity index was obtained by testing mortar mixes where 50% of Portland cement is replaced by GGBS. This means that for lower slag contents, the efficiency factor used could be higher. However, for mixes with higher percentages of replacement, a lower *k*-factor may need to be used, in order to obtain the same compressive strength. There is, therefore, one *k*-factor for each combination of slag and cement (as there is one activity index for each combination) that yields the same compressive strength as Portland-cement only concrete at 28 days.

The results also show that, for 56 days of age, the compressive strength increases with an increase in slag content at least for concrete with percentages of replacement up to 100% by mass of GGBS of the Portland cement content (50% of the total binder content). These results are also in agreement with the literature. As explained previously, the hydration of GGBS continues for longer periods of time, when compared to the hydration of Portland cement. This results on a higher compressive strength of the GGBS concrete at later ages. On the other hand, the denser microstructure of GGBS concrete also contributes to a higher strength, as long as sufficient hydration has occurred [Neville (2003)].

Compressive strength tests carried out by Gruyaert (2011) on concrete with different percentages of slag of the total binder content show similar results. From 28 days onwards, concrete qualities with up to 30% of GGBS of the total binder content showed higher strength than the reference Portland cement concrete at all ages, with the compressive strength increasing with an increase in slag content. As for concrete qualities with replacement levels between 50% and 85%, the compressive strength is lower even after one year. It seems, therefore, that there is a maximum percentage of replacement that yields the maximum mid-term strength of concrete, which is about 50% of the total binder content (i.e., 100% of GGBS replacement). These results support the recommendation presented in Neville (2003).

5.2.1.2. Influence of the air content of concrete

Figure 5.2 presents the results for the average compressive strength at 7, 28 and 56 days of age, for concrete mixes with 50% GGBS (Mix 3 and Mix 5) cured in a water bath at 20ºC, both produced with the same efficiency factor, but with different targeted air contents (4.5±0.5% for Mix 3, and 6.0±0.5% for Mix 5).

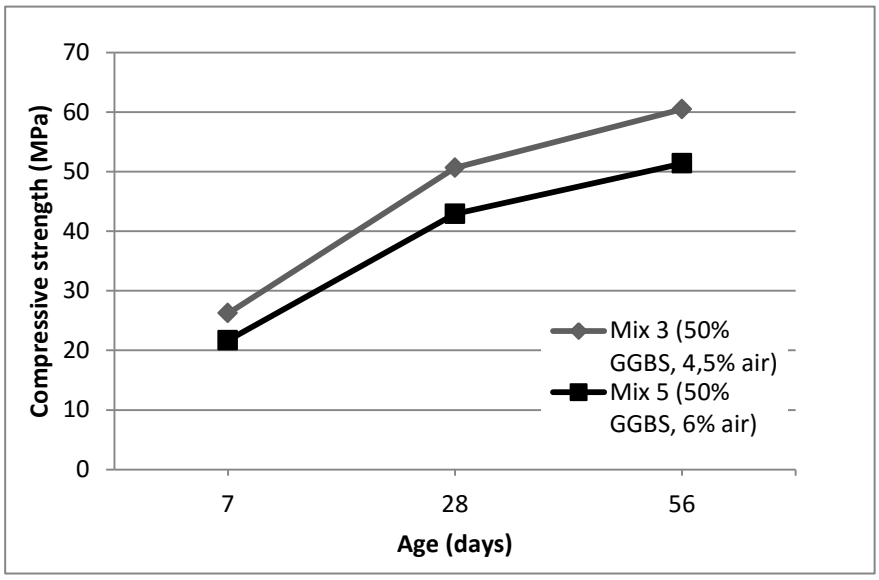

Figure 5.2 - Compressive strength development of concretes with 50% GGBS, k=0.6, cured at 20ºC, and with different air contents. Tests performed at 7, 28 and 56 days of age. Tested according to SS-EN 12390-3 (2009).

The results show that the concrete quality with higher amount of air (Mix 5, with air content between 5.5% and 5.6%, measured according to EN 12350-7) presents lower compressive strength at all ages than Mix 3 (air content between 4.1% and 4.9%). These results were expected. Since the compressive strength of concrete is directly related with its density, and given that an increase in the air content will reduced the density of the paste, it will also lead to a lower compressive strength [Neville (2003)].

According to the literature, a 1% increase in the volume of air pores in concrete results on an average compressive strength loss between 5.5% [Neville (2003)] and 6% [Domone and Illston (2010)]. Considering an average value of 4.5% for the air content of Mix 3, and 5.55% for Mix 5 (according to the results obtained for the pressure gauge method described in SS-EN 12350-7), the results obtained show a drop in compressive strength of between 15% and 17% for 1% increase of air content, for all ages of testing. This value is much higher than the 6% mentioned in the literature. The reasons for these results are unclear, but might be related with the accuracy of the measurements of the air content of the concrete qualities. Even though the results obtained for the pressure method according to SS-EN 12350-7 reveal air contents within the targeted limits for each of the mixes, the results obtained with the AVA show a higher air content for both mixes, with Mix 3 presenting an average air content of 5.85% and Mix 5 and average air content of 9.3%. According to the results of

the Air Void Analyser the difference between the average air content for Mixes 3 and 5 is 3.45%. Considering an average decrease of 5.5% in the compressive strength for each 1% of increase in the air content, a total decrease of approximately 19% is obtained for Mix 5, which is closer to the results obtained.

On the other hand, as referred before, the slump obtained for both batches of Mix 3 was extremely high, which may have favoured escape of air during handling of concrete. However, the slump obtained for both batches of Mix 5 was 170mm, which is fluid enough to adequately entrain air, but not excessively fluid that will enable loss of air while the concrete is being worked [Ramachandran (1995)]. Therefore, there is also a possibility that the air content of the hardened Mix 3 is lower than the value measured in the fresh concrete, which may also explain the difference in the compressive strength of these concrete qualities. Further investigation should have been carried out to assess the actual air content in the hardened concrete for both of these mixes.

The results also reveal similar strength development for both concrete mixes. As referred, the difference between the compressive strength of both mixes for each age varies between 17% at 7 days and 15% at 28 and 56 days of age. These results indicate that an increase in the air content of concrete affects the ultimate compressive strength of concrete, but not the rate of strength development, as displayed by the similar slope of the lines of Figure 5.2 for both concrete qualities.

5.2.1.3. Influence of the efficiency factor

Figure 5.3 shows the average strength development of Mixes 3 and 6, both with 50% of GGBS and 4.5±0.5% of targeted air content, water cured at 20ºC, and with different efficiency factors.

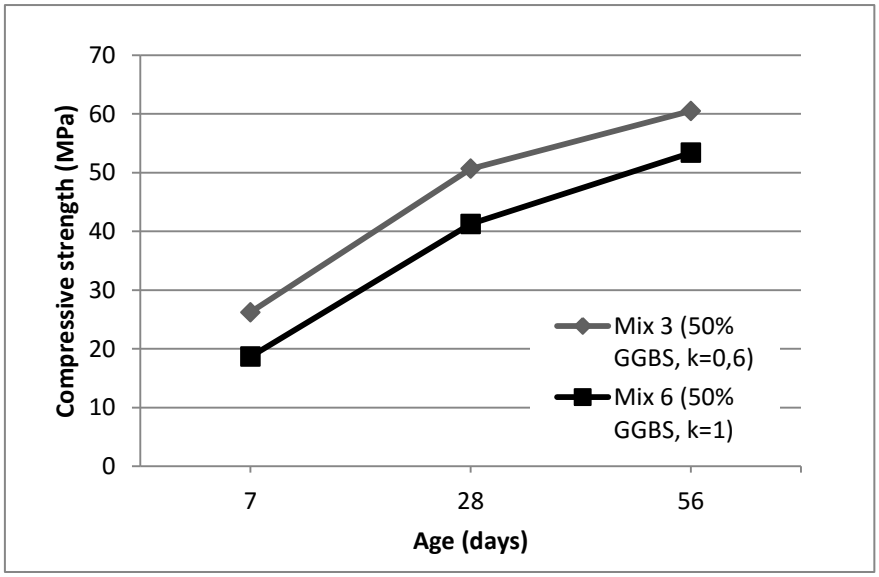

Figure 5.3 - Compressive strength development of concretes with 50% GGBS, air= 4.5%, cured at 20ºC and with different efficiency factors. Tests performed at 7, 28 and 56 days of age. Tested according to SS-EN 12390-3 (2009).

The results displayed in Figure 5.3 show that Mix 6, with a *k*-factor of 1, presents a lower compressive strength at all ages of testing than Mix 3, produced with an efficiency factor of 0.6.

The compressive strength of concrete with additions depends on the activity index of the addition. Given that the rate of strength development of concrete with additions in general, and GGBS in particular, is lower than that of Portland cement-only concrete, an efficiency factor concept was developed. The compressive strength of concrete depends highly on the water/cement ratio. Therefore, one way to achieve higher strength while using additions is to decrease the water/binder ratio. This means that, in order to achieve similar compressive strength at 28 days, for the same water content, the mass of addition used must be larger than the mass of cement that it is replacing. Thus, according to the *k*-factor concept, the mass of addition (A) replaces a mass of *k*A of Portland cement. In this approach, instead of using the water/binder ratio, an equivalent water/cement ratio is used, which is defined by equation (1) [Domone and Illston (2010)]. A *k*-factor of 1 means that the addition replaces the exact same amount of cement, which is the case for Mix 6. A *k*-factor lower than 1 means a larger amount of cementitious material and, therefore, a lower actual water/binder ratio (Mix 3). A *k*-value of 0.6 was used, as recommended in SS 13 70 03 (2008) for GGBS additions. As it can be seen in Table 4.3, the equivalent water/cement ratio is 0.45 for both Mixes. However, for Mix 3 (with an efficiency factor of 0.6), the water/binder ratio is 0.39, whereas for Mix 6 (with a *k*-factor of 1) the w/b ratio is 0.45. Given that the compressive strength increases with a reduction of water/(cementitious material) ratio [Neville (2003)], Mix 6 would theoretically show lower compressive strength, which is in accordance with the results obtained.

The results presented show, once again, effectiveness of the use of the efficiency factor concept in reducing the influence of the addition of GGBS in the compressive strength of concrete at all ages. It is important to notice, however, that the rate of strength gain is comparable for both mixes, i.e., the use of an efficiency factor does not influence the rate of strength development of concrete, but rather its compressive strength at each age.

It is also important to notice that Mix 6 presents a lower cement than Mix 3. Even though the water/binder ratio was kept constant for both mixes, the different cement contents used for both mixes may have also influenced their compressive strength.

According to Figure 4.1, the activity index for the GGBS used (Slagg Bremen) combined with the Portland cement Cementa Anläggningscement (CEM I 42.5 MH/SR/LA) used is 77% (at 28 days of age). This would mean that the compressive strength of a concrete quality with the GGBS replacing the same amount of cement (*k*-factor of 1) would present a compressive strength at 28 days that is 77% of the compressive strength of Portland cement concrete. Figure 5.4 compares the compressive strength of the Portland cement concrete (Mix 1) at ages between 7 and 56 days with the compressive strength of concrete with 50% GGBS replacement, produced with an efficiency factor of 1.

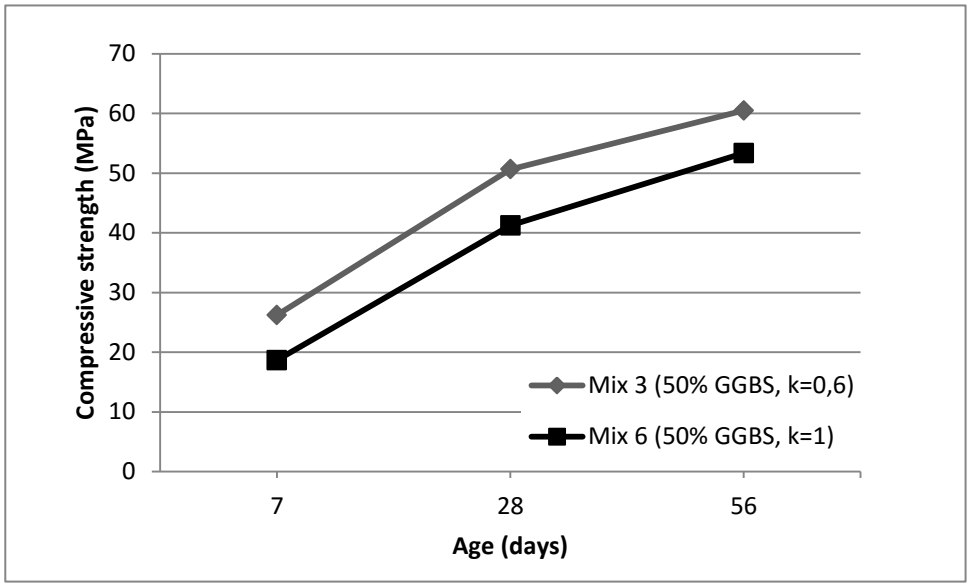

Figure 5.4 – Comparison between the compressive strength of the reference Portland-cement concrete and concrete with 50% GGBS replacement, k=1, air=4.5%. Tests performed at 7, 28 and 56 days of age. Tested according to SS-EN 12390-3 (2009).

As expected, the compressive strength is higher for Portland cement concrete than for concrete with 50% of GGBS replacement (Figure 5.4). However, the difference is more marked at early ages, and decreases with an increase in time: at the age of 7 days, the ratio between the compressive strength of Mix 6 to the compressive strength of Mix 1 is 57%; at the age of 28 days, the ratio is 80%; and finally, at the age of 56 days, the compressive strength of the GGBS concrete represents 92% of the compressive strength of Portland cement concrete.

The activity index obtained for Slagg Bremen mixed with Cementa Anläggningscement (CEM I 42.5 MH/SR/LA) shown in Figure 4.1 is 45% at 7 days of age and 77% at 28 days of age. The compressive strength obtained for Mix 6 at 7 days of age is, however, 57% of the value obtained for Mix 1, which is slightly higher than the 45% expected, according to the activity index concept. As for the age of 28 days, the ratio obtained (80%) was only 3% higher than the 77% expected. It must be noted that the activity index is obtained using a mortar sample in which the binder is composed by 50% of Portland cement and 50% of addition. However, Mix 3 is composed by 66% of cement and 33% of GGBS (Table 4.3). This difference may explain the higher ratio for the compressive strength obtained at 7 days of age, when compared with the activity index: since the amount of GGBS to cement in the mix is lower, the effect on the strength development at early ages will also be lower, thus resulting in a higher compressive strength at early ages. At the age of 28 days, however, the ratio between the compressive strength of Mix 6 and Mix 1 is more approximate to the activity index measured for a mix with the GGBS and cement used.

Figure 5.4 also shows that the strength development of concrete with GGBS continues at approximately the same rate after 28 days of age (at least up to the age of 56 days), slowing down significantly for Portland cement concrete. This fact is in accordance with the literature. As long as

there are some hydroxyl ions being released by the hydration of Portland cement, allied with the continuous release of alkalis by the hydration of GGBS, the hydration of slag continues months after the 28 days of age [Neville (2003)]. In fact, it is possible that Mix 6 would achieve the same compressive strength of Mix 1 after the 56 days of age, or even exceed it. The ACI Committee Report (2000) refers that long-term strength gain 20 years after mixing has been documented for Portland blast-furnace slag cement concrete exposed to moist or air curing.

5.2.1.4. Influence of the use of superplasticizers

Figure 5.5 compares the average compressive strength at different ages for mixes with 0% and 50% of GGBS replacement, with 4.5%±0.5% of targeted air content, efficiency factor of 0.6 (for the mixes containing GGBS), with and without superplasticizer.

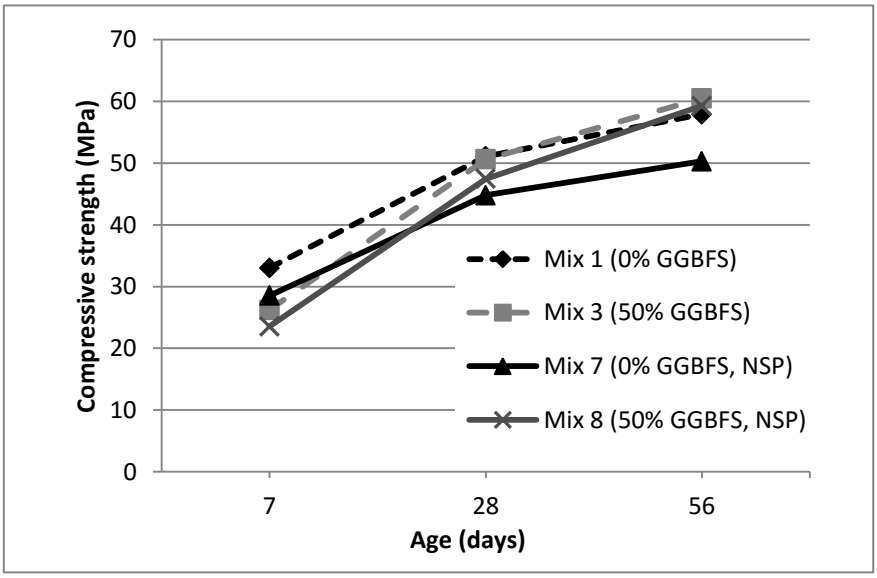

Figure 5.5 - Compressive strength development of concretes with 0% and 50% GGBS, k=0.6 for the mixes with addition, air=4.5%, with and without superplasticizer. Tests performed at 7, 28 and 56 days of age. Tested according to SS-EN 12390-3 (2009).

For the concrete mixes with 50% GGBS (Mix 3 and Mix 8), the compressive strength is slightly lower for concrete qualities without superplasticizer (Mix 8) than for concrete with superplasticizer. However, at 56 days of age, the compressive strength is similar for both concrete qualities. On the other hand, there is a marked difference between the compressive strength of Portland cement concrete with and without superplasticizer at all ages, with Mix 1 (with superplasticizer) displaying a much higher compressive strength than the comparable Mix 7 (without superplasticizer).

In order to achieve the same consistency for concrete without superplasticizer as for the concrete qualities with superplasticizer, a greater amount of air entraining agent was used in Mixes 7 and 8. The results of the air content in the fresh state according to SS-EN 12350-7 show that the air content varies from 4.8% and 4.6% for both batches of Mix 1 to 5.1% and 5.8% for both batches of Mix 7.

Also, the air content for Mix 3 obtained was 4.9% for batch number 1 and 4.1% for batch number 2, whereas the air contents obtained for batches 1 and 2 of Mix 8 were 4% and 5.3%, respectively. For both cases, the air content of mixes without superplasticizer is higher than for concrete qualities produced with superplasticizer, which may explain the higher compressive strength of the latter. As explained earlier, an increase in the air pores inside concrete reduces its density, which results in a lower compressive strength [Neville (2003)].

Moreover, the results obtained with the Air Void Analyser show even more significant differences between the air contents of mixes produced with and without superplasticizing admixture (Table 5.3) In fact, according to the AVA, batch number 1 of Mix 7 presents a total air content of 12.1%, which may explain the significant lower compressive strength of this concrete quality at all ages. On the other hand, the AVA results for Mix 8 reveal an air content of 2.2% for batch number 1, which may have contributed to the similar compressive strength of this mix at all ages, when compared with Mix 3 (and for the higher compressive strength at 56 days of age).

The differences in the compressive strength displayed between the concrete mixes casted with and without superplasticizer are, therefore, related with differences in the air content of the mixes, instead of the use of superplasticizing admixtures. In fact, the influence of the use of superplasticizers on the compressive strength of concrete is limited to its action in allowing a reduction of the water content, for the same desired workability [Ramachandran (1995)]. A decrease in the water/binder ratio results on a higher rate of strength gain, since the cement particles are closer to one another, and a continuous matrix of hydration products is established more rapidly [Neville (2003)]. Given that Mixes 1 and 7, and Mixes 3 and 8 were produced with the exact same water/(cementitious material) ratio, an effect of the use of superplasticizer in the compressive strength was not expected. Instead, the targeted slump was achieved using air entraining admixtures, which resulted on higher air content on the non-superplasticized mixes and, therefore, lower compressive strength of these mixes.

5.2.1.5. Influence of curing at increased temperature

One cube of Mix 4 (100% GGBS, targeted air content of 4.5%±0.5% and *k*-factor of 0.6) was cured at increased temperature, according to the procedure explained in section 4.5, and its compressive strength at 28 days of age was determined. Figure 5.6 compares the compressive strength at the 28th day of age of Mix 4 cured according to the standard (wet curing at 20ºC up to the age of testing, according to SS-EN 12390-2), and curing at increased temperature (wet curing at 20ºC until 7 days of age, and curing in water at 55ºC until the age of testing).

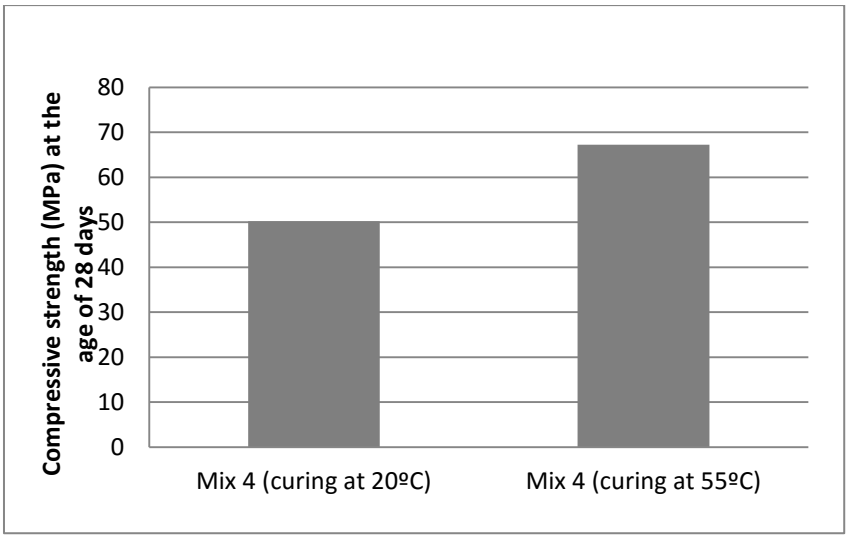

Figure 5.6 – Average compressive strength at 28 days of age for concrete with 100% of GGBS replacement, for different curing regimes. Tested according to SS-EN 12390-3 (2009).

The results show that an increase in the curing temperature results on an increase in the compressive strength at 28 days of age from 50.2MPa to 67.2MPa, for concrete with 100% of GGBS replacement. This result was expected. According to the ACI Committee 233 (2000), an increase in the curing temperature increases significantly the compressive strength of slag concrete, especially at early ages. Higher temperatures speed up the hydration reactions of the cementitious materials. Since the strength of concrete increases with the progress of hydration, a higher compressive strength for concrete cured at higher temperatures is obtained. On the other hand, an increase in temperature also contributes to an increase in the solubility of alkali hydroxides, which results on a higher reactivity of slag, and therefore, increased rate of strength gain of GGBS concrete [Neville (2003)].

Since the hydration of GGBS is slower than that of the Portland cement, and given that an increase in temperature results on a higher rate of strength gain, GGBS concrete is more affected by the curing temperature than Portland cement concrete. Also, the effect the curing temperature will be more pronounced for concrete mixes with high percentages of replacement, whose compressive strength depends mainly on the hydration of slag [Gruyaert (2011)].

In the present research, the effect of curing at increased temperature was only investigated for one concrete quality with 100% of slag replacement, and only at 28 days of age. The effect of curing at higher temperatures at later ages was not studied. Even though curing at higher temperatures increases significantly the early strength of concrete, it may lead to lower ultimate strengths. This fact is pointed out by Gruyaert (2011), citing Barnett et al. (2006), who found that the ultimate compressive strength obtained was lower for curing at higher temperatures. The authors believed that an increase in temperature at early ages resulted from a formation of dense hydrated particles around the unhydrated particles, which prevented the progress of hydration. The lower strength at later ages for concrete cured at higher temperatures is also mentioned by Domone and Illston (2010), and attributed to the fact that the C-S-H gel formed quickly in the hydration at higher temperatures is less uniform

and therefore weaker than the hydration products of concrete cured at lower temperatures. Neville (2003) also refers that the hydration products formed during the rapid reactions at very early ages present a poorer, more porous structure. This effect is more marked for concrete subjected to very high temperatures at very early ages (right after placing and setting). In order to minimize these adverse effects, the concrete cured at higher temperature during this research was placed in the water tank at 55ºC only after 7 days of standard water curing at 20ºC. According to Neville, delaying the increase in temperature at least a week leads to a higher strength than that of concrete subjected to increased temperature at very early ages.

Nevertheless, Neville (2003) refers that the harmful effect of curing at increased temperature on the compressive strength of concrete at later ages is less significant for slag concrete than for Portland cement concrete.

5.2.2. Rapid Chloride Migration

The resistance against chloride ingress was determined by the non-steady state migration test described in NT Build 492. Figure 5.7 to Figure 5.12 illustrate the average results obtained for the non-steady state migration coefficient of the specimens of all the mixes, determined according to equation (4). All raw data is presented in Appendix D.

5.2.2.1. Influence of the amount of Portland cement replacement by GGBS

Figure 5.7 shows the results for the average Rapid Chloride Migration coefficient, $D_{nssm,}$ for mixes with different percentages of GGBS replacement (between 0% and 100% of GGBS of the Portland cement content), cured at 20ºC, and measured at 28 and 56 days of age.

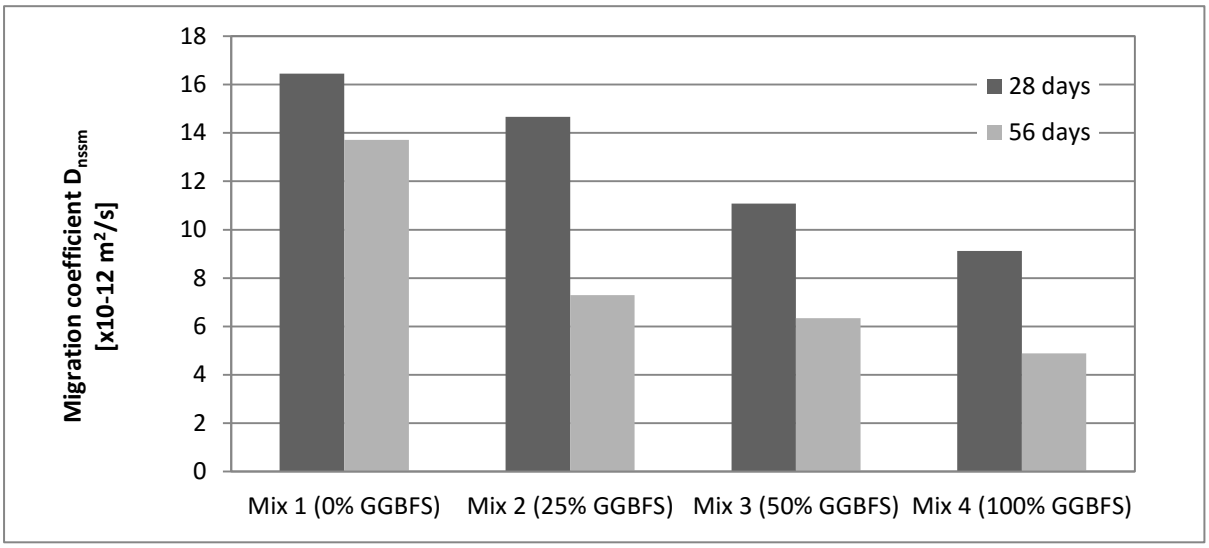

Figure 5.7 - Rapid chloride migration coefficient, D_{nssm}, for mixes cured at 20ºC with different additions of GGBS. Coefficient measured at 28 and 56 days of age. Tested according to NT Build 492.

The results show a lower chloride migration coefficient for the specimens tested at 56 days of age than for those tested at 28 days of age, for all concrete qualities. These results are in accordance with the literature: the resistance against chloride ingress depends on the permeability/penetrability of concrete, which in turn depends on the degree of hydration of concrete. The flow of liquids (and gases) through the concrete paste is facilitated through the larger capillary pores than through the smaller gel pores. With progress of hydration, the capillary pores in concrete are gradually filled with the C-S-H gel that is formed during the hydration reactions, i.e., the pore structure changes continuously, and the permeability of the paste is reduced with progress of hydration. Since the degree of hydration (amount of cement that has reacted, relative to the total amount of cement present in the mix) increases with time, the permeability will thus be reduced [Neville (2003)].

However, the effect of the hydration degree of concrete is more obvious for concrete mixes with GGBS addition than for the reference Portland-cement only concrete. For Portland cement concrete (Mix 1), the D_{nssm} coefficient decreases only 17% between specimens tested at 28 and 56 days of age, whereas for all concrete mixes with GGBS (Mixes 2, 3 and 4), a decrease between 43% and

50% is registered. Similar results were obtained by Gruyaert (2011), who determined the non-steady state migration coefficient according to NT Build 492 for concrete qualities with percentages of GGBS replacement of 0%, 50%, 70% and 85% of the total binder content, for ages between 1 and 12 months. The results obtained by the author showed a significant decrease of the migration coefficient with time for concrete qualities with high GGBS replacement levels. As for the reference Portland cement concrete, only a slight decrease of the migration coefficient after 28 days was registered. These results are related with the lower hydration rate of GGBS, which leads to a larger average pore size at early ages [Domone and Illston (2010)]. However, unlike the hydration of Portland cement, whose rate is greatly reduced after 28 days of age, the hydration of GGBS continues at a high rate, which leads to the continuous formation of gel and consequent reduction of the permeability of concrete with time [Gruyaert (2011)]. These results are also supported by Li et al. (2006), who determined the porosity of pastes containing 0%, 10%, 30% and 40% of slag, and found that the porosity of the pastes containing GGBS continues to decrease even after 90 days, while for Portland cement concrete, its changes only slightly after 28 days of age. The pore size distribution of concrete qualities with with 50% and 65% of GGBS of the total binder ratio was also investigated by Boukini et al. (2009), who found that the pore volume decreased with ageing for all specimens cured in moisture curing.

The results also display a clear decrease in the average chloride migration coefficient with the increase in the amount of GGBS replacement in the mix. That is the case for concrete specimens tested at both 28 days and 56 days of age. Gruyaert (2011) reached the same conclusion for the rapid chloride migration tests performed on concrete qualities with 0%, 50%, 70% and 85% of GGBS.

The positive influence of the increase in GGBS content in the improvement of the resistance against chloride migration may be due to different factors. On the one hand, an increase in the slag content results on a denser and less permeable concrete, which reduces the diffusion of chloride ions and slows down capillary suction [Neville (2003)]. This fact was observed by Cheng et al. (2005), cited by Gruyaert (2011), who determined the permeability coefficient of concrete qualities with 0%, 40% and 60% of slag of the total binder content at 91 days of age, and found that the permeability coefficient decreased with an increase in GGBS content. Another reason is the increase of the chemical and physical binding of chlorides provided by the presence of the GGBS in the concrete mix, as explained in Chapter 2.3.2.6, which contributes to a reduction of the free chlorides in the paste.

However, the influence of the amount of GGBS addition seems slightly different for concrete tested at different ages. In fact, the chloride penetration of the specimens tested at 28 days of age decreases gradually as the amount of slag increases. The D_{nssm} coefficient decreases 11% between Portland cement concrete and Mix 2, 24% between Mixes 2 and 3, and 18% between Mix 3 and Mix 4. On the other hand, for the specimens tested at 56 days of age, the reduction in the chloride migration is not regular. Instead, the results show a marked decrease (47%) in the D_{nssm} coefficient between Portland cement concrete (Mix 1) and concrete with 25% of slag replacement (Mix 2). As the percentage of slag replacement increases, the chloride migration coefficient is not significantly affected: the for concrete mixes with larger percentages of replacement, the Rapid Chloride Migration coefficient only

varies 13% between Mix 2 and Mix 3, and 23% between Mixes 3 and 4. The results show that, for concrete older than 28 days, an increase in the GGBS content does not translate in a proportional increase in the chloride resistance. Similar behaviour was observed by Gruyaert (2011) for mixes with high percentages of replacement (50%, 70% and 85% of GGBS of the total binder content), who displayed only slightly differences in the chloride migration coefficient measured between 1 and 12 months.

These results show that the addition of GGBS is very effective in reducing the chloride penetrability in concrete, when compared to Portland cement concrete, even for replacement levels as low as 25% of the cement content, as long as sufficient hydration of the GGBS is ensured. For earlier ages (at least for 28 days of age), higher percentages of GGBS are necessary to obtain significant reduction in the chloride ingress.

Moreover, even with the slower hydration of GGBS, the results show that the chloride migration coefficient is always lower for slag concrete than for Portland cement concrete of the same age, cured according to the same procedure, even at ages as early as 28 days, and for percentages of replacement as high as 100% of the cement content. These results indicate that, as long as proper curing is provided during the early days, the effect of the addition of GGBS in reducing the chloride ingress of concrete is able to offset the effect of the lower hydration rate, and consequent higher permeability of the slag concrete at early ages.

The results demonstrate a significant influence of the GGBS content in the improvement of the resistance against chloride ingress of concrete.

5.2.2.2. Influence of curing at increased temperature

Figure 5.8 presents the results for the Rapid Chloride Migration coefficient for the specimens of Mix 4 (with 100% of GGBS replacement), cured under different regimes: standard curing (curing in water at 20ºC until the age of testing) and curing at increased temperature (curing in water at 20ºC up to the age of 7 days, and curing in water at 55ºC until the age of testing).

As displayed in Figure 5.8, both at 28 and 56 days of age, the chloride migration coefficient is significantly lower for specimens cured at higher temperature. Curing at higher temperature increases the rate of hydration of concrete, which means that, at the same age, the degree of hydration of a concrete quality will be higher for concrete cured at increased temperature [Neville (2003)]. Since the permeability of concrete decreases with an increase in the hydration degree, the chloride ingress will be lower for concrete cured at higher temperature, as shown by the results.

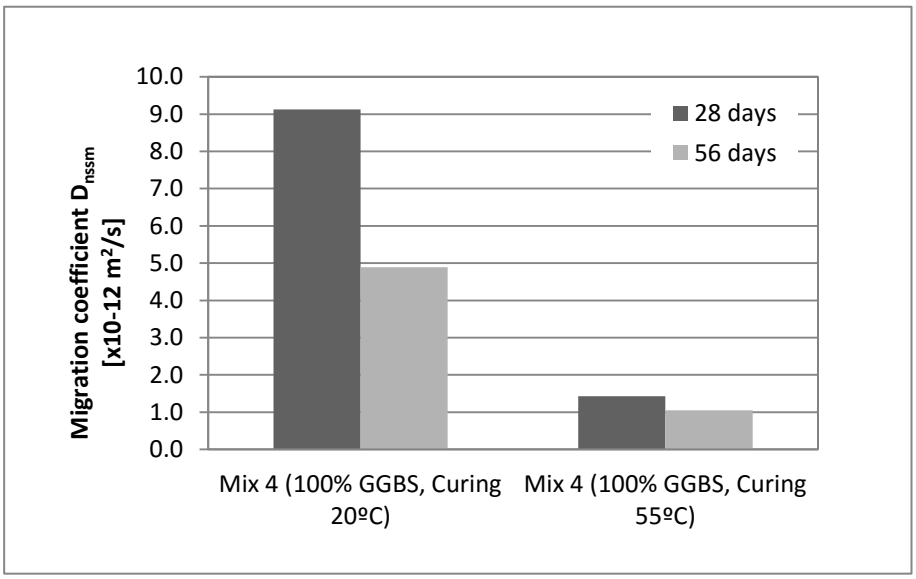

Figure 5.8 - Rapid chloride migration coefficient, D_{nssm}, for mixes with 100% GGBS, k=0.6 and 4.5% air content, cured at 20ºC and 55ºC. Coefficient measured at 28 and 56 days of age. Tested according to NT Build 492.

On the other hand, the progress of hydration also increases with time [Gruyaert (2011)]. Therefore, for both curing regimes, the D_{nssm} coefficient is lower for concrete qualities tested at 56 days of age than for the specimens tested after 28 days, as observed in Figure 5.8. This difference is, however, more significant for concrete cured at 20ºC than for concrete cured at 55ºC. Given that curing of concrete at increased temperature accelerates the rate of the hydration reactions, a larger percentage of the cementitious particles are already hydrated at early ages. Therefore, the effect of time in the increase of the degree of hydration will be less relevant, and, consequently, no significant difference in the chloride ingress is noticed at later ages. For concrete cured at lower temperatures, the slower hydration rate requires longer time for high degrees of hydration to be achieved, which results on a marked improvement of the resistance against chloride ingress at later ages.

The accuracy of the results obtained for the Rapid Chloride Migration coefficient of the specimens cured at 55ºC must, however, be regarded with caution. The non-steady state Rapid Chloride Migration test described in NT Build 492, and the parameters involved in the formula, were studied and defined to be used in Portland cement concrete cured according to the standard procedure described in SS-EN 12390-2 (water curing at 20ºC). There is no assurance that the exact same parameters can be used for concrete produced with additions, and cured under a different regime.

It is also important to refer that the decrease in the chloride migration coefficient obtained for concrete cured at higher temperature was attributed to the increase of the rate of hydration of the cementitious materials. However, the tests performed in this research tested concrete qualities of ages of 28 and 56 days only. Testing at ages later than 56 days could yield different results. In fact, both Gruyaert (2011) and Neville (2003) mention adverse effects of high temperatures in the resistance against chloride ingress of concrete. The authors attribute this detrimental effect to the fact that the amount of bound chlorides is lower at increased temperatures, which results on a higher content of free chloride

ions in the paste, and to an increase in the solubility of the Friedel's salt. Moreover, an increase in temperature also contributes for a lower resistance against chloride induced corrosion, by accelerating the corrosion reactions [Neville (2003)]. According to the results obtained, it seems that up to the age of 56 days, the effect of the temperature in the degree of hydration may be more significant for the chloride ingress.

5.2.2.3. Influence of the air content of concrete

Figure 5.9 illustrates the effect of the air content of concrete in the D_{nssm} coefficient. Two mixes (Mix 3 and Mix 5) both produced with 50% of cement replacement by GGBS and different targeted air contents (4.5% and 6%, respectively) were tested at the ages of 28 and 56 days.

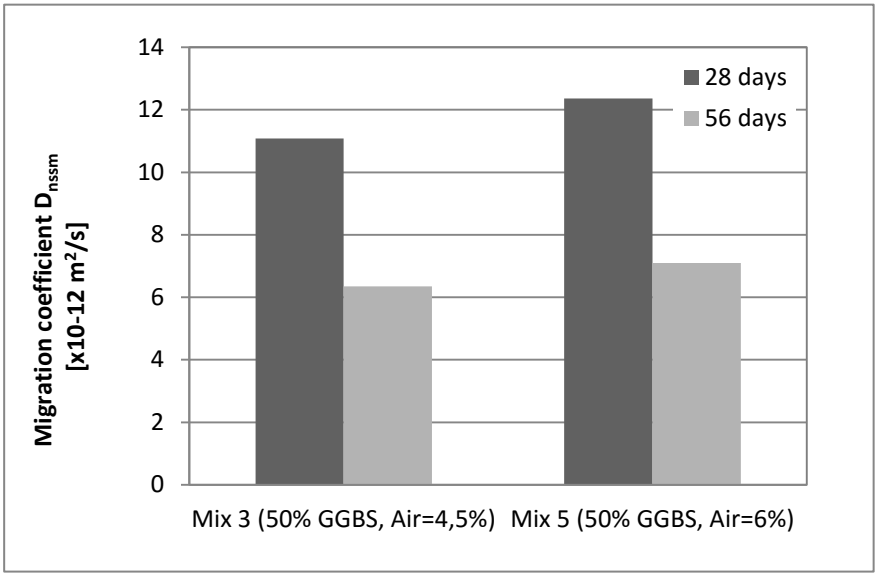

Figure 5.9 - Rapid chloride migration coefficient, D_{nssm}, for mixes with 50% GGBS, k=0.6 and different amount of air, cured at 20ºC. Coefficient measured at 28 and 56 days of age. Tested according to NT Build 492.

The results show a slight increase in the chloride migration coefficient for Mix 5 (with higher air content), when compared to Mix 3, both at 28 days and at 56 days of age.

The chloride ingress in concrete depends mainly on the penetrability of concrete, which is directly related to its air pore structure. It is therefore expected that an increase in the air content will lead to an increase in the permeability of concrete, due to an increase in the number of air voids throughout the paste. Also, an increase in the number of air pores in concrete due to the use of air entrainment admixtures often results in a reduced spacing factor, which shortens the continuous paths between the air voids in the paste, therefore facilitating the transport of chlorides. On the other hand, the permeability of concrete depends not only on the volume and distribution of voids, but also on the size and continuity of the air pores. Given that it is the capillary porosity which controls the permeability of concrete (which increases with an increase in the amount and size of capillary pores) [Neville (2003)], and since the air pores entrained using AEA are usually of a much smaller size, the effect of an

increase of the pores in the paste is not as marked as one would expect. For this reasons, only a slight increase in the chloride migration coefficient is obtained for concrete with increased air content (Figure 5.9).

The results also reveal that, even though an increase in the air content affects the overall resistance against chloride ingress, it does not influence the development of chloride resistance with ageing of concrete. In fact, the reduction in the D_{nssm} coefficient between the ages of 28 days and 56 days is 43% for both mixes, regardless of the air content. Moreover, the increase in the migration coefficient with the increase in the air content between Mixes 3 and 5 was 10% for both specimens tested at 28 and 56 days of age. This fact was expected since, as it was concluded in the tests of the compressive strength resistance, the air content in concrete affects only the air pore structure of concrete, and not the chemical reactions and the rate of hydration of concrete.

5.2.2.4. Influence of the efficiency factor

Figure 5.10 presents the results of the chloride migration coefficient determined according to NT Build 492 for two mixes with 50% GGBS (Mix 3 and Mix 6), and different *k* factors (0.6 and 1.0, respectively).

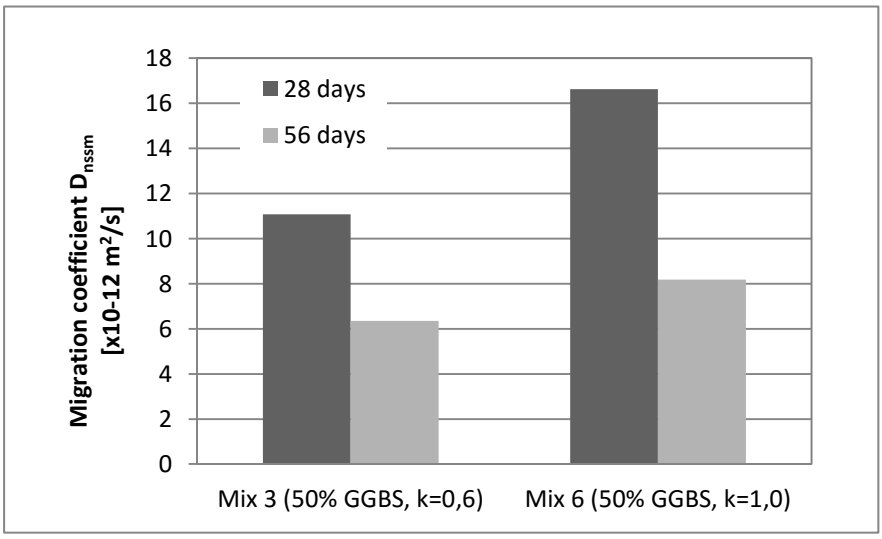

Figure 5.10 - Rapid chloride migration coefficient, D_{nssm}, for mixes with 50% GGBS, 4.5% air content and different *k*-factor, cured at 20ºC. Coefficient measured at 28 and 56 days of age. Tested according to NT Build 492.

The results show a higher value of the migration coefficient for the concrete specimens with an efficiency factor of 1.0 (Mix 6), both at 28 and at 56 days of age. These results were somewhat expected. In fact, the chloride ingress in concrete is closely related with the permeability of the paste, which in turn depends on the water/cement ratio. As it can be seen in Table 4.3, the equivalent water/cement ratio, determined according to equation (1) is 0.45 for both mixes. However, for Mix 3 (with an efficiency factor of 0.6), the water/binder ratio is 0.39, whereas for Mix 6 (with a *k*-factor of 1) the w/b ratio is 0.45. Lower water/cement ratios result in lower permeability of concrete [Neville (2003)]. Therefore, the migration coefficient is lower for Mix 3 than for Mix 6.

The increase in the D_{nssm} coefficient for a greater *k*-factor is more pronounced for concrete tested at 28 days of age, varying from 11.1 for Mix 3 to 16.6 for Mix 6, whereas for concrete tested at later ages (56 days), only a slight increase in the D_{nssm} coefficient is identified, increasing from 6.3 for 28 days to 8.2 at the age of 56 days. On the other hand, the decrease in the Rapid Chloride Migration coefficient between 28 and 56 days is very similar for both concrete qualities. In can be thus concluded that the difference in the *k*-factor / water/binder ratio does not strongly influence the development of the resistance against chloride ingress with the ageing of concrete.

Figure 5.11 compares the results obtained for Mix 6, with 50% of GGBS replacement of the mass of Portland cement and Portland cement concrete (Mix 1), both with the same actual water/binder ratio (0.45). It can be concluded that, for the age of 28 days, the D_{nssm} coefficient is similar for both concrete qualities. However, the tests performed at 56 days of age reveal a significant lower chloride migration coefficient for concrete with GGBS than for Portland cement concrete. These results are related with the slower hydration reactions of slag, which result in a higher porosity of GGBS concrete at early ages. With continuing hydration, however, concrete with addition of slag presents a higher resistance against chloride ingress than Portland cement concrete produced with the same w/c ratio. In fact, Pandey and Sharma (2000) showed that, at the age of 7 days, the average pore size is lower for Portland cement concrete than for concrete with 10% of slag replacement. With the continuing hydration of slag, the pore space is filled with gel, and this tendency is reversed between ages of 28 and 90 days, which explains the improved chloride resistance of GGBS concrete with ageing.

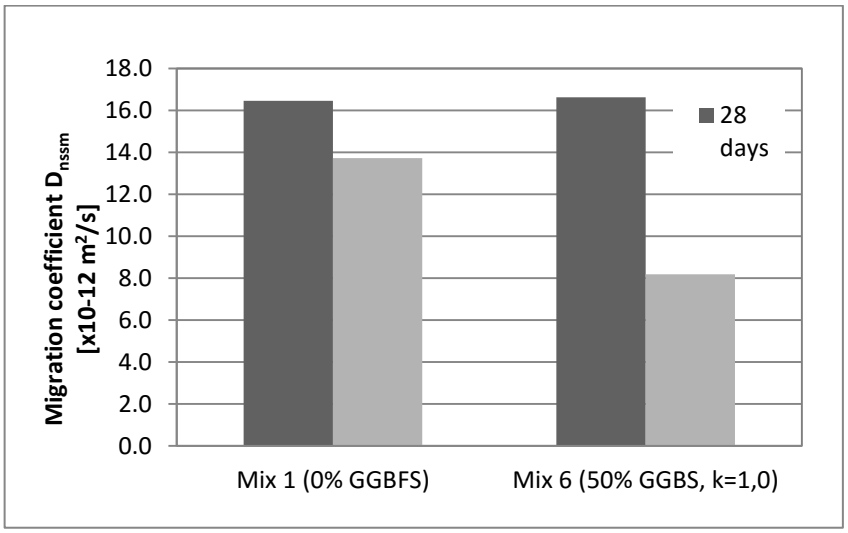

Figure 5.11 - Comparison between the rapid chloride migration coefficient, D_{nssm} of the reference Portland-cement concrete and concrete with 50% GGBS replacement, k=1, air=4.5%, both cured at 20ºC. Coefficient measured at 28 and 56 days of age. Tested according to NT Build 492.

The results obtained in this investigation show, therefore, that the addition of GGBS in concrete results in a significant improvement of the resistance against chloride ingress in concrete, even for efficiency factors equal to 1, as long as sufficient hydration is ensured.

These results also show that the efficiency factor concept is an effective way to deal with the compressive strength of concrete qualities with additions, but not necessarily its durability. In fact, the parameters required for high-quality concrete are usually related with minimum cement content, minimum cement class, maximum w/c ratio, and compressive strength achieved at 28 days of age. It is usually assumed that concrete that fulfils these requirements will present adequate protection against the aggressive agents. This is only partially true. As explained earlier, the majority of the deterioration mechanisms depend on the penetration of fluids or gases inside concrete, as it is the case of carbonation, chloride ingress, and frost scaling. And, as previously explained, the penetration of these agents in concrete depends on its porosity, which in turn depends on the water/cement ratio. There is, therefore, a base for determining an efficiency factor based on an equivalent water/cement ratio. However, this approach does not consider the effects of each addition on the microstructure of concrete – only on the compressive strength development. Therefore, new efficiency factors should be studied considering the durability parameters.

As seen by the results obtained, GGBS concrete performs better at all ages than Portland cement concrete in what concerns resistance against chloride ingress. Therefore, the efficiency factor for this parameter should be higher than 1. Similar conclusions were reached by Gruyaert (2011), who studied the *k*-value of concrete mixes with different amounts of slag replacement for chloride ingress, and obtained values of 1.3, 1.6 and 1.9 for mixes with 50%, 70% and 80% of GGBS of the total binder content.

5.2.2.5. Influence of the use of superplasticizers

Figure 5.12 shows the results for the chloride migration coefficient of concrete mixes with different percentages of GGBS replacement (0 and 50%), produced with and without superplasticizer.

The results show an increase in the Rapid Chloride Migration coefficient for Portland cement concrete casted without superplasticizer (Mix 7), at the age of 28 days, when compared to the mix with superplasticizer (Mix 1). However, for the specimens tested at 56 days of age, this trend is inverted, being the D_{nssm} coefficient lower for Mix 7.

As for the mixes containing 50% of GGBS replacement, the chloride migration coefficient is higher for Mix 3, produced with superplasticizer, than for Mix 8, for both ages of testing. However, the difference in the chloride penetration between the two mixes is negligible, varying from 4% for tests carried out at 28 days to 16% for specimens tested at 56 days of age.

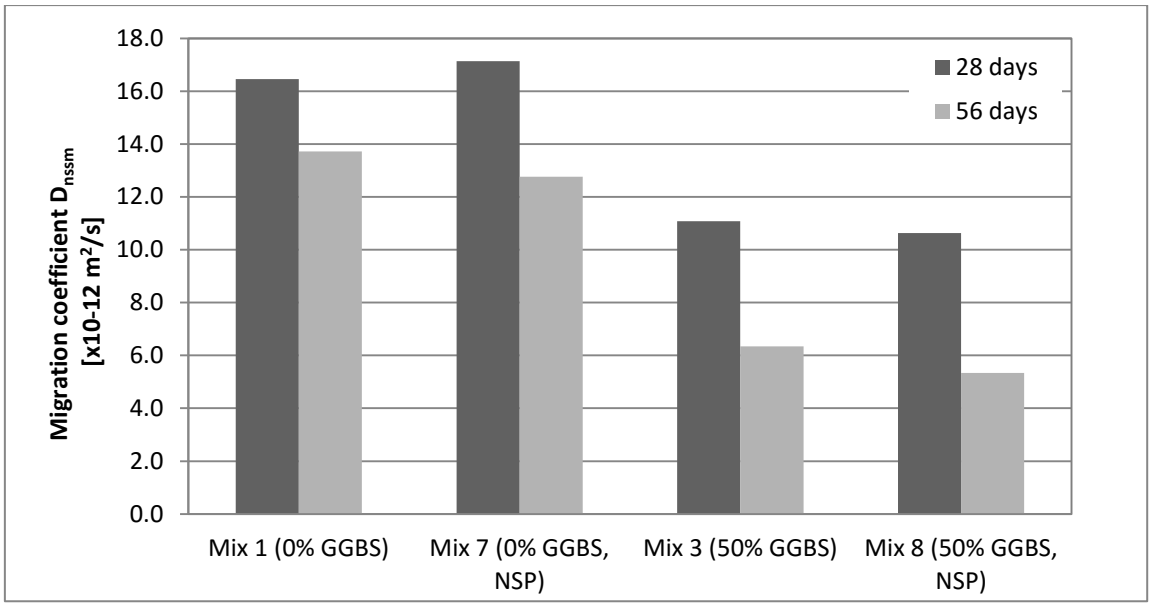

Figure 5.12 - Rapid chloride migration coefficient, D_{nssm}, for mixes with 0% and 50% GGBS, k=0.6 and 4.5% air content, with and without superplasticizer, cured at 20ºC. Coefficient measured at 28 and 56 days of age. Tested according to NT Build 492.

The results obtained are not conclusive in what concerns the influence of the use of superplasticizers in the chloride ingress of both Portland cement concrete and concrete with GGBS (at least for percentages of GGBS replacement up to 50% of the amount of Portland cement). According to the results, there is an apparent beneficial effect of not using superplasticizer, at least at the age of 56 days. This trend is not, however, followed by Portland cement concrete specimens tested at 28 days of age. Furthermore, the differences in the D_{nssm} coefficient registered between the mixes with and without superplasticizer for both concrete qualities (Portland cement-only concrete and concrete with 50% of slag replacement) and at both ages of testing all vary between 4% and 7% - except for 50% GGBS concrete at the age of 56 days, in which the migration coefficient decreases 16% for concrete without superplasticizer (Mix 8).

These minor differences are still within the margin of error, and may be due to a number of factors rather than the use of superplasticizer in the mix. One of the factors may be the precision of the operator when measuring the penetration depth. Another reason may be the difference in the air content of the concrete specimens tested. The air content measured in the fresh concrete was higher for Mix 7 than for Mix 1, which may explain the higher chloride migration coefficient observed for Mix 7 at 28 days of age. The reason behind the decrease of the chloride migration of Mix 7 for tests performed at 56 days of age is, however, unclear. On the other hand, the air contents obtained for Mixes 3 and 8 are very similar, which explains the comparable D_{nssm} coefficients obtained for both mixes, at both ages of testing.

5.2.2.6. General remarks

The results obtained with the Rapid Chloride Migration test clearly show a positive effect of the use of slag in concrete in the protection against chloride ingress. However, the test method described was prepared for Portland cement concrete, and not concrete with additions. For Portland cement concrete, NT Build 492 specifies a concentration of free chloride (c_d) of 0.07mol/l at the colour changing boundary given by a a 0.1M silver nitrate solution. This premise may not be true for concrete with additions.

In order to evaluate the correctness of using this test method in GGBS concrete, Gruyaert (2011) measured the chloride profiles for concrete containing slag (at replacement levels between 50% and 85% of the binder content), and determined the free chloride concentration at the colour change boundary for a 0.1 M silver nitrate solution. The author concluded that formula (4) gives a good approximation of the non-steady state migration coefficient for slag concrete, even for different percentages of slag replacement. Further investigation about this subject shall be carried out.

It must also be referred that the non-steady state migration coefficient determined by NT Build 492 gives only a relative comparison of the resistance against chloride ingress of different concrete qualities. In fact, there is no value for the Rapid Chloride Migration coefficient above which concrete can be described as not resistant. There is also no value below which concrete can be considered safe against chloride attack. Chloride ingress in concrete causes damage when it destroys the passivity layer around the reinforcement and corrosion initiates at the steel bars. Since the test methods used to evaluate the chloride ingress in concrete qualities cannot predict how long will it take for the free chloride ions to reach the reinforcement, and whether corrosion will begin during the service life of a structure, there is not a maximum migration coefficient value for concrete to be considered chloride resistant.

5.2.3. Scaling under freezing and thawing

The results of the salt-frost scaling resistance of concrete tested according to the Swedish Standard SS 13 72 44 (2008) are presented in this section. Raw data and pictures of the test specimens after 112 freeze/thaw cycles are presented in Appendix E.

The scaled material after 28, 56 and 112 cycles for all concrete mixes cured and pre-conditioned according to the standard procedures are presented in Figure 5.13.

A careful analysis of Figure 5.13 reveals some tendencies. The salt-frost resistance of concrete generally decreases with an increase in the addition of GGBS (as shown by the increase in the accumulated scaled material for Mixes 1 to 4). There is a markedly positive effect of the increase in the air content in the salt-frost resistance of concrete with GGBS (at least for replacement levels of 50% of the Portland cement weight), demonstrated by the comparison between Mixes 3 and 5. The results also indicate that an increase in the efficiency factor may lead to a more resistant concrete against freezing and thawing in the presence of salts, as demonstrated by the results for Mix 6, when compared to Mix 3. Moreover, the addition of superplasticizer seems to have a negative influence in the frost resistance of concrete with GGBS, as demonstrated by the decrease in the mass of scaled material obtained for the mixes produced without superplasticizer (Mixes 7 and 8), when compared to Mixes 1 and 3, respectively.

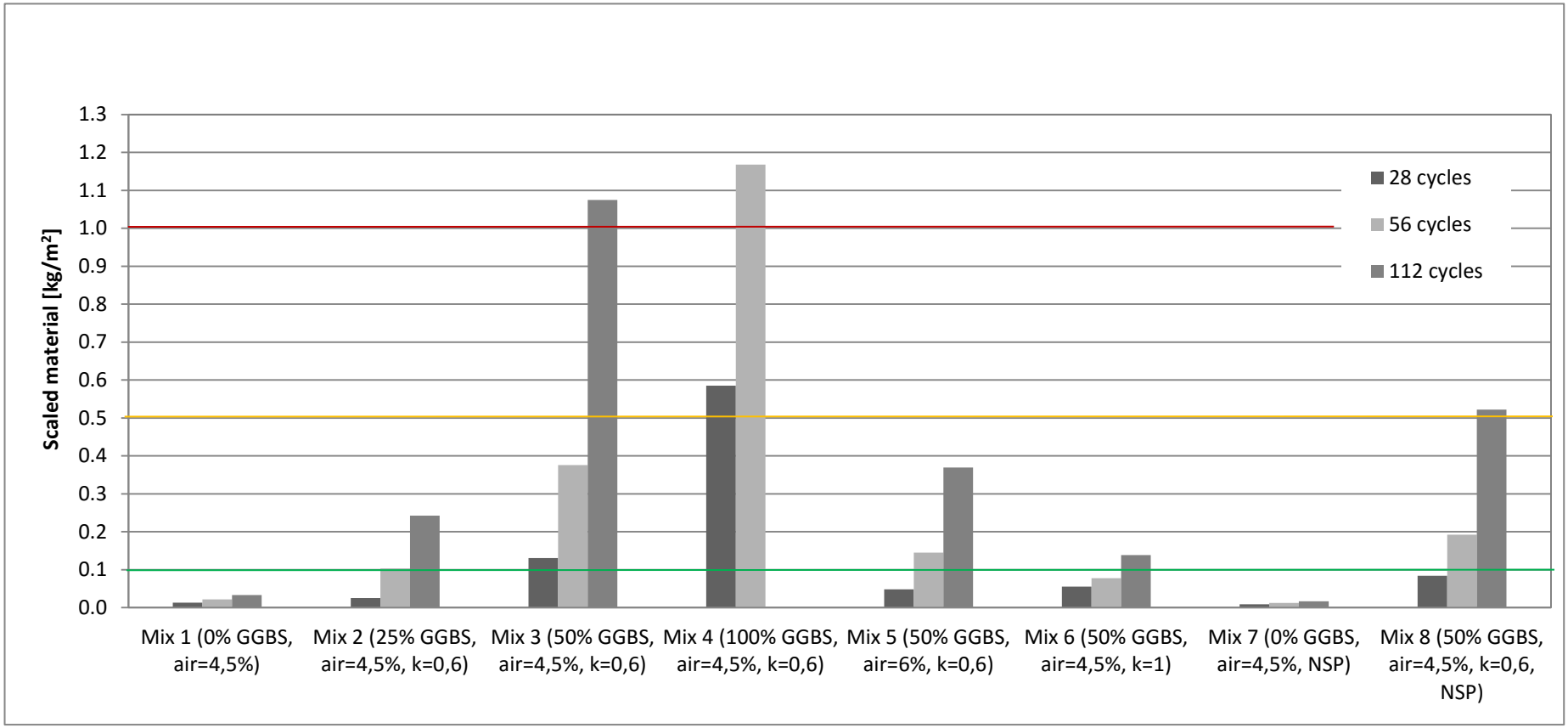

Figure 5.13 - Mean values of the accumulated mass of scaled material per area of freezing surface after 28, 56 and 112 cycles for concrete from all concrete mixes cured and pre-conditioned according to the standards. Tested according to SS 13 72 44 (2008).

5.2.3.1. Influence of the amount of Portland cement replacement by GGBS

Figure 5.14 presents the mean values for the mass of scaled material of concrete at each 7 cycles, for concrete mixes 1 to 4, with different percentages of GGBS replacement and the same efficiency factor (*k*=1) and targeted air content (4.5±0.5%).

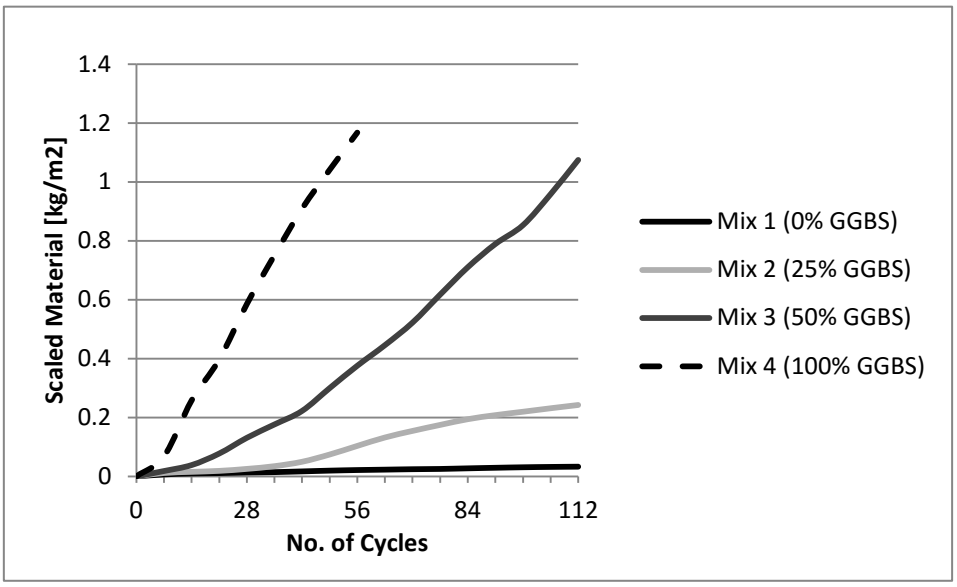

Figure 5.14 - Mean values from frost scaling for concrete cured according to the standard, with different amount of GGBS, k=0.6 and 4.5% air content, measured after each 7 cycles. Tested according to SS 13 72 44 (2008).

As seen in Figure 5.13 and Figure 5.14, the mass of scaled material increased significantly as the amount of GGBS increased. According to the acceptance criteria given by SS 13 72 44 (2008), the reference Portland cement-only concrete (Mix 1) showed very good frost resistance after 112 freeze/thaw cycles (presenting a total mass of scaled material below 0.1kg/m^2) . The mass of scaled material for Mix 2, with 25% of GGBS was 0.243kg/m^2 after 112 freeze-thaw cycles, which reveals good frost resistance, according to the Swedish Standard. As for concrete qualities with 50% of GGBS replacement or higher, both Mixes 3 (with 50% GGBS) and 4 (100% GGBS) were considered not resistant against salt-frost scaling. Mix 3 failed after 112 freeze/thaw cycles, with an average mass of scaled material of 1.075kg/m^2, whereas Mix 4 (with 100% of GGBS replacement) failed as early as the 56th cycle, reaching a scaling of 1.168kg/m^2. The poor salt-scaling resistance of concrete containing high amounts of GGBS is widely documented, even though some conflicting reports have been delivered over the years (especially between laboratory studies and field investigations), as exposed in Chapter 3.4.

Further analysis of the results obtained for the salt-frost scaling resistance of specimens of Mix 3 (Appendix E) show that, after 112 freeze/thaw cycles, only specimen C (casted from batch number 1) presented an accumulated scaled material lower than 1.0kg/m^2. Specimen B, on the other hand (casted from batch number 2), showed an accumulated scaled material higher than the maximum allowed already at the 84th cycle. The average accumulated scaled material after

112 cycles obtained for the specimens casted from batch number 2 (specimens B and D) was 21% higher than the results obtained for batch number 1. In fact, the scaled material of the specimens of batch number 1 was 0.948kg/m^2 after 112 cycles, which is still within the acceptable limits, unlike the 1.202 kg/m^2 obtained for the specimens of batch number 2.

The results for the air content in the fresh concrete of Mix 3 show a lower air content for batch number 2, measured both with the AVA and according SS-EN 12350-7, with differences of 0.7% and 0.8%, respectively. The specific surface and spacing factor obtained for both batches were very similar though, as showed in Table 5.3. These results reveal that the spacing factor and specific surface of concrete are not, independently, an indication of the resistance against frost attack of a concrete mix. The total air content must also be known. As previously explained, being the specific surface the ratio between the total surface area of the air pores divided by their total volume, the total volume of air pores must be known to assess the significance of the specific surface. A higher total volume of air pores means a higher surface area of the pores, which implies a finer pore structure. If the spacing factor is the same, it means that the average pore size is lower. Air voids with smaller sizes contain less freezable water, which results in a lower degree of saturation of the paste and, therefore, consequently, the hydraulic and osmotic pressures caused by freezing will be lower Neville (2003). This fact may explain the differences observed between the results of the two batches casted from Mix 3.

Mix 4 (with 100% of GGBS replacement) failed as early as the 56th cycle, with 3 out of the 4 specimens failing at this age, reaching an average scaled material of 1.168kg/m^2. In fact, after 49 freeze/thaw cycles, specimens C and D already presented a mass of scaled material higher than 1.0 kg/m^2, as shown in Appendix E.

As previously referred, all specimens from Mix 4 to be tested to salt-scaling resistance were collected from batch number 2, whose air avoid parameters measured according to the Air Void Analyser (specific surface and spacing factor) were within the limits for frost resistant concrete. The air content measured with the AVA was, also, higher for batch number 2 (8.80%, against 4.90% measured for batch number 1). However, even though all test specimens were produced from a batch of concrete whose air void parameters fulfilled the usually accepted limits for adequate salt-frost resistant concrete, the results show that the concrete mix was not resistant, according to the acceptance criteria described in SS 14 72 44 (2008). The results obtained seem to indicate that an adequate air void structure is not enough to ensure good salt-frost resistance of concrete, at least for GGBS concrete with 50% of the binder content replaced by slag. These results should, however, be regarded with caution. The results obtained for the air content measured according to SS-EN 12350-7 contradict the results obtained with the AVA, being higher for batch number 1 (4.50%) than for batch number 2 (4.20%). An air void analysis in the hardened concrete of Mix 4 should be carried out to verify if the air pore structure in the hardened concrete correlates with the results obtained by the AVA in the fresh concrete.

Another parameter that may have influenced the salt-frost scaling of Mixes 3 and 4 could be the high slump obtained for both batches of both of these concrete qualities (which vary between 210 and 220mm). As referred in section 5.1.1., concrete mixes with slumps higher than 178mm may reveal loss of air during handling and placing [Ramachandran (1995)]. Therefore, the air content of the hardened mixes may be lower than that measured in the fresh concrete, with a consequent negative effect on the frost resistance of these concrete qualities. In order to accurately evaluate the effect of the slag content and air pore parameters in the salt-frost scaling of concrete with high percentages of GGBS replacement, an evaluation of the air pore parameters of the hardened specimens would have been of great interest.

The results obtained support the limitation of 25% of cement replacement by slag prescribed by SS 13 70 03 (2008) for concrete exposed to freezing environments where de-icing salts are used. However, it might be possible to increase the percentage of replacement, even for the same air content and efficiency factor. The salt-frost resistance of concrete mixes with replacement levels between 25% and 50% should be investigated. Also, the possibility to produce frost resistant concrete with 50% of GGBS replacement by making some changes in the mix should also be studied.

5.2.3.2. Influence of the air content of concrete

Figure 5.15 shows the average mass of accumulated scaled material for concrete mixes 3 and 5, with 50% of the weight of cement being replaced by GGBS, produced with different targeted air contents (4.5±0.5% and 6±0.5%, respectively), and measured after each 7 freeze/thaw cycles.

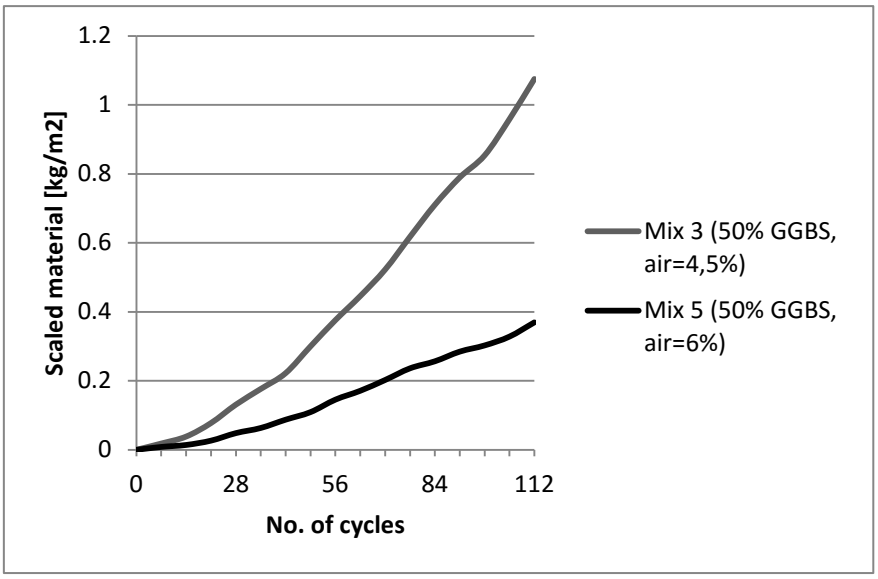

Figure 5.15 - Mean values from frost scaling for concrete cured according to the standard, with 50% GGBS, k=0.6 and different air content, measured after each 7 cycles. Tested according to SS 13 72 44 (2008).

The results plotted in Figure 5.15 reveal a markedly positive effect of the increase of the air content on the performance of concrete subjected to freeze/thaw cycles in the presence of salts. As it can be seen, the total accumulated scaled material for Mix 3 (with targeted air content of 4.5%) after 112 freeze/thaw cycles was 1.075kg/m^2, which is considered not acceptable according to SS 13 72 44 (2008). Mix 6, however, with targeted air content of 6% (and average air content measured according to the pressure method of 5.55%) presented good frost resistance after the finish of the test, with an average scaled material of 0.370kg/m^2.

According to these results, an increase in the air content from 4.5% to 5.55% changes the salt-scaling resistance of concrete with 50% of GGBS replacement from not acceptable to good. The positive effect of air entrainment in the improvement of the salt-frost resistance of concrete is widely described in the literature. The positive effect of an increase in the air content on a concrete mix with 50% of Portland cement replaced by GGBS had also already been found in the present experimental research. As explained in the previous section, the results obtained for Mix 3 showed that the specimens casted from concrete with 4.9% of air content presented an average accumulated salt-frost scaling under 1.0kg/m^2 after 112 freeze/thaw cycles, whereas both specimens with an air content of 4.1% failed.

The air contents used in the comparison of the results were the values obtained using the pressure gauge method described in SS-EN 12350-7 (2009). The other air void structure parameters determined for Mix 3 were already discussed in the previous section. In the analysis of the results of the salt-frost scaling resistance of Mix 5, the air void parameters determined by the AVA should also be considered.

There is a marked discrepancy between the air content results obtained for the pressure method (according to SS-EN 12350-7) and the AVA. Air contents of 5.50% and 5.60% were obtained using SS-EN 12350-7 for batches number 1 and 2, respectively. The values obtained with the AVA were, however, much higher, with batch number 1 achieving 9.20% of air content, and batch number 2 reaching 9.40%, which are quite excessive values of air content for concrete. As mentioned before, the compressive strength obtained for Mix 5 was 15 to 17% higher than the compressive strength of Mix 3. According to the literature, 1% increase in the air content of a concrete mix results in a decrease in the compressive strength of 5 to 6%. Therefore, according to the results of the compressive strength of concrete, there is a possibility that Mix 5 presented a higher air content than measured with the pressure method. A petrographic analysis should be carried out to assess the actual air content of the hardened concrete mixes.

The analysis of the other air pore parameters measured with the AVA shows a clear correlation between the increase of air content and the decrease in the spacing factor, with the spacing factor changing from a mean value of 0.215mm for Mix 3 to 0.12mm for Mix 5. The specific surface is also higher for Mix 5 (22.7mm^{-1}) than for Mix 3 (19.8mm^{-1}), which reveals an average pore size lower for Mix 5 than for Mix 3.

As referred earlier, it would be important to determine the actual air content in the hardened concrete mixes, in order to assess if the values obtained with the AVA for Mix 5 are indeed much higher than the 5.50% and 5.60% values obtained according to the pressure method, or, instead, if it is actually possible to obtain a similar air void structure and salt-frost scaling resistance with an air content between 5% and 6%.

These results show, nevertheless, that it is possible to produce concrete with GGBS replacement levels up to 50% of the cement content that presents good salt-frost resistance, as long as proper air entrainment is provided.

Frost scaling tests performed by Fagerlund (1982) in concrete with slag cement show exactly the opposite tendency, with the concretes made with the highest addition of slag (cement with 65% of slag) having the highest resistance against freeze/thaw scaling. However, Fagerlund also refers a better performance for concretes without entrained air. Therefore, mixes of concrete with high additions of GGBS and no entrained air should be tested.

5.2.3.3. Influence of the efficiency factor

Figure 5.16 presents the results for the mass of scaled material of concrete mixes with 50% of GGBS replacement and same targeted air content, produced with different efficiency factors: Mix 3 presents a *k*-factor of 0.6, recommended by SS 13 70 03 (2008), whilst Mix 5 was produced with an efficiency factor of 1.0, with GGBS replacing Portland cement in one-to-one basis.

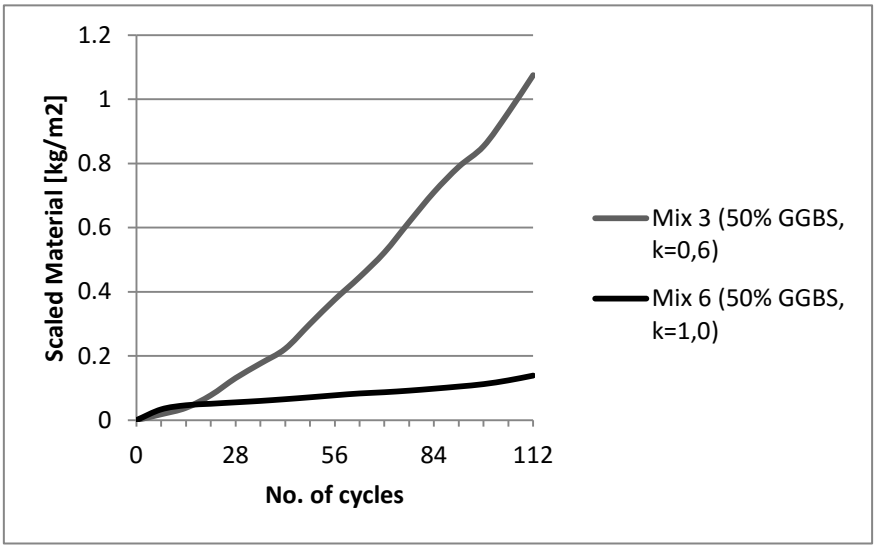

Figure 5.16 - Mean values for frost scaling for concrete cured according to the standard procedures, with 50% of GGBS replacement, air content of 4.5% and different *k* factor, measured after each 7 cycles. Tested according to SS 13 72 44 (2008).

The results of the salt frost scaling test according to SS 13 72 44 (2008) show that Mix 6, produced with an efficiency factor of 1.0, reveals a better performance against salt-frost scaling

than Mix 3, with the *k*-factor of 0.6 recommended by SS 13 70 03 (2008). As shown in Figure 5.16, while specimens of Mix 3 present an accumulated scaled material higher than the acceptable limit (1.0kg/m^2) at the end of the test, the mean value of the scaled material of the specimens of Mix 6 is under 0.5kg/m^2 (0.139kg/m^2, to be precise) after 112 freeze/thaw cycles, which reveals, therefore, good frost resistance.

The reasons behind a better performance of concrete produced with additions using a *k*-factor of 1.0, in comparison with mixes where a lower efficiency factor is used, are unclear. As explained in the previous chapters, the *k*-factor concept is used in concrete when additions replace cement, in order to offset the slower hydration of the additions and obtain similar compressive strength at 28 days of age. An *S* amount of slag replaces a *kS* amount of cement, for the same equivalent water/cement ratio, according to equation (1). By using a *k*-factor lower than 1, the water/binder ratio is lower: Table 4.3 shows that, even though the equivalent water/cement ratio is 0.45 for both mixes, the water/binder ratio is 0.45 for Mix 6, and 0.39 for Mix 3. Theoretically, and as explained in Chapter 3.2.1, an increase in the water/cement ratio will lead to a poorer performance of concrete under freezing conditions: a higher w/c ratio usually results in a more porous concrete, thus more able to absorb water, which results in a higher degree of saturation. Consequently, the hydraulic and/or osmotic pressures inside the paste will increase, resulting in a higher chance of damage due to freeze/thaw cycles [Neville (2003)]. The higher permeability of Mix 6, when compared to Mix 3, was already found in the results for the Rapid Chloride Migration test, with Mix 6 presenting a higher migration coefficient than Mix 3 at both ages of testing (28 and 56 days of age), as shown in Figure 5.10. Furthermore, an increase in water/cement ratio results in a lower strength of the paste, as concluded from the results for the compressive strength of Mixes 3 and 6 (Figure 5.3): Mix 6, with *k*-factor of 1, presented a lower compressive strength than Mix 3. Given that the tensile and compressive strength are affected in the same manner by mix proportioning [Neville (2003), Hogan and Meusel (1981)], one may conclude that the tensile strength for Mix 6 is also lower. The cement paste must be able to withstand the osmotic and hydraulic pressures caused by the freeze/thaw cycles, which means that a paste that presents a lower tensile strength will be more susceptible to damage [Bager (2010)].

These facts are in contradiction with the salt frost scaling results obtained for Mixes 3 and 6. Therefore, in this case, the pore structure of each of the concrete qualities may have played a more important role in the salt-frost resistance of the mixes than the water/binder ratios and permeability of the concrete mixes. The air void parameters shall, therefore, be analysed.

All specimens of Mix 6 to be cured and tested against salt-frost scaling according to SS 13 72 44 (2008) were taken from batch number 1. As displayed in Table 5.2, the air content of Mix 6 measured according to the pressure method described in SS-EN 12350-7 (2009) was the targeted 4.5% for both batches, thus comparable with the average value of 4.5% obtained for Mix 3 (Table 5.2). The results from the Air Void Analyser, however, reveal a slightly higher air content for Mix 6 (with 6% for batch number 1) than for Mix 3 (6.2% and 5.5% for batches 1 and 2, respectively). The specific surface measured for batch number 1 of Mix 6 was 23.7mm^{-1} (Table

5.3), which is higher than the 19.4 and 20.2 mm^{-1} obtained for Mix 3, and closer to the $25mm^{-1}$ recommended by the AVA manufacturer. Moreover, the spacing factor obtained for Mix 6 was 0.18mm, which lies within the limits recommended by the literature for satisfactory salt-frost resistance of a concrete quality (<0.20mm), unlike the spacing factor determined for Mix 3 (0.215mm).

Considering the results obtained by the AVA for Mixes 3 and 6, it seems that a slight increase in the air content (from 5.85% to 6%) may result in relevant differences regarding the air void structure of concrete (increase of the specific surface and reduction of the spacing factor). Further investigation should have been carried out to determine the air content of the concrete mixes in the hardened state, in order to determine the actual air void parameters of both concrete mixes, and therefore assess whether the higher mass of scaled material obtained for Mix 3, when compared to Mix 6, was actually due to the slight difference in the air pore structures of both concrete qualities obtained for the fresh concrete, or, instead, the hardened concrete revealed a much significant difference in the air void systems.

Nevertheless, the results show that it is possible to produce salt-frost resistant concrete with 50% of slag replacement using efficiency factors larger than the recommended by the standards, at least as high as 1.0.

According to these results, it also seems that ensuring an adequate air pore system affects more significantly the performance of concrete under freeze/thaw cycles than the water/cementitious material ratio and the tensile strength of concrete. This fact raises the question of the adequacy of the use of efficiency factors. In fact, the *k*-factors recommended in the literature and standards were determined solely based on the strength development of a concrete mix with additions, when compared with ordinary Portland cement concrete, by adjusting the water/cement ratio. However, even though the w/c ratio and the mechanical strength of concrete are important parameters that influence several degradation mechanisms (as observed in the results of this investigation), there may be other paramenters that have more influence in the durability of a concrete quality that are not considered in the efficiency factor concept. This fact had already been observed for the chloride ingress of GGBS concrete, as is now perceived in the results obtained for the salt-frost scaling. There is not, therefore, a straight correlation between the efficiency factor and the durability of a concrete mix. The use of different *k*-factors for durability purposes should be further investigated.

5.2.3.4. Influence of the use of superplasticizers

Figure 5.17 and Figure 5.18 present the results for the salt-frost scaling resistance of mixes with 0% and 50% of GGBS replacement, produced with the same efficiency factor (*k*=0.6) and targeted air content (4.5±0.5%), with and without superplasticizer.

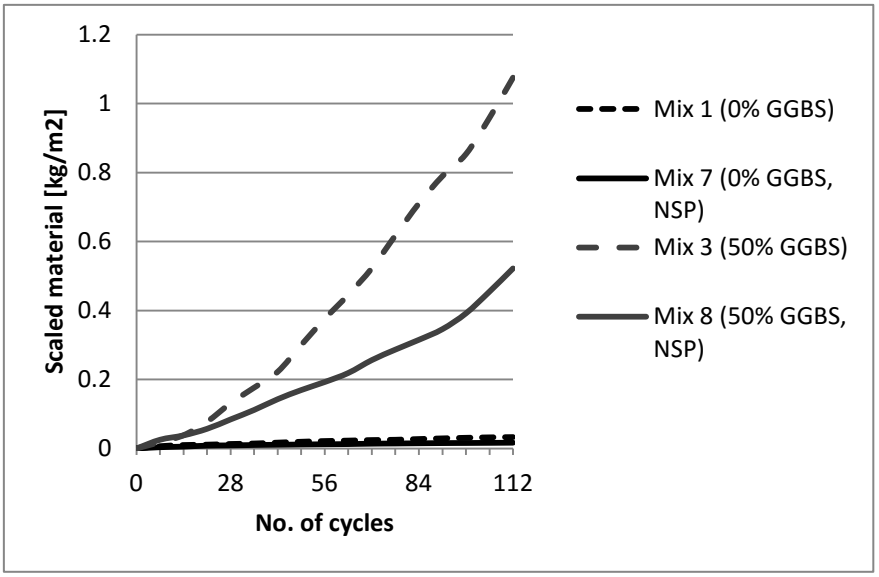

Figure 5.17 - Mean values for frost scaling measured at each 7 freeze/thaw cycles, for concrete mixes with 0% and 50% GGBS, 4.5% air content, with and without plasticizer, pre-conditioned according to the standard. Tested according to SS 13 72 44 (2008).

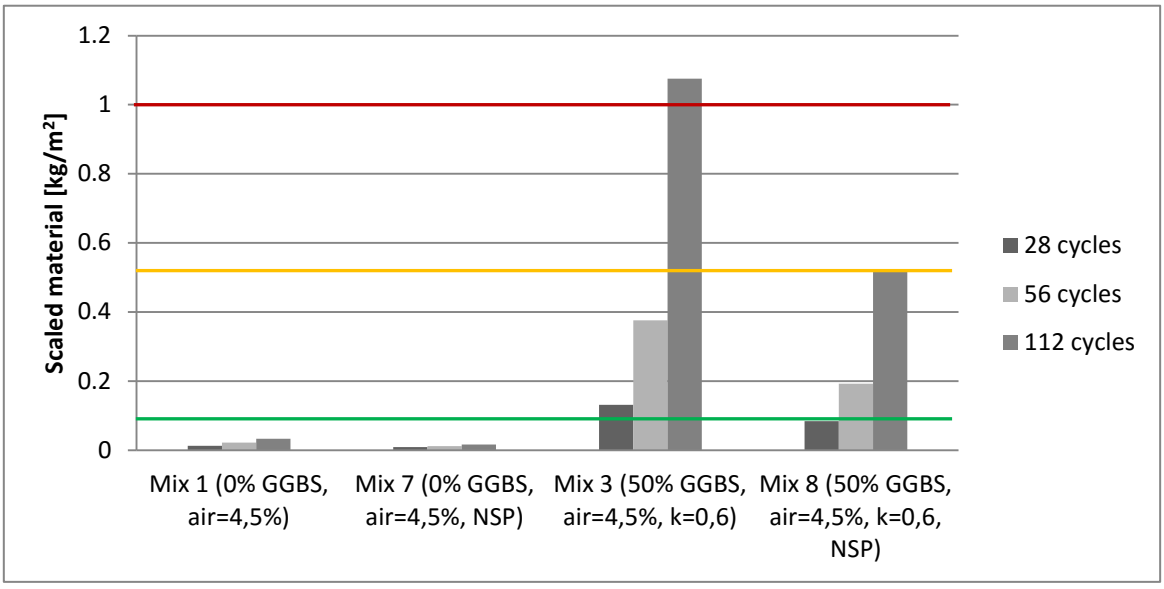

Figure 5.18 - Mean values from scaling under freeze/thaw after 28, 56 and 112 cycles for concrete mixes with 0 and 50% GGBS, 4.5% air content, with and without plasticizer, pre-conditioned according to the standard. Tested according to SS 13 72 44 (2008).

Figure 5.17 and Figure 5.18 show that the mixes produced without superplasticizer (Mixes 7 and 8) reveal a better scaling resistance than the comparable mixes produced with superplasticizer (Mixes 1 and 3, respectively), both for Portland cement concrete and for concrete with 50% of GGBS replacement.

The results obtained for Portland cement concrete (Mixes 1 and 7) are, however, probably related with the air pore structure of the concrete mixes, instead of the use of superplasticizer. All the specimens of Mix 7 tested against salt-frost scaling were casted from batch number 2, which presents a higher air content than both batches of Mix 1, both measured according to SS-EN 12350-7 (2009) and with the Air Void Analyser (Table 5.2). Moreover, the specific surface measured for the fresh Mix 7 was higher than for the comparable Mix 1, and the spacing factor was lower. These results agree with the literature, which correlates high air contents, low spacing factors and high specific surfaces with a good performance of concrete in freeze/thaw environments.

As for concrete with 50% of GGBS replacement, the causes for the better salt-frost resistance shown by Mix 8 (produced without superplasticizer), when compared to Mix 3 are dubious. On the one hand, the air content determined according to SS-EN 12350-7 resulted in higher air content for both batches of Mix 8 than for batches from Mix 3, which is in accordance with the results obtained. However, the scaled material results for Mix 8 presented in Appendix E show that specimens B and C, casted from batch number 2 (5.30% air content) presented a larger accumulated scaled material after 112 cycles than specimens A and D, casted from batch number 1, with lower air content (4.0%). In fact, specimens A and D, present a mean value of scaled material lower than 0.5kg/m^2, i.e., they show good frost resistance according to acceptance criteria defined in SS 13 72 44 (2008), whilst specimens B and C exceed that value, revealing only acceptable performance. These findings contradict the usual assumption that an increase in air content yields improved salt scaling resistance of concrete.

On the other hand, according to the results of the AVA, the air content obtained for batch number 1 of Mix 8 was lower than half of the air content achieved for either of the batches of Mix 3, which resulted on a larger spacing factor for Mix 8. The AVA results for batch number 2 were dismissed due to failure of the equipment, as referred before. Once again, it seems that a higher air content did not result in better salt-frost resistance of concrete.

Even though the air content was lower and spacing factor was higher for Mix 8, the specific surface was higher. According to the results obtained for the air pore structure and deicer scaling resistance of Mixes 8 and 3, it seems that the pore size distribution has a more relevant effect on the resistance against frost attack than the spacing factor. In fact, Mix 8 presents a spacing factor much larger than the maximum 0.20mm recommended (0.26mm), whereas Mix 3 presents a spacing factor closer to the maximum limit (0.21 and 0.22mm). On the other hand, the specific surface obtained for Mix 8 is within desirable limits (26.4mm^{-1}), whereas for Mix 3 it is lower than recommended (19.4 and 20.2mm^{-1}).

According to these results, it seems that the use of air entraining agents alone, without superplasticizer, results in a more refined air void structure of concrete, which leads to an improved salt frost resistance of concrete, even for low percentages of air content. These results agree with the literature. In fact, Neville (2003) states that the use of superplasticizers usually

results in increase of pore size and spacing factor. Ramanchadran (1995), on the other hand, refers that an adequate air void structure of concrete may be difficult to achieve when using superplasticizers together with AEA, as the superplasticizers may coalesce the air bubbles (which results in larger bubble size) and even entrain large bubbles in concrete during mixing, even after good vibration.

Superplasticizing admixtures are used to achieve the desired consistency without affecting the compressive strength of the concrete (instead of, for instance, increasing the w/c ratio). However, as seen in Table 5.1, it is possible to achieve S3 class of consistency (at least for concrete with 50% GGBS) just by adding air entraining agent, without exceeding the recommended dosage of AEA. Therefore, the use of AEA alone might be a good solution to improve the frost resistance of concrete with GGBS, and still maintain the desired w/c ratio and workability/placeability. For Portland cement concrete produced without superplasticizer, only class S2 of slump was achieved. The dosage of AEA could still be increased in order to improve the consistency. However, unlike Mix 8, the air content obtained for Mix 7 exceeded the desired amount. It is, therefore, not advisable to increase the amount of AEA, since an increase in air content results in loss of compressive strength of concrete. The mix proportions of concrete, especially w/c ratio and dosage of AEA must, therefore, be carefully investigated, in order to balance a satisfactory freeze/thaw resistance without compromising its workability and, more importantly, its mechanical strength.

These results should, nevertheless, be regarded with caution. The fact that the results for the air void analysis of one of the batches from Mix 8 could not be obtained means that a complete analysis of the results could not be accomplished. Also, an air void analysis in the hardened concrete specimens should have been carried out, in order to resolve the discrepancies between the results obtained for SS-EN 12350-7 and the AVA for Mix 8. Moreover, the fact that Mix 3 presented slumps higher than 170mm may have resulted in some loss of air content of the hardened specimens [Ramanchadran, (1995)], which may have influenced the results for the salt-frost resistance obtained. Again, an air pore structure analysis of the hardened concrete would be of great interest to study the freeze/thaw performance of the concrete qualities tested.

5.2.3.5. Influence of curing at increased temperature

Figure 5.19 and Figure 5.20 present the results for the scaling under freeze/thaw in the presence of salts for two mixes (Mix 4 and Mix 6, with 100% and 50% of GGBS replacement, respectively), cured according to a different regime: instead of moving the test specimens to the climate chamber after 7 days of water curing at 20ºC, the specimens were placed in a water curing bath at 55ºC until the 21st day of age, and were only then placed in the climate chamber. Figure 5.19 and Figure 5.20 also presents the results for Mixes 4 and 6 curing according to the standard procedure described in SS 13 72 45, for comparison of the results.

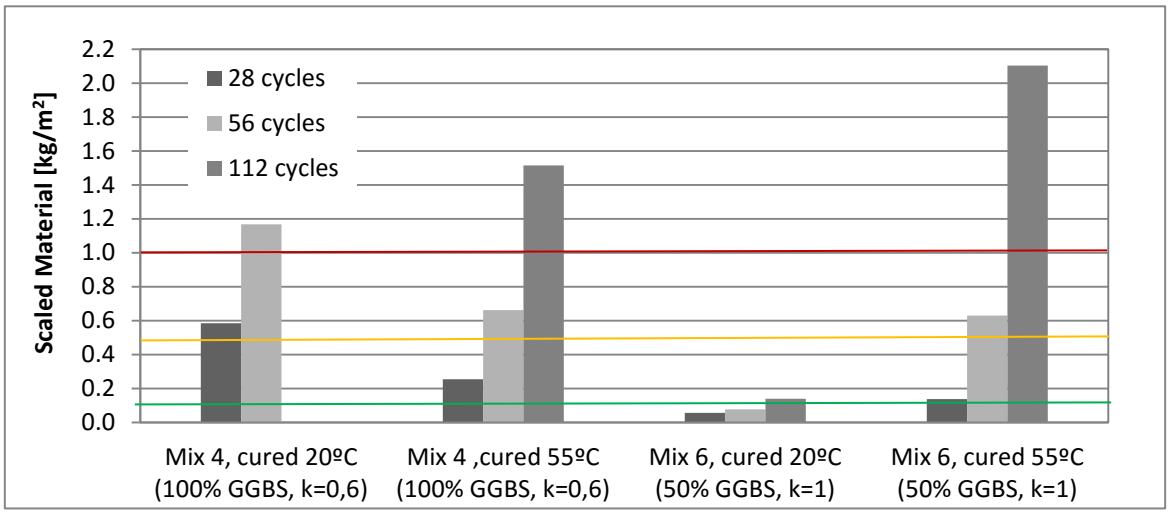

Figure 5.19 - Mean values from scaling under freeze/thaw after 28, 56 and 112 cycles for two different mixes, both with 4.5% air content, but with different amount of GGBS and different k factor and submitted to different curing regimes. Tested according to SS 13 72 44 (2008).

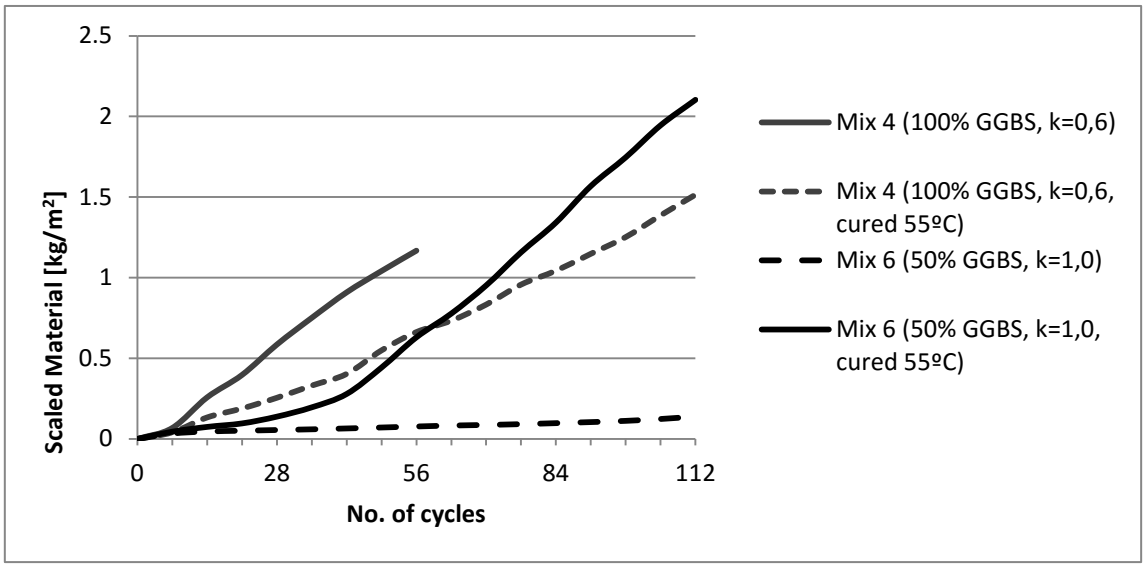

Figure 5.20 - Mean values for frost scaling for two different mixes, both with 4.5% air content, but with different amount of GGBS and different k factor and submitted to different curing regimes, measured after each 7 cycles. Tested according to SS 13 72 44 (2008).

The aim of this test was to evaluate the effect of curing at increased temperature in the resistance against salt-frost scaling of concrete. As seen in Figure 5.19 and Figure 5.20, the effect is different for Mixes 4 and 6: while for Mix 6, with 50% GGBS replacement and *k*=1, the accumulated scaled material for the specimens cured at increased temperature is higher than for concrete subjected to standard curing at all ages, the opposite happens for Mix 4 (100% GGBS, *k*=0.6). In fact, the accumulated scaled material of the specimens of Mix 4 subjected to standard

curing exceeds 1kg/m^2 as early as the 56th cycle, whereas concrete cured at 55ºC fails only after the 77th cycle (See Appendix E).

The reasons for the different influence of curing at higher temperature in the salt-frost scaling resistance of the two mixes are unclear.

As for Mix 4, with 100% GGBS, the better performance shown by the specimens cured at higher temperature is probably due to the influence of temperature in the hydration reactions in concrete. Higher temperatures increase the rate of hydration of the concrete, which, in turn, results in a higher compressive strength at a given age [Neville (2003)]. This phenomenon was already observed in the results for the compressive strength of specimens from Mix 4 cured at different temperatures. As seen in Figure 5.6, the specimen cured at 55ºC presents a compressive strength at the 28th day of age (age at which the pre-conditioning of the freeze/thaw test starts) 17 MPa higher than the specimens cured at 20ºC. Given that the compressive strength and tensile strength of concrete are affected in the same manner by temperature [Neville (2003)], it means that the specimens cured at 55ºC are able to withstand higher tensile stresses due to the hydraulic/osmotic pressures than specimens cured at lower temperature. Thus, less damage due to freeze/thaw cycles would occur.

Contrarily, for specimens of Mix 6, the concrete cured at 55ºC shows worst performance under freeze/thaw than the concrete cured at lower temperatures. In this case, even though the tensile strength of the material is probably higher for concrete cured at higher temperature, the specimens present more scaled material at all ages. The reasons for the different behaviour may be related with the percentage of GGBS replacement for both mixes. Mix 4 presents 100% of GGBS replacement, with an efficiency factor of 0.6, whereas for Mix 6 the percentage of GGBS is only 50%, with a *k*-factor of 1.0. Given that the rate of hydration of slag is lower than that of Portland cement, the use of an “accelerator” that enables faster hydration reaction is more important for higher GGBS contents. This may explain why the increase in the mechanical strength of concrete cured at increased temperature was relevant for the results of the salt-frost scaling of concrete from Mix 4, but seemed not to have such impact on Mix 6. Moreover, there are no results for the compressive strength of concrete from Mix 6 cured at 55ºC, therefore one can only speculate theoretically about the improvement in the mechanical strength.

This also means that, for Mix 6, there is probably another factor that has more influence in the freeze/thaw scaling than the mechanical strength. One explanation may be an increase in the degree of saturation of the specimens cured at increased temperature. As previously described, the procedure for curing at higher temperature consists of moving the specimens from a water bath at 20ºC to a water bath at 55ºC at the age of 7 days, where they remain up until the 21st day of age. The specimens cured according to the standard procedure, on the other hand, are moved to the climate chamber at the age of 7 days. This means that the specimens cured at 20ºC start drying 14 days before the specimens cured at increased temperature. The freeze/thaw resistance of a concrete mix depends highly on the drying period before the first freeze/thaw cycle [Neville

(2003)]. Specimens cured at 55ºC, with a smaller drying period, probably presented a higher degree of saturation at the beginning of the test, and therefore reached the critical degree of saturation earlier than specimens that were allowed to dry for a longer period (14 days longer). For Mix 4, it seems that the effect of the increase in the degree of hydration on the scaling resistance during the first 30 days outweighs the negative effect of the possible increase in the degree of saturation due to the water-curing.

Nevertheless, the results show that both mixes cured at increased temperature fail after 112 freeze/thaw cycles. In fact, as it can be seen in Appendix E all specimens cured at increased temperature fail. There is, therefore, an apparent severe negative effect of the curing at increased temperature in the salt frost resistance of concrete. The reasons for this are unclear. However, they might be related with the poorer microstructure of concrete cured at higher temperatures, already mentioned in Chapter 5.2.1.5. In fact, Gruyaert (2011) refers that the rapid hydration provided by curing at increase temperatures results in the formation of dense hydration products around the unhydrated particles, which will prevent further hydration. This means, therefore, that there is a portion of capillary pores that will always remain unfilled, and a porous concrete is obtained [Neville (2003)]. An increase in the amount of large capillary pores results on a higher degree of saturation of concrete and, consequently, poorer frost resistance. This explanation is also given by Schulson (1998), who refers that, although few, there are some reports that correlate a high temperature with a decrease in the resistance against salt frost damage, and attributes this fact to the coarsening of the pore structure of concrete.

5.2.3.6. Influence of prolonged hydration before starting of the freeze/thaw test

GGBS concrete presents a slower rate of hydration than Portland cement concrete, which may lead to a lower degree of hydration at the age of 28 days. A lower degree of hydration usually results on a more porous concrete, with lower compressive and tensile strengths. Given that the freeze/thaw test starts at 31 days of age, the salt-frost resistance of concrete with GGBS may be adversely affected by its lower hydration degree, when compared with Portland cement concrete. The effect of a prolonged hydration of slag concrete before the start of the freeze/thaw test was evaluated for two concrete mixes (Mix 3 and Mix 5), both with 50% of GGBS replacement and *k*-factor of 0.6, and different air content, by leaving the specimens in the climate chamber for 14 days after sawing, before the water being poured onto the freezing surface.

Figure 5.21 and Figure 5.22 compare the results of the specimens of Mix 3 and Mix 5 tested according to the standard procedure, and hydrated for 14 more days. As previously explained, the test specimens subjected to prolonged pre-treatment were sawn from the unused half of the cubes used in the standard freeze/thaw test of the same concrete qualities. Since the test specimens result from the same cube, the results obtained for the same mix with different pre-treatment procedures are not, therefore, significantly affected by mechanical properties and different air pore structures.

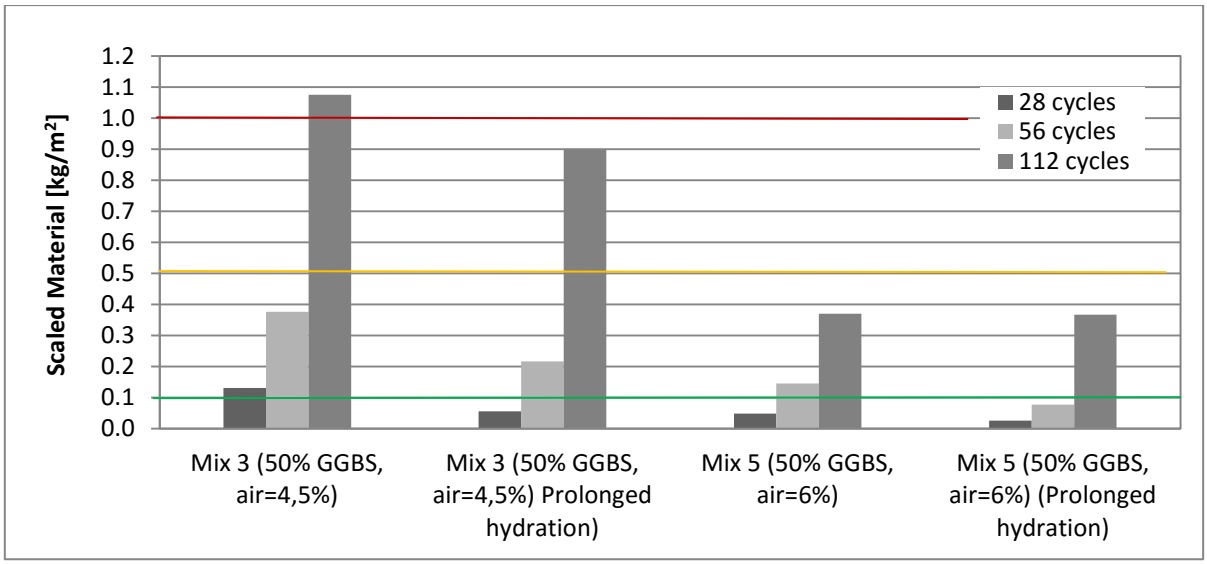

Figure 5.21 - Mean values from scaling under freeze/thaw after 28, 56 and 112 cycles for concrete mixes with 50% GGBS, k=1 but different air content. Two of the mixes were pre-treated according to the standard, and the other two were left in the climate chamber 14 days longer before the start of the test. Tested according to SS 13 72 44 (2008)

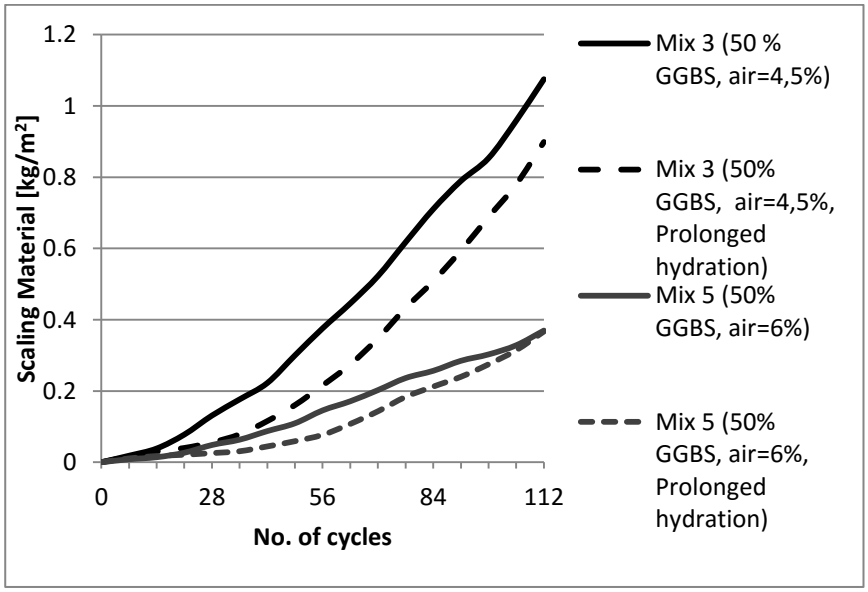

Figure 5.22 - Mean values for frost scaling for concrete mixes with 50% GGBS, k=1 and different air content, measured after each 7 cycles. Two of the mixes were pre-treated according to the standard, and the other two were left in the climate chamber 14 days longer before the start of the test. Tested according to SS 13 72 44 (2008).

As seen in Figure 5.21 and Figure 5.22, the specimens subjected to prolonged hydration before the start of the freeze/thaw test generally present a lower mass of scaled material than the specimens tested at 31 days of age, for both Mixes 3 and 5. The specimens of Mix 3 subjected to prolonged pre-treatment show a better performance than the specimens pre-treated according to the standard at all ages. In fact, the specimens of Mix 3 pre-treated according to the standard fail after 112 cycles, whereas the mix that was allowed to hydrate longer presents acceptable frost

resistance at the end of testing. As for Mix 5, the specimens tested at 45 days of age reveal a slight better frost resistance throughout the test, but not as evident as for Mix 3. However, at the end of the test, the accumulated scaled material is approximately the same for both mixes.

These results were somewhat expected. On the one hand, the specimens that remained 14 more days in the climate chamber were allowed to cure (moist curing at 20ºC, 65% R.H.) for a longer period before the first freeze/thaw cycle. This means that the hydration degree of these specimens was higher at the start of the test, i.e., the specimens presented higher compressive (and tensile) strength, and reduced amount of capillary porosity, which positively influences the salt-frost resistance of concrete. On the other hand, the specimens subjected to prolonged pre-treatment in the climate chamber were not in contact with water, which may have allowed prolonged drying of the test specimens before the first freezing took place (21 days, instead of 7 days for the specimens pre-conditioned according to SS 13 72 44). In fact, according to Neville (2003), drying of concrete before the exposure to freeze/thaw cycles improves its scaling resistance (as long as adequate wet curing was provided prior to drying, in order to ensure extensive hydration). Drying of the specimens lowers the degree of saturation of concrete, which means that the critical degree of saturation is not reached as early as for mixes which were not allowed to dry, and, therefore, less damage is obtained.

This may, in turn, explain why the mass of scaled material of the specimens tested at 45 days of age is significantly lower than the specimens tested at the 31st day of age in the first freeze/thaw cycles, but not as much in the last. As seen in Figure 5.21, the mean accumulated scaled material of the concrete qualities subjected to prolonged pre-treatment increases significantly after 56 cycles, with Mix 5 reaching the same value after 112 cycles as the specimens pre-treated according to the standard. This may be related with the lower degree of hydration of the mixes tested at 45 days of age at the start of the test. The critical degree of saturation is achieved earlier for the specimens tested at 31 days of age, which results in increased damage in the early cycles. After the critical degree of saturation is reached for mixes tested at 45 days of age, the effect of the freeze/thaw cycles in the presence of salts is similar for mixes tested at both ages.

The positive influence of the prolonged pre-treatment in the climate chamber seems more pronounced for Mix 3 than for Mix 5. This fact may be related with the different air content of the two mixes. The targeted air content for Mix 3 was 4.5±0.5% (with an actual average air content between the two batches of 4.5% according to SS-EN 12350-7), and 6±0.5% (with an actual average air content of 6%) for Mix 5. The results show, therefore, that the influence of the degree of hydration of concrete in the protection against frost scaling is more significant for concrete with lower air contents. This would be expected, since concrete with lower air contents have less voids to which the water can move when ice starts to form. The critical degree of saturation is, therefore, reached earlier.

Research carried out by Utgennant (2004) showed that drying has a relatively small, but usually positive effect on the scaling resistance of both Portland cement concrete and GGBS concrete, especially at early ages (up to 31 days of age). The author also found that this positive effect is more pronounced for GGBS concrete than for Portland cement concrete, and that it increases with an increase in slag content.

These results show that, after adequate curing, GGBS concrete structures shall be allowed to dry for a long period of time before being exposed to the first freeze/thaw cycle.

These results also raise a question of the applicability of the salt-frost scaling test described in SS 13 72 44 (2008) for concrete with additions. This test method was developed for Portland cement concrete, and the first freeze-thaw cycle occurs at 31 days of age. The maturity of Portland cement concrete does not increase significantly after 28 days of age [Neville (2003)], which means that the age of testing is probably adequate for Portland cement concrete. However, for concrete with additions, the maturity of concrete continues to develop long after the 28 days of age, depending on the type, reactivity and amount of addition. Therefore, there is a possibility that this test method underestimates the salt frost resistance of concrete qualities with additions. One possibility could be to start the test at a later age. This subject should be further investigated.

6. Conclusions and suggestions for future research

6.1. Main conclusions of the research

From the results of this investigation, a general conclusion can be drawn: concrete with addition of GGBS (fulfilling SS-EN 15167-1) up to 25% of replacement of cement (maximum amount of replacement permitted by SS 13 70 03 for exposure class XF4) presents adequate salt-frost resistance. Other conclusions are summarized below:

- The frost resistance of concrete generally decreases with an increase of the addition of GGBS, for concrete with 4 to 5% of air content by volume. This fact may be due to the slower hydration of GGBS when compared to Portland cement concrete, which yields a more porous concrete at the age of the start of the freeze/thaw test. The results showed, however, that it is possible to produce frost resistant concrete with GGBS amounts up to 50% (of the weight of CEM I), by changing some properties of the mix (such as increasing the air content), i.e., it is possible to produce salt-frost resistant concrete with percentages of GGBS replacement higher than the limit defined by SS 13 70 03 (2008) for exposure class XF4 (25% of the weight of CEM I).

- For concrete with 50% of the weight of cement replaced by GGBS, the results for frost resistance after 112 cycles changed from unacceptable for concrete with an air content of 4,5% to good for concrete with 6% of air. These results show that the beneficial effect of an adequate air pore structure in the salt-frost resistance of concrete is also valid for concrete with GGBS. The results also showed that amounts of GGBS up 50% of the cement weight can be safely used in freezing environments where de-icing salts are used, as long as proper air entrainment is provided.

- Addition of GGBS in concrete significantly improves the resistance against chloride ingress, when compared to Portland cement concrete. The results show that the performance of concrete against chloride penetration increases with increased cement replacement levels (up to 100% of the Portland cement weight). The resistance of GGBS concrete against chloride is mainly related to its denser and more refined microstructure, which results on a less permeable concrete and, consequently, on a slower diffusion of the Cl^- ions. On the other hand, GGBS has also been shown to improve both the physical and chemical binding of chloride ions, which also contributes to a reduction of the free chlorides in the concrete paste.

- The results also show that GGBS concrete outperforms Portland cement concrete at all ages, and all percentages of replacement, even if the slag replaces the cement on a one-to-one basis (i.e., for a *k*-factor of 1.0). The efficiency factor concept is based on the water/cement ratio and

compressive strength development of a concrete quality with additions, in comparison to Portland cement concrete, and no durability aspects were taken into account. The present results raise questions about the applicability of the efficiency factors when durability issues are concerned.

6.2. Suggestions for future studies

In this research project, the results showed that it is possible to obtain salt-frost resistant concrete even for amounts of GGBS replacement up to 50% by weight of CEM I. However, this study did not include investigations on aged concrete. Being the changes in the microstructure due to carbonation of GGBS concrete the factor that most authors indicate as the reason for the poorer salt-frost resistance of GGBS concrete, further research should be conducted to assess if the results are affected by the ageing of concrete.

The air void system is one of the most important factors that influence frost resistance of concrete. However, it is still very hard to obtain a correct measurement of the pore size distribution in the fresh concrete. Further investigation is needed to show the correlation between the results given by the AVA and the air void parameters of concrete in the hardened state, as well as to find a way to obtain a representative sample of the fresh concrete for the air void analysis.

Moreover, an increase in the efficiency factor revealed no significant negative effect on the compressive strength and chloride ingress of concrete mixes with 50% of GGBS replacement but resulted, instead on a significant improvement on the salt-frost resistance of the GGBS concrete. Further investigation should be conducted to assess if the *k*-factors determined according to the compressive strength of concrete at 28 days of age shall be considered for durability issues.

Some authors report a significant increase of the salt-scaling resistance of concrete qualities produced with a very low water/cement ratio (sometimes lower than 0.35). Further research should be carried out on GGBS concrete to assess whether a significant reduction in the water/binder ratio would yield an improvement in the salt-frost resistance of this concrete quality.

The applicability and possible adaptation of the salt-frost scaling test method described in SS 13 72 44 (2008) to concrete qualities with additions shall also be investigated.

7. References

ACI Committee 232 (1996), *Use of Fly Ash in Concrete*, ACI 232.2R-96.

ACI Committee 233 (2000), *Ground Granulated Blast-Furnace Slag as a Cementitious Constituent in Concrete*, ACI 233R-95.

Bager, Dirch H. (2010), *Qualitative description of the micro ice body freeze-thaw damage mechanism in concrete*, Workshop proceeding from a Nordic miniseminar, 4–5 March 2010, Vedbaek, Denmark.

Barnett, S. J., Soutsos, M. N., Millard, S. G. and Bungey, J. H. (2006), *Strength development of mortars containing ground granulated blast-furnace slag: Effect of curing temperature and determination of apparent activation energy,* Cement and Concrete Research 36.

Bortz, B. (2010), *Salt-scaling durability of fly ash concrete*, Master Thesis, Department of Civil Engineering, College of Engineering, Kansas State University, Kansas, USA

Bouikni, A., Swamy, R. N. and Bali, A. (2009), *Durability properties of concrete containing 50% and 65% slag*, Construction and Building Materials 23: 2836-2845.

Chen, W. (2006), *Hydration of slag cement - theory, modeling and application,* Enschede, University of Twente, PhD: 223.

Cheng et al. (2005), *Influence of GGBS on durability and corrosion behavior of reinforced concrete*, Materials Chemistry and Physics 93

Çopuroğlu, O. (2006), *The characterisation, improvement and modelling aspects of Frost Salt Scaling of Cement-Based Materials with a High Slag Content.* Ph.D. Thesis. Delft, 2006, ISBN-10: 90-9020622-1

Dhir, R. K., El-Mohr, M. A. K. and Dyer, T. D. (1996), *Chloride binding in GGBS concrete*, Cement and Concrete Research 26(12): 1767-1773.

Domone, P. Illston, J. (2010), *Construction materials, their nature and behaviour*, Spon Press, 4th Edition, New York, USA

Due, L. and Folliard, K. J. (2004), *Mechanisms of air entrainment of concrete*, Concrete Durability Center (CDC), The University of Texas at Austin, United States

Ellis, W.E. Jr., Riggs, E.H. and Butler, W.B., (1991), *Comparative Results of Utilization of Fly Ash, Silica Fume and GGBFS in Reducing the Chloride Permeability of Concrete*, Proceedings of the Second CANMET/ACI International Conference on

Durability of Concrete, Montreal, Canada, V.M. Malhotra, Ed., ACI Publication SP-126

Fagerlund (1995), *Freeze-thaw resistance of concrete. Destruction mechanisms. Concrete Technology. Test Methods. Quality control*, A contribution to the BRITE/EURAM project BREU-CT92-0591 "The Residual Service Life of Concrete Structures", Lund University of Technology, Report TVBM-3060, Lund, Sweden

Fagerlund G. (1977), *The critical degree of saturation method of assessing the freeze/thaw resistance of concrete*, Materials and Structures, Vol. 10. No. 58, 1977.

Fagerlund G. (1982), *The influence of slag cement on the frost resistance of the hardened concrete*, Swedish Cement and Concrete Research Institute, Research report 1:82, Stockholm, Sweden, 1982.

Fagerlund, G (1988), *Effect of air-entraining and other admixtures on the salt scaling resistance of concrete*, Durability of concrete: Aspects of admixtures and industrial by-products, International seminar, April 1988, pp. 233-266.

Fulton, F. S. (1974), *The Properties of Portland Cement Containing Milled Granulated Blast-Furnace Slag*, Monograph, Portland Cement Institute, Johannesburg, 1974

German Instruments, *Air Void Analyser (AVA) info*

Giergiczny, Z., Glinicki, M. A. and Sokolowski, M. Z., M. (2009), *Air void system and frost salt scaling of concrete containing slag-blended cement*, Construction and Building Materials 23: 2451-2456.

Gruyaert, E. (2011), *Effect of blast-furnace slag as cement replacement on hydration, microstructure, strength and durability of concrete,* Dissertation (monograph), Department of Structural Engineering, University of Ghent, Ghent, Belgium, ISBN: 978-9-0857-8412-8

Harnic, A. B., Meier, V., and Rosli, A. (1980), *Combined influence of Freezing and De-icing Salt on Concrete - Physical Aspect,* Durability of Building Materials and Components, ASTM, STP 691.

Hewlett, P. (2004), *Lea's Chemistry of Cement and Concrete,* Fourth Edition, Butterworth-Heinemann, ISBN: 978-0-7506-6256-7

Hogan, F. J., and Meusel, J. W., *Evaluation for Durability and Strength Development of a Ground Granulated BlastFurnace Slag*, Cement, Concrete, and Aggregates, V. 3, No. 1, Summer, 1981

Jain, D. K. et al. (2007), *Ground Granulated Blast Furnace Slag blended concrete*, Department of Civil Engineering, I. I. T. Roorkee, NBMCW, November 2007

Khatib, J. M. and Hibbert, J. J. (2005), *Selected engineering properties of concrete incorporating slag and metakaolin*, Construction and Building Materials 19: 460-472.

Li et al. (2006), *A study on the relationship between porosity of the cement paste with mineral additives and compressive strength of mortar based on this paste*, Cement and Concrete Research 36

Lindmark, S. (1998), *Mechanisms of salt-frost scaling of Portland cement-bound materials: Studies and hypothesis*, Ph.D. Thesis, Report TVBM 1017, Lund University, Lund Institute of Technology, Division of Building Materials, ISBN 91-628-3285-9 Lund, Sweden

Marchand, J., et al. (1994), *The deicer salt scaling deterioration of concrete - An overview*, Third international conference on Durability of concrete, ACI, SP-145, Nice, France.

Neville, A. M, (2003), *Properties of concrete*. Pearson Education Limited, Edinburgh

NORDTEST (1999), *Concrete, Mortar and Cement Based Repair Materials: Non Steady-State Migration Experiments*, NT Build 492, NORDTEST, Espoo

Osborne, G. J., *Carbonation and Permeability of BlastFurnace Slag Cement Concretes from Field Structures*, Fly Ash, Slag and Natural Pozzolans in Concrete, V. M. Malhotra, Ed., SP-114, American Concrete Institute, Detroit

Ozyildirim, C. (1994), *Resistance to Penetration of Chlorides into Concretes Containing Latex, Fly Ash, Slag and Silica Fume*, Durability of Concrete, Third International Conference, Nice, France, Publication SP-145, American Concrete Institute, Farmington Hills, Michigan

Petersen, C. G. (2009), *Air void analyser (AVA) for fresh concrete, latest advances*, Ninth ACI International Conference on Superplasticizers and Other Chemical Admixtures in Concrete – Sevilla, Spain

Pigeon, M and M. Langlois (1991), Canadian Journal of Civil Engineering, 18(4): 581-589.

Pigeon, M., Pleau, R. (1995), *Durability of concrete in cold climates*, Modern concrete technology 4, E & FN Spon, London, England. 1995.

Powers, T. C. (1949) 'The air requirement of frost-resistant concrete', Proceedings of the Highway Research Board, 29

Powers, T. C. (1965), *The mechanisms of frost action in concrete*, in Stanton Walker Lecture Series on the Material Science, Lecture No. 3, November, 1965.

Powers, T.C. (1975) 'Freezing effects in concrete', ACI Special publication SP-47, American Concrete

Powers, T.C., Helmuth, R.A. (1953), *Theory of volume changes in hardened Portland cement paste during freezing*, Proceedings of the Highway Research Board, 32

Ramachandran, V.S. (1995), *Concrete Admixtures Handbook – Properties, Science, and Technology*, 2nd Edition, William Andrew Publishing, ISBN 0-8155-1373-9

Rönning, T. F. (2001), *Freeze-thaw resistance of concrete effect of: curing conditions moisture exchange and materials*, Dr. Ing. Thesis, The Norwegian Institute of Technology, Division of Structural Engineering, Concrete Section, Trondheim, Norway, 2001. ISBN 82-7984-165-2

Rösli, A. and Harnik, A. B. (1980), *Improving the Durability of Concrete to Freezing and Deicing Salts*, Durability of Building Materials and Components, ASTM STP 691, P.J. Sereda and G.G. Litvan,Eds. American Society for Testing and Materials, 1980.

Schlorholtz and Hooton (2008), *Deicer scaling resistance of concrete pavements, bridge decks, and other structures containing slag cement, Phase I: site selection and analysys of field cores*, Final Report, National Concrete Pavement Technology Center, Iowa State University, September of 2008

Schulson, E. M. (1998), *Ice damage to concrete*, US Army Corps of Engineers, CRREL technical publications, Special Report 98-6

Setzer, M. J. (2002), *Development of the micro-ice-lens model. Frost resistance of concrete*, Essen,Germany, RILEM

Stark, J. and Ludwig, H.-M. (1997), *Freeze-deicing salt resistance of concretes containing cement rich in slag*, Proceedings of the International RILEM Workshop on Resistance of Concrete to Freezing and Thawing with or without De-icing Chemicals, University of Essen, RILEM Proceedings 34, Essen, Germany

Thomas Concrete Group (2012), *Teknisk Information Slagg Bremen (Technical sheet for Slagg Bremen, in Swedish)*

Utgenannt, P. (2004), *The influence of ageing on the salt-frost resistance of concrete*, Ph.D. Thesis. Lund Institute of Technology. Division of Building Materials. ISBN 91-628-6000-3

Virtanen, J. (1982), *Freeze-thaw resistance of concrete containing blast-furnace slag, fly-ash or silica fume*, CBI Report 2.83

Wimpenny, D. E., Ellis, C. M., and Higgins, D. D. (1989), *The Development of Strength and Elastic Properties in Slag Cement under Low Temperature Curing Conditions*, Proceedings, 3rd International Conference on Fly Ash, Silica Fume, Slag and Natural Pozzolans in Concrete, V. M. Malhotra, Ed., SP-114, American Concrete Institute, Detroit, V. 2, Trondheim, Norway

Standards

ASTM C457, *Standard test method for microscopical determination of parameters of the air void system in hardened concrete*

ASTM 666, *Standard Test Method for Resistance of Concrete to Rapid Freezing and Thawing*

ASTM C 672 (2003), *Standard Test Method for Scaling Resistance of Concrete Surfaces Exposed to Deicing Chemicals*

ASTM C989, *Standard Specification for Slag Cement for Use in Concrete and Mortars*

CDF Test, *Capillary Suction of De-icing Chemicals and Freeze-Thaw Tests*

EN 196-1, *Methods Of Testing Cement - Part 1: Determination Of Strength*

EN 196-2, *Methods of Testing Cement - Part 2: Chemical Analysis of Cement*

EN 196-3, *Methods Of Testing Cement - Part 3: Determination Of Setting Times And Soundness*

SIS, Swedish Standard Institute (2009), SS-EN 12350-2, *Testing fresh concrete - Part 1: Sampling.*

SIS, Swedish Standard Institute (2009): SS-EN 12350-7, *Testing of fresh concrete – Part 7: Air content – Pressure Methods.*

SIS, Swedish Standard Institute (2001), SS-EN 12390-1, *Testing hardened concrete - Part 1: Shape, dimensions and other requirements for specimens and moulds*

SIS, Swedish Standard Institute (2009), SS-EN 12390-2, *Testing hardened concrete - Part 2: Making and curing specimens for strength tests*

SIS, Swedish Standard Institute (2009), SS-EN 12390-3, *Testing hardened concrete - Part 3: Compressive strength of test specimens*

SIS, Swedish Standard Institute (2005), SS-EN 15167-1, *Ground granulated blast furnace slag for use in concrete, mortar and grout – Part 1: Definitions, specifications and conformity criteria.*

SIS, Swedish Standard Institute (2005), SS-EN 197-1, *Cement - Part 1: Composition, specifications and conformity criteria for common cements*

SIS, Swedish Standard Institute (2005), SS-EN 206, *Concrete – Part 1: Specifications, properties, production and conformity*

SIS, Swedish Standard Institute (2008), SS 13 70 03, *Concrete – Usage of EN 206-1 in Sweden*

SIS, Swedish Standard Institute (2005), SS 13 72 44, *Concrete testing - Hardened concrete - Scaling at freezing*

SIS, Swedish Standard Institute (1995), SS 13 72 45, *Concrete testing - Hardened concrete - Concrete cubes for freeze-testing*

APPENDIX A:

Air Void Analyser – Technical Specifications

GI AVA

Purpose

The AVA (Air Void Analyzer) is used to measure the air-void parameters of samples of fresh air-entrained concrete.

Background

The durability of concrete subjected to wetting and cycles of freezing and thawing can be enhanced by deliberately introducing many, small and closely spaced air bubbles (voids) in the cement paste. During freezing, the ice formed in the capillary pores of the paste will expand into adjacent air voids without damaging the paste, provided the air-void spacing and the size distribution of the air voids are within certain limits. To characterize the air voids, the spacing factor (the maximum distance from any point in the cement paste to an air-void boundary) and the specific surface (the ratio of the surface area of the air voids to their volume) are used. In general, a good quality, frost resistant concrete requires a spacing factor < 0.20 mm and a specific surface greater than 25 mm^{-1}.

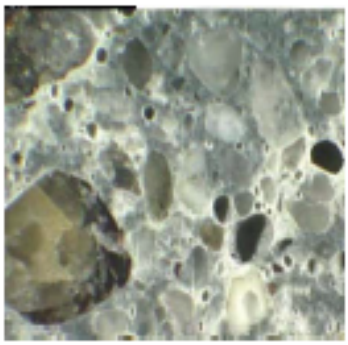

The spacing factor and the specific surface of the air-void system are determined typically according to ASTM C 457 "Test Method for Microscopical Determination of Parameters of the Air-Void System in Hardened Concrete." This method requires a sample cored from the hardened concrete on-site and prepared properly in the laboratory as illustrated in the photo to the left. The spacing factor and the specific surface are then measured manually by the linear traverse method using a microscope, or by an automated image analyses system as illustrated on page 16. Determination of the air-void structure in this manner cannot produce timely information during construction, which would be needed to make adjustments to the concrete mixture if the measured parameters are not within specified limits.

Timely information is important, as practice has shown that the air-void structure created by air entraining agents can easily change during construction, e.g., due to the type and dosage of normal or high-range water-reducing admixtures, by changes in sources of cementitious materials, by pressure influences in concrete pumps, by high hydrostatic pressure, or by over-vibration.

With the AVA, the air-void structure is measured while the concrete is still fresh, thereby providing timely information of the spacing factor and the specific surface of the air-void system in the cement paste of the concrete. The time of testing is 25 minutes or less.

Principle

The air bubbles entrained in a mortar sample, which is removed from fresh concrete, are transferred to a blue AVA release liquid as the mortar is stirred. Provided the release liquid has the proper viscosity and hydrophilic character, the bubbles released from the mortar retain their original size and neither coalesce nor disintegrate into smaller bubbles.

Above the blue AVA release liquid there is a column of water through which the air bubbles rise. According to Stoke's Law, larger bubbles will rise faster than smaller bubbles.

The air bubbles rising through the water column are collected under an inverted and submerged pan attached to a sensitive balance. As air bubbles accumulate in the top of the pan, the apparent mass of the pan decreases as water is displaced by air. The apparent mass of the pan is recorded over time.

On the basis of the recorded change in apparent mass of the pan, an algorithm calculates the size distribution of the collected air bubbles. From the size distribution, the spacing factor and the specific surface are calculated. The algorithm ensures the parameters are the same as obtained from ASTM C 457 linear traverse measurements.

Correlation and Variability

The results from the AVA have been correlated to ASTM C 457 determinations. Among the published reports are:

- Brite Euram Project No: BE-3376-89, Task 2, "Quantitative and Qualitative Determination of the Air Void structure in Fresh Concrete," Dansk Beton Teknik A/S, Hellerup, Denmark, Feb. 1994
- FHWA-SA-96-062, "Air Void Analyzer Evaluation," Federal Highway Administration, Washington DC, USA, 1995
- Price, B., "Measuring Air Voids in Fresh Concrete," CONCRETE, July/August 1996
- Wojakowski, J., "Air in Portland Cement Concrete Pavements," Kansas Department of Transportation, USA, 2002
- Crawford, G.L., Wathne, L.G., and Mullarky, J.I.: "A 'Fresh' Perspective on Measuring Air in Concrete," Federal Highway Administration, Washington DC, 2003 Bridge Conference, USA

The general conclusion is that the AVA results in air-void parameters that are within ± 10 % of those obtained by ASTM C 457. The repeatability coefficients of variation for the AVA spacing factor and the specific surface determinations are normally 8 to 10 %.

Testing Example



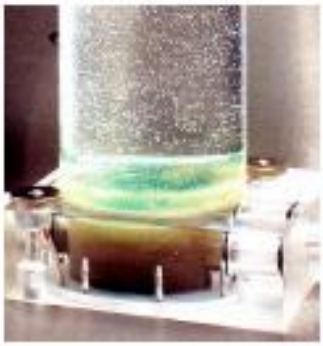

- A sample of the mortar fraction of the air-entrained concrete is taken by vibrating a wire cage into the plastic concrete (left above). The mortar enters the cage, which excludes particles larger than 6 mm. A syringe is used to collect a 20 cm^3 mortar test specimen from within the cage.
- The specimen is injected into the riser column (center above). The riser column has the blue AVA release liquid at the bottom and water above it. The mortar and the liquid are stirred gently by a magnetic stirrer for 30 seconds, and the air voids are released (right above).
- The bubbles rise through the liquids at rates that depend on their size, providing a separation in time when different sizes arrive at the top of the column.
- The bubbles are collected under a submerged pan attached to a balance. A computer connected to the balance records the change in mass of the pan as a function of time.
- In the early stages of the measurement, the size distribution of the air bubbles collecting under the pan range from a few mm to a few micrometers. For each succeeding period, the size of the bubbles that collect under the pan decrease.
- The measurement continues for 26 minutes unless there is no mass change recorded for 2 consecutive minutes, in which case the measurement is stopped.
- The AVA software processes the balance readings and calculates the air-void parameters including the spacing factor and the specific surface as indicated on the following page.
- In addition, the software produces a graph of the bubble size distribution and a histogram of the different bubble sizes, also illustrated on the following pages.

AVA System Features

Two AVA systems are available: the AVA-2000 and the AVA-3000.

AVA-2000

The AVA-2000 is the daily workhorse, and is based on the original Dansk Beton Teknik (BTK) design from the late 1980s. This model features:

- A complete system, ready-to-use, including a laptop computer with the AVA-2000 software and an installed PCMCIA card with driver software
- Optimized sensitivity of the balance for eliminating the effects of external vibrations during testing

AVA-3000

Recently developed, the AVA-3000 features:

- Latest microprocessor technology with components minimized in size and number
- Only one USB cord connecting the laptop computer and the base unit
- Incorporates a mini balance that can withstand rough treatment during transport and/or testing
- Elimination of the influence of external vibrations on the test results, including the introduction of a wind shield positioned on top of the riser column
- Improved stirrer operation with constant rotational speed independent of the load applied on the stirrer
- Incorporates a 35-L temperature bath tank for automated de-aerating and tempering of the water and the AVA release liquid for testing. The bath tank may also function as ballast for stabilizing the base unit
- In addition to the calculation of the spacing factor and the specific surface for chord length <2 mm (as in the AVA-2000), the AVA-3000 calculates the air-void parameters for chord length <1 mm, as required by the latest ASTM C 457-06 standard

Example of AVA-2000 printout, documenting:

- The change in mass of the buoyancy pan (x-axis) as a function of time (y-axis),
- The results of the analyses, including the spacing factor and the specific surface, and
- Comments

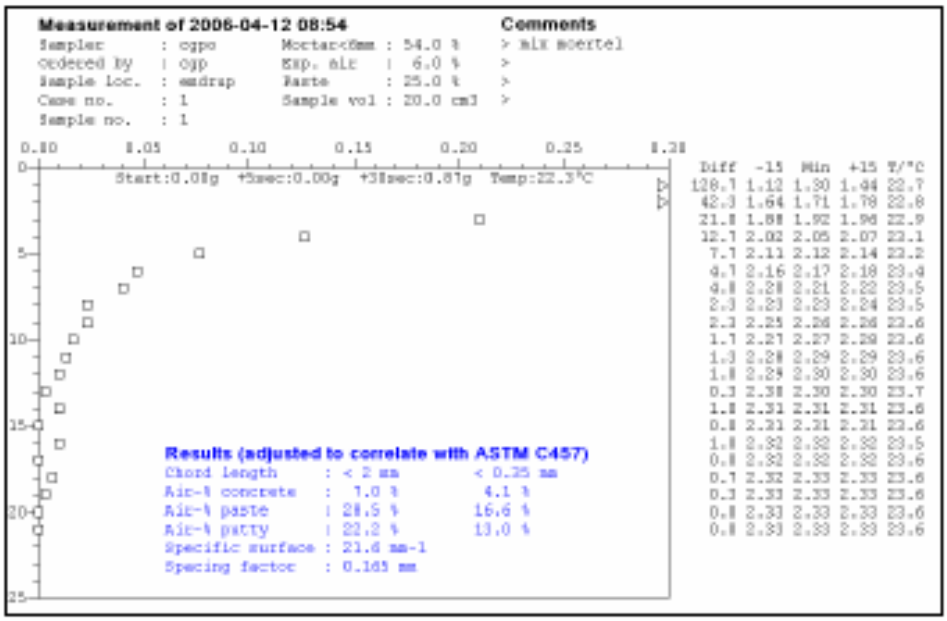

Example of AVA-3000 printout, documenting:

- The change in mass of the buoyancy pan (x-axis) as a function of time (y-axis),
- The results of the analyses, including the spacing factor and the specific surface, and
- Comments

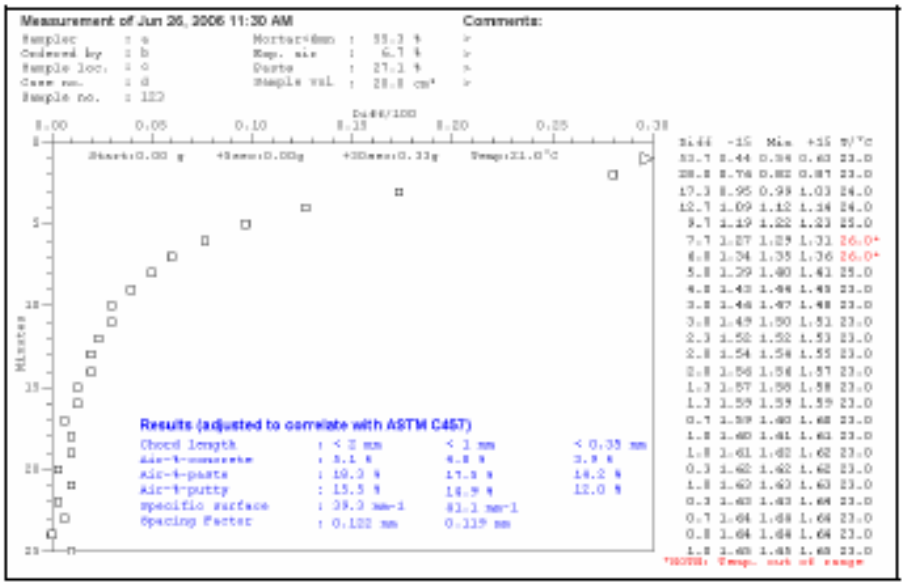

Example of AVA-2000 or AVA-3000 printout, documenting:

- The size distribution of air voids < 2 mm (left), and
- A histogram of air void sizes < 2 mm (right).

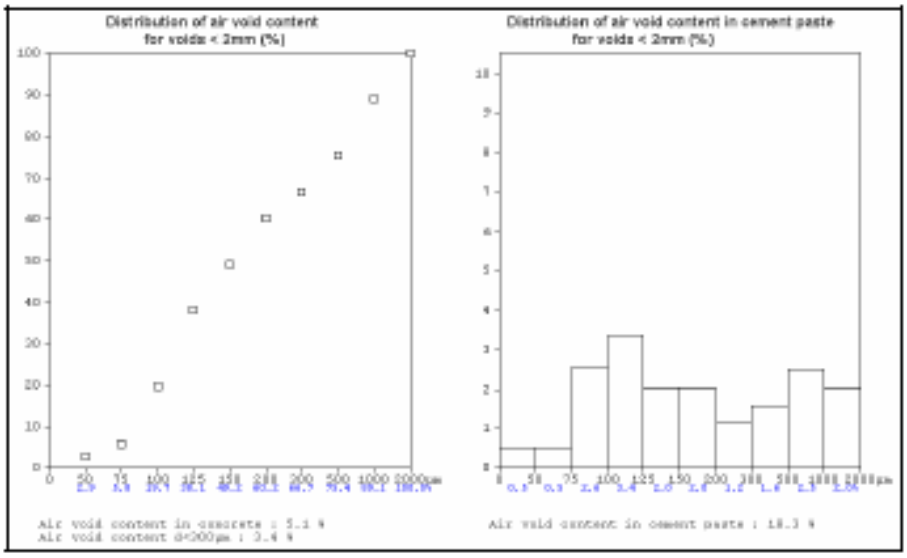

The AVA-2000 System

AVA-2000 System
Supplied in a rugged transport case

The AVA-2000 base unit with riser column, buoyancy pan and laptop computer

AVA-2000 System Ordering Numbers

Item	Order #
Base unit	AVA-2010
Riser column	AVA-2020
Piston with temperature sensor	AVA-2030
Buoyancy pan	AVA-2040
Vibrating cage	AVA-2050
Vibrating collector	AVA-2060
Electric drill	AVA-2070
Funnel for insertion of AVA release liquid into riser column	AVA-2080
Sampling syringes, 5 pcs	AVA-2090
Digital thermometer	AVA-2100
Heating element	AVA-2110
Bottle for heating AVA release liquid	AVA-2120
Laptop computer	AVA-2250

Item	Order #
Brush	AVA-2130
Plexiglas plate with hole for sampling	AVA-2140
Bucket for de-aeration of water	AVA-2150
Connector box	AVA-2160
Interface cord, connector box to PC	AVA-2170
Cord, PC to balance	AVA-2180
PCMCIA card and driver software	AVA-2190
Manual for PCMCIA card	AVA-2200
CD-ROM for PCMCIA card	AVA-2210
AVA-2000 software diskette	AVA-2220
AVA-2000 manual	AVA-2230
AVA release liquid, 5 L	AVA-2240

The AVA-2240 release liquid comes in 5-L containers with controlled batch number and certificate that it has the proper viscosity and hydrophilic characteristics.

Each test requires 200 mL of liquid.

Delivered separately is the AVA-2260 verification kit (calibrated masses applied to weighing rod).

Offered separately is a one-day course by an AVA specialist.

The AVA-3000 System

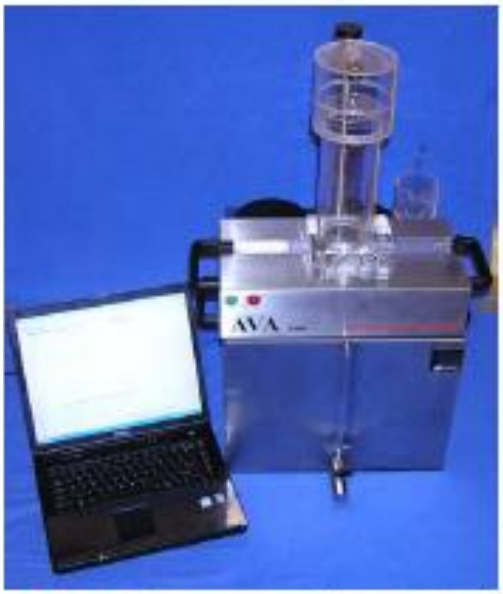

AVA-3000 *System composed of base unit, riser column, temperature bath and laptop computer*

AVA-3000 *accessories as described below*

AVA-3000 System Ordering Numbers

Item	Order #
Base unit	AVA-5010
Riser column	AVA-5020
Piston	AVA-5030
Buoyancy pan	AVA-5040
Vibrating cage	AVA-5050
Vibrating collector	AVA-5060
Electric drill	AVA-5070
Funnel for insertion of AVA release liquid into riser column	AVA-5080
Sampling syringes, 5 pcs	AVA-5090

Item	Order #
Bottle for heating AVA release liquid	AVA-5120
Brush	AVA-5130
Plexiglas plate with hole for sampling	AVA-5140
Laptop computer	AVA-5150
Cord, PC to base unit	AVA-5160
AVA-3000 software diskette	AVA-5220
AVA-3000 manual	AVA-5230
AVA release liquid, 5 L	AVA-2240

As with the AVA-2000, the AVA-2260 verification kit for checking the balance is offered separately as well as a 1-day training course by an AVA specialist.

APPENDIX B:

NT Build 492

nordtest method

NT BUILD 492

Approved 1999–11

1(8)

UDC 691.32/691.53/691.54

CONCRETE, MORTAR AND CEMENT-BASED REPAIR MATERIALS:
CHLORIDE MIGRATION COEFFICIENT FROM NON-STEADY-STATE MIGRATION EXPERIMENTS

Key words: Chlorides, concrete, diffusion, mortar, repair materials, migration, test method

1 SCOPE

This procedure is for determination of the chloride migration coefficient in concrete, mortar or cement-based repair materials from non-steady-state migration experiments.

2 FIELD OF APPLICATION

The method is applicable to hardened specimens cast in the laboratory or drilled from field structures. The chloride migration coefficient determined by the method is a measure of the resistance of the tested material to chloride penetration. This non-steady-state migration coefficient cannot be directly compared with chloride diffusion coefficients obtained from the other test methods, such as the non-steady-state immersion test or the steady-state migration test.

3 REFERENCES

/1/ NT BUILD 201, "Concrete: Making and curing of moulded test specimens for strength tests", 2nd ed., Approved 1984-05.

/2/ NT BUILD 202, "Concrete, hardened: Sampling and treatment of cores for strength tests", 2nd ed., Approved 1984-05.

/3/ NT BUILD 208, "Concrete, hardened: Chloride content", 2nd ed., Approved 1984-05.

/4/ Tang, L and Sørensen, H.E., "Evaluation of the Rapid Test Methods for Chloride Diffusion Coefficient of Concrete, NORDTEST Project No. 1388-98", SP Report 1998:42, SP Swedish National Testing and Research Institute, Borås, Sweden, 1998.

4 DEFINITIONS

Migration: The movement of ions under the action of an external electrical field.

Diffusion: The movement of molecules or ions under a concentration gradient or, more strictly, chemical potential, from a high concentration zone to a low concentration zone.

5 SAMPLING

The method requires cylindrical specimens with a diameter of 100 mm and a thickness of 50 mm, sliced from cast cylinders or drilled cores with a minimum length of 100 mm. The cylinders and cores should meet the requirements described in NT BUILD 201 and NT BUILD 202 respectively. Three specimens should be used in the test.

6 TEST METHOD

6.1 Principle

An external electrical potential is applied axially across the specimen and forces the chloride ions outside to migrate into the specimen. After a certain test duration, the specimen is axially split and a silver nitrate solution is sprayed on to one of the freshly split sections. The chloride penetration depth can then be measured from the visible white silver chloride precipitation, after which the chloride migration coefficient can be calculated from this penetration depth.

6.2 Reagents and apparatus

6.2.1 Reagents

- Distilled or de-ionised water.
- Calcium hydroxide: $Ca(OH)_2$, technical quality.
- Sodium chloride: NaCl, chemical quality.
- Sodium hydroxide: NaOH, chemical quality.
- Silver nitrate: $AgNO_3$, chemical quality.
- Chemicals for chloride analysis as required by the test method employed (optional, see 6.4.6).

6.2.2 Apparatus

- Water-cooled diamond saw.
- Vacuum container: capable of containing at least three specimens.
- Vacuum pump: capable of maintaining a pressure of less than 50 mbar (5 kPa) in the container.

Published by NORDTEST P.O. Box 116 FIN–02151 ESPOO FINLAND Phone + 358 9 455 4600 Fax + 358 9 455 4272

ISSN 0283–7153 Proj. 1388–98

- Migration set-up: One design (see Appendix 1) includes the following parts:
  - Silicone rubber sleeve: inner/outer diameter 100/115 mm, about 150 mm long.
  - Clamp: diameter range 105 – 115, 20 mm wide, stainless steel (see Figure 2 in Appendix 1).
  - Catholyte reservoir: plastic box, 370 × 270 × 280 mm (length × width × height).
  - Plastic support: (see Figure 3 in Appendix 1).
  - Cathode: stainless steel plate (see Figure 3 in Appendix 1), about 0.5 mm thick.
  - Anode: stainless steel mesh or plate with holes (see Figure 4 in Appendix 1), about 0.5 mm thick.

  Other designs are acceptable, provided that temperatures of the specimen and solutions during the test can be maintained in the range of 20 to 25 °C (see 6.4.2).
- Power supply: capable of supplying 0 – 60 V DC regulated voltage with an accuracy of ±0.1 V.
- Ammeter: capable of displaying current to ±1 mA.
- Thermometer or thermocouple with readout device capable of reading to ±1 °C.
- Any suitable device for splitting the specimen.
- Spray bottle.
- Slide calliper with a precision of ±0.1 mm.
- Ruler with a minimum scale of 1 mm.
- Equipment for chloride analysis as required by the test method employed (optional, see 6.4.6).

6.3 Preparation of the test specimen

6.3.1 Test specimen

If a drilled core is used, the outermost approximately 10 – 20 mm thick layer should be cut off (Note 1) and the next 50 ± 2 mm thick slice should be cut as the test specimen. The end surface that was nearer to the outermost layer is the one to be exposed to the chloride solution (catholyte).

If a Ø100 × 100 mm cast cylinder is used, cut a 50 ± 2 mm thick slice from the central portion of the cylinder as the test specimen. The end surface that was nearer to the as-cast surface is the one to be exposed to the chloride solution (catholyte).

If a Ø100 × 200 mm cast cylinder is used, prepare the test specimen by first cutting the cylinder into two halves (i.e. into two Ø100 × 100 mm cylinders), and then cutting a 50 ± 2 mm thick slice from one half. The end surface that was nearer to the first cut (the middle surface) is the one to be exposed to the chloride solution (catholyte).

Measure the thickness with a slide calliper and read to 0.1 mm.

Note 1: The term 'cut' here means to saw perpendicularly to the axis of a core or cylinder, using a water-cooled diamond saw.

6.3.2 Preconditioning

After sawing, brush and wash away any burrs from the surfaces of the specimen, and wipe off excess water from the surfaces of the specimen. When the specimens are surface-dry, place them in the vacuum container for vacuum treatment. Both end surfaces must be exposed. Reduce the absolute pressure in the vacuum container to a pressure in the range of 10–50 mbar (1–5 kPa) within a few minutes. Maintain the vacuum for three hours and then, with the vacuum pump still running, fill the container with the saturated $Ca(OH)_2$ solution (by dissolving an excess of calcium hydroxide in distilled or de-ionised water) so as to immerse all the specimens. Maintain the vacuum for a further hour before allowing air to re-enter the container. Keep the specimens in the solution for 18 ± 2 hours.

6.4 Procedure

6.4.1 Catholyte and anolyte

The catholyte solution is 10 % NaCl by mass in tap water (100 g NaCl in 900 g water, about 2 N) and the anolyte solution is 0.3 N NaOH in distilled or de-ionised water (approximately 12 g NaOH in 1 litre water). Store the solutions at a temperature of 20–25 °C.

6.4.2 Temperature

Maintain the temperatures of the specimen and solutions in the range of 20–25 °C during the test.

6.4.3 Preparation of the test

- Fill the catholyte reservoir with about 12 litres of 10 % NaCl solution.
- Fit the rubber sleeve on the specimen as shown in Figure 4 in Appendix 1 and secure it with two clamps. If the curved surface of the specimen is not smooth, or there are defects on the curved surface which could result in significant leakage, apply a line of silicone sealant to improve the tightness.
- Place the specimen on the plastic support in the catholyte reservoir (see Figure 1 in Appendix 1).
- Fill the sleeve above the specimen with 300 ml anolyte solution (0.3 M NaOH).
- Immerse the anode in the anolyte solution.
- Connect the cathode to the negative pole and the anode to the positive pole of the power supply.

6.4.4 Migration test

- Turn on the power, with the voltage preset at 30 V, and record the initial current through each specimen.
- Adjust the voltage if necessary (as shown in Table 1 in Appendix 2). After adjustment, note the value of the initial current again.

- Record the initial temperature in each anolyte solution, as shown by the thermometer or thermocouple.
- Choose an appropriate test duration according to the initial current (see Table 1 in Appendix 2).
- Record the final current and temperature before terminating the test.

6.4.5 Measurement of chloride penetration depth

- Disassemble the specimen by following the reverse of the procedure in 6.4.3. A wooden rod is often helpful in removing the rubber sleeve from the specimen.
- Rinse the specimen with tap water.
- Wipe off excess water from the surfaces of the specimen.
- Split the specimen axially into two pieces. Choose the piece having the split section more nearly perpendicular to the end surfaces for the penetration depth measurement, and keep the other piece for chloride content analysis (optional).
- Spray 0.1 M silver nitrate solution on to the freshly split section.
- When the white silver chloride precipitation on the split surface is clearly visible (after about 15 minutes), measure the penetration depth, with the help of the slide calliper and a suitable ruler, from the centre to both edges at intervals of 10 mm (see Figure 5 in Appendix 1) to obtain seven depths (notes 2, 3 and 4). Measure the depth to an accuracy of 0.1 mm.

Note 2: If the penetration front to be measured is obviously blocked by the aggregate, move the measurement to the nearest front where there is no significant blocking by aggregate or, alternatively, ignore this depth if there are more than five valid depths.

Note 3: If there is a significant defect in the specimen which results in a penetration front much larger than the average, ignore this front as indicative of the penetration depth, but note and report the condition.

Note 4: To obviate the edge effect due to a non-homogeneous degree of saturation or possible leakage, do not make any depth measurements in the zone within about 10 mm from the edge (see Figure 5 in Appendix 1).

6.4.6 Surface chloride content (optional, Note 5)

- From the other axially split specimen, cut an approximately 5 mm thick slice (Note 6) parallel to the end surface that was exposed to the chloride solution (catholyte).
- Determine the chloride content in the slice in accordance with NT BUILD 208 or by a similar method with the same or better accuracy.

Note 5: Information on chloride binding capacity of the tested material can be estimated from the surface chloride content.

Note 6: The thickness of the slice should always be less than the minimum penetration depth.

6.5 Expression of results

6.5.1 Test results

Calculate the non-steady-state migration coefficient from Equation (1):

$$D_{nssm} = \frac{RT}{zFE} \cdot \frac{x_d - \alpha\sqrt{x_d}}{t} \quad (1)$$

where:

$$E = \frac{U-2}{L} \quad (2)$$

$$\alpha = 2\sqrt{\frac{RT}{zFE}} \cdot \mathrm{erf}^{-1}\left(1 - \frac{2c_d}{c_0}\right) \quad (3)$$

D_{nssm}: non-steady-state migration coefficient, m^2/s;

z: absolute value of ion valence, for chloride, $z = 1$;

F: Faraday constant, $F = 9.648 \times 10^4$ J/(V·mol);

U: absolute value of the applied voltage, V;

R: gas constant, $R = 8.314$ J/(K·mol);

T: average value of the initial and final temperatures in the anolyte solution, K;

L: thickness of the specimen, m;

x_d: average value of the penetration depths, m;

t: test duration, seconds;

erf^{-1}: inverse of error function;

c_d: chloride concentration at which the colour changes, $c_d = 0.07$ N for OPC concrete;

c_0: chloride concentration in the catholyte solution, $c_0 = 2$ N.

Since $\mathrm{erf}^{-1}\left(1 - \frac{2 \times 0.07}{2}\right) = 1.28$, the following simplified equation can be used:

$$D_{nssm} = \frac{0.0239(273+T)L}{(U-2)t}\left(x_d - 0.0238\sqrt{\frac{(273+T)L\,x_d}{U-2}}\right) \quad (4)$$

where:

D_{nssm}: non-steady-state migration coefficient, $\times 10^{-12}$ m^2/s;

U: absolute value of the applied voltage, V;

T: average value of the initial and final temperatures in the anolyte solution, °C;

L: thickness of the specimen, mm;

x_d: average value of the penetration depths, mm;

t: test duration, hour.

6.6 Accuracy

6.6.1 Repeatability

The coefficient of variation of repeatability is 9 %, according to the results from the Nordic round-robin test between six laboratories /4/.

6.6.2 Reproducibility

The coefficient of variation of reproducibility is 13 % for Portland cement concrete or for concrete mixed with silica fume, and 24 % for concrete mixed with slag cement, according to the results from the Nordic round-robin test between six laboratories /4/.

6.7 Test report

The test report should, if known, include the following information:

a) Name and address of the test laboratory.

b) Date and identification number of the test report.

c) Name and address of the organisation or person who ordered the test.

d) Name and address of the manufacturer or supplier of the material or object tested.

e) Date of arrival of the material or object tested.

f) Description of the material or object tested, including sampling, composition, and curing age.

g) Purpose of the test.

h) Test method.

i) Any deviation from the test method.

j) Name and address of the person who performed the test.

k) Date of the test.

l) Test results, including the specimen dimensions, applied voltage, initial and final currents, initial and final temperatures, average and individual data of penetration depth and migration coefficient.

m) Any observation of an abnormal penetration front due to a defect in the specimen.

n) Optional information about surface chloride content.

o) Date and signature.

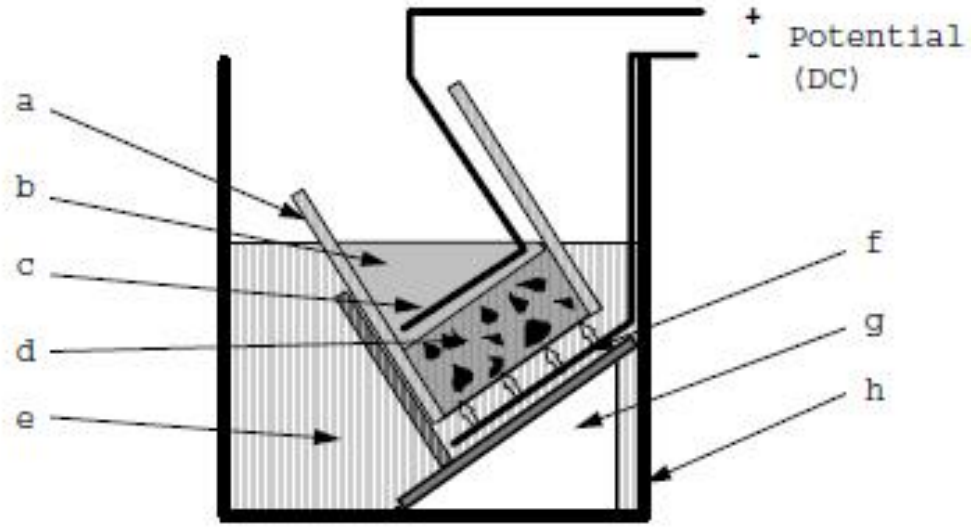

a. Rubber sleeve
b. Anolyte
c. Anode
d. Specimen
e. Catholyte
f. Cathode
g. Plastic support
h. Plastic box

Fig. 1. One arrangement of the migration set-up.

Fig. 2. Stainless steel clamp.

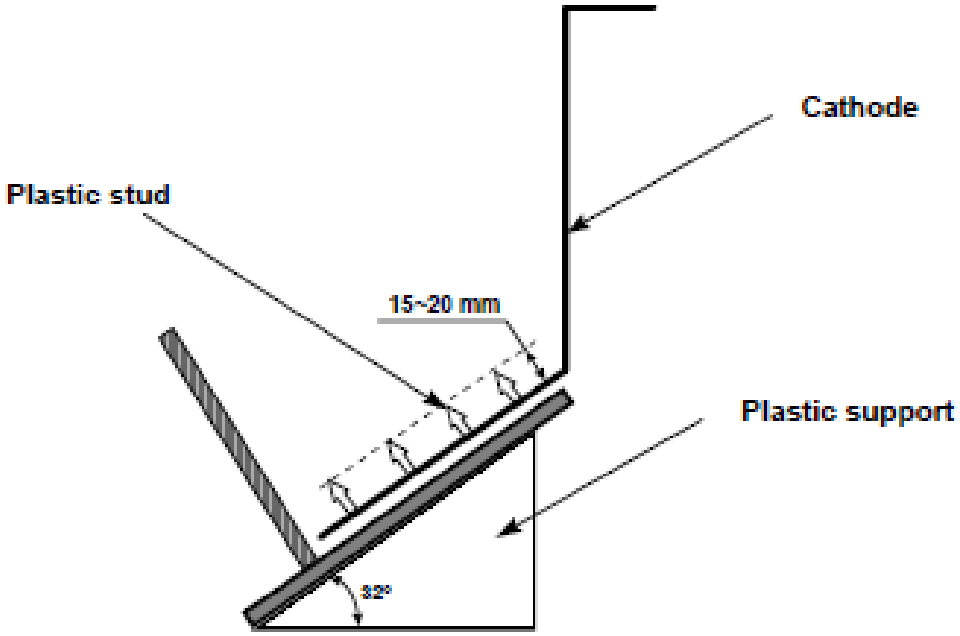

Fig. 3. Plastic support and cathode.

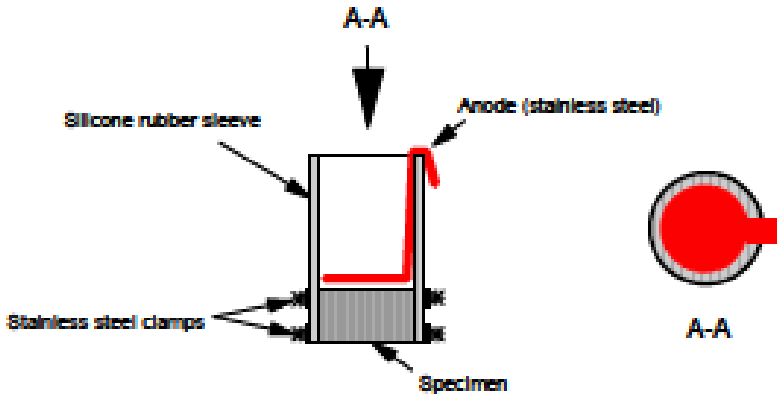

Fig. 4. Rubber sleeve assembled with specimen, clamps and anode.

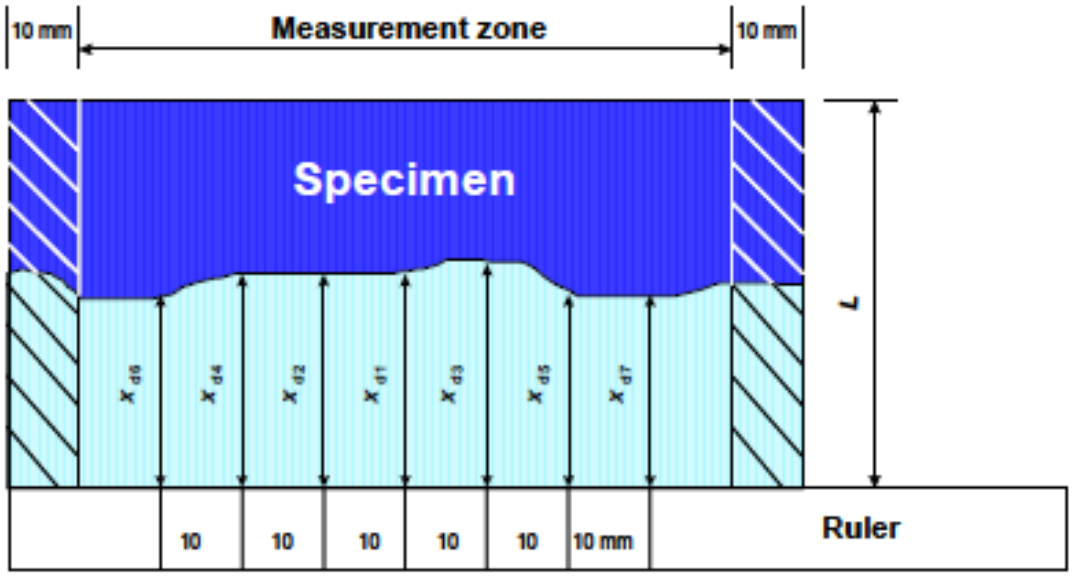

Fig. 5. Illustration of measurement for chloride penetration depths.

Table 1. Test voltage and duration for concrete specimen with normal binder content.

Initial current I_{30V} (with 30 V) (mA)	Applied voltage U (after adjustment) (V)	Possible new initial current I_0 (mA)	Test duration t (hour)
$I_0 < 5$	60	$I_0 < 10$	96
$5 \le I_0 < 10$	60	$10 \le I_0 < 20$	48
$10 \le I_0 < 15$	60	$20 \le I_0 < 30$	24
$15 \le I_0 < 20$	50	$25 \le I_0 < 35$	24
$20 \le I_0 < 30$	40	$25 \le I_0 < 40$	24
$30 \le I_0 < 40$	35	$35 \le I_0 < 50$	24
$40 \le I_0 < 60$	30	$40 \le I_0 < 60$	24
$60 \le I_0 < 90$	25	$50 \le I_0 < 75$	24
$90 \le I_0 < 120$	20	$60 \le I_0 < 80$	24
$120 \le I_0 < 180$	15	$60 \le I_0 < 90$	24
$180 \le I_0 < 360$	10	$60 \le I_0 < 120$	24
$I_0 \ge 360$	10	$I_0 \ge 120$	6

Note: For specimens with a special binder content, such as repair mortars or grouts, correct the measured current by multiplying by a factor (approximately equal to the ratio of normal binder content to actual binder content) in order to be able to use the above table.

APPENDIX C:

Compressive strength Results

Appendix C: Compressive Strength Results

The results for compressive strength are presented in this appendix. The tests were performed at 7, 28 and 56 of age for cubes (150 mm × 150 mm × 150 mm) according to SS-EN 12390-3 (2009), for specimens cured at either 20°C or 55°C. In Tables C.1 - C.3, the results from each specimen and the mean value for each mix are presented. In Table C.4 are presented the strength classes at 28 days of age, evaluated according to SS 13 70 03 (2008).

Table C. 1 - Results for 7-day compressive strength, tested according to SS-EN 12390-3.

Compressive Strength

7 days

		1	2	3	Mean value	
Mix 1	**Weight**	7766	7913	-	7839,5	**g**
	Density	2294,409	2305,149	-	2299,8	**kg/m^3**
	Load	730,8	770,2	-	750,5	**kN**
	Strength	32,386	33,655	-	33,0	**MPa**
Mix 2	**Weight**	7963	7843	-	7903,0	**g**
	Density	2318,701	2303,124	-	2310,9	**kg/m^3**
	Load	696,1	682,1	-	689,1	**kN**
	Strength	30,404	30,045	-	30,2	**MPa**
Mix 3	**Weight**	7951	7913	-	7932,0	**g**
	Density	2295,903	2286,168	-	2291,0	**kg/m^3**
	Load	580,3	629,9	-	605,1	**kN**
	Strength	25,135	27,298	-	26,2	**MPa**
Mix 4	**Weight**	7784	-	-	7784,0	**g**
	Density	2283,033	-	-	2283,0	**kg/m^3**
	Load	529,9	-	-	529,9	**kN**
	Strength	23,313	-	-	23,3	**MPa**
Mix 5	**Weight**	7884	7678	-	7781,0	**g**
	Density	2276,310	2236,446	-	2256,4	**kg/m^3**
	Load	500,3	490,7	-	495,5	**kN**
	Strength	21,667	21,440	-	21,6	**MPa**
Mix 6	**Weight**	7843	-	-	7843,0	**g**
	Density	2283,033	-	-	2283,0	**kg/m^3**
	Load	424,2	-	-	424,2	**kN**
	Strength	23,313	-	-	23,3	**MPa**
Mix 7	**Weight**	7699	7700	-	7699,5	**g**
	Density	2255,869	2256,906	-	2256,4	**kg/m^3**
	Load	642,1	656,2	-	649,2	**kN**
	Strength	28,22107	28,8503	-	28,5	**MPa**
Mix 8	**Weight**	-	-	-	-	**g**
	Density	-	-	-	-	**kg/m^3**
	Load	537,4	538,3	528,9	534,9	**kN**
	Strength	23,529	23,641	23,126	23,4	**MPa**

Table C. 2 - Results for 28-days compressive strength, tested according to SS-EN 12390-3.

Compressive Strength

28 days

		1	2	3	Mean value	
Mix 1	**Weight**	7872	7826	7886	7861,3	**g**
	Density	2307,067	2305,494	2294,026	2302,2	**kg/m^3**
	Load	1139	1141	1210	1163,3	**kN**
	Strength	50,071	50,420	52,798	51,1	**MPa**
Mix 2	**Weight**	7887	7800	7867	7851,3	**g**
	Density	2321,413	2297,327	2303,829	2307,5	**kg/m^3**
	Load	1150	1136	1143	1143	**kN**
	Strength	50,773	50,188	50,209	50,4	**MPa**
Mix 3	**Weight**	7996	7980	7934	7970	**g**
	Density	2308,148	2318,841	2311,266	2312,8	**kg/m^3**
	Load	1154,0	1161,0	1175,0	1163,3	**kN**
	Strength	49,968	50,605	51,344	50,6	**MPa**
Mix 4	**Weight**	7787	7798	7897*	7792,5	**g**
	Density	2276,401	2273,138	2287,742*	2274,8	**kg/m^3**
	Load	1142,0	1151,0	1547*	1146,5	**kN**
	Strength	50,077	50,328	67,224*	50,2	**MPa**
Mix 5	**Weight**	7871	7919	7734	7841,3	**g**
	Density	2273,804	2283,778	2267,503	2275,0	**kg/m^3**
	Load	999,7	1018	938,9	985,5	**kN**
	Strength	43,291	44,060	41,311	42,9	**MPa**
Mix 6	**Weight**	7897	7868	7911	7892	**g**
	Density	2294,722	2300,080	2311,384	2302,1	**kg/m^3**
	Load	967,8	950,1	909,5	942,5	**kN**
	Strength	42,184	41,662	39,860	41,2	**MPa**
Mix 7	**Weight**	7766	7807	7781	7784,7	**g**
	Density	2282,272	2278,252	2289,961	2283,5	**kg/m^3**
	Load	1030	1009	1015	1018	**kN**
	Strength	45,404	44,167	44,807	44,8	**MPa**
Mix 8	**Weight**	7871	7788	7880	7846,3	**g**
	Density	2309,566	2297,091	2301,822	2302,8	**kg/m^3**
	Load	1077	1100	1058	1078,3	**kN**
	Strength	47,403	48,667	46,358	47,5	**MPa**

Table C. 3 - Results for 56-days compressive strength, tested according to SS-EN 12390-3.

Compressive Strength

56 days

		1	2	3	Mean value	
Mix 1	**Weight**	7809	7785	-	7797,0	**g**
	Density	2314,621	2302,456	-	2308,5	**kg/m^3**
	Load	1239	1389	-	1314	**kN**
	Strength	54,660	61,196	-	57,9	**MPa**
Mix 2	**Weight**	7874	7968	7868	7903,3	**g**
	Density	2308,668	2315,858	2288,041	2304,2	**kg/m^3**
	Load	1415	1346	1397	1386	**kN**
	Strength	62,232	58,681	60,938	60,6	**MPa**
Mix 3	**Weight**	7986	7979	-	7982,5	**g**
	Density	2306,759	2299,258	-	2303,0	**kg/m^3**
	Load	1388,0	1407,0	-	1397,5	**kN**
	Strength	60,139	60,817	-	60,5	**MPa**
Mix 4	**Weight**	7854	-	-	7854,0	**g**
	Density	2293,725	-	-	2293,7	**kg/m^3**
	Load	1431,0	-	-	1431,0	**kN**
	Strength	62,688	-	-	62,7	**MPa**
Mix 5	**Weight**	7786	7775	-	7780,5	**g**
	Density	2278,857	2263,464	-	2271,2	**kg/m^3**
	Load	1169,0	1177,0	-	1173	**kN**
	Strength	51,323	51,397	-	51,4	**MPa**
Mix 6	**Weight**	8008	7972	-	7990,0	**g**
	Density	2329,261	2321,322	-	2325,3	**kg/m^3**
	Load	1221	1224	-	1222,5	**kN**
	Strength	53,272	53,461	-	53,4	**MPa**
Mix 7	**Weight**	7809	7785	-	7797,0	**g**
	Density	2280,333	2285,840	-	2283,1	**kg/m^3**
	Load	1135	1155	-	1145	**kN**
	Strength	49,715	50,870	-	50,3	**MPa**
Mix 8	**Weight**	7849	7864	-	7856,5	**g**
	Density	2288,755	2295,388	-	2292,1	**kg/m^3**
	Load	1355	1309	-	1332	**kN**
	Strength	59,26736	57,31173	-	58,3	**MPa**

Table C. 4 – Strength classes for each mix at 28 days, according to SS 13 70 03 (2008)

Mix	$f_{c,\ mean}$ -4 MPa [MPa]	$f_{c,\ min}$ -4 Mpa [MPa]	$f_{ck,\ cube}$ [MPa]	Strength class
Mix 1	51,1	54,1	51,1	C32/40
Mix 2	50,4	54,2	50,4	C32/40
Mix 3	50,6	54,0	50,6	C32/40
Mix 4	50,2	54,1	50,2	C32/40
Mix 5	42,9	45,3	42,9	C32/40
Mix 6	41,2	43,9	41,2	C32/40
Mix 7	44,8	48,2	44,8	C32/40
Mix 8	47,5	50,4	47,5	C32/40

APPENDIX D:
Rapid Chloride Migration Results

Appendix D: Rapid Chloride Migration Results

Table D. 1 - Results from Chloride Migration coefficient, D_{nssm}, from non-steady state migration experiments for Mix 1 (0% GGBS, 4.5% Air) at 28 days of age. Tested according to NT Build 492.

Specimen ID:	**Mix 1: 0% GGBFS , Air=4,5%**			
Age at the start of test, day:	28 days			
Mean value of D_{nssm}:	**16,5**	x10^{-12} m^2/s		
Standard deviation:	1,1	x10^{-12} m^2/s		
Coefficient of Variation:	6,6	%		
Specimen No.:	**1**	**2**	**3**	
Diameter *d*	100	100	100	mm
Thickness *L*	45,6	46,5	45,2	mm
Chloride concentration c_0	10	10	10	NaCl%
Applied potential *U*	20,0	20,0	20,0	V
Current at start I_i	70,00	70,00	80,00	mA
Temperature at start T_i	292,16	292,16	292,16	K
Test duration *t*	24,0	24,0	24,0	hr
Current at end I_t	60,0	70,0	70,0	mA
Temperature at end T_t	295,46	295,46	295,46	K
Average penetration depth x_d	25,3	26,6	24,1	mm
Migration coefficient D_{nssm}	**16,4**	**17,6**	**15,4**	x10^{-12} m^2/s
Individual chloride penetration depths				
Penetration depth x_{d1}	25,6	24,5	23,8	mm
Penetration depth x_{d2}	25,9	24,1	24,1	mm
Penetration depth x_{d3}	25,2	25,8	23,0	mm
Penetration depth x_{d4}	23,6	26,7	23,6	mm
Penetration depth x_{d5}	25,1	28,0	26,8	mm
Penetration depth x_{d6}	25,6	28,3	26,0	mm
Penetration depth x_{d7}	26,2	29,0	21,5	mm

Table D. 2 - Results from Chloride Migration coefficient, D_{nssm}, from non-steady state migration experiments for Mix 1 (0% GGBS, 4.5% Air) at 56 days of age. Tested according to NT Build 492.

Specimen ID:	**Mix 1: 0% GGBFS , Air=4,5%**			
Age at the start of test, day:	56 days			
Mean value of D_{nssm}:	**13,7**	x10^{-12} m^2/s		
Standard deviation:	0,7	x10^{-12} m^2/s		
Coefficient of Variation:	4,8	%		
Specimen No.:	**1**	**2**	**3**	
Diameter *d*	100	100	100	mm
Thickness *L*	49,5	48,9	49,0	mm
Chloride concentration c_0	10	10	10	NaCl%
Applied potential *U*	20,0	20,0	20,0	V
Current at start I_i	68,00	65,00	65,00	mA
Temperature at start T_i	290,16	290,16	290,16	K
Test duration *t*	24,0	24,0	24,0	hr
Current at end I_t	55,0	55,0	54,0	mA
Temperature at end T_t	292,16	292,16	292,16	K
Average penetration depth x_d	19,4	21,4	20,2	mm
Migration coefficient D_{nssm}	**13,1**	**14,4**	**13,6**	x10^{-12} m^2/s
Individual chloride penetration depths				
Penetration depth x_{d1}	19,0	22,1	20,2	mm
Penetration depth x_{d2}	18,7	24,8	22,0	mm
Penetration depth x_{d3}	19,2	22,1	20,9	mm
Penetration depth x_{d4}	19,2	20,9	20,4	mm
Penetration depth x_{d5}	19,6	19,6	20,5	mm
Penetration depth x_{d6}	19,7	20,1	19,2	mm
Penetration depth x_{d7}	20,7	20,1	18,1	mm

Table D. 3 - Results from Chloride Migration coefficient, D_{nssm}, from non-steady state migration experiments for Mix 2 (25% GGBS, 4.5% Air) at 28 days of age. Tested according to NT Build 492.

Specimen ID:	**Mix 2: 25% GGBFS, k=0,6, Air=4,5%**			
Age at the start of test, day:	28 days			
Mean value of D_{nssm}:	**14,7**	x10^{-12} m^2/s		
Standard deviation:	0,9	x10^{-12} m^2/s		
Coefficient of Variation:	5,8	%		
Specimen No.:	**1**	**2**	**3**	
Diameter *d*	100	100	100	mm
Thickness *L*	45,3	48,9	45,0	mm
Chloride concentration c_0	10	10	10	NaCl%
Applied potential *U*	20,0	20,0	20,0	V
Current at start I_i	80,00	80,00	80,00	mA
Temperature at start T_i	295,16	295,16	295,16	K
Test duration *t*	24,0	24,0	24,0	hr
Current at end I_t	60,0	60,0	60,0	mA
Temperature at end T_t	296,16	296,16	296,16	K
Average penetration depth x_d	24,0	21,6	21,7	mm
Migration coefficient D_{nssm}	**15,5**	**14,8**	**13,8**	x10^{-12} m^2/s
Individual chloride penetration depths				
Penetration depth x_{d1}	21,3	24,7	21,7	mm
Penetration depth x_{d2}	23,2	22,1	22,4	mm
Penetration depth x_{d3}	24,3	19,4	22,7	mm
Penetration depth x_{d4}	24,8	19,7	22,6	mm
Penetration depth x_{d5}	24,8	21,9	19,1	mm
Penetration depth x_{d6}	23,2	20,9	20,5	mm
Penetration depth x_{d7}	26,6	22,5	23,1	mm

Table D. 4 - Results from Chloride Migration coefficient, D_{nssm}, from non-steady state migration experiments for Mix 2 (25% GGBS, 4.5% Air) at 56 days of age. Tested according to NT Build 492.

Specimen ID:	**Mix 2: 25% GGBFS, k=0,6, Air=4,5%**			
Age at the start of test, day:	56 days			
Mean value of D_{nssm}:	**7,3**	x10^{-12} m^2/s		
Standard deviation:	0,5	x10^{-12} m^2/s		
Coefficient of Variation:	6,8	%		
Specimen No.:	**1**	**2**	**3**	
Diameter *d*	100	100	100	mm
Thickness *L*	46,7	46,7	52,1	mm
Chloride concentration c_0	10	10	10	NaCl%
Applied potential *U*	25,0	25,0	25,0	V
Current at start I_i	57,00	60,00	59,00	mA
Temperature at start T_i	291,16	291,16	291,16	K
Test duration *t*	24,0	24,0	24,0	hr
Current at end I_t	47,0	51,0	45,0	mA
Temperature at end T_t	292,16	292,16	292,16	K
Average penetration depth x_d	14,3	13,8	14,2	mm
Migration coefficient D_{nssm}	**7,2**	**6,9**	**7,8**	x10^{-12} m^2/s
Individual chloride penetration depths				
Penetration depth x_{d1}	14,1	13,0	15,7	mm
Penetration depth x_{d2}	13,8	12,5	14,2	mm
Penetration depth x_{d3}	14,2	12,2	13,2	mm
Penetration depth x_{d4}	13,0	14,5	12,8	mm
Penetration depth x_{d5}	12,4	14,9	15,0	mm
Penetration depth x_{d6}	17,2	15,8	14,6	mm
Penetration depth x_{d7}	15,5	13,4	14,0	mm

Table D. 5 - Results from Chloride Migration coefficient, D_{nssm}, from non-steady state migration experiments for Mix 3 (50% GGBS, 4.5% Air, k=0,6) at 28 days of age. Tested according to NT Build 492.

Specimen ID:	**Mix 3: 50% GGBFS, k=0,6, Air=4,5%**			
Age at the start of test, day:	28 days			
Mean value of D_{nssm}:	**11,1**	x10^{-12} m^2/s		
Standard deviation:	1,3	x10^{-12} m^2/s		
Coefficient of Variation:	11,7	%		
Specimen No.:	**1**	**2**	**3**	
Diameter d	100	100	100	mm
Thickness L	47,0	46,5	46,8	mm
Chloride concentration c_0	10	10	10	NaCl%
Applied potential U	20,0	20,0	20,0	V
Current at start I_i	59,00	57,00	59,00	mA
Temperature at start T_i	293,16	293,16	293,16	K
Test duration t	24,0	24,0	24,0	hr
Current at end I_t	60,0	60,0	60,0	mA
Temperature at end T_t	295,16	295,16	295,16	K
Average penetration depth x_d	16,7	15,8	19,3	mm
Migration coefficient D_{nssm}	**10,7**	**10,0**	**12,5**	x10^{-12} m^2/s
Individual chloride penetration depths				
Penetration depth x_{d1}	15,9	14,0	20,4	mm
Penetration depth x_{d2}	15,7	13,9	18,6	mm
Penetration depth x_{d3}	16,6	14,7	18,8	mm
Penetration depth x_{d4}	15,4	17,0	18,7	mm
Penetration depth x_{d5}	14,9	15,4	18,3	mm
Penetration depth x_{d6}	18,0	18,5	20,2	mm
Penetration depth x_{d7}	20,2	16,9	20,0	mm

Table D. 6 - Results from Chloride Migration coefficient, D_{nssm}, from non-steady state migration experiments for Mix 3 (50% GGBS, 4.5% Air, k=0.6) at 56 days of age. Tested according to NT Build 492.

Specimen ID:	**Mix 3: 50% GGBFS, k=0,6, Air=4,5%**			
Age at the start of test, day:	56 days			
Mean value of D_{nssm}:	**6,3**	x10^{-12} m^2/s		
Standard deviation:	0,6	x10^{-12} m^2/s		
Coefficient of Variation:	8,8	%		
Specimen No.:	**1**	**2**	**3**	
Diameter *d*	100	100	100	mm
Thickness *L*	49,1	49,8	46,4	mm
Chloride concentration c_0	10	10	10	NaCl%
Applied potential *U*	25,0	25,0	25,0	V
Current at start I_i	50,00	50,00	50,00	mA
Temperature at start T_i	292,16	292,16	292,16	K
Test duration *t*	24,0	24,0	24,0	hr
Current at end I_t	50,0	50,0	50,0	mA
Temperature at end T_t	295,16	295,16	295,16	K
Average penetration depth x_d	11,7	11,5	14,0	mm
Migration coefficient D_{nssm}	**6,0**	**6,0**	**7,0**	x10^{-12} m^2/s
Individual chloride penetration depths				
Penetration depth x_{d1}	14,0	13,5	12,5	mm
Penetration depth x_{d2}	13,3	10,6	12,2	mm
Penetration depth x_{d3}	10,6	8,9	15,1	mm
Penetration depth x_{d4}	11,0	9,5	15,1	mm
Penetration depth x_{d5}	10,6	10,0	14,4	mm
Penetration depth x_{d6}	9,2	11,9	13,6	mm
Penetration depth x_{d7}	13,2	16,1	15,2	mm

Table D. 7 - Results from Chloride Migration coefficient, D_{nssm}, from non-steady state migration experiments for Mix 4 (100% GGBS, 4.5% Air, k=0.6), cured at 20ºC, at 28 days of age. Tested according to NT Build 492.

Specimen ID:	**Mix 4(a): 100% GGBFS, k=0,6, Air=4,5%, Curing 20ºC**			
Age at the start of test, day:	29 days			
Mean value of D_{nssm}:	**9,1**	x10^{-12} m^2/s		
Standard deviation:	0,5	x10^{-12} m^2/s		
Coefficient of Variation:	5,3	%		
Specimen No.:	**1**	**2**	**3**	
Diameter d	100	100	100	mm
Thickness L	45,7	47,4	47,5	mm
Chloride concentration c_0	10	10	10	NaCl%
Applied potential U	25,0	25,0	25,0	V
Current at start I_i	70,00	70,00	60,00	mA
Temperature at start T_i	292,16	292,16	292,16	K
Test duration t	24,0	24,0	24,0	hr
Current at end I_t	70,0	60,0	60,0	mA
Temperature at end T_t	296,16	296,16	296,16	K
Average penetration depth x_d	17,2	18,4	17,5	mm
Migration coefficient D_{nssm}	**8,6**	**9,6**	**9,1**	x10^{-12} m^2/s
Individual chloride penetration depths				
Penetration depth x_{d1}	18,4	18,0	17,9	mm
Penetration depth x_{d2}	18,1	17,0	17,4	mm
Penetration depth x_{d3}	16,8	18,6	16,2	mm
Penetration depth x_{d4}	17,1	18,7	17,6	mm
Penetration depth x_{d5}	16,5	17,2	17,6	mm
Penetration depth x_{d6}	16,7	18,1	18,0	mm
Penetration depth x_{d7}	17,1	21,1	18,0	mm

Table D. 8 - Results from Chloride Migration coefficient, D_{nssm}, from non-steady state migration experiments for Mix 4 (100% GGBS, 4.5% Air, k=0.6), cured at 20ºC, at 56 days of age. Tested according to NT Build 492.

Specimen ID:	**Mix 4(a): 100% GGBFS, k=0,6, Air=4,5%, Curing 20ºC**			
Age at the start of test, day:	56 days			
Mean value of D_{nssm}:	**4,9**	x10^{-12} m^2/s		
Standard deviation:	0,7	x10^{-12} m^2/s		
Coefficient of Variation:	13,5	%		
Specimen No.:	**1**	**2**	**3**	
Diameter *d*	100	100	100	mm
Thickness *L*	47,1	45,8	45,5	mm
Chloride concentration c_0	10	10	10	NaCl%
Applied potential *U*	30,0	30,0	30,0	V
Current at start I_i	40,00	50,00	40,00	mA
Temperature at start T_i	291,16	291,16	291,16	K
Test duration *t*	24,0	24,0	24,0	hr
Current at end I_t	40,0	50,0	40,0	mA
Temperature at end T_t	294,16	294,16	294,16	K
Average penetration depth x_d	12,0	13,4	10,5	mm
Migration coefficient D_{nssm}	**5,0**	**5,5**	**4,2**	x10^{-12} m^2/s
Individual chloride penetration depths				
Penetration depth x_{d1}	12,8	14,6	11,0	mm
Penetration depth x_{d2}	11,7	12,2	10,9	mm
Penetration depth x_{d3}	12,2	13,0	10,6	mm
Penetration depth x_{d4}	11,5	14,9	11,2	mm
Penetration depth x_{d5}	11,2	12,5	10,7	mm
Penetration depth x_{d6}	12,0	13,5	10,0	mm
Penetration depth x_{d7}	12,9	13,2	9,0	mm

Table D. 9 - Results from Chloride Migration coefficient, D_{nssm}, from non-steady state migration experiments for Mix 4(b) (100% GGBS, 4.5% Air, k=0.6), cured at 55ºC, at 28 days of age. Tested according to NT Build 492.

Specimen ID:	**Mix 4(b): 100% GGBFS, k=0,6, Air=4,5%, Curing 55ºC**			
Age at the start of test, day:	30 days			
Mean value of D_{nssm}:	**1,4**	x10^{-12} m^2/s		
Standard deviation:	0,2	x10^{-12} m^2/s		
Coefficient of Variation:	16,1	%		
Specimen No.:	**1**	**2**	**3**	
Diameter *d*	100	100	100	mm
Thickness *L*	47,4	48,2	47,0	mm
Chloride concentration c_0	10	10	10	NaCl%
Applied potential *U*	60,0	60,0	60,0	V
Current at start I_i	30,00	30,00	20,00	mA
Temperature at start T_i	295,16	295,16	295,16	K
Test duration *t*	23,0	23,0	23,0	hr
Current at end I_t	30,0	30,0	30,0	mA
Temperature at end T_t	296,16	296,16	296,16	K
Average penetration depth x_d	7,1	5,4	7,3	mm
Migration coefficient D_{nssm}	**1,5**	**1,2**	**1,6**	x10^{-12} m^2/s
Individual chloride penetration depths				
Penetration depth x_{d1}	8,7	5,5	6,1	mm
Penetration depth x_{d2}	7,1	5,1	5,8	mm
Penetration depth x_{d3}	6,5	5,6	6,3	mm
Penetration depth x_{d4}	6,5	5,3	7,3	mm
Penetration depth x_{d5}	6,7	6,4	8,8	mm
Penetration depth x_{d6}	7,4	5,0	8,6	mm
Penetration depth x_{d7}	6,9	4,7	8,3	mm

Table D. 10 - Results from Chloride Migration coefficient, D_{nssm}, from non-steady state migration experiments for Mix 4 (100% GGBS, 4.5% Air, k=0.6), cured at 55ºC, at 56 days of age. Tested according to NT Build 492.

Specimen ID:	**Mix 4(b): 100% GGBFS, k=0,6, Air=4,5%, Curing 55ºC**			
Age at the start of test, day:	56 days			
Mean value of D_{nssm}:	**1,0**	x10^{-12} m^2/s		
Standard deviation:	0,1	x10^{-12} m^2/s		
Coefficient of Variation:	10,4	%		
Specimen No.:	**1**	**2**	**3**	
Diameter *d*	100	100	100	mm
Thickness *L*	49,7	49,3	49,7	mm
Chloride concentration c_0	10	10	10	NaCl%
Applied potential *U*	60,0	60,0	60,0	V
Current at start I_i	20,40	18,70	17,80	mA
Temperature at start T_i	290,16	290,16	290,16	K
Test duration *t*	48,0	48,0	48,0	hr
Current at end I_t	30,0	24,5	18,8	mA
Temperature at end T_t	294,16	294,16	294,16	K
Average penetration depth x_d	8,7	10,6	9,4	mm
Migration coefficient D_{nssm}	**0,9**	**1,2**	**1,0**	x10^{-12} m^2/s
Individual chloride penetration depths				
Penetration depth x_{d1}	8,0	11,0	9,0	mm
Penetration depth x_{d2}	7,0	8,0	10,0	mm
Penetration depth x_{d3}	7,0	9,0	10,0	mm
Penetration depth x_{d4}	12,0	12,0	9,0	mm
Penetration depth x_{d5}	7,0	13,0	9,0	mm
Penetration depth x_{d6}	11,0	10,0	9,0	mm
Penetration depth x_{d7}	9,0	11,0	10,0	mm

Table D. 11 - Results from Chloride Migration coefficient, D_{nssm}, from non-steady state migration experiments for Mix 5 (50% GGBS, 6% Air, k=0.6) at 28 days of age. Tested according to NT Build 492.

Specimen ID:	**Mix 5: 50% GGBFS, k=0,6, Air=6%**			
Age at the start of test, day:	30 days			
Mean value of D_{nssm}:	**12,4**	x10^{-12} m^2/s		
Standard deviation:	1,3	x10^{-12} m^2/s		
Coefficient of Variation:	10,7	%		
Specimen No.:	**1**	**2**	**3**	
Diameter d	100	100	100	mm
Thickness L	45,9	46,7	46,3	mm
Chloride concentration c_0	10	10	10	NaCl%
Applied potential U	20,0	20,0	20,0	V
Current at start I_i	80,00	50,00	60,00	mA
Temperature at start T_i	295,16	295,16	295,16	K
Test duration t	24,0	24,0	24,0	hr
Current at end I_t	80,0	60,0	60,0	mA
Temperature at end T_t	296,16	296,16	296,16	K
Average penetration depth x_d	20,9	19,5	17,1	mm
Migration coefficient D_{nssm}	**13,5**	**12,7**	**10,9**	x10^{-12} m^2/s
Individual chloride penetration depths				
Penetration depth x_{d1}	20,6	21,7	17,3	mm
Penetration depth x_{d2}	21,7	18,9	15,7	mm
Penetration depth x_{d3}	21,6	17,9	15,6	mm
Penetration depth x_{d4}	21,6	17,7	17,4	mm
Penetration depth x_{d5}	20,2	20,2	17,9	mm
Penetration depth x_{d6}	20,6	20,8	17,3	mm
Penetration depth x_{d7}	20,3	19,0	18,5	mm

Table D. 12 - Results from Chloride Migration coefficient, D_{nssm}, from non-steady state migration experiments for Mix 5 (50% GGBS, 6% Air, k=0.6) at 56 days of age. Tested according to NT Build 492.

Specimen ID:	**Mix 5: 50% GGBFS, k=0,6, Air=6%**		
Age at the start of test, day:	57 days		
Mean value of D_{nssm}:	**7,1**	x10^{-12} m^2/s	
Standard deviation:	0,5	x10^{-12} m^2/s	
Coefficient of Variation:	6,6	%	
Specimen No.:	**1**	**3**	
Diameter *d*	100	100	mm
Thickness *L*	46,8	47,7	mm
Chloride concentration c_0	10	10	NaCl%
Applied potential *U*	25,0	25,0	V
Current at start I_i	60,00	60,00	mA
Temperature at start T_i	296,16	296,16	K
Test duration *t*	24,0	24,0	hr
Current at end I_t	60,0	50,0	mA
Temperature at end T_t	295,16	295,16	K
Average penetration depth x_d	14,6	13,2	mm
Migration coefficient D_{nssm}	**7,4**	**6,8**	x10^{-12} m^2/s
Individual chloride penetration depths			
Penetration depth x_{d1}	13,2	13,3	mm
Penetration depth x_{d2}	14,1	13,4	mm
Penetration depth x_{d3}	13,4	14,9	mm
Penetration depth x_{d4}	15,9	12,9	mm
Penetration depth x_{d5}	15,1	12,7	mm
Penetration depth x_{d6}	14,5	12,7	mm
Penetration depth x_{d7}	15,7	12,8	mm

Table D. 13 - Results from Chloride Migration coefficient, D_{nssm}, from non-steady state migration experiments for Mix 6 (50% GGBS, 4.5% Air, k=1) at 28 days of age. Tested according to NT Build 492.

Specimen ID:	**Mix 6: 50% GGBFS, k=1, Air=4,5%**			
Age at the start of test, day:	29 days			
Mean value of D_{nssm}:	**16,6**	x10^{-12} m^2/s		
Standard deviation:	0,7	x10^{-12} m^2/s		
Coefficient of Variation:	4,2	%		
Specimen No.:	**1**	**2**	**3**	
Diameter d	100	100	100	mm
Thickness L	46,0	45,9	46,9	mm
Chloride concentration c_0	10	10	10	NaCl%
Applied potential U	20,0	20,0	20,0	V
Current at start I_i	70,00	60,00	60,00	mA
Temperature at start T_i	296,16	296,16	296,16	K
Test duration t	24,0	24,0	24,0	hr
Current at end I_t	60,0	60,0	60,0	mA
Temperature at end T_t	295,16	295,16	295,16	K
Average penetration depth x_d	26,4	24,5	24,8	mm
Migration coefficient D_{nssm}	**17,4**	**16,0**	**16,5**	x10^{-12} m^2/s
Individual chloride penetration depths				
Penetration depth x_{d1}	28,4	25,6	27,2	mm
Penetration depth x_{d2}	31,4	25,3	25,5	mm
Penetration depth x_{d3}	25,5	23,1	24,5	mm
Penetration depth x_{d4}	25,1	23,9	24,4	mm
Penetration depth x_{d5}	19,9	25,6	24,9	mm
Penetration depth x_{d6}	25,5	24,7	23,2	mm
Penetration depth x_{d7}	29,2	23,4	24,1	mm

Table D. 14 - Results from Chloride Migration coefficient, D_{nssm}, from non-steady state migration experiments for Mix 6 (50% GGBS, 4.5% Air, k=1) at 56 days of age. Tested according to NT Build 492.

Specimen ID:	**Mix 6: 50% GGBFS, k=1, Air=4,5%**			
Age at the start of test, day:	56 days			
Mean value of D_{nssm}:	**8,2**	x10^{-12} m^2/s		
Standard deviation:	0,4	x10^{-12} m^2/s		
Coefficient of Variation:	4,6	%		
Specimen No.:	**1**	**2**	**3**	
Diameter d	100	100	100	mm
Thickness L	47,1	46,8	44,7	mm
Chloride concentration c_0	10	10	10	NaCl%
Applied potential U	25,0	25,0	25,0	V
Current at start I_i	60,00	60,00	60,00	mA
Temperature at start T_i	294,16	294,16	294,16	K
Test duration t	25,0	25,0	25,0	hr
Current at end I_t	50,0	50,0	50,0	mA
Temperature at end T_t	294,16	294,16	294,16	K
Average penetration depth x_d	17,3	16,0	17,2	mm
Migration coefficient D_{nssm}	**8,6**	**7,8**	**8,1**	x10^{-12} m^2/s
Individual chloride penetration depths				
Penetration depth x_{d1}	20,3	16,3	16,1	mm
Penetration depth x_{d2}	14,3	13,4	18,8	mm
Penetration depth x_{d3}	14,7	16,5	17,8	mm
Penetration depth x_{d4}	16,2	16,2	16,7	mm
Penetration depth x_{d5}	16,9	16,0	15,8	mm
Penetration depth x_{d6}	19,0	16,9	17,2	mm
Penetration depth x_{d7}	20,0	16,9	17,9	mm

Table D. 15 - Results from Chloride Migration coefficient, D_{nssm}, from non-steady state migration experiments for Mix 7 (0% GGBS, 4.5% Air, no superplasticizer) at 28 days of age. Tested according to NT Build 492.

Specimen ID:	**Mix 7: 0% GGBFS, Air=4,5%, no superplasticizer**			
Age at the start of test, day:	28 days			
Mean value of D_{nssm}:	**17,1**	x10^{-12} m^2/s		
Standard deviation:	2,0	x10^{-12} m^2/s		
Coefficient of Variation:	11,8	%		
Specimen No.:	**1**	**2**	**3**	
Diameter d	100	100	100	mm
Thickness L	44,9	46,6	47,0	mm
Chloride concentration c_0	10	10	10	NaCl%
Applied potential U	20,0	20,0	20,0	V
Current at start I_i	70,00	60,00	70,00	mA
Temperature at start T_i	292,16	292,16	292,16	K
Test duration t	24,0	24,0	24,0	hr
Current at end I_t	70,0	60,0	60,0	mA
Temperature at end T_t	295,16	295,16	295,16	K
Average penetration depth x_d	29,7	26,0	22,9	mm
Migration coefficient D_{nssm}	**19,1**	**17,2**	**15,1**	x10^{-12} m^2/s
Individual chloride penetration depths				
Penetration depth x_{d1}	27,2	25,2	23,2	mm
Penetration depth x_{d2}	28,8	24,4	23,1	mm
Penetration depth x_{d3}	34,5	23,1	20,1	mm
Penetration depth x_{d4}	33,0	25,6	23,0	mm
Penetration depth x_{d5}	30,1	28,9	23,0	mm
Penetration depth x_{d6}	28,1	27,1	23,9	mm
Penetration depth x_{d7}	26,5	27,7	24,1	mm

Table D. 16 - Results from Chloride Migration coefficient, D_{nssm}, from non-steady state migration experiments for Mix 7 (0% GGBS, 4.5% Air, no superplasticizer) at 56 days of age. Tested according to NT Build 492.

Specimen ID:	**Mix 7: 0% GGBFS, Air=4,5%, no superplasticizer**		
Age at the start of test, day:	56 days		
Mean value of D_{nssm}:	**12,8**	$x10^{-12}$ m^2/s	
Standard deviation:	0,0	$x10^{-12}$ m^2/s	
Coefficient of Variation:	0,1	%	
Specimen No.:	**1**	**2**	
Diameter d	100	100	mm
Thickness L	46,6	46,3	mm
Chloride concentration c_0	10	10	NaCl%
Applied potential U	20,0	20,0	V
Current at start I_i	66,00	71,00	mA
Temperature at start T_i	291,16	291,16	K
Test duration t	24,0	24,0	hr
Current at end I_t	54,0	57,0	mA
Temperature at end T_t	294,16	294,16	K
Average penetration depth x_d	19,8	19,9	mm
Migration coefficient D_{nssm}	**12,8**	**12,7**	$x10^{-12}$ m^2/s
Individual chloride penetration depths			
Penetration depth x_{d1}	18,7	22,0	mm
Penetration depth x_{d2}	19,7	21,2	mm
Penetration depth x_{d3}	18,9	21,1	mm
Penetration depth x_{d4}	19,8	20,2	mm
Penetration depth x_{d5}	18,8	19,1	mm
Penetration depth x_{d6}	20,1	17,1	mm
Penetration depth x_{d7}	22,9	18,4	mm

Table D. 17 - Results from Chloride Migration coefficient, D_{nssm}, from non-steady state migration experiments for Mix 8 (50% GGBS, 4.5% Air, k=0.6, no superplasticizer) at 28 days of age. Tested according to NT Build 492.

Specimen ID:	**50% GGBFS, k=0,6, Air=4,5%, no superplasticizer**			
Age at the start of test, day:	28 days			
Mean value of D_{nssm}:	**10,6**	x10^{-12} m^2/s		
Standard deviation:	0,7	x10^{-12} m^2/s		
Coefficient of Variation:	6,3	%		
Specimen No.:	**1**	**2**	**3**	
Diameter d	100	100	100	mm
Thickness L	46,7	46,5	46,9	mm
Chloride concentration c_0	10	10	10	NaCl%
Applied potential U	25,0	25,0	25,0	V
Current at start I_i	70,00	80,00	70,00	mA
Temperature at start T_i	294,16	294,16	294,16	K
Test duration t	24,0	24,0	24,0	hr
Current at end I_t	70,0	70,0	70,0	mA
Temperature at end T_t	296,16	296,16	296,16	K
Average penetration depth x_d	21,5	19,2	20,6	mm
Migration coefficient D_{nssm}	**11,2**	**9,9**	**10,8**	x10^{-12} m^2/s
Individual chloride penetration depths				
Penetration depth x_{d1}	21,9	17,6	20,0	mm
Penetration depth x_{d2}	22,9	18,0	18,3	mm
Penetration depth x_{d3}	22,9	18,2	18,6	mm
Penetration depth x_{d4}	22,3	19,1	18,5	mm
Penetration depth x_{d5}	21,9	19,1	22,0	mm
Penetration depth x_{d6}	19,4	20,6	22,7	mm
Penetration depth x_{d7}	19,5	21,9	24,0	mm

Table D. 18 - Results from Chloride Migration coefficient, D_{nssm}, from non-steady state migration experiments for Mix 8 (50% GGBS, 4.5% Air, k=0.6, no superplasticizer) at 56 days of age. Tested according to NT Build 492.

Specimen ID:	**50% GGBFS, k=0,6, Air=4,5%, no superplasticizer**			
Age at the start of test, day:	56 days			
Mean value of D_{nssm}:	**5,3**	x10^{-12} m^2/s		
Standard deviation:	1,1	x10^{-12} m^2/s		
Coefficient of Variation:	20,4	%		
Specimen No.:	**1**	**2**	**3**	
Diameter d	100	100	100	mm
Thickness L	45,9	46,8	45,9	mm
Chloride concentration c_0	10	10	10	NaCl%
Applied potential U	25,0	25,0	25,0	V
Current at start I_i	47,30	55,20	49,10	mA
Temperature at start T_i	292,16	292,16	292,16	K
Test duration t	24,0	24,0	24,0	hr
Current at end I_t	40,6	47,2	43,5	mA
Temperature at end T_t	294,16	294,16	294,16	K
Average penetration depth x_d	13,3	10,4	9,3	mm
Migration coefficient D_{nssm}	**6,5**	**5,1**	**4,4**	x10^{-12} m^2/s
Individual chloride penetration depths				
Penetration depth x_{d1}	11,8	10,8	11,0	mm
Penetration depth x_{d2}	13,2	10,7	10,2	mm
Penetration depth x_{d3}	12,8	9,5	10,6	mm
Penetration depth x_{d4}	16,2	10,2	8,9	mm
Penetration depth x_{d5}	15,1	10,1	7,8	mm
Penetration depth x_{d6}	11,3	11,0	8,1	mm
Penetration depth x_{d7}	12,5	10,2	8,2	mm

APPENDIX E:

Scaling under freeze/thaw

Results

Appendix E.1: Results of the scaled material measured at each 7 cycles

Appendix E.2: Results of the accumulated scaled material

Appendix E.3: Pictures of the specimens at the end of the freeze/thaw test

Table E. 1 - Measured values from scaling under freeze/thaw

		Scaled material [g] after each 7th cycle															
Mix	**Specimen**	**7 d**	**14 d**	**21 d**	**28 d**	**35 d**	**42 d**	**49 d**	**56 d**	**63 d**	**70 d**	**77 d**	**84 d**	**91 d**	**98 d**	**105 d**	**112 d**
Mix 1	A #1	0,175	0,073	0,032	0,049	0,053	0,119	0,148	0,116	0,047	0,067	0,023	0,082	0,080	0,038	0,037	0,015
	B #1	0,163	0,037	0,030	0,077	0,040	0,067	0,042	0,024	0,026	0,023	0,012	0,057	0,037	0,024	0,012	0,008
	C #2	0,184	0,109	0,027	0,033	0,022	0,028	0,030	0,028	0,035	0,024	0,029	0,028	0,036	0,045	0,045	0,039
	D #2	0,078	0,083	0,013	0,012	0,013	0,015	0,011	0,014	0,011	0,021	0,016	0,021	0,019	0,046	0,015	0,011
Mix 2	A #2	0,233	0,049	0,034	0,075	0,120	0,262	0,468	0,527	0,727	0,337	0,435	0,371	0,155	0,155	0,137	0,148
	B #2	0,326	0,143	0,164	0,353	0,400	0,551	1,038	1,099	1,118	0,925	0,776	0,473	0,685	0,419	0,368	0,310
	C #2	0,196	0,071	0,061	0,081	0,188	0,299	0,341	0,526	0,355	0,410	0,370	0,471	0,250	0,318	0,376	0,426
	D #2	0,284	0,087	0,044	0,092	0,127	0,235	0,366	0,485	0,371	0,340	0,251	0,437	0,147	0,148	0,178	0,119
Mix 3	A #1	0,405	0,526	1,075	1,583	1,422	1,006	1,862	1,165	1,485	1,685	1,794	1,765	2,206	1,814	2,643	3,264
	B #2	0,553	0,689	1,010	1,275	1,200	1,415	2,274	2,403	2,236	2,324	3,749	3,440	0,710	0,457	1,870	1,125
	C #1	0,295	0,229	0,493	0,896	0,560	0,523	0,929	0,979	0,791	0,896	1,151	1,296	1,779	1,431	1,908	2,791
	D #2	0,393	0,371	0,951	1,053	0,901	1,189	1,922	2,283	1,775	2,001	1,860	1,861	2,427	2,056	3,045	3,288
Mix 3 (45 days)	A #1	0,259	0,319	0,263	0,382	0,619	0,877	0,981	1,788	1,410	1,752	1,811	1,873	2,247	2,322	2,130	3,671
	B #2	0,496	0,445	0,186	0,249	0,627	0,893	1,040	1,220	1,397	2,046	2,170	1,735	2,004	2,432	2,037	2,609
	C #1	0,334	0,286	0,233	0,216	0,391	0,719	1,101	0,862	1,043	1,361	1,631	1,576	1,657	1,882	2,161	1,573
	D #2	0,342	0,259	0,182	0,555	0,406	0,858	0,921	1,105	1,425	1,442	2,031	1,614	1,824	1,856	1,923	2,841
Mix 4 (a)	A #2	1,079	4,291	2,995	4,230	3,590	3,450	0,298[a]	1,868	-	-	-	-	-	-	-	-
	B #2	1,316	3,530	2,982	4,238	3,526	3,367	1,940[a]	2,656	-	-	-	-	-	-	-	-
	C #2	2,096	4,789	2,849	4,230	3,751	3,134	4,469	4,488	-	-	-	-	-	-	-	-
	D #2	1,637	4,478	3,694	4,254	4,053	4,286	5,198	2,350	-	-	-	-	-	-	-	-
Mix 4 (55°C)	A #1	0,998	1,442	1,312	1,434	1,575	1,488	2,893	2,160	1,436	1,677	2,781	1,816	1,645	2,538	2,626	2,765
	B #2	0,631	2,808	1,318	1,305	1,579	1,796	4,263	2,761	1,713	2,026	2,706	2,263	2,723	2,453	3,319	2,847
	C #2	1,168	1,967	1,127	1,734	1,954	1,596	2,708	2,721	1,643	3,029	2,879	1,725	2,713	2,016	3,137	3,026

Table E. 1 - Measured values from scaling under freeze/thaw (cont.)

		Scaled material [g] after each 7th cycle															
Mix	**Specimen**	**7 d**	**14 d**	**21 d**	**28 d**	**35 d**	**42 d**	**49 d**	**56 d**	**63 d**	**70 d**	**77 d**	**84 d**	**91 d**	**98 d**	**105 d**	**112 d**
Mix 5	A #1	0,198	0,096	0,216	0,115	0,510	0,032	0,036	0,053	0,074	0,100	0,224	0,157	0,240	0,126	0,168	0,308
	B #2	0,106	0,056	0,110	0,344	0,460	0,462	0,585	0,877	0,577	0,594	0,496	0,478	0,580	0,512	0,604	1,297
	C #1	0,234	0,170	0,529	0,879	0,041	0,915	0,299[a]	0,844	0,374	0,250	0,352	0,344	0,537	0,381	0,825	1,003
	D #2	0,217	0,194	0,273	0,622	0,332	0,752	1,053	1,482	1,284	1,877	1,970	0,857	1,164	0,598	0,709	1,104
Mix 5 (45 days)	A #1	0,352	0,118	0,071	0,087	0,027	0,215	0,187	0,272	0,353	0,741	0,661	0,687	0,839	0,878	1,099	1,393
	B #2	0,211	0,114	0,069	0,056	0,106	0,219	0,245	0,417	1,200	0,962	0,962	0,705	0,637	1,128	0,892	1,393
	C #1	0,168	0,250	0,108	0,194	0,188	0,387	0,547	0,529	0,581	0,892	1,113	0,677	0,562	0,312	0,671	0,644
	D #2	0,235	0,125	0,068	0,088	0,141	0,402	0,338	0,390	0,621	0,594	0,902	0,535	0,433	0,842	0,896	1,293
Mix 6 (a)	A #1	0,496	0,179	0,099	0,118	0,045[a]	0,061[a]	0,204	0,190	0,137	0,022	0,040	0,066	0,066	0,064	0,105	0,170
	B #1	1,009	0,342	0,111	0,097	0,093[a]	0,100[a]	0,135	0,088	0,098	0,039	0,088	0,089	0,066	0,068	0,078	0,154
	C #1	0,726	0,277	0,084	0,091	0,043[a]	0,120[a]	0,074	0,121	0,108	0,130	0,108	0,123	0,135	0,138	0,301	0,224
	D #1	0,791	0,359	0,125	0,098	0,212	0,209[a]	0,111	0,169	0,172	0,151	0,211	0,272	0,328	0,411	0,571	0,794
Mix 6 (55°C)	A #2	1,159	0,854	0,633	1,137	1,495	1,970	4,244	4,310	3,681	4,876	4,274	4,294	6,457	2,749[a]	3,867	6,218
	B #2	1,152	0,673	0,463	0,985	1,539	2,268	4,141	4,758	2,954	3,479	5,525	4,112	5,191	4,768	4,903	3,541
	C #1	0,738	0,473	0,371	0,713	0,857	1,357	2,677	3,587	3,296	3,437	4,050	4,058	3,625	4,509	4,631	0,921
Mix 7	A #2	0,043	0,027	0,019	0,007	0,040	0,014	0,023	0,011	0,010	0,034	0,024	0,026	0,005	0,006	0,009	0,011
	B #2	0,217	0,099	0,049	0,019	0,013	0,014	0,014	0,033	0,017	0,020	0,013	0,008	0,013	0,006	0,008	0,018
	C #2	0,017	0,015	0,171	0,020	0,029	0,027	0,027	0,012	0,010	0,018	0,009	0,014	0,010	0,012	0,008	0,003
	D #2	0,058	0,012	0,021	0,024	0,007	0,009	0,009	0,009	0,006	0,033	0,004	0,004	0,021	0,005	0,009	0,010
Mix 8	A #1	0,298	0,291	0,247	0,133	0,273	0,250	0,156	0,317	0,255	0,682	0,807	1,037	0,720	0,789	1,135	2,279
	B #2	0,239	0,200	0,179	0,378	0,548	0,783	1,023	0,807	1,235	1,424	1,080	0,803	0,980	1,821	2,350	1,280
	C #2	0,829	0,301	0,755	1,074	0,984	1,151	0,853	0,718	0,410	0,545	0,505	0,418	0,697	0,952	1,324	1,412
	D #1	0,909	0,350	0,542	0,860	0,671	0,621	0,346	0,262	0,453	0,714	0,343	0,297	0,382	0,564	0,857	1,077

Table E. 2. 1 - Results from scaling under freeze/thaw, according to SS 13 72 44, method IA, for Mix 1 (0% GGBS, Air=4.5%), accumulated values [kg/m^2]

		Scaled material, accumulated [kg/m^2]																
Mix	**Specimen**	**m_7**	**m_{14}**	**m_{21}**	**m_{28}**	**m_{35}**	**m_{42}**	**m_{49}**	**m_{56}**	**m_{63}**	**m_{70}**	**m_{77}**	**m_{84}**	**m_{91}**	**m_{98}**	**m_{105}**	**m_{112}**	**m_{56}/m_{28}**
Mix 1	A	0,008	0,011	0,012	0,015	0,017	0,022	0,029	0,034	0,036	0,039	0,040	0,044	0,047	0,049	0,051	0,051	
	B	0,007	0,009	0,010	0,014	0,015	0,018	0,020	0,021	0,022	0,024	0,024	0,027	0,028	0,029	0,030	0,030	
	C	0,008	0,013	0,014	0,016	0,017	0,018	0,019	0,020	0,022	0,023	0,024	0,026	0,027	0,029	0,031	0,033	
	D	0,003	0,007	0,008	0,008	0,009	0,010	0,010	0,011	0,011	0,012	0,013	0,014	0,015	0,017	0,017	0,018	
	Mean value	0,007	0,010	0,011	0,013	0,014	0,017	0,020	**0,022**	0,023	0,024	0,025	0,027	0,029	0,031	0,032	**0,033**	**1,655**
	Standard deviation	0,002	0,003	0,003	0,003	0,004	0,005	0,008	0,010	0,010	0,011	0,011	0,012	0,014	0,013	0,014	0,014	
	Coefficient of variation [%]	32,5	25,4	25,2	25,2	26,3	31,5	39,3	44,3	44,6	45,4	44,3	45,1	46,0	43,1	42,7	41,9	

Table E. 2. 2 - Results from scaling under freeze/thaw, according to SS 13 72 44, method IA, for Mix 2 (25% GGBS, Air=4.5%, k=0.6), accumulated values [kg/m^2]

		Scaled material, accumulated [kg/m^2]																
Mix	**Specimen**	**m_7**	**m_{14}**	**m_{21}**	**m_{28}**	**m_{35}**	**m_{42}**	**m_{49}**	**m_{56}**	**m_{63}**	**m_{70}**	**m_{77}**	**m_{84}**	**m_{91}**	**m_{98}**	**m_{105}**	**m_{112}**	**m_{56}/m_{28}**
Mix 2	A	0,010	0,013	0,014	0,017	0,023	0,034	0,055	0,079	0,111	0,126	0,145	0,162	0,169	0,175	0,182	0,188	
	B	0,014	0,021	0,028	0,044	0,062	0,086	0,132	0,181	0,231	0,272	0,306	0,327	0,358	0,376	0,393	0,407	
	C	0,009	0,012	0,015	0,018	0,027	0,040	0,055	0,078	0,094	0,112	0,129	0,150	0,161	0,175	0,192	0,211	
	D	0,013	0,016	0,018	0,023	0,028	0,039	0,055	0,076	0,093	0,108	0,119	0,139	0,145	0,152	0,160	0,165	
	Mean value	0,012	0,015	0,019	0,025	0,035	0,050	0,074	**0,104**	0,132	0,155	0,175	0,194	0,208	0,220	0,231	**0,243**	**4,067**
	Standard deviation	0,003	0,004	0,007	0,012	0,018	0,024	0,039	0,052	0,066	0,079	0,088	0,089	0,100	0,105	0,108	0,111	
	Coefficient of variation [%]	22,0	26,9	34,7	48,8	51,9	49,0	52,0	49,8	50,1	50,9	50,5	45,9	48,2	47,9	46,8	45,7	

Table E. 2. 3 - Results from scaling under freeze/thaw, according to SS 13 72 44, method IA, for Mix 3 (50% GGBS, Air=4.5%, k=0.6), accumulated values [kg/m2]

		Scaled material, accumulated [kg/m^2]																
Mix	**Specimen**	m_7	m_{14}	m_{21}	m_{28}	m_{35}	m_{42}	m_{49}	m_{56}	m_{63}	m_{70}	m_{77}	m_{84}	m_{91}	m_{98}	m_{105}	m_{112}	m_{56}/m_{28}
Mix 3	A	0,018	0,041	0,089	0,160	0,223	0,267	0,350	0,402	0,468	0,543	0,623	0,701	0,799	0,880	0,997	1,142	
	B	0,025	0,055	0,100	0,157	0,210	0,273	0,374	0,481	0,580	0,684	0,850	1,003	1,035	1,055	1,138	1,188	
	C	0,013	0,023	0,045	0,085	0,110	0,133	0,174	0,218	0,253	0,293	0,344	0,402	0,481	0,544	0,629	0,753	
	D	0,017	0,034	0,076	0,123	0,163	0,216	0,301	0,403	0,482	0,571	0,653	0,736	0,844	0,935	1,071	1,217	
	Mean value	0,018	0,038	0,078	0,131	0,176	0,222	0,300	**0,376**	0,446	0,522	0,618	0,710	0,790	0,854	0,959	**1,075**	**2,868**
	Standard deviation	0,005	0,013	0,024	0,035	0,051	0,065	0,089	0,112	0,138	0,165	0,208	0,246	0,230	0,219	0,227	0,217	
	Coefficient of variation [%]	25,9	34,9	30,6	26,6	29,0	29,1	29,7	29,7	30,9	31,5	33,7	34,6	29,1	25,6	23,7	20,2	

Table E. 2. 4 - Results from scaling under freeze/thaw, according to SS 13 72 44, method IA, for Mix 3 (50% GGBS, Air=4.5%, k=0.6, carbonated), accumulated values [kg/m^2]

		Scaled material, accumulated [kg/m^2]																
Mix	**Specimen**	m_7	m_{14}	m_{21}	m_{28}	m_{35}	m_{42}	m_{49}	m_{56}	m_{63}	m_{70}	m_{77}	m_{84}	m_{91}	m_{98}	m_{105}	m_{112}	m_{56}/m_{28}
Mix 3 (tested at 45 days)	A	0,012	0,026	0,037	0,054	0,082	0,121	0,164	0,244	0,307	0,384	0,465	0,548	0,648	0,751	0,846	1,009	
	B	0,022	0,042	0,050	0,061	0,089	0,129	0,175	0,229	0,291	0,382	0,479	0,556	0,645	0,753	0,843	0,959	
	C	0,015	0,028	0,038	0,048	0,065	0,097	0,146	0,184	0,230	0,291	0,363	0,433	0,507	0,591	0,687	0,757	
	D	0,015	0,027	0,035	0,059	0,078	0,116	0,157	0,206	0,269	0,333	0,423	0,495	0,576	0,659	0,744	0,870	
	Mean value	0,016	0,030	0,040	0,056	0,078	0,116	0,160	**0,216**	0,274	0,348	0,433	0,508	0,594	0,688	0,780	0,899	3,878
	Standard deviation	0,004	0,008	0,007	0,006	0,010	0,014	0,012	0,026	0,033	0,045	0,052	0,057	0,067	0,079	0,078	0,111	
	Coefficient of variation [%]	27,8	25,0	17,1	11,0	12,9	11,7	7,7	12,2	12,1	12,8	12,0	11,1	11,2	11,4	10,0	12,3	

Table E. 2. 5 - Results from scaling under freeze/thaw, according to SS 13 72 44, method IA, for Mix 4(a) (100% GGBS, Air=4.5%, k=0.6), accumulated values [kg/m^2]

		Scaled material, accumulated [kg/m^2]																
Mix	**Specimen**	**m_7**	**m_{14}**	**m_{21}**	**m_{28}**	**m_{35}**	**m_{42}**	**m_{49}**	**m_{56}**	**m_{63}**	**m_{70}**	**m_{77}**	**m_{84}**	**m_{91}**	**m_{98}**	**m_{105}**	**m_{112}**	**m_{56}/m_{28}**
Mix 4 (a) – Curing 20ºC	A	0,048	0,239	0,372	0,560	0,719	0,873	0,886	0,969	0,969	0,969	0,969	0,969	0,969	0,969	0,969	0,969	
	B	0,058	0,215	0,348	0,536	0,693	0,843	0,929	1,047	1,047	1,047	1,047	1,047	1,047	1,047	1,047	1,047	
	C	0,093	0,306	0,433	0,621	0,787	0,927	1,125	1,325	1,325	1,325	1,325	1,325	1,325	1,325	1,325	1,325	
	D	0,073	0,272	0,436	0,625	0,805	0,996	1,227	1,331	1,331	1,331	1,331	1,331	1,331	1,331	1,331	1,331	
	Mean value	0,068	0,258	0,397	0,585	0,751	0,909	1,042	**1,168**	1,168	1,168	1,168	1,168	1,168	1,168	1,168	**1,168**	**1,995**
	Standard deviation	0,020	0,040	0,044	0,044	0,054	0,067	0,161	0,187	0,187	0,187	0,187	0,187	0,187	0,187	0,187	0,187	
	Coefficient of variation [%]	28,7	15,3	11,1	7,6	7,1	7,4	15,5	16,1	16,1	16,1	16,1	16,1	16,1	16,1	16,1	16,1	

Table E. 2. 6 - Results from scaling under freeze/thaw, according to SS 13 72 44, method IA, for Mix 4(b) (100% GGBS, Air=4.5%, k=0.6, cured at 55ºC), accumulated values [kg/m^2]

		Scaled material, accumulated [kg/m^2]																
Mix	**Specimen**	**m_7**	**m_{14}**	**m_{21}**	**m_{28}**	**m_{35}**	**m_{42}**	**m_{49}**	**m_{56}**	**m_{63}**	**m_{70}**	**m_{77}**	**m_{84}**	**m_{91}**	**m_{98}**	**m_{105}**	**m_{112}**	**m_{56}/m_{28}**
Mix 4 (b) - Curing 55ºC	A	0,044	0,108	0,167	0,230	0,300	0,367	0,495	0,591	0,655	0,730	0,853	0,934	1,007	1,120	1,236	1,359	
	B	0,028	0,153	0,211	0,269	0,340	0,419	0,609	0,732	0,808	0,898	1,018	1,119	1,240	1,349	1,496	1,623	
	C	0,052	0,139	0,189	0,266	0,353	0,424	0,545	0,666	0,739	0,873	1,001	1,078	1,198	1,288	1,427	1,562	
	Mean value	0,041	0,134	0,189	0,255	0,331	0,403	0,550	**0,663**	0,734	0,834	0,957	1,043	1,148	1,252	1,387	**1,515**	**2,594**
	Standard deviation	0,012	0,023	0,022	0,022	0,027	0,032	0,057	0,070	0,076	0,091	0,091	0,097	0,124	0,119	0,135	0,138	
	Coefficient of variation [%]	29,4	17,0	11,8	8,5	8,3	7,9	10,4	10,6	10,4	10,9	9,5	9,3	10,8	9,5	9,7	9,1	

Table E. 2. 7 - Results from scaling under freeze/thaw, according to SS 13 72 44, method IA, for Mix 5 (50% GGBS, Air=6%, k=0.6), accumulated values [kg/m2]

	Scaled material, accumulated [kg/m^2]

Mix	Specimen	m_7	m_{14}	m_{21}	m_{28}	m_{35}	m_{42}	m_{49}	m_{56}	m_{63}	m_{70}	m_{77}	m_{84}	m_{91}	m_{98}	m_{105}	m_{112}	m_{56}/m_{28}
Mix 5	A	0,009	0,013	0,023	0,028	0,050	0,052	0,053	0,056	0,059	0,064	0,074	0,080	0,091	0,097	0,104	0,118	
	B	0,005	0,007	0,012	0,027	0,048	0,068	0,094	0,133	0,159	0,185	0,207	0,229	0,254	0,277	0,304	0,362	
	C	0,010	0,018	0,041	0,081	0,082	0,123	0,136	0,174	0,190	0,202	0,217	0,232	0,256	0,273	0,310	0,355	
	D	0,010	0,018	0,030	0,058	0,073	0,106	0,153	0,219	0,276	0,359	0,447	0,485	0,537	0,563	0,595	0,644	
	Mean value	0,008	0,014	0,027	0,048	0,063	0,087	0,109	**0,145**	0,171	0,202	0,236	0,257	0,285	0,303	0,328	**0,370**	**3,003**
	Standard deviation	0,003	0,005	0,012	0,026	0,017	0,033	0,045	0,069	0,090	0,121	0,155	0,168	0,185	0,193	0,202	0,215	
	Coefficient of variation [%]	30,2	36,8	46,5	53,2	26,7	37,7	40,9	47,6	52,3	60,0	65,6	65,4	65,0	63,8	61,5	58,2	

Table E. 2. 8 - Results from scaling under freeze/thaw, according to SS 13 72 44, method IA, for Mix 5 (50% GGBS, Air=6%, k=0.6, carbonated), accumulated values [kg/m^2]

		Scaled material, accumulated [kg/m^2]																
Mix	Specimen	m_7	m_{14}	m_{21}	m_{28}	m_{35}	m_{42}	m_{49}	m_{56}	m_{63}	m_{70}	m_{77}	m_{84}	m_{91}	m_{98}	m_{105}	m_{112}	m_{56}/m_{28}
Mix 5 (tested at 45 days)	A	0,016	0,021	0,024	0,028	0,029	0,039	0,047	0,059	0,075	0,108	0,137	0,168	0,205	0,244	0,293	0,355	
	B	0,009	0,014	0,018	0,020	0,025	0,034	0,045	0,064	0,117	0,160	0,203	0,234	0,262	0,312	0,352	0,414	
	C	0,007	0,019	0,023	0,032	0,040	0,058	0,082	0,105	0,131	0,171	0,220	0,250	0,275	0,289	0,319	0,348	
	D	0,010	0,016	0,019	0,023	0,029	0,047	0,062	0,079	0,107	0,133	0,174	0,197	0,217	0,254	0,294	0,351	
	Mean value	0,011	0,017	0,021	0,026	0,031	0,044	0,059	**0,077**	0,108	0,143	0,183	0,212	0,240	0,275	0,314	**0,367**	**2,992**
	Standard deviation	0,003	0,003	0,003	0,005	0,007	0,010	0,017	0,021	0,024	0,028	0,036	0,037	0,034	0,032	0,028	0,032	
	Coefficient of variation [%]	32,6	16,3	15,3	20,7	21,7	23,0	28,7	27,1	22,3	19,8	19,9	17,5	14,3	11,5	8,9	8,6	

Table E. 2. 9 - Results from scaling under freeze/thaw, according to SS 13 72 44, method IA, for Mix 6(a) (50% GGBS, Air=4.5%, k=1), accumulated values [kg/m^2]

		Scaled material, accumulated [kg/m^2]																
Mix	**Specimen**	**m_7**	**m_{14}**	**m_{21}**	**m_{28}**	**m_{35}**	**m_{42}**	**m_{49}**	**m_{56}**	**m_{63}**	**m_{70}**	**m_{77}**	**m_{84}**	**m_{91}**	**m_{98}**	**m_{105}**	**m_{112}**	**m_{56}/m_{28}**
Mix 6 (a) - – Curing 20°C	A	0,022	0,030	0,034	0,040	0,042	0,044	0,053	0,062	0,068	0,069	0,071	0,074	0,077	0,079	0,084	0,092	
	B	0,045	0,060	0,065	0,069	0,073	0,078	0,084	0,088	0,092	0,094	0,098	0,102	0,105	0,108	0,111	0,118	
	C	0,032	0,045	0,048	0,052	0,054	0,060	0,063	0,068	0,073	0,079	0,084	0,089	0,095	0,101	0,115	0,125	
	D	0,035	0,051	0,057	0,061	0,070	0,080	0,085	0,092	0,100	0,107	0,116	0,128	0,143	0,161	0,186	0,222	
	Mean value	0,034	0,046	0,051	0,056	0,060	0,065	0,071	**0,078**	0,083	0,087	0,092	0,098	0,105	0,112	0,124	**0,139**	**1,395**
	Standard deviation	0,009	0,013	0,013	0,013	0,015	0,017	0,016	0,015	0,015	0,017	0,019	0,023	0,028	0,035	0,044	0,057	
	Coefficient of variation [%]	27,9	27,3	25,5	22,8	24,7	25,6	21,9	19,0	18,2	19,0	21,1	23,4	26,5	30,8	35,2	40,9	

Table E. 2. 10 - Results from scaling under freeze/thaw, according to SS 13 72 44, method IA, for Mix 6(b) (50% GGBS, Air=4.5%, k=1, cured at 55ºC), accumulated values [kg/m^2]

		Scaled material, accumulated [kg/m^2]																
Mix	**Specimen**	**m_7**	**m_{14}**	**m_{21}**	**m_{28}**	**m_{35}**	**m_{42}**	**m_{49}**	**m_{56}**	**m_{63}**	**m_{70}**	**m_{77}**	**m_{84}**	**m_{91}**	**m_{98}**	**m_{105}**	**m_{112}**	**m_{56}/m_{28}**
Mix 6 (b) - Curing 55°C	A	0,052	0,089	0,118	0,168	0,235	0,322	0,511	0,702	0,866	1,083	1,273	1,463	1,750	1,873	2,044	2,321	
	B	0,051	0,081	0,102	0,145	0,214	0,315	0,499	0,710	0,841	0,996	1,242	1,424	1,655	1,867	2,085	2,242	
	C	0,033	0,054	0,070	0,102	0,140	0,200	0,319	0,479	0,625	0,778	0,958	1,138	1,300	1,500	1,706	1,747	
	Mean value	0,045	0,075	0,097	0,139	0,196	0,279	0,443	**0,630**	0,778	0,952	1,157	1,342	1,568	1,747	1,945	**2,103**	**4,551**
	Standard deviation	0,011	0,019	0,024	0,034	0,050	0,068	0,107	0,131	0,132	0,157	0,173	0,177	0,238	0,214	0,208	0,311	
	Coefficient of variation [%]	23,7	24,9	24,9	24,3	25,3	24,4	24,2	20,8	17,0	16,5	15,0	13,2	15,2	12,2	10,7	14,8	

Table E. 2. 11 - Results from scaling under freeze/thaw, according to SS 13 72 44, method IA, for Mix 7 (50% GGBS, Air=4.5%, no superplasticizer), accumulated values [kg/m^2]

		Scaled material, accumulated [kg/m^2]																
Mix	**Specimen**	**m_7**	**m_{14}**	**m_{21}**	**m_{28}**	**m_{35}**	**m_{42}**	**m_{49}**	**m_{56}**	**m_{63}**	**m_{70}**	**m_{77}**	**m_{84}**	**m_{91}**	**m_{98}**	**m_{105}**	**m_{112}**	**m_{56}/m_{28}**
Mix 7	A	0,002	0,003	0,004	0,004	0,006	0,007	0,008	0,008	0,009	0,010	0,011	0,012	0,013	0,013	0,013	0,014	
	B	0,010	0,014	0,016	0,017	0,018	0,018	0,019	0,020	0,021	0,022	0,023	0,023	0,024	0,024	0,024	0,025	
	C	0,001	0,001	0,009	0,010	0,011	0,012	0,014	0,014	0,015	0,015	0,016	0,016	0,017	0,017	0,018	0,018	
	D	0,003	0,003	0,004	0,005	0,005	0,006	0,006	0,007	0,007	0,008	0,009	0,009	0,010	0,010	0,010	0,011	
	Mean value	0,004	0,005	0,008	0,009	0,010	0,011	0,012	**0,012**	0,013	0,014	0,015	0,015	0,016	0,016	0,016	**0,017**	**1,356**
	Standard deviation	0,001	0,001	0,003	0,003	0,003	0,004	0,004	0,004	0,004	0,004	0,004	0,004	0,004	0,004	0,004	0,004	
	Coefficient of variation [%]	24,8	18,0	34,9	33,5	31,5	33,2	33,7	32,2	31,5	26,1	25,2	25,5	23,1	23,7	23,0	21,4	

Table E. 2. 12 - Results from scaling under freeze/thaw, according to SS 13 72 44, method IA, for Mix 8 (50% GGBS, Air=4.5%, k=0.6, no superplasticizer), accumulated values [kg/m^2]

		Scaled material, accumulated [kg/m^2]																
Mix	**Specimen**	**m_7**	**m_{14}**	**m_{21}**	**m_{28}**	**m_{35}**	**m_{42}**	**m_{49}**	**m_{56}**	**m_{63}**	**m_{70}**	**m_{77}**	**m_{84}**	**m_{91}**	**m_{98}**	**m_{105}**	**m_{112}**	**m_{56}/m_{28}**
Mix 8	A	0,013	0,026	0,037	0,043	0,055	0,066	0,073	0,087	0,099	0,129	0,165	0,211	0,243	0,278	0,328	0,430	
	B	0,011	0,020	0,027	0,044	0,069	0,103	0,149	0,185	0,240	0,303	0,351	0,387	0,430	0,511	0,616	0,672	
	C	0,037	0,050	0,084	0,132	0,175	0,226	0,264	0,296	0,314	0,339	0,361	0,380	0,411	0,453	0,512	0,575	
	D	0,040	0,056	0,080	0,118	0,148	0,176	0,191	0,203	0,223	0,255	0,270	0,283	0,300	0,325	0,363	0,411	
	Mean value	0,025	0,038	0,057	0,084	0,112	0,143	0,169	**0,193**	0,219	0,256	0,287	0,315	0,346	0,392	0,455	**0,522**	**2,287**
	Standard deviation	0,016	0,018	0,029	0,047	0,059	0,072	0,080	0,086	0,089	0,092	0,091	0,084	0,089	0,109	0,133	0,124	
	Coefficient of variation [%]	61,4	47,0	50,7	56,0	52,7	50,2	47,2	44,4	40,9	35,7	31,7	26,7	25,9	27,7	29,4	23,8	

Appendix E.3: Pictures of the specimens at the end of the freeze/thaw test

Figure E. 1 – Picture of specimen A, Mix 1 (0% GGBS, 4,5% Air) after 112 freeze/thaw cycles

Figure E. 2 - Picture of specimen B, Mix 1 (0% GGBS, 4,5% Air) after 112 freeze/thaw cycles

Figure E. 3 – Picture of specimen C, Mix 1 (0% GGBS, 4,5% Air) after 112 freeze/thaw cycles

Figure E. 4 – Picture of specimen D, Mix 1 (0% GGBS, 4,5% Air) after 112 freeze/thaw cycles

Figure E. 5 – Picture of specimen A, Mix 2 (25% GGBS, 4,5% Air, k=0.6) after 112 freeze/thaw cycles

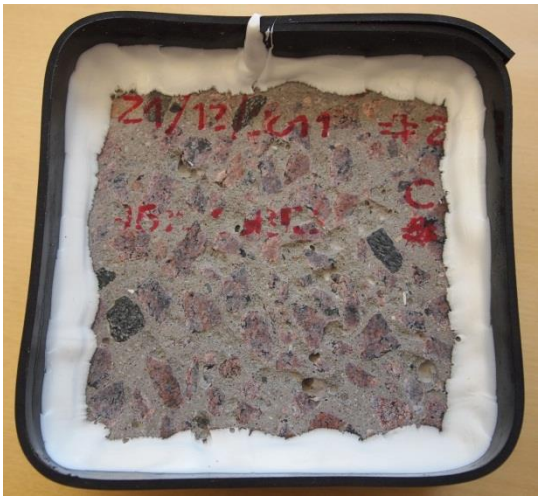

Figure E. 6 – Picture of specimen B, Mix 2 (25% GGBS, 4,5% Air, k=0.6) after 112 freeze/thaw cycles

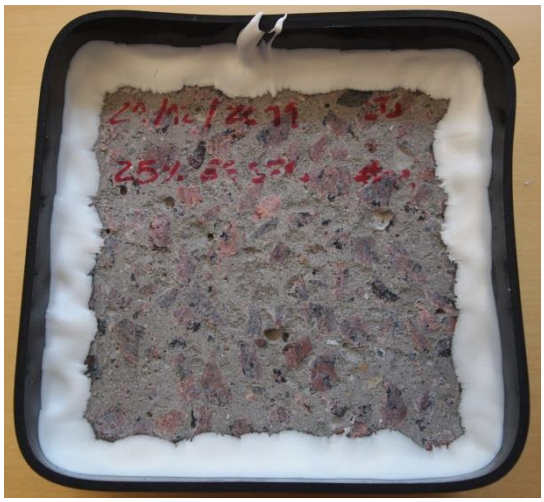

Figure E. 7 – Picture of specimen C, Mix 2 (25% GGBS, 4,5% Air, k=0.6) after 112 freeze/thaw cycles

Figure E. 8 – Picture of specimen D, Mix 2 (25% GGBS, 4,5% Air, k=0.6) after 112 freeze/thaw cycles

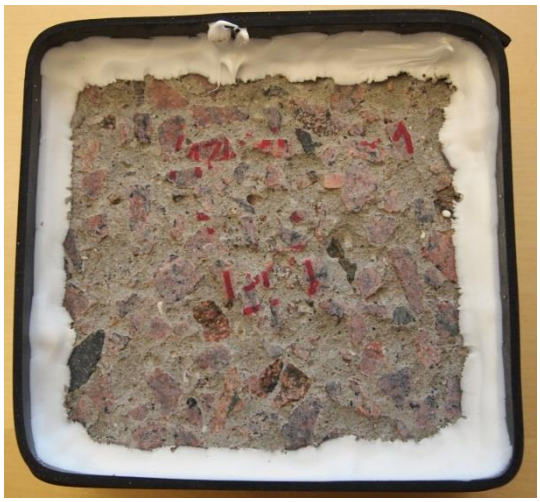

Figure E. 9 – Picture of specimen A, Mix 3 (50% GGBS, 4,5% Air, k=0.6) after 112 freeze/thaw cycles

Figure E. 10 – Picture of specimen B, Mix 3 (50% GGBS, 4,5% Air, k=0.6) after 112 freeze/thaw cycles

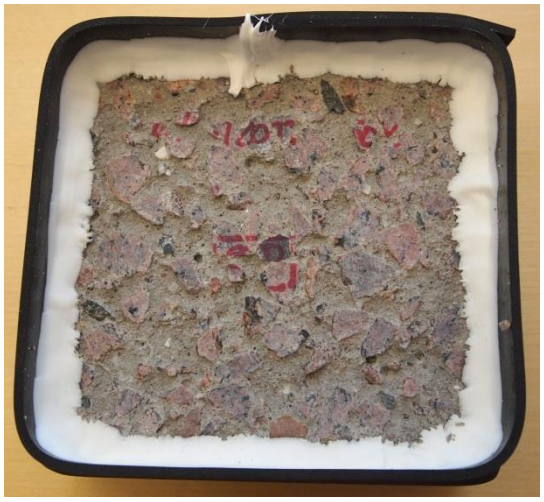

Figure E. 11 – Picture of specimen C, Mix 3 (50% GGBS, 4,5% Air, k=0.6) after 112 freeze/thaw cycles

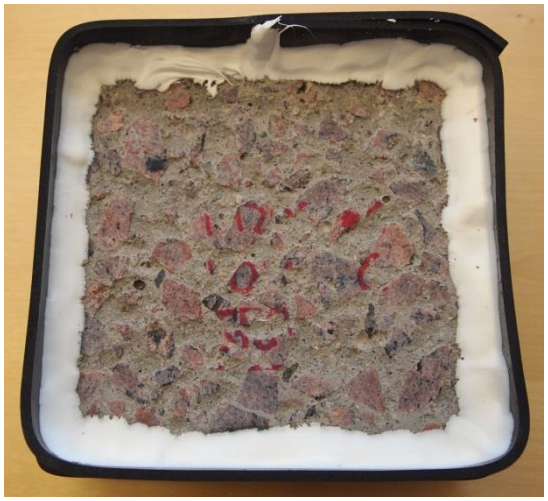

Figure E. 12 – Picture of specimen D, Mix 3 (50% GGBS, 4,5% Air, k=0.6) after 112 freeze/thaw cycles

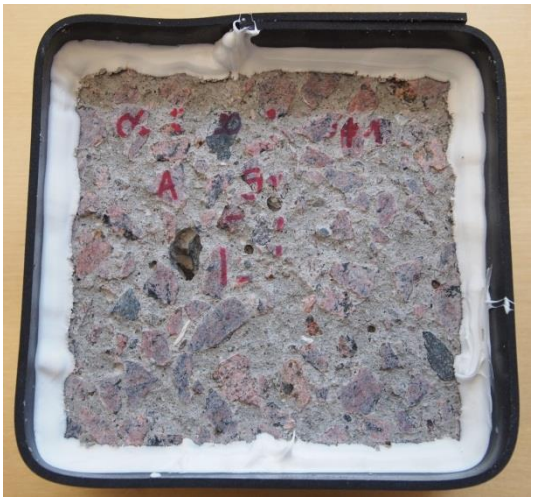

Figure E. 13 – Picture of specimen A, Mix 3 (50% GGBS, 4,5% Air, k=0.6, carbonated) after 112 freeze/thaw cycles

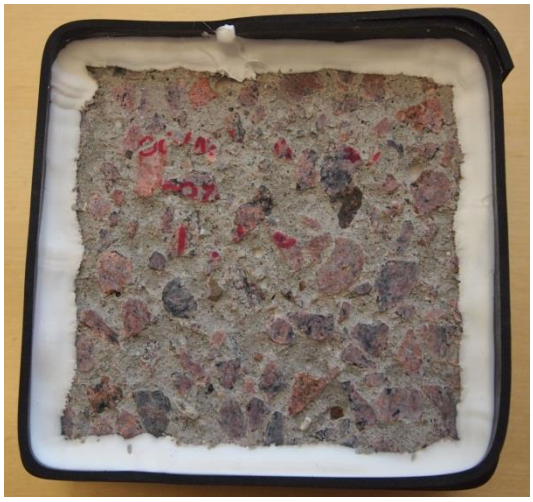

Figure E. 14 – Picture of specimen B, Mix 3 (50% GGBS, 4,5% Air, k=0.6, carbonated) after 112 freeze/thaw cycles

Figure E. 15 – Picture of specimen C, Mix 3 (50% GGBS, 4,5% Air, k=0.6, carbonated) after 112 freeze/thaw cycles

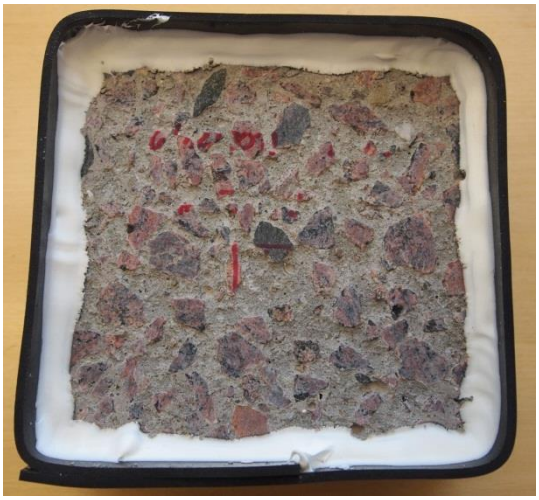

Figure E. 16 – Picture of specimen D, Mix 3 (50% GGBS, 4,5% Air, k=0.6, carbonated) after 112 freeze/thaw cycles

Figure E. 17 – Picture of specimen A, Mix 4(a) (100% GGBS, 4,5% Air, k=0.6) after 112 freeze/thaw cycles

Figure E. 18 – Picture of specimen B, Mix 4(a) (100% GGBS, 4,5% Air, k=0.6) after 112 freeze/thaw cycles

Figure E. 19 – Picture of specimen C, Mix 4(a) 100% GGBS, 4,5% Air, k=0.6) after 112 freeze/thaw cycles

Figure E. 20 – Picture of specimen D, Mix 4(a) (100% GGBS, 4,5% Air, k=0.6) after 112 freeze/thaw cycles

Figure E. 21 – Picture of specimen A, Mix 4(b) (100% GGBS, 4,5% Air, k=0.6, cured at 55ºC) after 112 freeze/thaw cycles

Figure E. 22 – Picture of specimen B, Mix 4(b) (100% GGBS, 4,5% Air, k=0.6, cured at 55ºC) after 112 freeze/thaw cycles

Figure E. 23 – Picture of specimen C, Mix 4(b) (100% GGBS, 4,5% Air, k=0.6, cured at 55ºC) after 112 freeze/thaw cycles

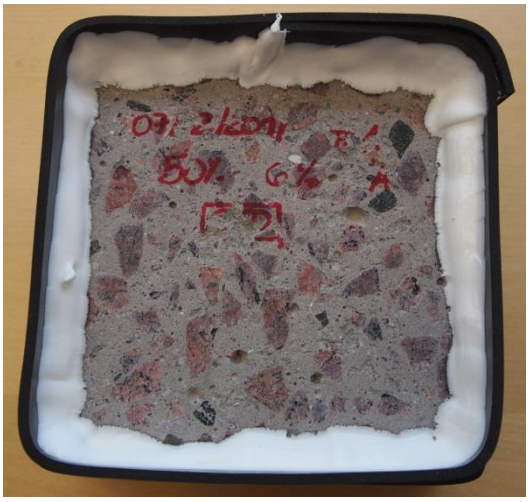

Figure E. 24 – Picture of specimen A, Mix 5 (50% GGBS, 6% Air, k=0.6), after 112 freeze/thaw cycles

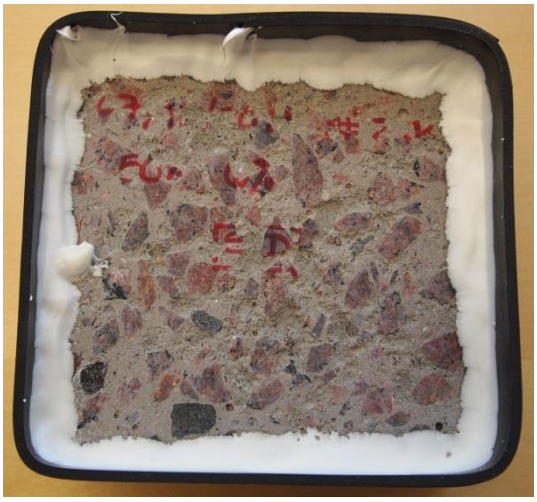

Figure E. 25 – Picture of specimen B, Mix 5 (50% GGBS, 6% Air, k=0.6), after 112 freeze/thaw cycles

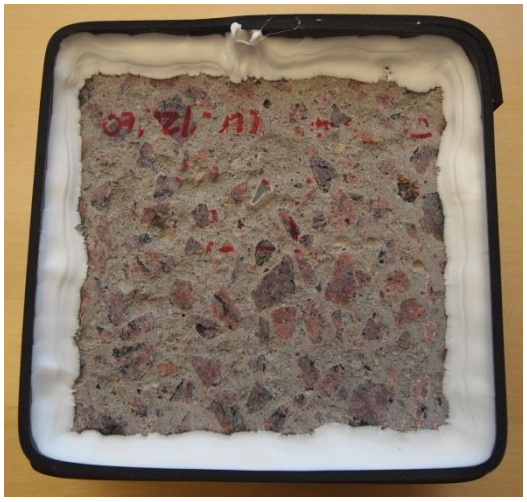

Figure E. 26 – Picture of specimen C, Mix 5 (50% GGBS, 6% Air, k=0.6), after 112 freeze/thaw cycles

Figure E. 27 – Picture of specimen D, Mix 5 (50% GGBS, 6% Air, k=0.6), after 112 freeze/thaw cycles

Figure E. 28 – Picture of specimen A, Mix 5 (50% GGBS, 6% Air, k=0.6, carbonated), after 112 freeze/thaw cycles

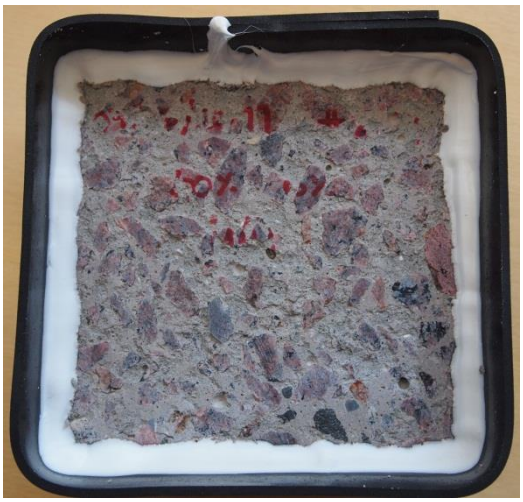

Figure E. 29 – Picture of specimen B, Mix 5 (50% GGBS, 6% Air, k=0.6, carbonated), after 112 freeze/thaw cycles

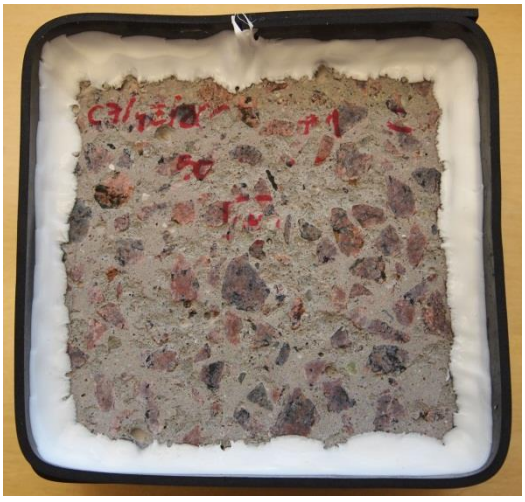

Figure E. 30 – Picture of specimen C, Mix 5 (50% GGBS, 6% Air, k=0.6, carbonated), after 112 freeze/thaw cycles

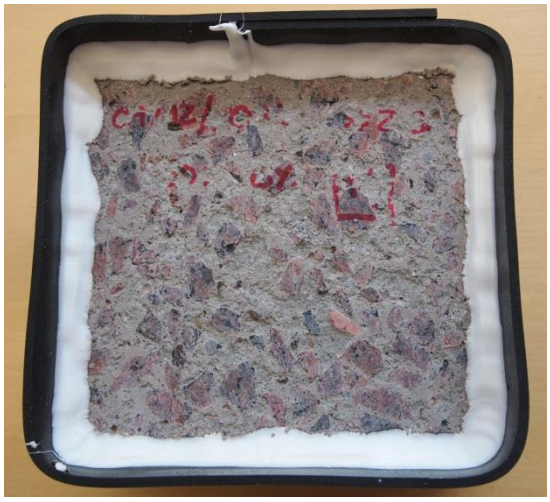

Figure E. 31 – Picture of specimen A, Mix 5 (50% GGBS, 6% Air, k=0.6, carbonated), after 112 freeze/thaw cycles

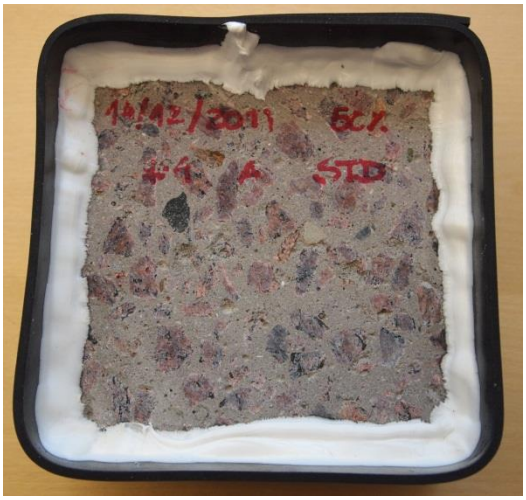

Figure E. 32 – Picture of specimen A, Mix 6(a) (50% GGBS, 4,5% Air, k=1), after 112 freeze/thaw cycles

Figure E. 33 – Picture of specimen B, Mix 6(a) (50% GGBS, 4,5% Air, k=1), after 112 freeze/thaw cycles

Figure E. 34 – Picture of specimen C, Mix 6(a) (50% GGBS, 4,5% Air, k=1), after 112 freeze/thaw cycles

Figure E. 35 – Picture of specimen D, Mix 6(a) (50% GGBS, 4,5% Air, k=1), after 112 freeze/thaw cycles

Figure E. 36 – Picture of specimen A, Mix 6(b) (50% GGBS, 4,5% Air, k=1, cured at 55ºC), after 112 freeze/thaw cycles

Figure E. 37 – Picture of specimen B, Mix 6(b) (50% GGBS, 4,5% Air, k=1, cured at 55ºC), after 112 freeze/thaw cycles

Figure E. 38 – Picture of specimen C, Mix 6(b) (50% GGBS, 4,5% Air, k=1, cured at 55ºC), after 112 freeze/thaw cycles

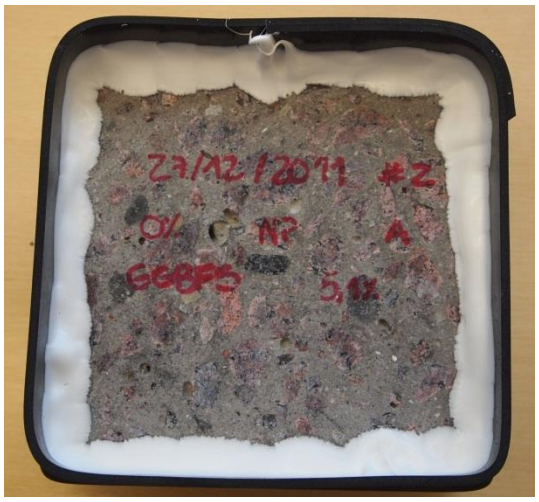

Figure E. 39 – Picture of specimen A, Mix 7 (0% GGBS, 4,5% Air, no superplasticizer) after 112 freeze/thaw cycles

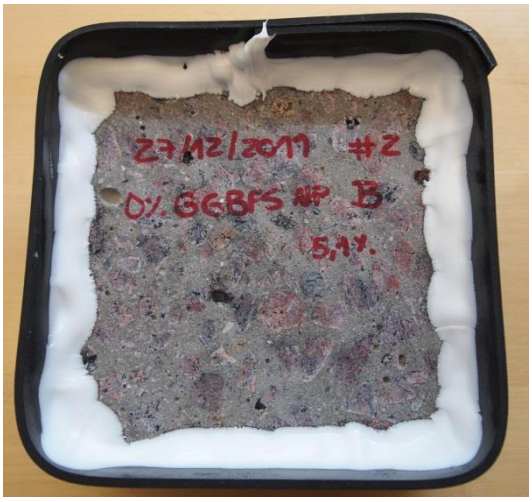

Figure E. 40 – Picture of specimen B, Mix 7 (0% GGBS, 4,5% Air, no superplasticizer) after 112 freeze/thaw cycles

Figure E. 41 – Picture of specimen C, Mix 7 (0% GGBS, 4,5% Air, no superplasticizer) after 112 freeze/thaw cycles

Figure E. 42– Picture of specimen D, Mix 7 (0% GGBS, 4,5% Air, no superplasticizer) after 112 freeze/thaw cycles

Figure E. 43 – Picture of specimen A, Mix 8 (50% GGBS, 4,5% Air, k=0.6, no superplasticizer) after 112 freeze/thaw cycles

Figure E. 44 – Picture of specimen B, Mix 8 (50% GGBS, 4,5% Air, k=0.6, no superplasticizer) after 112 freeze/thaw cycles

Figure E. 45 – Picture of specimen C, Mix 8 (50% GGBS, 4,5% Air, k=0.6, no superplasticizer) after 112 freeze/thaw cycles

Figure E. 46 – Picture of specimen D, Mix 8 (50% GGBS, 4,5% Air, k=0.6, no superplasticizer) after 112 freeze/thaw cycles